The Impact of Permafrost Thaw on Soil Carbon Cycling in Boreal Peatlands

by

William Heffernan

A thesis submitted in partial fulfillment of the requirements for the degree of

Doctor of Philosophy

in

Soil Science

Department of Renewable Resources

University of Alberta

Abstract

Permafrost peatlands in northern regions store a significant proportion of global soil carbon and have historically played an important role in global carbon cycling. Recent warming is accelerating permafrost thaw and causing thermokarst formation. Thermokarst formation in peatlands leads to a drastic increase in wetness and the colonization of *Sphagnum* mosses which may increase the capacity of peatlands to sequester carbon dioxide, as organic matter in newly formed peat. Thermokarst formation also exposes vast stores of previously frozen soil organic carbon to microbial decomposition, and potential mineralization and release as greenhouse gases to the atmosphere. The net effect of thermokarst formation on peatland carbon storage, greenhouse gas exchange, and the controls on decomposition in peatlands have been poorly understood, at both the short- and long-term perspective.

In this thesis I aimed to use several complimentary approaches to assess the net effect of thermokarst formation on carbon storage, greenhouse gas exchange, and the controls on decomposition at a peatland site in the sporadic-discontinuous permafrost zone of boreal western Canada (59.5°N, 117.2°W). I used a space-for-time chronosequence approach along two thaw transects to determine the impacts of thawing on carbon storage and the microbial constraints on peat decomposition. I used carbon stocks and annual carbon balances calculated from carbon dioxide (CO_2) and methane (CH_4) surface fluxes to measure the former, and soil enzyme activity to measure the latter. All three approaches yielded consistent findings, suggesting that mineralization of recently thawed peat was slow and largely balanced by rapid peat accumulation at the surface.

Peat core analysis showed that surficial peat accumulation offset losses of previously frozen carbon. Peat humification indices did not indicate any significant increase in decomposition of previously frozen peat upon thawing. Over a three-year measurement period, the functional response and controls of greenhouse gas fluxes differed between the recently thawed and mature bog stages. This resulted in asynchronous annual C fluxes. Due to the interannual variability of environmental drivers, this approach was unable to determine whether the long-term net carbon balance of recently thawed and more mature thermokarst bogs differed. However, it did demonstrate that the recently thawed thermokarst bogs in the study region are unlikely to experience rapid net C losses, although they do represent an area of high CH_4 emissions which may have significant implications for radiative forcing.

Soil enzyme activity, peat humification indices, and C stores showed that previously frozen peat was largely unaffected at this site by permafrost thaw. Annual carbon balances and microbial decomposition were governed by biotic and abiotic conditions at the surface. These findings demonstrate that 1) previously frozen carbon may not be vulnerable to rapid decomposition following permafrost thaw and 2) the large carbon stores found at this boreal peatland complex in western Canada, are not at risk to enhanced loss following thaw.

Permafrost peatlands within the sporadic-discontinuous permafrost zones of western Canada are unlikely to experience rapid mineralization of previously frozen carbon following thaw. Recently thawed thermokarst bogs within this region are unlikely to represent a period of rapid net carbon loss on the landscape.

Preface

Contributions of authors

All co-authored work presented in this dissertation follows the author order convention of first author is lead author, followed by authors in order of contribution, with the last author as the Principal Investigator. Each chapter in this thesis represents a collaborative, scientific effort resulting in manuscript publication or preparation for submission to peer-reviewed journals, as detailed below. For all chapters , L.H. and D.O. designed the study with input from co-authors; L.H. led field and laboratory work, data analysis, and manuscript writing; prior to publication all co-authors contributed, or will contribute, to writing.

Chapter 2: Heffernan, L., Estop-Aragonés, C., Knorr, K-H., Talbot, J., Olefeldt, D. Long-term impacts of permafrost thaw on carbon storage in peatlands: deep losses offset by surficial accumulation. *Journal of Geophysical Research: Biogeosciences. doi.org/10.1029/2019JG005501*

Chapter 3: Heffernan, L., Estop-Aragonés, C., Knorr, K-H., Olefeldt, D. Asynchronous interannual variability of the greenhouse gas exchange of young and mature thermokarst bogs due to differences in dominant environmental controls. A version of this is in preparation for submission to *Global Biogeochemical Cycles.*

Chapter 4: Heffernan, L., Jassey, V.E., MacKenzie, M.D., Frederickson, M., Olefeldt, D. Stability of soil carbon following permafrost thaw: no evidence of increased soil enzyme activity in recently thawed peat and elevated activity in near-surface peat is driven by vegetation succession. In preparation for submission to *Global Change Biology.*

“Between my finger and my thumb

The squat pen rests.

I’ll dig with it.”

“Digging” by Seamus Heaney, 1966.

Acknowledgements

Firstly, I would like to sincerely thank my supervisor and mentor Dr. David Olefeldt who has guided me throughout my PhD. with patience, encouragement, and commitment. David's enthusiasm for science, his knowledge of boreal ecosystems, and ability to identify and communicate the story has provided me with the tools to be a successful scientist. His outlook and approach to science is something I admire and aspire to.

Funding for this work, without which this research would not have been possible, came from the Natural Science and Engineering Research Council grant (RGPIN-2016-04688), the Campus Alberta Innovation Program, the University of Alberta Northern Research Awards, and the International Peatland Society Allan Robertson Grants for Research Students and Young Professionals.

I thank my supervisory committee, Dr. M. Derek MacKenzie, Dr. Merritt Turetsky, and the late Dr. Christian Blodau, for sharing their time and expertise in peatlands, permafrost, and biogeochemistry. This research has been greatly strengthened with their insight. I also thank Dr. Cristian Estop-Aragonés for stimulating conversations about peatlands, advice on study design, and for always asking the right questions.

To my family, Pat, Ita, Fiona, and Deirdre, it has been a long *aul* road. Thank you for your support and encouraging me to pursue my goals and interests. To my new Canadian family, thank you for making me feel so welcome and providing a real home away from home.

I have been very lucky to have shared the past five years with an incredible lab group. CAWS members, past and present, you have all inspired me to be better. Thank you, McKenzie Kuhn, Carolyn Gibson, Katheryn Burd, Emily Pugh, Christopher Schulze, Lauren Thompson, Rebecca

Frei, Julia Orlova, and Lorna Harris, for the countless cups of coffee, laughs, and kilometers driven. The advice, support, and feedback you have provided has helped immeasurably along the way. A special thanks to our field grandparents, Eric and Vi, 60th will always be my favourite.

Finally, to Julia Seymour, mo ghrá, thank you for always being an inspiration, a friend, and for driving me forward each and every day. I am so grateful to have had your support over these past five years, and even luckier to have it in the future. Here's to many more chapters together.

Port Láirge abú.

Table of Contents

List of Tables

List of Figures

1. General Introduction

1.1 Northern peatlands

Northern peatlands, i.e. those located between 50 – 70°N, cover ~3% of the global land surface and are widespread across the boreal and tundra biomes (Gorham, 1991; Xu et al., 2018). They are a wetland ecosystems characterised by cool, acidic, anoxic waterlogged conditions that facilitate the slow accumulation of partially decomposed organic matter, known as peat, to a depth of >30cm over millennia (Zoltai and Vitt, 1995). In northern peatlands these cool, acidic, anoxic conditions, coupled with the dominance of vegetation with complex and poor-quality litter, such as *Sphagnum* mosses, restrains microbial activity and decomposition (Clymo, 1984; Laiho, 2006). These restricted rates of microbial activity are exceeded by net plant productivity, leading to the long-term accumulation of globally significant carbon (C) stores (Clymo, Turunen, and Tolonen, 1998; Moore and Basiliko, 2006). Current estimates suggest that northern peatlands stores of 547 ± 74 Pg C (Yu et al., 2010) represent ~30% of global soil C (Yu, 2012), and that they have the capacity to increase their C stores (Gallego-Sala et al., 2018), potentially to 875 ± 125 Pg C before the end of the present interglacial (Alexandrov et al., 2020). A significant fraction, 345 ± 50 Pg C, of the northern peatland C store is found within the permafrost region (continuous, discontinuous, sporadic, isolated), an area where approximately 20% is covered by peatlands (Hugelius et al., 2014; Tarnocai et al., 2009). Permafrost soils store roughly 43% of northern peatland C (Hugelius et al., 2014) due to the widespread expansion of permafrost peatlands following the Holocene thermal maximum (Treat and Jones, 2018). Rapid warming at these higher latitudes threatens the stability of permafrost peatlands and the globally significant stores of soil C found there.

Peat initiation and peatland development at higher latitudes became widespread following the end of the last glaciation (Jones and Yu, 2010; Morris et al., 2018), however there is evidence of extensive peat accumulation at latitudes >40°N up to 130 ka, particularly during warmer periods (Treat et al., 2019). Following their widespread development, they have played an important role in the Holocene global C cycle and have long acted as a persistent net sink of atmospheric C of 20 – 30 g C m^{-2} yr^{-1} (Loisel et al., 2014; Yu, 2011). Through photosynthesis and net plant productivity they sequester carbon dioxide (CO_2), while at the same time emitting CO_2 and

methane (CH_4) derived from the mineralization and microbial decomposition of soil organic C (Blodau, 2002). Peatland C is also lost via the production and export of dissolved organic C (DOC), which can range from 1.5 – 50 g m^{-2} yr^{-1} and 2.8 – 7.3 g m^{-2} yr^{-1} in permafrost free and permafrost peatland catchments respectively (Fraser, Roulet, and Moore, 2001; Olefeldt et al., 2013). The rapid development of northern peatlands following the last glaciation (Gorham et al., 2007) contributed to the decrease of atmospheric CO_2 and increase of atmospheric CH_4 (MacDonald et al., 2006), and following further lateral expansion likely played a role in the rise of atmospheric CH_4 observed in ice cores in the late Holocene (Korhola et al., 2010). Overall, northern peatlands have had a net removal of ~70 Pg C (CO_2 and CH_4) and a net negative radiative forcing effect on the atmosphere (Frolking and Roulet, 2007), resulting in a high C density of 50 – >500 kg C m^{-2} (Frolking et al., 2011). Despite the interannual variability observed in individual peatlands (Roulet et al., 2007), undisturbed northern peatlands are likely to remain acting as a net sink for atmospheric C (Moore, Roulet, and Waddington, 1998). However, this will depend on the response of peatland C to the intensified impacts of anthropogenic climate change at northern latitudes (Holland and Bitz, 2003; Xia et al., 2014) and particularly the impact of permafrost thaw on C stores (Schuur et al., 2008).

1.2 Carbon cycling in northern peatlands

The uptake and fixation of atmospheric C, as CO_2, in northern peatlands is a result of plant photosynthesis or gross primary productivity (GPP), while the loss and release of C, as CO_2, CH_4, and DOC, is a result of microbial respiration and decomposition (Ahlström et al., 2015). Peatlands are structured both vertically as peat profiles and laterally in peat microforms, such as hummocks and hollows (Blodau, 2002). Vertically, peatlands are comprised of an upper, oxic layer known as the acrotelm, however seasonal saturation and anoxic conditions can occur, that is positioned above an anoxic layer called the catotelm (Clymo, 1984). Above the acrotelm, the upper, live vegetated portion of the vertical peat profile contains <2% of the C store, whereas the acrotelm and catotelm combined contain >98% of the peatlands C store (Gorham, 1991). The majority of organic matter decomposition in peatlands occurs in the oxic acrotelm, with only ~10% of the leaf litter mass reaching the catotelm where decomposition occurs at ~1% the rate seen in the acrotelm (Clymo et al., 1998; Frolking et al., 2001). Thus, the long-term accumulation of peatland C is dependant on organic matter decomposition in the catotelm.

Across their lateral structure, peatlands are spatial heterogeneous which can result in differing rates of long-term peat accumulation (Malmer and Wallén, 1999) and annual C balances (Waddington and Roulet, 2000) within an individual peatland. Both vertically and laterally, decomposition in northern peatlands is controlled by the water table position and its direct influence on oxygen availability and the redox boundary, and temperature, and indirectly by impacts on the vegetation community and its litter inputs (Blodau, 2002; Laiho, 2006).

The ability of a peatland to act as a net sink of atmospheric C is closely coupled with its hydrological regime and local water table position (Chivers et al., 2009; Strack and Waddington, 2007). The water table position defines the oxic/anoxic boundary, i.e. the availability of oxygen for respiration, and anoxic conditions are found 1-3 cm beneath the water table (Blodau, Basiliko, and Moore, 2004). The emission of CH_4 in peatlands is a result of methanogenic microbial activity under anoxic conditions below the water table. The production of CH_4 occurs via the acetoclastic or hydrogenotrophic methanogenic pathways and is primarily derived from the upper layers of the anaerobic catotelm. Prior to being emitted to the atmosphere at the surface CH_4 is partially oxidized in the aerobic layer above.

The majority of CO_2 emissions from peatlands to the atmosphere are derived from aerobic autotrophic (root respiration) and heterotrophic (soil microbial) respiration, that combined represent ecosystem respiration (ER), with some contribution by anaerobically produced CO_2 via organic matter oxidation or fermentation (Keller and Bridgham, 2007). Lower water tables allow for increased diffusion of oxygen into peat and enables aerobic decomposition and the production of CO_2 2.5 – 6 times greater than under anerobic conditions (Bridgham et al., 1995; Moore and Dalva, 1993). While lowered water tables have been shown to lead to increased CO_2 emissions (Bubier et al., 2003; Riutta, Laine, and Tuittila, 2007) and the importance of heterotrophic respiration for overall ER (Olefeldt et al., 2017), others have suggested little to no impact of lowered water tables on CO_2 emissions (Lafleur et al., 2005; Laine et al., 2019) However, across peatland microforms water table position, along with soil temperatures have been shown to act as significant controls on ER (Juszczak et al., 2013).

1.3 Constraints on peat decomposition

The kinetics and rate of decomposition of organic matter are highly sensitive to temperature (Davidson and Janssens, 2006). Several studies have shown temperature to be a dominant

control on peat decomposition and that increases in soil temperature corresponds with increases in peatland ER and CH_4 production (Dorrepaal et al., 2009; Kettridge and Baird, 2008; Mäkiranta et al., 2009; Silvola et al., 1996; Treat et al., 2007). Low temperatures in northern peatlands constrain rates of microbial decomposition and the ER and CH_4 Q_{10} values i.e. the relative change in the rate of respiration over a 10°C increase in temperature, can vary with a higher Q_{10} for recalcitrant peat compared to labile peat where there is lower required activation energy for microbial decomposition (Blodau, 2002; Davidson and Janssens, 2006; Michaelis et al., 1913). However, deep recalcitrant catotelm peat has been shown to not be sensitive to increased temperatures (Wilson et al., 2016), which may be a result of low hydraulic conductivity and the accumulation of decomposition end-products resulting in anaerobic decomposition having reached its thermodynamic threshold (Beer and Blodau, 2007; Beer et al., 2008). The response of heterotrophic respiration to temperature is dependant on the chemical composition and nutrient availability of the dissolved organic matter substrate provided by the vegetation community (Tfaily et al., 2013; Updegraff et al., 1995).

The vegetation community, through its litter inputs, provides the substrate and nutrients, i.e. the energy source, for the microbial decomposer community and thus regulates the composition and activity of the microbial community (Borga, Nilsson, and Tunlid, 1994; Briones et al., 2014; Ward et al., 2015). Peat decomposition is regulated by the efficiency of extracellular enzymes in cool, saturated, acidic conditions produced by the microbial community in response to the chemistry and quality of litter inputs (Limpens et al., 2008; Sinsabaugh et al., 2005). The activity of extracellular hydrolytic enzymes controls the rate of organic matter solubilization and at which degraded substrates become available for microbial metabolism (Bengtson and Bengtsson, 2007; Bell et al., 2013). They control the rate limiting step of decomposition, mediating the decomposition and mineralization of organic matter into greenhouse gases (Marx, Wood, and Jarvis, 2001; Luo, Meng, and Gu, 2017). The water table position and saturation conditions influences the structure of the vegetation community (Breeuwer et al., 2009; Robroek et al., 2007) and thus impacts the quality of litter inputs and substrate available for microbial decomposition (Laiho et al., 2003). Predicted increases in temperature and lowering of water tables in northern peatlands (Roulet et al., 1992) can have a significant impact on the dominant *Sphagnum* moss vegetation community and favours the colonization of vascular plants (Churchill et al., 2014; Weltzin et al., 2003). Shifts in the vegetation community due to water

table change can have large implications for C cycling and can lead to enhanced C losses (Strack et al., 2006; Walker et al., 2016). Shifts in vegetation results in differing quality of litter inputs and substrate availability impacting the composition and activity of microbes (Crow and Wieder, 2005; Bubier, 1995), and potentially affects the sensitivity of decomposition to temperature (Fierer et al., 2005). Both of which can lead to enhanced microbial decomposition (Bragazza et al., 2013).

Sphagnum moss plays a vital role in C decomposition by producing decay resistant litter with poor organic matter quality (Hájek et al., 2011). Phenolic compounds that inhibit the activity of extracellular hydrolytic enzymes and microbial activity (Jassey et al., 2011) are produced by *Sphagnum* and the quantity produced is species, season, and microhabitat dependant (Rasmussen, Wolff, and Rudolph, 1995; Chiapusio et al., 2018). Oxidative enzymes are involved in the degradation of phenolic compounds (Sinsabaugh, 2010) and can completely oxidize phenolics from inhibitory and simple aromatics to complex and non-inhibitory polyphenols (Durán et al., 2002). The presence of oxygen has been shown to be a strong constraint on oxidative enzyme activity (Freeman et al., 2002), along with low temperatures (Freeman et al., 2001) and low pH (Criquet et al., 1999; Pind, Freeman, and Lock, 1994). Oxidative enzyme activity is highest in the upper oxic peat layers and while they are still produced under saturated conditions, activity decreases with depth below the water table and increasing anoxic conditions (Fenner and Freeman, 2011; Fenner, Freeman, and Reynolds, 2005; Freeman et al., 2004). Phenolic compounds can accumulate in peat due to low oxidative activity (Freeman et al., 2002) potentially inhibiting hydrolytic enzyme activity and microbial decomposition (Freeman et al., 2004). However, previous research has highlighted that variations in plant litter inputs are of greater importance to decomposition than water table position and oxygen availability (Kaštovská et al., 2018; Straková et al., 2012). Shifts in vascular plant communities due to changing water tables, temperature, and nutrient status (Bragazza, 2006; Dieleman et al., 2015) can have important implications for microbial communities and activity, leading to increased enzyme activity and C decomposition (Bragazza et al., 2015; Robroek et al., 2016). Previous studies indicate that litter type and chemistry, in particular that derived from *Sphagnum* spp., may be the most important control on microbial decomposition and C mineralization in to CO_2 and CH_4 (Limpens, Bohlin, and Nilsson, 2017; Sjögersten et al., 2016; Strakova et al., 2011).

Increased evapotranspiration and water table drawdown due to accelerated circumpolar temperatures have the potential to destabilize the controls on decomposition and C balance of northern peatlands (Alm et al., 1999; Manabe and Wetherald, 1986). Rapidly rising temperatures as a result of anthropogenic climate change are amplified at northern latitudes and are predicted to accelerate throughout the 21st century (IPCC, 2019). Projected increases in soil temperatures are greatest at the higher latitudes in permafrost regions (Koven, Riley, and Stern, 2013; Soong et al., 2020), leading to the widespread degradation and thawing of permafrost soils (Grosse et al., 2016; Jorgenson et al., 2010; Park, Kim, and Kimball, 2016), particularly in permafrost peatlands (Payette et al., 2004; Swindles et al., 2015).

1.4 Permafrost peatlands

Permafrost, i.e. perennially frozen ground that ranges from continuous, discontinuous, sporadic, and isolated (Everett, 1989), has an affinity for peat soils due to the insulating thermal properties of *Sphagnum* moss (Vitt, Halsey, and Zoltai, 2000) and peatlands are the most abundant permafrost terrain across the discontinuous and sporadic permafrost zone (Tarnocai et al., 2009). Northern peatlands within the permafrost region store an estimated 345 ± 50 Pg C (Hugelius et al., 2014) with large quantities of this C currently frozen, unavailable for microbial decomposition and it remains unclear as to how this vast C store will respond to rapid and widespread permafrost thaw (Abbott et al., 2016; Schuur et al., 2015; Schuur et al., 2008).

Permafrost aggradation in peatlands results in ice rich permafrost peat plateaus that are raised ~1 – 2 m above the surrounding landscape (Quinton, Hayashi, and Chasmer, 2009), with the majority of expansion occurring in mineral layer beneath the peat deposit (Kanevskiy et al., 2014). Permafrost can aggrade epigenetically whereby the majority of the peat accumulated prior to permafrost aggradation (Zoltai, 1993) or syngenetically with peat accumulation (Kanevskiy et al., 2014). Aggradation can have a significant impact on the properties and quality of accumulated peat (Treat et al., 2016). The formation of raised peat plateaus results in a hydraulic gradient between the plateau and surrounding wetlands (Quinton, Hayashi, and Chasmer, 2011) and the development of a dry, oxic active layer <80 cm thick above the permafrost (Shur and Jorgenson, 2007). Early plateau development is dominated by mesic *Sphagnum* spp. with further drying leading to a dominance of lichens (such as *Cladonia* spp.), black spruce (*Picea mariana*), feathermosses, and ericaceous shrubs such as Labrador Tea (*Rhododendron groenlandicum*)

(Kuhry, 2008). The development of this dry oxic layer, and dominance of the associated vegetation communities, leads to the accumulation of sylvic peat. A natural cycle of permafrost aggradation and degradation can occur within the same peatland complex, resulting in the formation of peat plateaus interspersed with permafrost free, thermokarst bogs (Zoltai, 1993). However due to rising temperatures, recent permafrost degradation and the development of thermokarst bogs is occurring at an accelerated rate (Camill, 2005) with further thawing expected to accelerate throughout the 21st century (Zhang, Chen, and Riseborough 2008).

Thawing in permafrost peatlands leads to thermokarst formation, whereby interactions between hydrology, geomorphology, soil properties, vegetation, and disturbances (such as increasing temperatures or fire severity and frequency) lead to the thawing and loss of ground ice and subsequent surface subsidence (Jorgenson et al., 2010; Kokelj and Jorgenson, 2013; Zimov, Schuur, and Chapin, 2006). Thermokarst bog development (Fig. 1.1) results in the inundation of the peat profile and a drastic, sharp shift from the dry black spruce and lichen dominated plateau vegetation to hydrophilic species such as *Sphagnum riparium*, *Carex* spp., and *Eriophorum* spp. (Baltzer et al., 2014; Beilman, 2001). Following centuries of peat accumulation and autogenic succession, the peat surface becomes drier once again, favouring the colonization and dominance of more mesic ombrotrophic bog species such as such as *Sphagnum fuscum*, *Sphagnum magellanicum*, ericaceous shrubs, and some black spruce regrowth (Camill, 2005; Robinson and Moore, 2000; Vitt, Halsey, and Zoltai, 1994). Thermokarst bog development, due to shifts in the hydrological regime and vegetation community, increased soil temperatures, exposure of previously frozen peat to enhanced microbial decomposition can have significant consequences for permafrost peatland C.

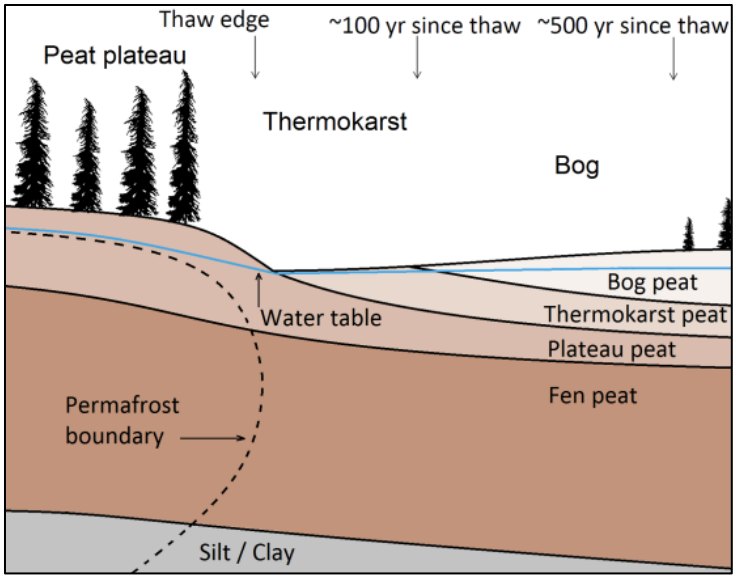

Figure 1.1 Stages of thaw and thermokarst bog succession in a permafrost peatland. (Image credit; Olefeldt, David).

The controls of peatland C decomposition are in a highly dynamic state following permafrost thaw and thermokarst formation has significant implications for C accumulation and decomposition. Surface inundation in the initial stages of thermokarst development causes a shift to anoxic conditions, reducing aerobic respiration and CO_2 emissions, as well a switch to a productive vegetation community leading to high rates of GPP and C accumulation at the surface (Camill et al., 2001; Robinson and Moore, 2000). Warm, wet anaerobic conditions and increased hydrophilic vascular plants leads to increased CH_4 emissions as C fixed during GPP may be used for microbial CH_4 production, as well as through plant-mediated transport (Prater, Chanton, and Whiting, 2007). The exposure of previously frozen peat to enhanced microbial decomposition and mineralization into CO_2 and CH_4 can cause a loss of C to the atmosphere, further amplifying anthropogenic climate change (Deng et al., 2014; Mauritz et al., 2017; Wickland et al., 2006). While previous studies have indicated increased rates of C accumulation following thaw (Jones et al., 2013), others have indicated significant losses of C, as high a 30% of previously frozen C stores (Jones et al., 2017; O'Donnell et al., 2012), and increased CO_2 and CH_4 emissions (Johnston et al., 2014; Turetsky et al., 2002) particularly in the initial decades following thaw. The soil C pool in thawed permafrost peatlands is far greater than the vegetative C pool

accumulating at the surface, thus the adjustment or removal of constraints on decomposition following thaw, due to shifts in water table regime, increased labile litter and substrate availability, or increasing temperatures, may accelerate net C loss and the permafrost C climate feedback. Currently, the magnitude of the response of permafrost peatland C to widespread permafrost thaw is unknown (Schuur et al., 2015).

1.5 Permafrost peatlands of western Canada

The Mackenzie River Basin in western Canada represents a circumpolar region with one of the greatest density of northern peatlands, that span from north to south across all permafrost zones (Wu et al., 2017; Zoltai, 2007). Permafrost peatland complexes in this region cover an area of ~151,000 km^2 and represent a globally significant terrestrial soil C store (Hugelius et al., 2014). Peatland development in the sporadic-discontinuous permafrost zone of western Canada began ~9,000 years ago (Halsey, Vitt, and Bauer 1998), with permafrost aggradation occurring following the Holocene Thermal Maximum (Zoltai, 1995) and more widespread following regional climate cooling ~1,200 years ago (Pelletier et al., 2017). The permafrost peatland complexes found here consist of peat plateaus, thermokarst bogs, permafrost free bogs, channel fens and ponds (Vitt, Halsey, and Zoltai, 1994). Permafrost in this region is found primarily in peatlands and is thin, warm (near 0 °C), shallow and susceptible to thaw (Smith et al., 2009; Holloway and Lewkowicz, 2019). Total permafrost loss for this area is predicted during the 21st century (Chasmer and Hopkinson, 2017). Permafrost peatland complexes in the sporadic-discontinuous permafrost region of western Canada are well suited to studying both the impacts of permafrost thaw on peatland C due to the high density of C rich permafrost peatlands found there and their vulnerability to accelerated permafrost thaw.

The main objective of this doctoral dissertation is to understand how, on the scale from decades to millennia, vast boreal permafrost peatland C stores will be affected by inevitable permafrost thaw, and to assess whether boreal peatlands will become hotspots for C loss. The dissertation is divided in to five chapters, including an introduction, three data chapters, and conclusion. In Chapter 2 I focus on the impact of permafrost thaw on long-term C storage in a boreal peatland complex and establish that the assumptions of the chronosequence approach used throughout the dissertation are met. Chapter 3 examines the effect of permafrost thaw on surface greenhouse gas fluxes and estimates the impact of thaw on the annual greenhouse gas exchange balance (CO_2

and CH_4), assessing whether recently thawed thermokarst bogs act as large net sources of C to the atmosphere. Chapter 4 investigates the impacts of permafrost thaw on soil enzyme activities and assess the vulnerability of previously frozen peat to increased decomposition following thaw. In Chapters 2 and 3 I assess the long- and short-term effects of thaw on net C storage. Chapter 4 focuses on controls of belowground decomposition of previously frozen peat, highlighting potential mechanisms for identified changes in long- and short-term C balances. In my fifth and final chapter I draw overall conclusions from my three data chapters on the impact of permafrost thaw on boreal peatland C and suggest future steps to better understand and predict how boreal peatlands will respond to permafrost thaw.

2. Long-term impacts of permafrost thaw on carbon storage in peatlands: deep losses offset by surficial accumulation

Abstract

Peatlands in northern permafrost regions store a significant proportion of global soil carbon. Recent warming is accelerating peatland permafrost thaw and thermokarst collapse, exposing previously frozen peat to microbial decomposition and potential mineralization into greenhouse gases. Here we show from a site in the sporadic-discontinuous permafrost zone of western Canada that thermokarst collapse leads to neither large losses nor gains following thaw, as deep carbon losses are offset by surficial accumulation. We collected peat cores along two thaw chronosequences, from peat plateau, through young (~30 years since thaw), intermediate (~70 years) and mature (~200 years) thermokarst bog locations. Macrofossil and ^{14}C analysis showed synchronicity of peatland development until recent thaw, with wetland initiation ~8,500 cal yr BP followed by succession through peatland stages prior to permafrost aggradation ~1,800 cal yr BP. Analysis and modelling of soil carbon stocks indicated 8.7 ± 12.4 kg C m^{-2} of carbon accumulated prior to thaw was lost in ~200 years post-thaw. Despite these losses, there was no observed increase in peat humification as assessed by FTIR and C:N ratios. Rapid peat accumulation post-thaw (9.8 ± 1.6 kg C m^{-2} over 200 years) offset deeper losses. Our approach constrains the net carbon balance to be between uptake of 27.3 g C m^{-2} yr^{-1} and loss of 106.6 g C m^{-2} yr^{-1} over 200 years post-thaw. While our approach cannot determine whether thermokarst bogs in the sporadic-discontinuous permafrost zone act as long-term carbon sinks or sources post-thaw, our study better constrains post-thaw C losses and gains.

2.1 Introduction

Northern peatlands are a globally significant stock of soil organic carbon (C), with an estimated 345 ± 50 Pg C stored within the northern permafrost region (Yu 2012; Hugelius et al., 2014). Long-term C accumulation in northern peatlands since the last deglaciation has been facilitated by cold and waterlogged conditions (Blodau, 2002). Roughly 43% of the accumulated C in northern peatlands has become incorporated into permafrost (Hugelius et al., 2014), with particularly widespread permafrost expansion following the Holocene thermal maximum (Treat and Jones, 2018). Recently, increased warming at northern latitudes (Xin-Gang and Ping, 2010) and accelerated permafrost thaw in northern peatlands (Camill, 2005; Payette et al., 2004) has exposed vast stores of C to enhanced microbial decomposition, potentially releasing previously frozen C to the atmosphere as CO_2 and CH_4 (Dorrepaal et al., 2009; Turetsky et al., 2002). Studies estimating the magnitude and timing of emissions derived from recently thawed non-peatland soils predict a positive feedback to climate warming (Grosse et al., 2011; Koven et al., 2015; Schuur et al., 2015). Large-scale predictions of thawing peatland C related feedbacks to climate warming are difficult to make due to the heterogeneity of the landscape, permafrost history, and peat properties (Jorgenson et al., 2001; Treat et al., 2016). It remains unclear how permafrost thaw will impact the complex regulatory ecohydrological feedbacks that govern long-term C storage in peatlands (Waddington et al., 2014; Wu et al., 2011), and to what degree peatland developmental and permafrost history influences this.

Permafrost aggradation in boreal peatlands influences the peat type and quality that is accumulated (Treat et al., 2016). The development of raised permafrost peat plateaus influences local hydrology and vegetation cover (Camill et al., 2009; Quinton et al., 2009), and leads to the accumulation of sylvic peat, i.e. peat dominated by mesic *Sphagnum* spp., ericaceous shrubs, feathermosses, lichens, and black spruce remains, in a dry, oxic active layer. During their early development peat plateaus often continue to be dominated by *Sphagnum* spp., as dominated in the preceding bog stage, but continued peat plateau development causes further drying of the site and a shift in vegetation towards dominance of lichens (such as *Cladonia* spp.), black spruce (*Picea mariana*), and ericaceous shrubs such as Labrador Tea (*Rhododendron groenlandicum*) (Kuhry, 2008). Peat plateaus have lower apparent C accumulation rates than surrounding non-permafrost peatlands (Robinson and Moore, 1999) and have increased aerobic decomposition of

active layer peat (Turetsky et al., 2007). However, monitoring of the greenhouse gas exchange has shown peat plateaus and adjacent non-permafrost peatlands to have similar annual net C balances (Olefeldt et al., 2012; Pelletier et al., 2017; Helbig, Chasmer, Desai, et al., 2017). This suggests that accumulation of less labile sylvic peat and reduced soil temperatures in the permafrost layer, compared to peat from non-permafrost peatlands, may result in comparatively similar rates of C accumulation.

Peat in areas where permafrost formed epigenetically, i.e. where most of the peat deposit was already present when permafrost formed, has undergone centuries to millennia of decomposition (Zoltai, 1993) and is likely humified and not labile upon thawing . Peat quality and humification are important controls for peat decomposition in thawed permafrost peatlands (Sjögersten et al., 2016; Treat et al., 2014), which highlights the potential importance of permafrost history, and resulting organic matter quality, when considering the future of thawing peatland C stores.

Permafrost thaw in ice-rich peat plateaus can have significant consequences on the net C balance as thaw may lead to land subsidence (1 – 3 m) and development of thermokarst bogs (Zimov et al., 2006) resulting in the inundation of the peat profile. Thermokarst development causes a complete shift in the vegetation community and is associated with high rates of productivity and C inputs at the surface (Beilman, 2001; Jones et al., 2013), in the order of ~150 g C m^{-2} yr^{-1} over 200 years following thaw (Camill et al., 2001). Inundation results in anaerobic conditions associated with elevated emissions of CH_4 (Wickland et al., 2006), but can also restrict respiration of old C that previously was respired aerobically in the active layer (Schädel et al., 2016) further enhancing C accumulation. Despite high accumulation rates of surface peat following thaw, studies along Alaskan thaw chronosequences indicated large net losses of C in the initial decades to centuries following thaw, in the order of <500 to 3,500 g C m^{-2} yr^{-1} during the first decade following thaw (O'Donnell et al., 2012; Jones et al., 2017). However, various field studies from areas with different permafrost and developmental histories have found no direct evidence of losses of old soil C as CO_2 or CH_4 following thaw at the magnitude that would be necessary for such large net C losses (Klapstein et al., 2014; Cooper et al., 2017; Estop-Aragonés, Cooper, et al., 2018; Estop-Aragonés, Czimczik, et al., 2018). Projections suggest increased permafrost degradation and thermokarst formation over the next 100 years, with total loss of permafrost from warm discontinuous permafrost regions in the next few decades

(Chasmer and Hopkinson, 2017). This emphasizes the importance of developing a better approach to assess post-thaw C balance, and to understand if there are differences between sites, and how those differences arise.

Peatlands of the southern Mackenzie River Basin (Fig. 2.1a) are well suited to assess the impact of permafrost thaw on C storage due to the significance of the C stores found there and, due to their history of epigenetic permafrost aggradation and degradation, this C store is potentially recalcitrant upon thawing (Zoltai and Tarnocai 1975; Beilman et al., 2008). The space-for-time chronosequence approach has been used to determine the impacts of thawing on C storage by comparing C stocks or fluxes among sites that differ only with regards to their time since permafrost thaw. Using this approach previous studies have indicated long-term changes in peatland C storage via measured C stocks (O'Donnell et al., 2012), assessed annual C balances from measured CO_2 and CH_4 surface fluxes (Johnston et al., 2014; Helbig, Chasmer, Kljun, et al., 2017), identified increased peat humification following thaw (Jones et al., 2017), and used ^{14}C analysis to determine the contribution of old soil C to CO_2 lost at the surface (Estop-Aragonés, Cooper, et al., 2018; Estop-Aragonés, Czimczik, et al., 2018). While these approaches have their individual strengths and weaknesses, in order to accurately detect the long-term impact of thaw on C stocks the assumptions of the chronosequence approach must be met. A key assumption of chronosequences is that developmental histories, and soil forming factors, have been similar for all stages of the chronosequence up until the timing of permafrost thaw. Verifying that the developmental histories across the chronosequence are identical ensures that differences in C storage are due to the effects of permafrost thaw and not due to differing C accumulation histories prior to thaw.

In this study, the main objective was to estimate the impact of permafrost thaw on the long-term C storage of a boreal peatland complex. We evaluated the assumptions of the chronosequence approach, ensuring that each site along the chronosequence had the same developmental history in order to assess the impact of thaw on C storage. We collected and analyzed multiple peat cores along two thaw transects, each core collected from an area that thawed at different times over the past ~ 200 years. This approach allowed us to determine both how permafrost thaw impacted stores of C that accumulated prior to thaw, as well as accumulation of new C at the surface following thaw. By determining the timing of peatland initiation, permafrost aggradation and

permafrost thaw, we assessed the vulnerability of peatland C stores to loss with regards to both time-since-thaw and peat properties. We hypothesize that; (1) there are net losses of C in the initial decades following thaw, where losses of old C is accompanied by increased peat humification; and that (2) in the centuries following thaw peat humification stabilizes, and losses of old C slow and are outweighed by new C accumulation at the surface resulting in a net C gain. This study highlights the importance of developmental history and how spatially varied the impacts of permafrost thaw are on C stores across the boreal landscape.

2.2 Methods

2.2.1 Site Description

The study site is located in the sporadic-discontinuous permafrost zone of the Mackenzie River Basin in western Canada (59.5°N, 117.2°W) (Brown et al., 1997; Heginbottom, Dubreuil, and Harker, 1995) (Fig. 2.1a). The climate at Meander River 50 km south of the study site is continental, with an average annual air temperature of -1.8°C (Climate-Data.org, 2019). January is the coldest month (-22.8°C), July is the warmest (16.1°C), and average annual precipitation is 391 mm. The study area is a heterogenous landscape with a mix of upland forests and peatlands, with permafrost only found in the peatlands. These peatland complexes are in turn comprised of permafrost-affected peat plateaus interspersed with non-permafrost thermokarst bogs, fens, and ponds. Peatland formation in this region began 8000 – 9000 years ago following deglaciation (Halsey, Vitt, and Bauer, 1998). A cooling of the climate ~6,000 years ago following the Holocene thermal maximum (Porter et al., 2019) lead to the earliest permafrost aggradation in the area, but this became more widespread following further cooling ~1200 years ago (Loisel et al., 2014; Pelletier et al., 2017). Permafrost peatlands make up >25% of land cover and peat deposits vary in thickness from 2 – 6 m throughout the sporadic-discontinuous permafrost zone of boreal western Canada (Hugelius et al., 2014; Vitt et al., 2000; Beilman et al., 2008; Bauer et al., 2003). Permafrost in this region is warm (near 0 °C), fragmented, and susceptible to extensive and rapid permafrost thaw (Carpino et al., 2018; Gibson et al., 2018; Smith et al., 2009).

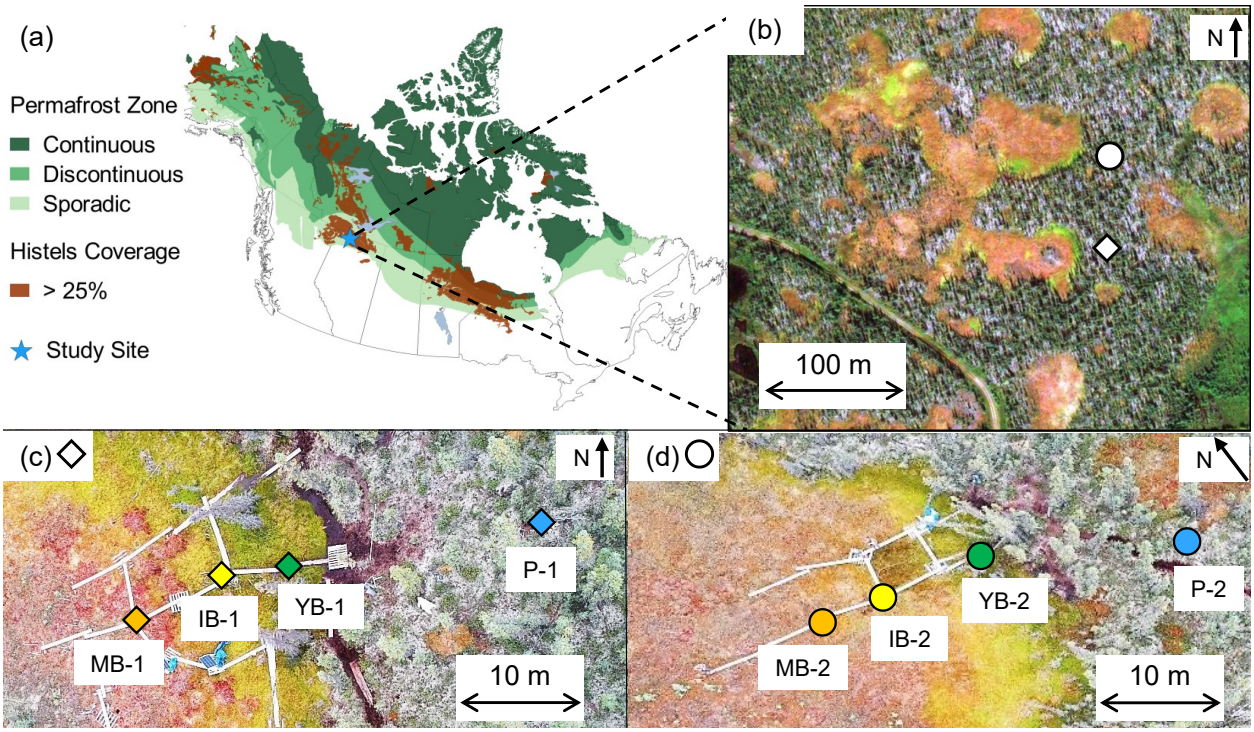

Figure 2.1. Study site location within North America, and site characteristics and soil sampling locations shown on satellite and drone imagery. (a) Study site (Lutose, Alberta, Canada 59.5°N, 117.2°W) location within permafrost zonation (Brown et al., 1997) and permafrost peatland extent (histel soils) (Hugelius et al., 2014) in North America. (b) Geoeye satellite image of study site obtained online at https://zoom.earth/, 0.46 m resolution. Diamond symbol represents the peat plateau sampling location in transect one, circular symbol represent peat plateau sampling location intransect 2. (c) Aerial image from 2018 of transect 1 (diamond), obtained from drone at an altitude of ~50 m showing location of plateau (P-1; blue diamond), young (YB-1; green diamond), intermediate (IB-1; yellow diamond), and mature bog (MB-1; orange diamond) cores. (d) Same as for (c) but for transect 2, showing locations of plateau (P-2; blue circle), young (YB-2; green circle), intermediate (IB-2; yellow circle), and mature bog (MB-2; orange circle) cores. (Aerial photo credit: Olefeldt, David).

The study site includes two transects, each with cores collected from an intact permafrost peat plateau and adjacent thermokarst bog (Fig. 2.1b, c, d). The peat plateau is raised 1 – 2 m above the surrounding thermokarst bogs due to ice expansion and presence of segregated ice. The peat plateau has an average active layer depth of ~55 cm. Vegetation on the peat plateau is characterized by a stunted, open canopy black spruce (*Picea mariana*) forest, Labrador tea

(*Rhododendron groenlandicum*) shrubs, and ground cover of lichens (*Cladonia* spp.) and sparse hummocks dominated by dry-adapted *Sphagnum fuscum*. Within each of the two thermokarst bogs we differentiate between young, intermediate, and mature bog stages based on water table position, vegetation composition, and proximity to the thawing edge (Fig. 2.1b, c, d). The young bog stage is located adjacent to the peat plateau and is <5 m wide. Active thaw is occurring in the young bog stage as indicated by the presence of dying *Picea mariana* that are toppling over. It has an average growing season water table position of 2 cm beneath the peat surface and is dominated by hydrophilic *Sphagnum riparium* and Rannoch-rush (*Scheuchzeria palustris*). The intermediate bog has an average growing season water table depth of 7 cm beneath the peat surface, is dominated by *Sphagnum riparium, Sphagnum angustifolium, Scheuchzeria palustris*, and Leather leaf shrub (*Chamaedaphne calyculata*), and is located 5 – 10 m from the thawing edge. The mature bog is the driest area of the thermokarst bog with an average growing season water table depth of 24 cm beneath the peat surface and is located >10 m from the thawing edge. It is dominated by *Sphagnum fuscum* and *Sphagnum magellanicum, Chamaedaphne calyculata* and Bog Rosemary (*Andromeda polifolia*) shrubs, scattered cotton-grass (*Eriophorum vaginatum*) tussocks, and some *Picea mariana* regrowth.

2.2.2 Chronosequence Approach and Site History

We used a space-for-time chronosequence approach to assess the impact of permafrost thaw on C storage by collecting cores at several locations across the two thaw transects (Transect 1 and Transect 2). In August 2015, we extracted eight cores in total along two 20 m transects with 4 cores taken from each. The two peat plateau cores (P-1 and P-2) were collected ~15 m apart and had similar understory vegetation. From both thermokarst bog transects we extracted cores from the young bog (YB-1 and YB-2), the intermediate bog (IB-1 and IB-2), and the mature bog (MB-1 and MB-2). Surface cores (top 40 cm) were extracted using 10.2 cm diameter PVC tubes. Below 40 cm we used a Russian peat corer (4.5 cm inner-diameter, Eijkelkamp, Giesbeek, Netherlands) in thermokarst bog peat, and a Snow, Ice, Permafrost Research Establishment (SIPRE) coring auger (10 cm inner diameter) in frozen, plateau peat. Cores taken with the Russian corer were taken at each location from two boreholes located ~30 cm apart, alternating between both in 50 cm long sections with a 10 cm overlap, in order to avoid sampling peat disturbed by the tip of the corer. Cores using the SIPRE corer were taken from a single borehole,

the top and bottom 1 cm of each core segment was not used for analysis to avoid interference from disturbance. Each core section was then placed in a halved PVC tube, wrapped in cellophane, and transported frozen on dry ice back to the laboratory where it was cut in to 1 cm sections for various analysis. The P-1 and MB-1 cores, which represent the beginning and end of our thaw chronosequence, were chosen for ^{14}C and peat properties analysis for a more detailed comparison of peat age and peat humification between the intact permafrost peat plateau (P-1) and an area that thawed longest ago (MB-1).

Plant macrofossils were collected and described every 5 – 15 cm in all eight cores using the Mauquoy et al., (2010) protocol for preparation and identification. Once cut, we sampled 5 – 7.5 cm^3 of peat from a single 1 cm section and visually estimated the main peat components. We estimated the presence of *Sphagnum*, brown moss, sedge, ligneous matter, and ericaceous rootlets using five ranges (≤ 1%, 1 – 10%, > 10 – 50%, > 50 – 90%, and > 90%) of percentage of peat volume acquired from the average of five different estimates per 1 cm section. For sedges, only above-ground fragments were used for vegetation reconstruction. Plant needles and leaves are reported as individuals per cm^3. We assessed macrofossil information at all depths sampled in all cores, along with bulk density, loss-on-ignition, and radiocarbon dated material, to understand peatland developmental history and identify the main transitions between macrofossil assemblages, peatland stages, and permafrost history at the study site. Macrofossil data for each core was assessed using C2 Version 1.5 (Juggins, 2003) to visualise paleoenvironmental data.

Peat samples were dated using ^{14}C analysis with accelerator mass spectrometry (AMS) from all eight cores. For the dating 50 – 100 mg of clean, identifiable dried plant macrofossils were sent to the A. E. Lalonde AMS Laboratory, Ottawa. Dates were calibrated using the IntCall13 calibration curve (Reimer et al., 2013). We selected 10 samples for ^{14}C analysis from both P-1 and MB-1, which we used to obtain core chronologies and estimate the age of ecosystem transitions. Basal peat was considered to be the first peat layer with an organic matter content over 75%. Basal peat samples from P-2, YB-1, and MB-2 were ^{14}C dated to assess the variability in age of the basal peat. Visual inspection of the core stratigraphy and paleoenvironment data, including organic matter content and bulk density, allowed us to determine the transition from peat plateau to thermokarst bog, which we used to infer time of thaw. We sampled 1 cm deeper than the identified transition from peat plateau to thermokarst bog in all thermokarst cores for

^{14}C analysis, except in the MB-2 core. The age of the transition from peat plateau to thermokarst bog for the MB-2 core (at 85 cm depth) was estimated by calculating an average peat accumulation rate (0.6302 cm $year^{-1}$), obtained from the post-thaw peat in the IB and MB cores, and applying it to the known depth of the thaw transition in MB-2 (85 cm). Samples of the transition from peat plateau to thermokarst bog for YB-1, YB-2, and IB-2 cores, and above the transition in the MB-2 core, had a fraction modern ($F^{14}C$) > 1 indicating modern carbon, which adds uncertainty to the time of thaw in those locations. For samples with a $F^{14}C$ >1, we obtained calendar ages using http://calib.org/CALIBomb/ (Stuiver et al., 2019) and report the age as the median of the 1-σ probability distribution. Age-depth models were estimated using a Bayesian approach for P-1 and MB-1 with the *Bacon* software (Blaauw and Christen, 2011) in the R computing environment (R Core Team, 2015).

We used Fourier transform infrared (FTIR) spectroscopy and molar C:N ratios from elemental analysis to determine peat humification, i.e. the degree of decomposition of peat. Both have previously been shown to be good proxies for decomposition in peatlands (Biester et al., 2014). We analyzed 30 and 32 samples from MB-1 and P-1, respectively, for FTIR on an Agilent 660 FT-IR spectrometer (Agilent Technologies Inc., Santa Clara, CA, USA). Spectra were recorded in a range of 4000-6500 cm^{-1} (4 cm^{-1} resolution) on KBr pellets (2 mg sample in 200 mg KBr) (Sadoh et al., 2014). After baseline correction, peak height ratios were calculated for absorption at ~1630 cm^{-1} and 1090 cm^{-1} to determine the abundance of aromatic and carboxylate moieties relative to polysaccharides (Artz et al., 2008; Broder et al., 2012). An FTIR ratio of aromatic/polysaccharides based on the peak maxima around those wavenumbers was used as an index of peat humification, where higher values represent a higher degree of humification. C:N ratios in P-1, YB-1, and MB-1 were determined from 15 depths in each core. Total carbon and total nitrogen content, and calculated molar C:N ratios, were determined using a Eurovector EA 3000 Elemental Analyzer (HEKAtech, Wegberg, Germany) from a homogenized sample.

2.2.3 Soil Carbon Measurements and Accumulation

We calculated the C stocks of all cores. To do so, we first measured bulk density (g cm^{-3}) and loss-on-ignition according to Chambers et al., (2011) every 5 – 10 cm from 1 cm^3 peat sections in all eight cores. Samples were oven dried at 100 °C over night and weighed to calculate bulk density. Loss-on-ignition was determined for each sample by placing dried samples in a muffle

furnace at 550°C for 4 hours and weighed once cool to calculate organic matter (OM) content (%). We used the measured bulk density to interpolate between measured depths so that every 1 cm increment of the core had a bulk density value. The mass of organic C of each 1 cm section was calculated by multiplying bulk density by the average C content (45%) and the total mass of organic C of the core was calculated by adding all 1 cm sections for each core.

The long-term rate of carbon accumulation (LORCA; g C m^{-2} yr^{-1}) and apparent carbon accumulation rates (ACAR; g C m^{-2} yr^{-1}) were calculated for all cores. The LORCA was calculated by dividing the C content of the entire core by the basal age of each core. Basal dates used for IB-1, YB-2, and IB-2 are an average of the dated bog core (YB-1, MB-1, and MB-2) basal dates. The ACAR is similar but calculated for different developmental stages. The ACAR was calculated for *Sphagnum* peat that accumulated post-thaw (thermokarst bog stage) and for peat that accumulated during the preceding peat plateau, bog and fen stages based on the C content of that core section and the estimated age of permafrost thaw and the transition from marsh to fen (detailed ^{14}C analysis results are available in the supplementary). Transitions indicating marsh to fen peat transition and permafrost aggradation (bog to peat plateau peat transition) were measured only in P-1 and MB-1; an average of these dates (6901- and 1785-years BP respectively) are used across all cores. We are confident in using these dates as they are similar to previously reported peatland formation (Halsey, Vitt, and Bauer, 1998) and permafrost aggradation (Pelletier et al., 2017) dates for western Canada. The ACAR values are meant to be compared for the same developmental peat stage. Comparing ACARs between different stages can be misleading as older stages have had a longer time to decompose.

More information regarding the C accumulation rate for different developmental stages was obtained by modeling both C inputs and rates of decomposition. To quantify rates of C accumulation, and to determine changes in decomposition following thaw, we used calculated C stores and ^{14}C transition ages of peatland stages along both thaw chronosequences. We assume that the net change in C storage (kg C m^{-2}) over time, as described by the exponential decay model, is governed by annual inputs (I; kg C m^{-2} yr^{-1}), the fractional first-order decomposition constant (k; yr^{-1}), and the C stocks in a given year (C(t)) (Clymo, 1984). The C balance for any given year can then be calculated using the equation

$$dC/dt = I - kC(t). \quad (1)$$

Assuming the initial C concentration begins at zero, solving Equation (1) produces

$$C_{(t)} = \left(\frac{I}{k}\right) \times (1 - e^{-kt}) \quad (2)$$

By fitting Equation (2) to the C stocks and ^{14}C age (cal yr BP) of developmental peat stage transitions we calculated *I* and *k* rate constants from plateau and bog cores for the peat stages identified as the sites developmental history. This allowed us to compare *k* for any developmental peat stage between the bog and peat plateau cores. Increased *k* in the bog core peat stages would be an indication of increased decomposition in those layers post-thaw. Using calculated *I* rate constants we could confirm that modelled annual C inputs (*I*) are similar for peat stages across all cores. This further ensured us that the assumptions of our chronosequence method were being met and that reductions in C stores in the bog cores following thaw are due to increased decomposition (*k*), and not due to reduced inputs.

When calculating *I* and *k*, we combined P-1 and P-2 to represent plateau cores, and YB-1, IB-1, MB-1, YB-2, IB-2 and MB-2 were combined to represent bog cores. When calculating *I* and *k* for peatland stages we combined the bog, fen and marsh (BFM) peat stages for both the plateau and bog cores together. Combining peat cores and combining peat stages was due to a low number ^{14}C peat dates for individual cores which was required to calculate *I* and *k* model parameters. We calculated *I* and *k* for the (a) post-thaw (bog cores only), (b) peat plateau, and (c) bog, fen, and marsh (BFM) peat stages for plateau and bog cores. Greater bog core *k* values than those from the plateau cores in the same peat stages would indicate increased decomposition post-thaw.

To infer potential C loss from pre-thaw peat in the bog locations more accurately, we standardized the C stock in the bog cores relative to the plateau cores. The plateau core locations had longer time to accumulate sylvic peat than the thawed bog cores. Thus, directly comparing the measured stocks of C in the plateau and bog cores that accumulated prior to thaw could overestimate loss. To account for such potential overestimation in C loss, we estimated the additional C stock of sylvic peat that would have potentially accumulated in the bog locations. We did so by fitting Equation (2) with the peat plateau peat stage *I* and *k* rate constants from the plateau cores (Table 2; $I = 49.33$ g C m^{-2} yr^{-1} and $k = 0.0014$ yr^{-1}) and the timing of permafrost thaw from each bog location (Table 2.1). This estimated C stock was then added to the measured

C at each bog core and provided us with a adjusted bog pre-thaw C stock. With this addition, differences in C stocks across the chronosequence could be interpreted as post-thaw losses of pre-thaw peat.

Table 2.1. Carbon stocks, LORCA, and ACAR for plateau and bog cores along both thaw transects. LORCA and ACAR calculated using measured basal ages, post-thaw using thaw transition age, and pre-thaw peatland using an averaged marsh – fen transition date (5901 BP) between P-1 and MB-1 cores as these were the only two cores with this transition dated. Total C is carbon content from entire measured peat profile. Pre-thaw peatland C is carbon content from the fen, bog, and peat plateau peat stages. Post-thaw C is carbon content from peat that accumulated after permafrost thaw

Core	Full profile depth cm	Marsh – Fen depth cm	Post-thaw depth cm	Basal age cal yr BP	Thaw age cal yr BP	Total C kg m^{-2}	Pre-thaw peatland C kg m^{-2}	Post-thaw C kg m^{-2}	LORCA g C m^{-2} yr^{-1}	Pre-thaw peatland g C m^{-2} yr^{-1}	Post-thaw ACAR g C m^{-2} yr^{-1}
P-1	596*	475	NA	8103*	NA	154.9	120.5	NA	19	20.2	NA
P-2	592*	500	NA	8170*	NA	166.9	134.3	NA	20.3	22.5	NA
YB-1	496	403	29	8301	-28	174.2	118.5	2.9	20.8	19.9	78.4
IB-1	513	403	41	NA	76	201.6	116.5	5.4	23.6	19.5	38.3
MB-1	523	425	71	8274	150	201.5	105.9	8.9	24.2	17.8	41.4
YB-2	509	405	22	NA	-33	196.2	126.9	0.7	23	21.3	21.9
IB-2	516	415	44	NA	-20	200.6	119.5	7.2	23.5	20	160
MB-2	530	426	85	8835	70**	201.5	118.5	11.1	22.6	19.9	82.2

* = basal peat not reached, these values indicate deepest depth reached and age at that depth. ** = estimated age of thaw transition based on average.

To test the sensitivity of our chronosequence approach to indicate significant changes of both C that accumulated prior to thaw and net C stocks post-thaw we used a simple linear regression. We calculated the change in (a) C stocks that accumulated prior to thaw (with the additional adjusted C stock that would have accumulated had it never thawed) and (b) measured net C stocks over the time since each site had thawed. In calculating the rate of change in C over time following thaw for (a) and (b) we also determined the 95% confidence intervals (CI) for this regression. The error (95% CI) of our regression represents the range of C that can be either gained or lost each year without representing a significant change and is the sensitivity of our chronosequence approach.

2.2.4 Statistical Analysis

All statistical analysis was carried out in R (Version 3.4.4) (R Core Team, 2015). We used an ANCOVA to determine whether peat age, peat stage, and peat depth were significantly influencing FTIR and C:N ratios. We used two-way ANOVAs and t-test to evaluate differences in FTIR and C:N ratios of peat from peatland stages in P-1, YB-1, and MB-1 cores. We performed linear regressions to test whether there was a significant change in C stocks that accumulated over time following permafrost thaw. These regressions were carried out for C stocks of peat accumulated (a) post-thaw, (b) prior to thaw, and (c) net C stocks. We performed t-tests to evaluate differences in averaged LORCA and ACAR values between permafrost and non-permafrost cores for different peat stages. We used t-tests to test for differences between input (I) and decomposition constants (k) from plateau and bog cores. For all t-tests, the homogeneity of variances was checked using an F test. For ANOVAs distribution of the data was inspected visually and with the Shapiro-Wilk test, the homogeneity of variances was then tested using the Levene test in the car package (Fox and Weisberg, 2011). When appropriate we report average values with ± one standard deviation. We define the statistical significance level at 5%.

2.3 Results

2.3.1 Peatland Developmental History

Macrofossil analysis and radiocarbon dating across all eight cores suggested that the site had a common developmental history with largely synchronous transitions between different peatland stages across all cores up until the recent permafrost thaw. The site initiated as a marsh, then transitioned through fen, bog, and peat plateau stages before permafrost thaw started to affect the site (Fig. 2.2, Fig. 2.3). The ^{14}C age of organic matter increased with depth in all cores. Initiation of organic matter accumulation at the site occurred 8,470 ± 316 (n = 3) cal yr BP (Table 2.1), as indicated by the ^{14}C age of basal peat samples in the thermokarst bog cores. We were unable to reach the underlying silt when coring in the peat plateau (>6 m deep). However, the deepest peat samples from the plateau cores had ages of 8,103 (P-1) and 8,170 (P-2) cal yr BP, which were only ~400 cal yr BP younger than the basal date of the bog cores. Transitions between peatland stages were determined from shifts in macrofossil assemblages and increases in bulk density that signify a shift to drier plateau vegetation and *Sphagnum* spp. (Fig. 2.2). A more detailed paleoenvironmental record is available in Appendix 1 (Fig. A1.1).

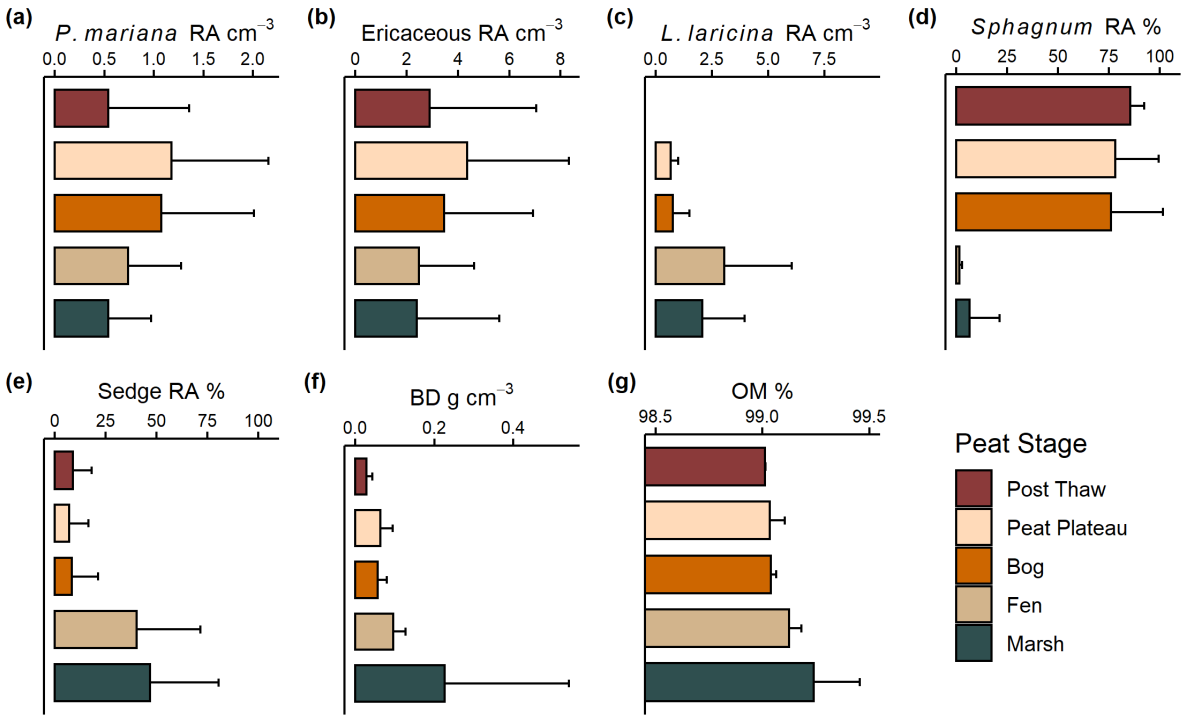

Figure 2.2. Main macrofossil groups (relative abundance; RA), organic matter (%; OM), and bulk density (g cm^{-3}; BD) used to determine transitions between peat stages. (a) – (g) shows averaged data across all eight cores. For detailed information on macrofossil assemblage and OM and bulk density trends with depth in each core see the supplementary. Error bars represent + 1 standard deviation.

The earliest organic matter accumulating stage identified was a marsh stage characterized by abundant sedge remains and high bulk density (Fig. 2.2e, f). The transition to the subsequent fen stage occurred 5901 ± 380 (n = 2) cal yr BP and was indicated by increasing abundance of *Larix laricina* (Fig. 2.2c), decreasing bulk density (Fig. 2.2f), and decreasing brown moss spp. abundance. The transition from fen to ombrotrophic bog was inferred from an increased presence of *Sphagnum* spp. (Fig. 2.2d), *Picea mariana* (Fig. 2.2a), and ericaceous leaves (Fig. 2.2b), as well as a decrease in *Larix laricina* (Fig. 2.2c) and sedge remains (Fig. 2.2e). The age-depth model (available in the Appendix 1, Fig. A1.2) shows this transition occurring 5379 ± 153 (n = 2) cal yr BP. The bog stage was the dominant peat stage of the site's developmental history, with between 2 and 3 m of bog peat in all eight cores.

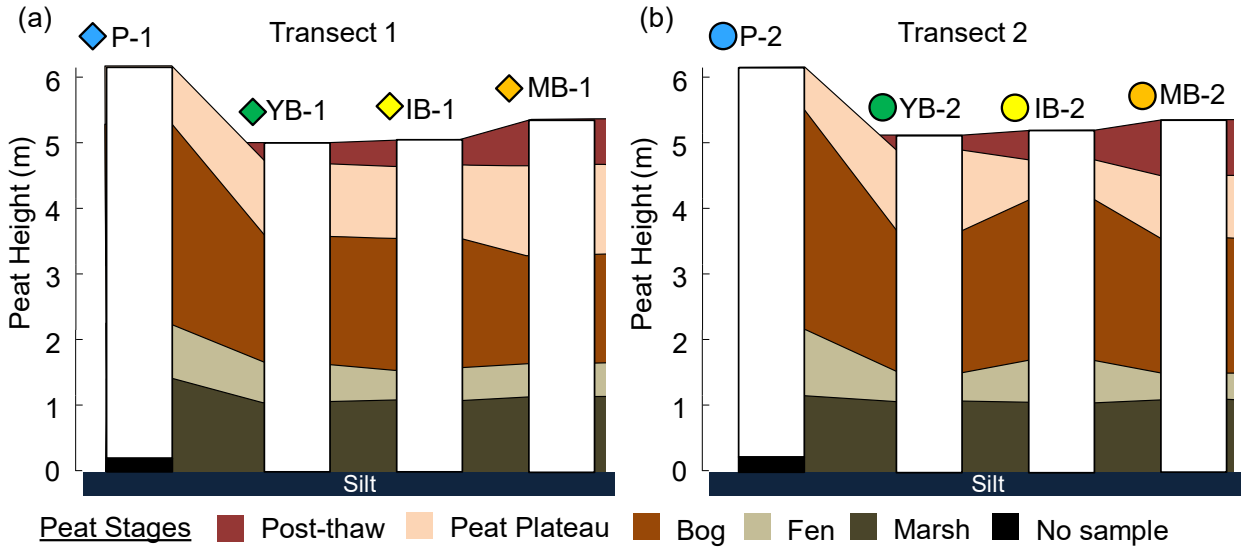

Figure 2.3. Schematic depicting soil profiles established at (a) Transect 1 and (b) Transect 2 based on macrofossil record analysis. The panels show peat accumulated over the various stages that the site has gone through during its developmental history: marsh, fen, bog,

permafrost bog, and post-thaw peat. Each coring location is shown, labelled with the appropriate label, colour, and symbol from Fig. 2.1c, d, with transitions between peatland stages at each coring location to scale. Silt, mineral stage samples of both plateau cores were not collected (No sample), resulting in incomplete cores at these two locations.

Permafrost is interpreted to have aggraded at the site 1785 ± 151 (n = 2) cal yr BP when there was a transition from bog to peat plateau peat. This transition was characterised by an increase in bulk density (Fig. 2.2f), an increase in loss-on-ignition (Fig. A1.1), and the presence of macrofossil indicator taxa indicative of drier conditions such as *Picea mariana* (Fig. 2.2a), *Rhododendron groenlandicum* (Labrador Tea), and other ericaceous rootlets (Fig. 2.2b) (Oksanen, 2006; Sannel and Kuhry, 2008). Permafrost aggradation at this site was thus epigenetic, as most of the currently present peat deposit had already accumulated when permafrost formed. In the peat plateau cores, only the upper ~70 – 90 cm of the total 6 m peat deposit accumulated under permafrost conditions. The dominant macrofossil taxa for much of the peat plateau stage were *Sphagnum*. spp, and ericaceous shrubs such as *Rhododendron groenlandicum*. However, a shift from Sphagnum dominance to rootlet, sylvic peat was observed near the surface in the peat plateau cores. This relative shift towards sylvic peat accumulation occurred 314 ± 19 (n = 1) cal yr BP and was 26 cm beneath the peat surface.

The oldest evidence of permafrost thaw was found in the MB-1 core, where thaw occurred 150 cal yr BP, while in the MB-2 core the thaw transition was dated to 70 cal yr BP. The transition from peat plateau to thermokarst bog stage was clearly visible in the stratigraphy in all thermokarst bog cores, and characterized by a reduction of *Picea mariana* (Fig. 2.2a), *Larix laricina* (Fig. 2.2c) and ericaceous rootlets (Fig. 2.2b), and an increase in wetter macrofossil indicator species such as *Sphagnum* spp. (Fig. 2.2d) and sedges (Fig. 2.2e). Time since permafrost thaw increased in both transects from young to mature bog cores, with thaw having occurred in the YB-1, YB-2 and IB-2 cores after the ^{14}C bomb-peak in the early 1960s (Table 2.1).

2.3.2 Carbon Stocks and Accumulation

The average carbon content of peat was 45 ± 3.6% (n = 45, 15 depths in each P-1, YB-1, and MB-1). Total C stocks among cores varied between 154.9 and 201.6 kg C m^{-2} (Table 2.1). There was no significant difference (p = 0.178, two-sample t-test) between average plateau LORCA (19.6 g C m^{-2} yr^{-1}; n = 2) and average thermokarst bog LORCA (22.9 g C m^{-2} yr^{-1}; n = 6) (Table 2.1). Direct comparisons of total C stocks and LORCA along the thaw transects were however not appropriate since we could not reach the basal peat in the plateau cores. Although the deepest ^{14}C dates from the peat plateau cores were only slightly younger than the basal dates of the bog cores (8137 vs 8470 cal yr BP on average, respectively), this may significantly have influenced the total carbon storage due to the very high bulk density in the basal peat of the bog cores (Fig. 2.2d).

Carbon stocks above the peat plateau – thermokarst bog transition (post-thaw C) increased from the young (YB) to mature (MB) thermokarst bog cores in both transects (Fig. 2.4a). Post-thaw ACAR averaged 70.3 g C m^{-2} yr^{-1} and varied between 21.9 and 160 g C m^{-2} yr^{-1}. The post-thaw ACAR was generally higher in the early stages of thaw (YB and IB) cores but there was no trend (R^2 = 0.12, p = 0.51) across the chronosequence (Table 2.1).

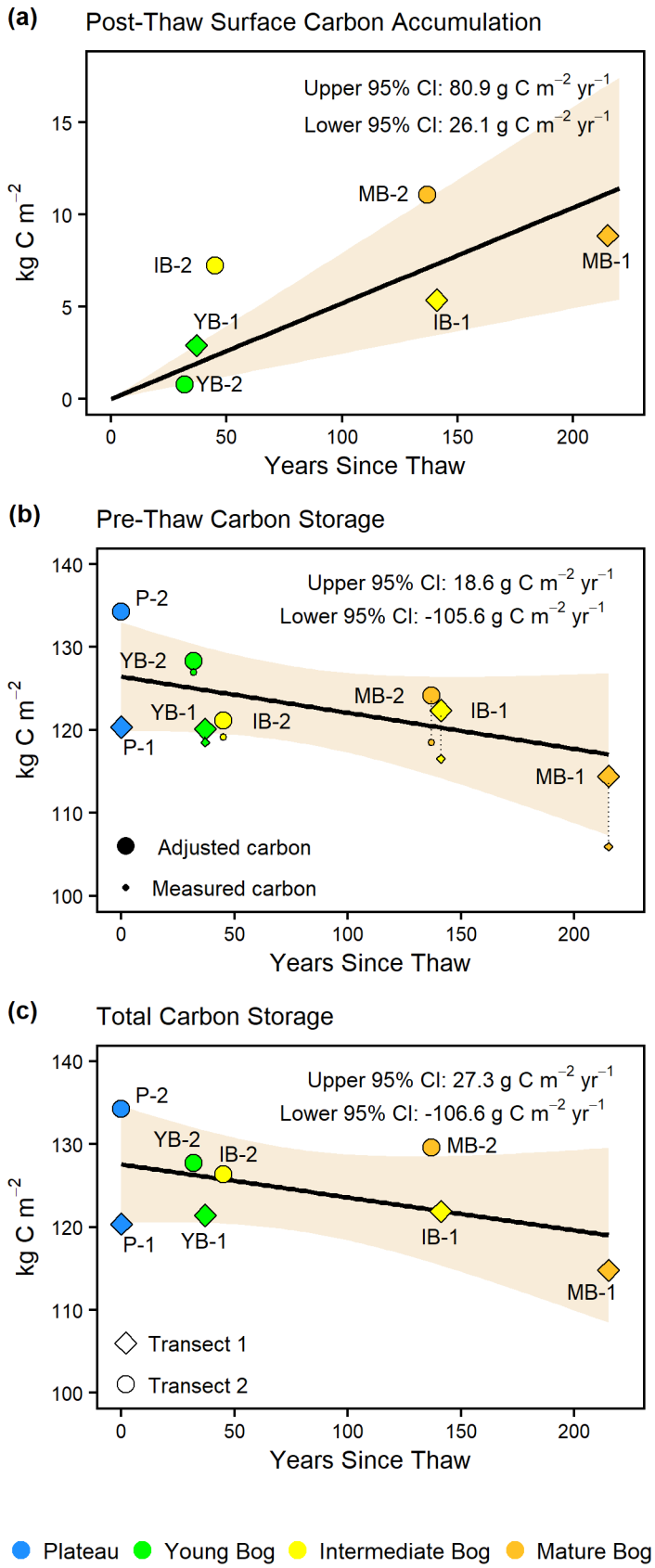
(a)
Post-Thaw Surface Carbon Accumulation
Upper 95% CI: 80.9 g C m^{-2} yr^{-1}
Lower 95% CI: 26.1 g C m^{-2} yr^{-1}
MB-2
IB-2
MB-1
YB-1
IB-1
YB-2
kg C m^{-2}
Years Since Thaw
(b)
Pre-Thaw Carbon Storage
Upper 95% CI: 18.6 g C m^{-2} yr^{-1}
Lower 95% CI: -105.6 g C m^{-2} yr^{-1}
P-2
YB-2
MB-2
IB-1
YB-1
IB-2
P-1
MB-1
Adjusted carbon
Measured carbon
kg C m^{-2}
Years Since Thaw
(c)
Total Carbon Storage
Upper 95% CI: 27.3 g C m^{-2} yr^{-1}
Lower 95% CI: -106.6 g C m^{-2} yr^{-1}
P-2
YB-2
IB-2
MB-2
P-1
YB-1
IB-1
MB-1
Transect 1
Transect 2
kg C m^{-2}
Years Since Thaw
Plateau
Young Bog
Intermediate Bog
Mature Bog

Figure 2.4. Carbon stocks at each coring location along both thaw chronosequences, for different peat stages. (a) Carbon in new, post-thaw peat which accumulated at the surface following permafrost thaw. (b) Carbon that accumulated prior to permafrost thaw (old carbon). Small icons represent measured pre-thaw C stocks. Large icons represent adjusted C stock that allow for an assessment of losses of pre-thaw C stocks following thaw, by adding pre-thaw carbon that would have accumulated in the absence of permafrost thaw. This adjusted C was calculated using *I* and *k* values (Table 2; 49.33 g C m^{-2} yr^{-1} and 0.0014 yr^{-1} respectively) for the peat plateau stage from the plateau cores, and thaw age (Table 2.1). (c) Total stocks of measured carbon. Regression lines represent the change in C over time and the dark area on each graph represent 95% confidence intervals. Text in graphs a - c indicate the 95% CI of the regressions, expressed as annual change in total C storage over 200 years following thaw. Diamond symbols represent Transect 1. Circular symbols represent Transect 2. Blue = Plateau cores. Green = Young bog cores. Yellow = Intermediate bog cores. Orange = Mature bog cores. Panels (b) and (c) exclude C stocks of the marsh stage from all cores.

Carbon stocks between the marsh – fen transition and the top of the peat plateau stage varied between 105.9 and 126.9 kg m^{-2} (Table 2.1; Pre-thaw peatland C) and decreased along both transects from the plateau cores (average 127.4 kg C m^{-2}) to the mature thermokarst bog cores (average 112.2 kg C m^{-2}) (Fig. 2.4b). The linear relationship between the pre-thaw C stocks and the time since permafrost thaw was significant ($R^2 = 0.64$, $p < 0.05$; Fig. 2.4b), suggesting that 8.7 ± 12.4 kg C m^{-2} was lost over the first 200 years post-thaw. Measured C stocks for a mature bog core that has been thawed for 200 years was thus 13.1% lower (16.7 kg m^{-2} less) than found in a peat plateau core. Similarly, ACAR of the pre-thaw C decreased along the transects from the plateau cores to the mature thermokarst bog cores (averages 21.4 vs 18.9 g C m^{-2} yr^{-1}, respectively).

This significant decline in pre-thaw C stocks following thaw was likely not entirely due to decomposition and C mineralization following thaw, but can also be a result of thermokarst bogs having a shorter time to accumulate pre-thaw C. We adjusted the pre-thaw C stores for the thermokarst bogs by adding the estimated amount of pre-thaw soil C which would have accumulated if the site had not thawed, thus allowing us to isolate the effect of post-thaw peat mineralization on soil C stocks that accumulated prior to permafrost thaw. Using *I* and *k* values

for peat plateau stage (see below) along with the time since thaw in Equation 2, we thus added between 1.4 and 8.5 kg C to the adjusted pre-thaw soil C stocks for a comparison that isolates the effect of permafrost thaw on soil stocks. Despite this adjustment of soil C stocks, there was still a decrease in adjusted pre-thaw soil C along the chronosequences which thus needs to be interpreted as being due to post-thaw decomposition of pre-thaw C. However, this decrease in adjusted pre-thaw C was not statistically significant ($R^2 = 0.33$, $p < 0.137$; Fig. 2.4b), with 95% CI between +18.6 and -105.6 g C m^{-2} yr^{-1} (Fig. 2.4b). This suggests that while C stocks for a mature bog core that has been thawed for 200 years are 6.8% lower (8.7 kg m^{-2} less) than found in a peat plateau core, our approach could not detect a significant overall change in C stocks.

An unbiased comparison of peat C stocks along the thaw transects could be done when only considering peat above the marsh – fen transition, a transition which was clearly identified in all cores. Cores taken at the peat plateau sites did not reach the silt, mineral layer and thus had less marsh peat than found in the bog cores. The total C stocks above the marsh – fen transition varied between 114.8 and 129.6 kg C m^{-2} among all six bog cores (Table 2.1; Pre-thaw peatland C plus Post-thaw C). The plateau core C stocks above the marsh – fen transitions were 120.5 and 134.3 kg C m^{-2}. The average peat plateau C stocks above the marsh – fen transition was thus higher, but not significantly higher, than that of the averaged thermokarst bog cores (127.4 vs 123.6 kg C m^{-2}, respectively; $p = 0.55$ two-sample t-test). The linear relationship between C stocks above the marsh – fen transition and the time since thaw (0 years for peat plateau cores) was non-significant ($R^2 = 0.26$, $p = 0.20$; Fig. 2.4c). Similarly, ACAR between the fen-marsh transitions and the top of the cores were non-significantly higher in the peat plateau cores than the thermokarst bog cores (21.4 vs 20.7 g C m^{-2} yr^{-1}, respectively).

2.3.3 Sensitivity of the Chronosequence Approach

We tested the ability of our chronosequence approach to detect a significant change in C stocks using a linear regression of the change in C stocks (Table 2.1) over time since thaw. We determined that the decline in pre-thaw C stocks, that had been adjusted to not overestimate loss, was not a significant reduction (Fig. 2.4b). The average rate of loss of adjusted pre-thaw C was -43.5 g C m^{-2} yr^{-1} over 200 years. The uncertainty of the regressions (95% CI) constrains the carbon balance of pre-thaw peat following thaw to be between a loss of 105.6 and a gain of 18.6 g C m^{-2} yr^{-1}.

Similarly, using a linear regression we determined that the average rate of net C loss, a -39.7 g C m^{-2} yr^{-1} decline in our net C stocks over ~200 years, was not a significant change (Fig. 2.4c). To detect either a net gain or net loss of C using our approach the rate of change must lie outside the 95% CI range of -106.6 – +27.3 g C m^{-2} yr^{-1} (Fig. 2.4c). Thus, either a minimum 4.3% (5.5 kg C m^{-2}) net gain or 16.8% (21.3 kg C m^{-2}) net loss of C is required to significantly detect changes in C stocks using our chronosequence approach.

2.3.4 Modelling C Accumulation

Estimates of *k* (decomposition constant; yr^{-1}) and organic C accumulation, *I* (inputs; g C m^{-2} yr^{-1}), calculated using Eqn. 2, for corresponding peat stages did not vary between the plateau and bog cores (Table 2.2; Fig. 2.5). Calculated *k* values for the peat plateau peat stages in the bog cores (0.0009 yr^{-1}) were not significantly different (p = 0.713, two-sample t-test) from those calculated from plateau cores (0.0014 yr^{-1}) (Table 2.2; Fig. 2.5). The calculated annual C inputs (*I*; Table 2.2) for plateau and bog cores (44.09 and 49.33 g C m^{-2} yr^{-1} respectively) did not differ either (p = 0.64 two-sample t-test).

Table 2.2. Summary of peat carbon accumulation parameters (*I* = input rate; *k* = decomposition constant) calculated from Eqn. 2 (Fig. 2.5) using measured ^{14}C age (years) (available in Appendix 1, Table A1.1) of peat samples and the carbon content. Values in parentheses represent 95% confidence intervals of calculated *I* and *k* values.

Core	Peat Stages	*I*; g C m^{-2} yr^{-1}	*k*; yr^{-1}
Bog	Post-thaw	82.99 (33.57 – 157.67)	0.0049 (-0.0037 – 0.0135)
	Peat Plateau	44.09 (34.01 – 55.35)	0.0009 (0.0005 – 0.0013)
	Bog, Fen, and Marsh	40.41 (36.12 – 44.93)	0.0002 (0.0001 – 0.0002)
Plateau	Peat Plateau	49.33 (4.64 – 128.25)	0.0014 (-0.001 – 0.004)
	Bog, Fen, and Marsh	37.73 ± (30.55 – 45.66)	0.0002 (0.0001 – 0.0002)

The calculated *k* for the bog, fen, and marsh (BFM) peat stages were also not significantly different (p = 0.89, two-sample t-test) between bog (Fig. 2.5c) and plateau (Fig. 2.5e) cores at 0.0002 yr^{-1} in both. Similarly, there was no significant difference (between calculated *I* values (Table 2.2) for the bog (40.41 g C m^{-2} yr^{-1}) and plateau cores at 40.41 and 37.73 g C m^{-2} yr^{-1} respectively (p = 0.30, two-sample t-test).

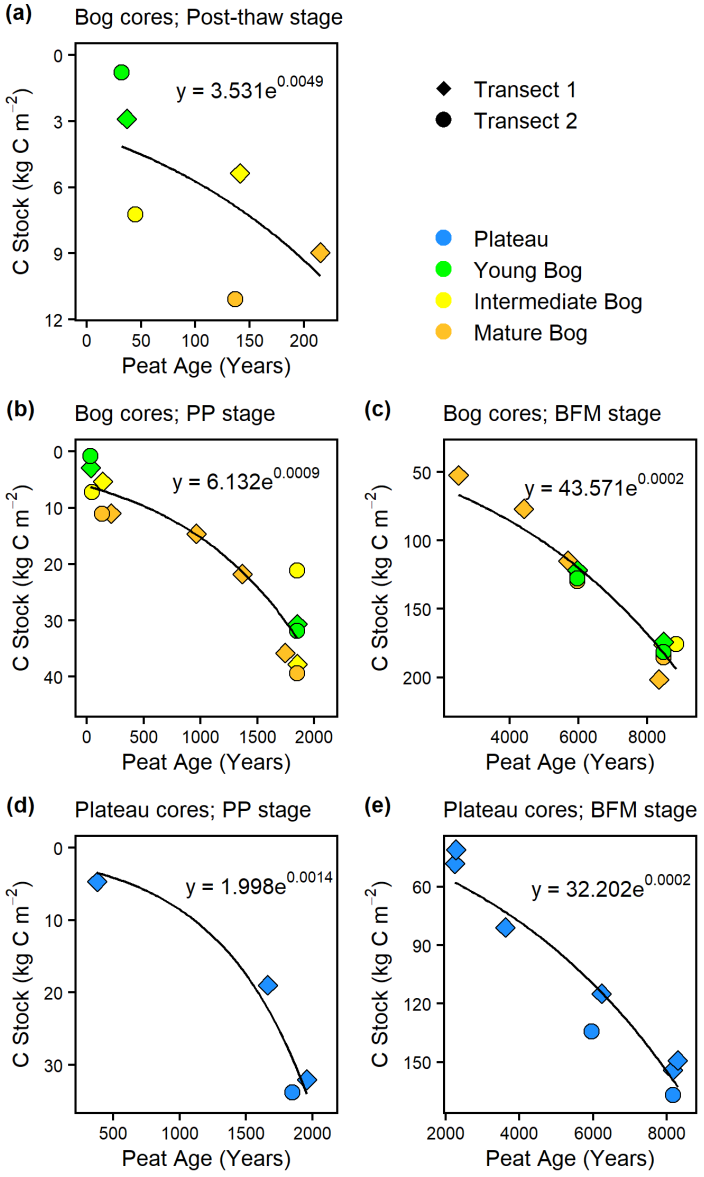

Figure 2.5. Increase in cumulative carbon stocks over time for the (a) post-thaw, (b) peat plateau (PP), and (c) bog, fen and marsh (BFM) peat stages in all bog cores, and for the (d)

peat plateau, and (e) bog, fen and marsh peat stages in the two plateau cores. Calculated using measured carbon stocks and ^{14}C age (years) of peat. Diamond symbols represent Transect 1. Circular symbols represent Transect 2. Blue = plateau core. Green = young bog core. Orange = intermediate bog core. Orange = mature bog core.

2.3.5 Peat Quality

Peat humification indices (FTIR and C:N ratios) increased with depth similarly across the P-1, YB-1 and MB-1 cores (Fig. 2.6). Comparing peat of the same stage and age between P-1, YB-1 and MB-1 cores indicate that up to ~200 years of thaw had no significant impact on its degree of humification, as indicated by the FTIR and C:N ratios (Fig. 2.6).

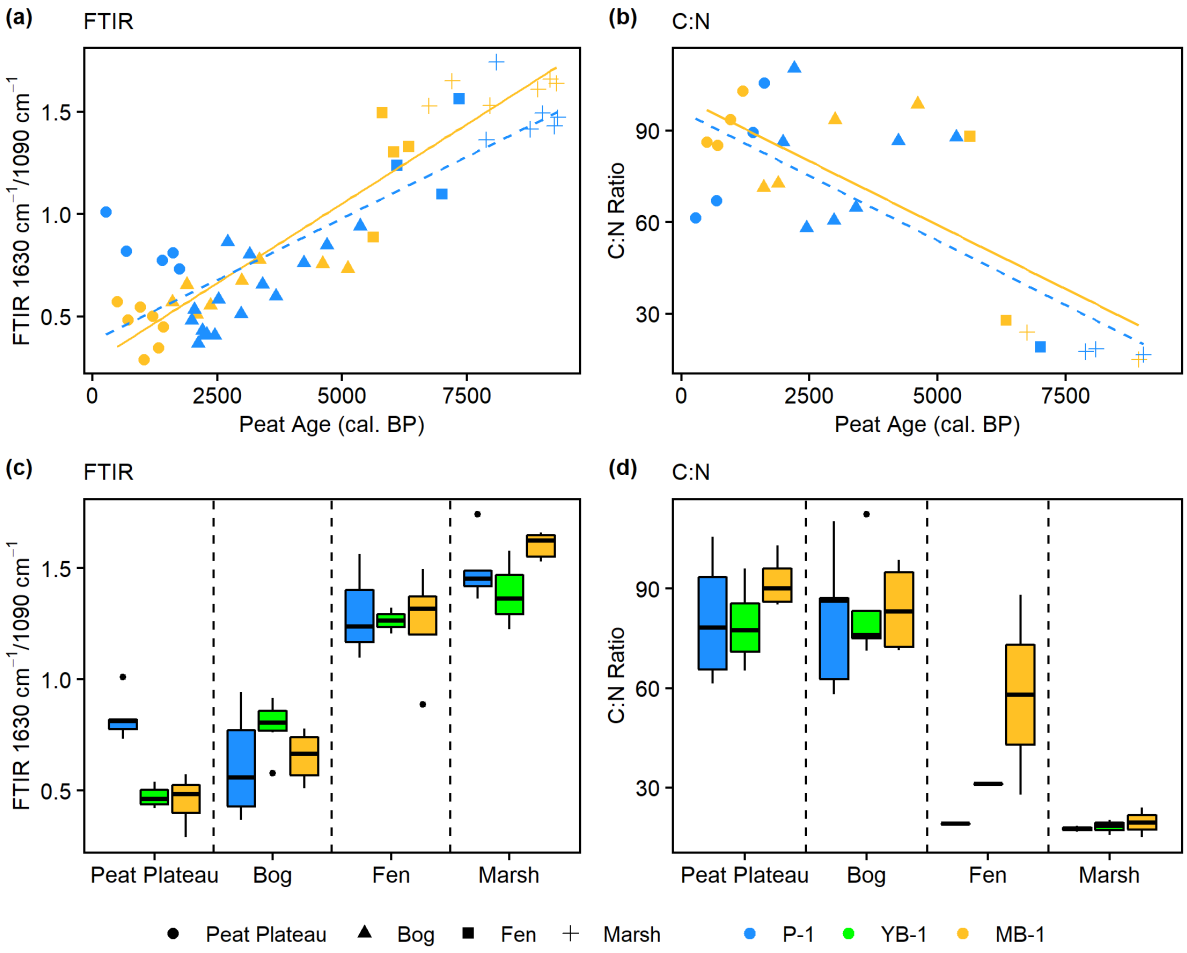

Figure 2.6. Peat humification indices from different peat stages found in each of the P-1, YB-1, and MB-1 cores. Increases in humification indices with peat age (cal BP) calculated using

Bacon model (available in the supplementary) for different peat stages from MB-1 (yellow) and P-1 (blue) cores. (a) FTIR (1630 cm^{-1}/1090 cm^{-1}) ratios are not significantly different between P-1 and MB-1 cores across peat stages after controlling for age (ANCOVA; $F_{(5, 49)} = 64.94$, $p = 0.644$). (b) C:N ratios decrease across peat stages but there is no significant difference between P-1 and MB-1 cores (ANCOVA; $F_{(5, 21)} = 12.31$, $p = 0.137$) after controlling for age. Dashed blue lines in (a) and (b) represent change in FTIR and C:N ratios over peat age in the P-1 core. Solid golden lines in (a) and (b) represent change in FTIR and C:N ratios over peat age in the MB-1 core. (c) FTIR (1630 cm^{-1}/1090 cm^{-1}) values for each peat stage across all 3 cores. No significant difference in FTIR ratios between cores (Two-way ANOVA; $F_{(2, 66)} = 0.694$, $p = 0.503$) but there is between peat stages (Two-way ANOVA; $F_{(3, 66)} = 113.26$, $p < 0.001$). (d) C:N ratios for each peat stage across all 3 cores. No significant difference in C:N ratios across all 3 cores (Two-way ANOVA; $F_{(2, 34)} = 1.18$, $p = 0.319$) but there is between peat stages (Two-way ANOVA; $F_{(3, 34)} = 37.77$, $p < 0.001$).

The increase in peat humification with age was determined for MB-1 and P-1 by plotting FTIR and C:N ratios at each sampled depth against the age of that peat depth as calculated by the *Bacon* age-depth model (Blaauw and Christen, 2011). FTIR ratios were not significantly different between P-1 and MB-1 cores across peat stages after controlling for age (ANCOVA; $F_{(5, 49)} = 64.94$, $p = 0.64$). (Fig. 2.6a). FTIR ratios were slightly higher for peat of the same age in MB-1 except for peat from the peat plateau stage in P-1. Peat humification increased with peat age through all peat stages similarly in both P-1 and MB-1 cores.

The C:N ratios results from the bog and fen stages were combined when comparing between stages and cores due to low sample numbers from the fen stage. C:N ratios decreased with age across peat stages but there was no significant difference between P-1 and MB-1 cores (ANCOVA; $F_{(5, 21)} = 12.31$, $p = 0.14$) after controlling for age (Fig. 2.6b).

The degree of humification of peat from similar peat stages did not differ across the P-1, YB-1 and MB-1 cores. A two-way ANOVA was run to examine the effect of core and peat stage on FTIR and C:N ratios. There was a significant interaction between the effects of core and peat stage on FTIR ratios ($F_{(6, 60)} = 5.84$, $p < 0.001$). Peat stage had a significant effect on FTIR ratios ($p < 0.001$), but there was no difference in FTIR ratios between cores ($p = 0.37$). There was no significant interaction between the effects of core and peat stage on C:N ratios ($F_{(6, 28)} = 0.536$, p

= 0.78) across the P-1, YB-1 and MB-1 cores. However, C:N ratios were different for different peat stages ($p < 0.001$) across the three cores.

2.4 Discussion

By analyzing peat cores collected along two peatland thaw chronosequences, we have been able to constrain the post-thaw C balance to preclude both rapid net C losses and gains over the first 200 years following permafrost thaw. The overall neutral net C balance following thaw found at our site is in contrast to sites in Alaska where large net C losses have been suggested (O'Donnell et al., 2012; Jones et al., 2017), but also contrasts to studies that have suggested rapid C gains, but which only considered change in C stocks near the peat surface, (Camill, 1999; Robinson and Moore, 2000). Our results of 6.8 ± 9.8% (95% CI) losses of deep, pre-thaw C over 200 years following permafrost thaw were largely offset by accumulation of new surface peat. Peat decomposition rate constants (k) were not higher in thermokarst bogs which had been thawed for decades to centuries, which suggested similar decomposition for similar peat stages along the chronosequence. FTIR and C:N ratios show an increase in peat humification with peat age and depth, but there was no evidence of significant increases in peat humification 200 years after thaw. This study highlights the spatial heterogeneity of the response of boreal peatland C to permafrost thaw and suggests that sites with epigenetic permafrost i.e. majority of peat deposit present when permafrost forms, may not experience large net changes of C stores following thaw.

2.4.1 Validity of the Chronosequence Approach

Previous studies have shown how fine-scale spatially heterogeneity of peatland microtopography, vegetation communities, and surface moisture content can lead to spatial variability of C accumulation in individual boreal peatlands, sometimes by up to 100% (Chaudhary et al., 2018; Waddington and Roulet 2000; Weltzin et al., 2001). Considering how dynamic permafrost and developmental history can be at a single peatland and the spatial heterogeneity in C accumulation due to this (Pelletier et al., 2017), meeting the assumptions of the chronosequence approach is required in order to assess the impact of thaw on C storage.

These assumptions can be satisfied if all locations within the peatland transitioned concurrently between peatland stages up until the most recent permafrost thaw.

Careful consideration of the plant macrofossil record, ^{14}C dating of transitions, and peat organic matter characterization were crucial to ensure that the study site had gone through the same developmental history (Fig. 2.3), and thus that the assumptions of the chronosequence are met. Spatial heterogeneity in vegetation, ice content, active layer depth, nutrient levels, hydrology, and soil temperatures can affect plateau C accumulation rates at small spatial scales (Loisel et al., 2014), and could likely explain the 10% difference between our plateau C stocks (Table 2.1; Fig. 2.4b, c). Combining C stock measurements with comparisons of LORCA and ACAR following thaw reduced uncertainty in assessing post-thaw C storage. The lack of ^{14}C-dated transitions, and use of assumed dates, introduces uncertainty into these rates. However, the similarities in site history (Fig. 2.3), along with similar dates previously reported for peatland formation and permafrost aggradation in western Canada (Zoltai, 1995; Sannel and Kuhry, 2008; Pelletier et al., 2017), bolsters our comparison of C stocks along the chronosequence. While spatial variability complicates the detection of net C gains or losses, we estimated that using our study design of 8 collected cores the change in C stocks required to infer net C gains or losses, should exceed -16.6% for pre-thaw C loss (Fig. 2.4b) and -16.8 – +4.3% for net C stock (Fig. 2.4c) over 200 years following thaw.

2.4.2 Stability of Old Carbon Following Thaw

In this study we assessed the stability of old C following thaw using three lines of evidence: the first was with measured carbon stocks, the second by modelling C accumulation and decay constants, and the third by assessing whether peat humification indices (FTIR and C:N ratio) indicated substantial degradation of peat 200 years post-thaw. All three approaches found a statistically non-significant loss of C stocks and non-significantly increased degradation of peat that accumulated prior to permafrost thaw. We did not detect any significant difference in peat humification or in decay constants (k) between similar peat stages of plateau and mature bog locations (Fig. 2.6 and Fig. 2.5 respectively). This suggests that while thaw resulted in non-significant losses of pre-thaw C, this degradation of pre-thaw peat may be too small to be detected clearly with k values and humification indices.

Our measurements indicate that adjusted pre-thaw C stocks were on 6.8 ± 9.8% (95% CI) lower (8.7 ± 12.4 kg C m^{-2}; 95% CI) in the bog over the first 200 years following thaw compared to the plateau (Fig. 2.4b), which could be attributed to microbial decomposition (Schuur et al., 2015). This implies an average rate of loss of 43.5 g C m^{-2} yr^{-1} over the 200 years. This 6.8% indicated loss of pre-thaw C post-thaw suggests that decomposition of pre-thaw peat following thaw at the site is slow compared to other thawing permafrost peatlands, where 30% losses have been indicated (O'Donnell et al., 2012; Jones et al., 2017). These suggested 30% losses represent an average rate of 305 g C m^{-2} yr^{-1} (Jones et al., 2017) decline in net C stocks over ~200 years post-thaw, such a rate of C loss is three times greater than even or most liberal estimates. While there are differences in study design, this may be due to the epigenetic formation of permafrost at our study site and that a significant proportion of peat that accumulated prior to thaw is recalcitrant upon thawing as it has already undergone millennia of anaerobic decomposition (Beer et al., 2008; Zoltai, 1993). Areas where soil C accumulated syngenetically with permafrost have more labile C available to microbial decomposition and are more at risk of experiencing large loss of C post-thaw (Heslop et al., 2019; Knoblauch et al., 2013; Strauss et al., 2015). We observed non-significant losses of C which were smaller than those reported from similar sites (O'Donnell et al., 2012; Jones et al., 2017) and we were unable to detect any significant increase to peat humification. This finding highlights the potential importance of site permafrost history when considering potential losses of C following thaw and agrees with the observation of limited C release from recalcitrant catotelm peat in a non-permafrost boreal peatland exposed to *in situ* warming (Wilson et al., 2016).

Our findings of small pre-thaw C losses following thaw are complimented by previous work at the study site where the contribution of aged soil C to late-season soil respiration could not be detected using $^{14}CO_2$ measurements in the thermokarst bog locations YB-1 and MB-1 (Estop-Aragonés, Czimczik, et al., 2018). It is possible that the losses indicated in our study may have been too small to be identified using $^{14}CO_2$ measurements. Also, a significant proportion of C may be released as CH_4 (Wickland et al., 2006; Johnston et al., 2014) or lost as dissolved organic carbon (DOC) following thaw, which may be pathways for old C loss not previously measured at the site. This is important with regards to the permafrost C climate feedback as increased CH_4 emissions from northern peatlands can lead to increased net radiative forcing (Frolking et al., 2006) and the lateral flux of highly labile permafrost DOC can lead to enhanced microbial

respiration and C release to the atmosphere (Liu et al., 2019). However, studies from similar sites suggest limited contribution of aged soil C released as CH_4 (Klapstein et al., 2014; Cooper et al., 2017). Our estimated average loss of 43.5 g C m^{-2} yr^{-1} is greater than estimated CH_4 emissions (~30 g C m^{-2} yr^{-1}) from all thermokarst landscapes that thawed <100 years ago (Olefeldt et al., 2013). As such, increased losses due to CH_4 while important for greenhouse gas budgets are likely not the sole driver of pre-thaw C losses. The export of DOC may be an important pathway of old C loss, particularly in the YB as it receives water from the plateau and acts as a channel for runoff to adjacent fens (Quinton et al., 2003). However, many thermokarst bogs in boreal western Canada are isolated, and thus have no means for DOC export (Quinton, Hayashi, and Chasmer, 2009).

The *k* decomposition constants we calculated for C accumulation are similar to previously reported values for different peat types for both permafrost and non-permafrost peatlands and show no evidence of change following thaw. This indicates that there is not a statistically significant increase to decomposition of old peat from any peat stage following thaw. The calculated *k* values for the peat plateau stage in both plateau and bog cores are consistent with the higher decomposition of peat seen in drier peatland forests ($k = 0.019$) (Trumbore and Harden, 1997). The calculated *k* values from the BFM peat stages of both the plateau and bog cores (Fig. 2.3) are consistent with previously reported *k* values ($k = 0.0005 – 0.0009$ yr^{-1}) from deep organic layers in *Sphagnum* dominated ombrotrophic bogs (Trumbore and Harden, 1997). The high *k* values for post-thaw peat stages are similar to previously reported *k* values of thermokarst bogs ($k = 0.045$ yr^{-1}) (Trumbore and Harden, 1997) and fresh plant litter ($k = 0.02 – 0.14$ yr^{-1}) (Moore et al., 2007). Our calculated *k* model parameters are similar across plateau and bog cores. The long-term decomposition constant (*k*) for peat plateau and BFM peat stages were not significantly different between plateau and bog cores (Table 2.2; Fig. 2.5). In both plateau and bog cores, the *k* value calculated for the peat plateau peat stage was greater than that calculated for BFM peat stages. This increase in peat humification is likely due to aerobic respiration and increased C mineralization of this peat in the active layer during the peat plateau peat stage (Turetsky et al., 2007).

Our results from FTIR analysis and C:N ratios also do not indicate a detectable increase in humification and thus, enhanced decomposition of peat after 200 years of thaw. Peat

humification increased with peat age and depth similarly across all peat stages and cores, but we did not find a significant difference in humification between similarly aged peat of the plateau and mature bog cores. However, there was a slightly, not significantly, higher humification in the BFM peat stages of MB-1 (Fig. 2.6a, c). While not significantly greater, these higher humification values in MB-1 indicate increased degradation of pre-thaw peat following 200 years of thaw, which may account for our indicated non-significant loss of old C (Fig. 2.4b). However, we cannot exclude that these differences arose due to heterogeneity in hydrology, nutrients, or temperature (Loisel et al., 2014; Broder et al., 2012). The age-depth and humification analysis of multiple cores would be required to conclusively attribute an increase of humification to increased decomposition following thaw.

A decrease in C:N ratios also indicates increased decomposition (Kuhry and Vitt, 1996). The similarity in C:N ratios for peat stages in the P-1, YB-1 and MB-1 cores suggests that this proxy cannot detect increased peat decomposition following thaw. C:N ratios are initially high in all cores, decrease with depth, and are lowest in the marsh stage. This pattern of peat decomposition increasing with depth is seen in most non-permafrost northern bogs (Wang et al., 2014). C:N ratios from peat plateau and BFM peat stages fall within range of reported C:N ratios for boreal ombrotrophic bogs (Szumigalski and Bayley, 1996; Loisel et al., 2014). This suggests that there has been little impact from permafrost aggradation and degradation on C:N ratios at the site, likely due to the epigenetic formation of permafrost and peat properties prior to permafrost aggradation (Treat et al., 2016, 2014).

The sensitivity of FTIR analysis and C:N ratios, as a proxy for decomposition, may not be able to detect the increases to decomposition that lead to C losses following thaw at the timescale of the study site. Peat humification indices, such as FTIR analysis and C:N ratios, are typically related to changes in environmental conditions and their impact on decomposition processes in the upper, more dynamic, fresh peat layers (Borgmark and Schoning, 2006; Kuhry and Vitt, 1996). However, the combination of both does provide a powerful tool for our approach. Peat from depth found across the chronosequence accumulated under the same conditions and was recalcitrant prior to permafrost aggradation. Even with increased decomposition at depth, the large changes to peat humification post-thaw necessary to be detected by FTIR analysis and C:N ratios were unlikely. Most of the peat profile accumulated under ombrotrophic bog conditions

and once it thaws it returned to similar conditions, with little impact on decomposition and peat humification at depth.

2.4.3 Net Carbon Balance Post-Thaw

Using our chronosequence approach we were unable to identify any significant loss or gain of C following thaw and net C stores remained relatively unchanged (Fig. 2.4c). This study highlights that net losses of C from thawing boreal peatlands where permafrost has formed epigenetically may not be as large as those indicated from sites where permafrost aggraded syngenetically (O'Donnell et al., 2012; Jones et al., 2017) and that C gains post-thaw at these sites (Robinson and Moore, 2000; Turetsky et al., 2000) can compensate for losses.

Post-thaw accumulation in thermokarst bog cores was greatest in the initial decades following thaw, which agrees with previously reported values (Camill, 1999) and this accumulation slows with increased time-since-thaw as has also been previously reported (Turetsky et al., 2007) (Fig. 2.4a). Overall, we found no significant change in net C balance over the first 200 years post-thaw (Fig. 2.4c) due to gains of new surface peat compensating the losses of old C (Fig. 2.4b).

Our long-term C accumulation rates (LORCA) are consistent with peatlands in western Canada and the average rates of northern peatlands over the Holocene (Pelletier et al., 2017; Loisel et al., 2014). Our LORCA remained similar following permafrost thaw, suggesting that the thermokarst sites are similar to non-permafrost northern peatlands (Clymo, 1984; Trumbore and Harden, 1997; Roulet et al., 2007). However, we find that over the first 200 years following permafrost thaw the average net C balance is unchanged. This suggests that over this time the C sink potential may be reduced from a weak sink to neutral. The LORCA and ACAR for plateau and thermokarst bog cores are similar (Table 2.1), suggesting permafrost aggradation and degradation had limited impact on long-term C accumulation. This may be due to permafrost aggrading epigenetically, not syngenetically, which results in less labile organic matter available for microbial decomposition upon thawing. Other thermokarst landscapes, including bogs and lakes, experience large losses of old C following thaw (Jones et al., 2017; Walter Anthony et al., 2018) and represent a net loss of permafrost C to the atmosphere. Our results here highlight that in order to improve permafrost C feedback modelling there needs to be a better understanding of what drives old C losses following thaw and thermokarst formation.

2.5 Conclusions

This study supports the use of the chronosequence approach to study the long-term impact of permafrost thaw on peatland C stores, once a set of assumptions for each site with regards to its developmental history are validated. Using this approach, we ruled out any change in net C stores representing losses greater than 106.6 g C m^{-2} yr^{-1} or gains of 27.3 g C m^{-2} yr^{-1} over the first 200 years following thaw at a site with an epigenetic permafrost history. We did not find any evidence of permafrost thaw having a detectable impact on peat humification indices. While we estimated that 200 years following thaw results in an average loss of 6.8% (8.7 kg C m^{-2}) of the pre-thaw C store, these losses were compensated by the accumulation of new C. Our results differ from previous studies using similar approaches where 30% of the original pre-thaw C stores was reported to be lost post-thaw (O'Donnell et al., 2012; Jones et al., 2017). Differences in site history and the aggradation of epigenetic vs. syngenetic in boreal peatlands may influence the rates of C loss following thaw in these ecosystems and partially explain such discrepancies. Future work should include more well dated chronosequence studies that directly compare sites at the regional scale with similar environmental conditions but with differing developmental and permafrost histories and other approaches that provide synergistic information such as peat incubation studies or microbial community composition and activity analysis. In conclusion, our study shows that losses of old, previously frozen C stores from thawing boreal peatlands may not be as substantial as previously thought and proposes that differences in permafrost history determine peat properties, which may be important factors controlling the magnitude of C loss following thaw.

3. Asynchronous interannual variability of the greenhouse gas exchange of young and mature thermokarst bogs due to differences in dominant environmental controls

Abstract

Peatlands in permafrost regions have acted as long-term net sinks of atmospheric carbon (C) and store a significant proportion of global soil C. Recent warming is accelerating permafrost thaw in peatlands, leading to thermokarst collapse and the potential mineralization of previously frozen C into greenhouse gases. Here we show that following permafrost thaw, thermokarst bogs in the sporadic-discontinuous permafrost zone of western Canada are unlikely to act as a large net source of atmospheric C. Over three years we monitored greenhouse gas exchange (CO_2 and CH_4), and environmental variables from young (~30 years) and mature (~200 years) thermokarst bog locations along thaw chronosequences. We find that the functional relationship and controls of CO_2 and CH_4 fluxes differ between young and mature bog stages, which results in asynchronous cumulative annual C fluxes. The annual net C balance in the young bog is governed by the sensitivity of fluxes, particularly gross primary production, to variability in the water table. Whereas the net C balance in the mature bog is sensitive to variability in shallow depth soil temperatures and the response of ecosystem respiration. Due to the interannual variability of environmental drivers, and the sensitivity of net annual C fluxes to these drivers, our approach can not determine whether the long-term net ecosystem carbon flux differs between young and mature bog stages. However, it does highlight that recently thawed thermokarst bogs in our study region are unlikely to represent a period of rapid net losses of C to the atmosphere.

3.1 Introduction

High latitude peatland ecosystems have acted as a long-term sink of atmospheric carbon (C) since the end of the last glaciation (Gallego-Sala et al., 2018; Treat and Jones 2018), and store approximately 547 ± 74 Pg C (Yu 2012) with over two-thirds of this C found within the permafrost region (Hugelius et al., 2014). This long-term net accumulation of C is due not to high gross primary production (GPP) but rather to restricted, slow rates of ecosystem respiration (ER) under cool, anoxic soil conditions (Turunen et al., 2002). The stability of a peatlands capacity to act as a C sink is closely coupled with its hydrological regime (Laine et al., 2019) that defines the oxic-anoxic peat boundary (Blodau et al., 2004) and vegetation community (Mäkiranta et al., 2018), along with temperature and its controls on ER (Lafleur et al., 2005), methane (CH_4) production and emissions (Frolking and Roulet, 2007), and GPP (Jensen et al., 2019). Rapidly warming temperatures are causing increased permafrost thaw in ice-rich peatlands and leading to thermokarst development (Kokelj and Jorgenson, 2013). While thermokarst development has been shown to lead to increased rates of surficial peat accumulation (Turetsky et al., 2007), the rapid loss of previously frozen C stores in the initial decades following thaw (O'Donnell et al., 2012; Jones et al., 2017) has been indicated from soil organic C stocks. Permafrost thaw exposes previously frozen soil organic C to potential rapid mineralization (Schuur et al., 2008) and release to the atmosphere as both carbon dioxide (CO_2) and CH_4 (Helbig, Chasmer, Kljun, et al., 2017; Helbig, Chasmer, Desai, et al., 2017), particularly in recently thawed areas where the potential for increased microbial decomposition is greatest.

Peatland complexes in the sporadic-discontinuous permafrost zone of western Canada include peat plateaus, thermokarst bogs, channel fens, and ponds, and represent an area of ~151,000 km^2 (Vitt et al., 1994; Hugelius et al., 2014). Peatland development in the sporadic-discontinuous permafrost zone of western Canada began ~9,000 years ago (Heffernan et al., 2020), with the first appearance of permafrost aggradation occurring after the Holocene Thermal maximum (Zoltai, 1995) but more widespread, rapid expansion of permafrost occurred 1,200 – 1,600 years ago following climate cooling (Pelletier et al., 2017; Heffernan et al., 2020). At its southernly extent permafrost is relatively warm and thin (Smith et al., 2005) and due to increased disturbances leading to permafrost thaw (Lara et al., 2016), the peatland complexes in this area are predicted to be permafrost-free within the 21st century (Chasmer and Hopkinson, 2017).

Thermokarst bog formation in ice-rich raised peat plateaus leads to surface subsidence and inundation (Quinton et al., 2009), causing a rapid shift in the hydrological regime and soil temperatures (Baltzer et al., 2014; Quinton and Baltzer, 2013), and a ~30% increase in species diversity (Beilman, 2001). The saturated early stages of thermokarst bog formation are colonized by hydrophilic vegetation, such as *Sphagnum riparium*, and sedge species (Robinson et al., 1999) that are associated with higher rates of productivity and C accumulation at the surface (Camill et al., 2001) and relatively labile plant litter (Turetsky, 2003). Over time, thermokarst bogs undergo autogenic succession and peat accumulation results in drier surface conditions allowing more drought-tolerant vegetation, but with less-labile plant litter, to colonize such as *Sphagnum fuscum* and ericaceous shrubs (Camill, 1999).

The net ecosystem exchange (NEE), i.e. the balance between ER and GPP, of intact boreal peat plateaus indicates that they act as a weak net sink of atmospheric CO_2 and do not significantly differ from surrounding permafrost free peatlands (Olefeldt et al., 2012). Increasing temperatures and the ecological shifts associated with permafrost thaw have the potential to destabilize this net sink by impacting the components of the NEE, as well as CH_4 emissions. Peatland plants are adapted to the saturated conditions that define peatlands (Sottocornola et al., 2009), thus the shifting water table regime, vegetation community, and increased nutrient availability following thaw can result in increased GPP and C uptake compared to the plateau understory vegetation (Camill et al., 2001; Keuper et al., 2012). However, when the water table is high and oxygen availability is low GPP can be significantly reduced (Chivers et al., 2009). Inundation of the peat profile results in anaerobic conditions which constricts the respiration of C previously aerobically respired in the plateau (Schädel et al., 2016) and can lead to low ER but high CH_4 emissions (Alm et al., 1999). Alternatively, drier conditions (Sulman et al., 2009) and warmer temperatures (Walker et al., 2017) can lead to increased above-ground biomass and GPP, provided there is no long-term impact on GPP due to moisture stress (Robroek et al., 2007). While warmer conditions can stimulate GPP, they have the potential to stimulate greater rates of ER (Cai et al., 2010), particularly when peat is exposed to oxygen and aerobic ER (Chimner et al., 2017). Warming temperatures have been shown to lead to increased emissions of CO_2 and CH_4 (Voigt et al., 2017), with increasing importance being placed on non-growing season warming and CO_2 (Commane et al., 2017) and CH_4 (Zona et al., 2016) emissions in non-peatland permafrost regions. Shifts in the hydrological regime and increasing temperatures further impact

peatland NEE as they provide favourable conditions for the colonization of vegetation with labile inputs (Dieleman et al., 2015), leading to increased decomposition of organic matter (Straková et al., 2012) and enhanced ER (Walker et al., 2016) and CH_4 emissions (Prater et al., 2007).

Several studies have demonstrated that permafrost thaw in boreal peatlands can lead to enhanced C accumulation (Robinson and Moore, 2000; Camill et al., 2001; Turetsky et al., 2007), however these studies only consider changes in near-surface C stores. Whereas others have indicated that there are rapid and substantial losses of deep, previously frozen C in the initial decades following thaw (O'Donnell et al., 2012; Jones et al., 2017), which would not be captured by surface C accumulation rates. In order for such large losses to occur in the initial decades following thaw, enhanced decomposition and emissions of previously frozen C would be required to exceed C accumulation at the surface. Deep peat warming has been shown to lead to enhanced CO_2 and CH_4 emissions (Gill et al., 2017), and increased CH_4 emissions have previously been reported from recently thawed thermokarst bogs (Johnston et al., 2014; Turetsky et al., 2002). Warmer temperatures at depth, the exposure of previously frozen, labile peat following thaw, and potential downward transport of labile surface dissolved organic matter in the initial decades following thaw may lead to enhanced CO_2 and CH_4 production and emissions (Schuur et al., 2015; Chanton et al., 2008). However previous studies have found little to no evidence of aged soil C contributing to CO_2 and CH_4 surface emissions in thermokarst bogs (Estop-Aragonés, Cooper, et al., 2018; Cooper et al., 2017). Thus, questions remain regarding the fate of previously frozen C following permafrost thaw and whether recently thawed thermokarst bogs are hotspots for enhanced C loss on the landscape.

In this study, the main objective was to assess differences in the annual C balance between recently thawed, young thermokarst bogs and mature thermokarst bogs that thawed ~200 years ago in order to determine whether the young stage represents a hotspot for net C losses in a boreal peatland complex. We used measured greenhouse gas fluxes and environmental variables along two thaw chronosequences to construct annual C balances. This approach allowed us to determine how permafrost thaw impacted the annual C balance of a boreal peatland complex, and the response of greenhouse gas fluxes to shifts in hydrological regimes, soil temperatures, and vegetation composition. By determining the functional response of CO_2 and CH_4 surface fluxes to thaw induced environmental changes, we assessed the vulnerability of the C sink

function, with regards to time-since-thaw, of a boreal peatland. We hypothesize that: (1) there are net losses of C to the atmosphere in the initial decades following thaw due to enhanced, deep losses of CO_2 and CH_4 that exceed CO_2 uptake; and that (2) in the centuries following thaw, C loss to the atmosphere is offset by C sequestration and there are net gains of atmospheric C. This study highlights the spatial variability in the functional response of greenhouse gas fluxes to permafrost thaw and the necessity for long-term monitoring of these functional responses in thawing boreal peatlands.

3.2 Methods

3.2.1 Site Description

Our peatland study site ("Lutose", 59.5°N, 117.2°W; Fig. 3.1a) is located in the sporadic-discontinuous permafrost zone of the Mackenzie River Basin, western Canada (Brown et al., 1997; Heginbottom, Dubreuil, and Harker, 1995). The climate is continental with an average annual air temperature at Meander River (50 km to the south) of -1.8°C, with July being the warmest (16.1°C) and January being the coldest (-22.8°C) (Climate-Data.org, 2019). Annual average precipitation is ~391 mm with nearly two-thirds of annual precipitation falling as rain (239 mm) between May and September. The Lutose peatland is characteristic of peatlands in the region, composed of a fine-scale mosaic of permafrost peat plateaus affected by permafrost interspersed with bogs, fens, and ponds without permafrost. Permafrost is predominantly found in peatlands in the study region, and only sporadically in other forested ecosystems (Holloway and Lewkowicz, 2019). Peatlands in boreal western Canada cover >25% of the landscape and have peat deposits that vary in thickness from 2 – 6m (Hugelius et al., 2014; Vitt, Halsey, and Zoltai, 2000).

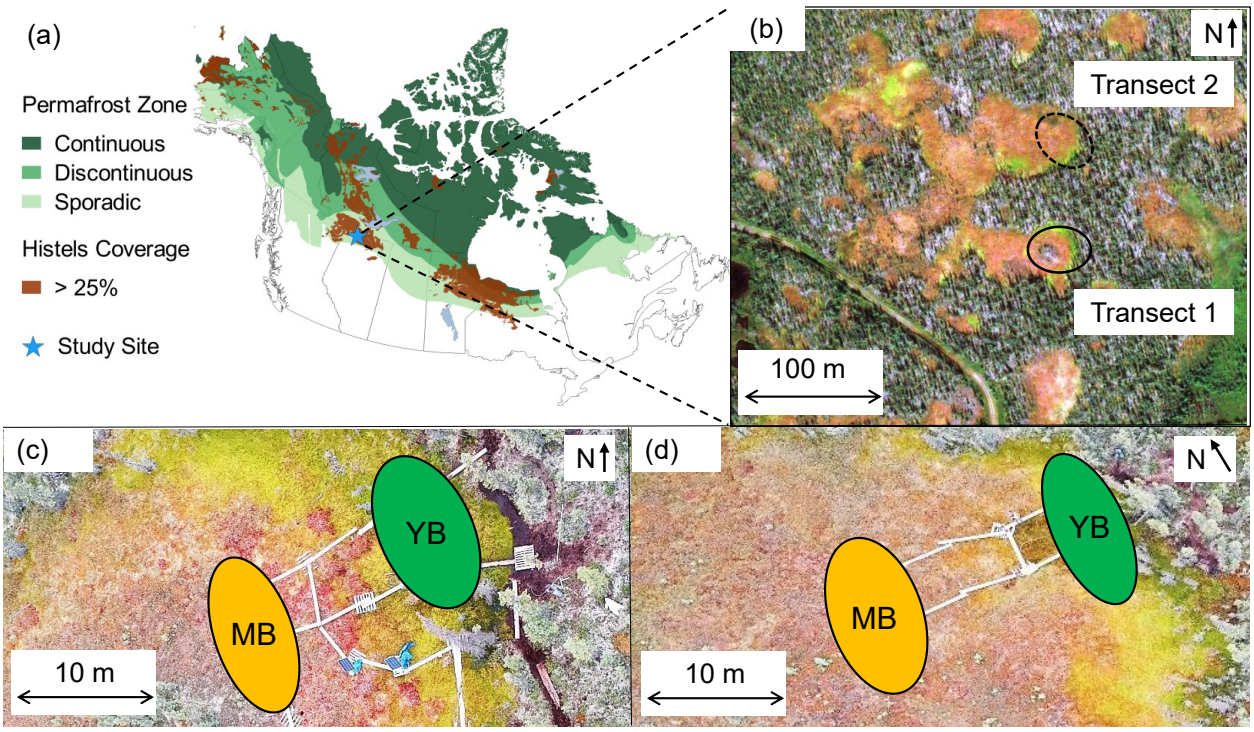

Figure 3.1. Site location and study design for the Lutose peatland. a) Site location in boreal western Canada (59.5°N, 117.2°W), where green shading indicates the distribution of permafrost zonation (Brown et al., 1997) and brown shows areas which contain >25% coverage of Histel (permafrost peatland) soils (Hugelius et al., 2014). b) Locations of the two studied thermokarst bog transects within the Lutose peatland (image from https://zoom.earth/). c) Transect 1 and d) transect 2 including locations of collars for gas flux measurements in the young bog (YB, green) and mature bog (MB, orange) sections of each transect (Aerial photo credit: Olefeldt, David).

The study includes two thaw transects that include the transitions from peat plateau to young thermokarst bog, and from young to mature thermokarst bog (Fig. 3.1b, c, d). The peat plateau is raised 1 – 2 m above the adjacent thermokarst bogs, and has an active layer thickness of ~50 cm. Vegetation in the peat plateau is typical of peat plateau vegetation in western Canada (Vitt, Halsey, and Zoltai, 1994) and is characterized by a stunted open black spruce (*Picea mariana*) forest, low-lying ericaceous shrubs such as Labrador tea (*Rhododendron groenlandicum*), lichens (*Cladonia* spp.) and dry-adapted *Sphagnum fuscum* hummocks. Each thermokarst bog is differentiated between young and mature bog stage determined by vegetation community, water

table position, and proximity to the plateaus thawing edge (Fig. 3.1b, c, d). The young bog (YB) stage thawed most recently, is narrow (<5m wide) and adjacent to the intact plateau with active thaw occurring as indicated by *Picea mariana* that are dying and drooping over. The surface of the YB stage is inundated, with an average growing season water table position of -1.3 ± 4.9 cm below the peat surface and its vegetation community is dominated by the hydrophilic species *Sphagnum riparium,* rannoch rush (*Scheuchzeria palustris)*, and bog-sedge (*Carex limosa)*. The mature bog (MB) thawed between 70 – 150 cal yr. BP and is relatively drier with an average growing water table depth of -22.9 ± 9.3 cm. It is located >10m from the thawing edge and its vegetation consists of *Sphagnum fuscum, Sphagnum magellanicum,* leather leaf (*Chamaedaphne calyculata),* bog rosemary *(Andromeda polifolia),* cloudberry *(Rubus chamaemorus), Eriophorum vaginatum* tussocks, and some black spruce (*Picea mariana)* regrowth. There were no differences in water table position and vegetation composition between the two thaw transects.

Boardwalks for both thaw transects were constructed in 2015 to minimize disturbance. Six collars with 39 cm diameter were permanently inserted to a depth of ~20 cm in to each young and mature bog, totalling 24 collars over two thaw transects. Collars were flush with the peat surface and care was taken to ensure minimal disturbance to vegetation during collar installation. It was determined that each collar was representative of its bog stage and suitable for greenhouse gas flux measurements.

3.2.2 Climate and water table records

A weather station (Hobo RX3000 Remote Monitoring weather station) was established at the Lutose site in July 2015. The weather station included air temperature, solar irradiation, and rainfall sensors. Air temperature was recorded every five minutes using a Hobo 12-bit Temperature Smart Sensor S-TMB-M002 (Onset Computer, Bourne, MA, USA). Incoming photosynthetically active radiation (PAR; µE) was measured every 5 minutes using a Hobo Photosynthetic Light Smart Sensor S-LIA-M003 (Onset Computer, Bourne, MA, USA). Rainfall (mm) was measured using a tipping bucket and Hobo Pendant Event RG3-M data logger (Onset Computer, Bourne, MA, USA). Both PAR and air temperature were measured at ~1.5 m height PAR, air temperature, and rainfall were measured from the August 2015 – present.

Continuous bi-hourly measurements of soil temperature (°C) were recorded using loggers (Hobo 8k Pendant Onset Computer, Bourne, MA, USA) installed at 5 and 40 cm in all bog stages from July 2015 to July 2019. All continuous measurements were aggregated to, or used to estimate, data for one-hour intervals.

In addition, we measured soil temperature at 5 and 40 cm, water table position, thaw depth manually at each collar during each gas flux measurement. Daily water level records between May 1st and October 31st each year were constructed by interpolating between manual measurements. Soil temperatures were measured at 5 and 40 cm depth manually at each collar and flux occasion using handheld thermometers, or taken from previously installed temperature sensors at 5 and 40 cm when the surface was frozen.

3.2.3 Measurements of greenhouse gas fluxes

Greenhouse gas flux measurements (CO_2 and CH_4) were taken using the static chamber method (Carroll and Crill 1997). We used a transparent cylindrical Plexiglass chamber with a basal area of 0.12 m^2, height of 0.40 m, and volume of 47.8 L. The chamber was equipped with three fans (Micronel Ventilator D341T012GK-2, BEDEK GmbH) to mix air during measurements, a PAR sensor identical to the PAR sensor installed on the site weather station, and a temperature sensor (RH Smart Sensor, S-THB-M002) that was shaded from direct sunlight (Burger et al., 2016). Each collar had a ~1.5 cm deep well around its upper circumference and an airtight seal was created between the chamber base and the collar by pouring water around this well during measurements.

Winter flux measurements were taken using an opaque chamber with a basal area of 0.12 m^2, height of 0.26 m, and volume of 31.1 L. Three collars from each bog stage were marked during the growing season to identify their position underneath the winter snowpack. Snow was removed from each collar a minimum of 30 minutes prior to each flux measurement to allow for any gas trapped in the snowpack to be released. The chamber was sealed as in the growing-season and loose snow was packed around the chamber base. Ambient air temperature outside the chamber was measured using a handheld thermometer at the beginning and end of each flux measurement.

Net ecosystem exchange (NEE) was measured under ambient light conditions and was followed by measurements of ecosystem respiration (ER) in darkened conditions by covering chambers with a reflective shroud. Our gross primary production (GPP) estimate was determined as the difference between NEE and ER where;

$$NEE = GPP + ER \quad (1)$$

Fluxes of CH_4 were captured simultaneously with CO_2 and CH_4 fluxes captured under dark conditions are reported here. Chambers were closed for 5 minutes and CO_2 and CH_4 concentrations were determined at a temporal resolution of 1s using an Ultraportable Greenhouse Gas Analyser (Los Gatos Research, CA, USA). Fluxes were monitored in real-time using the VNV® Viewer (RealVNC® Limited, UK) application with an iPad mini 2 (Apple Inc.). Fluxes were calculated using linear regression of the change in gas concentration inside the chamber over time and the ideal gas, average air temperature inside the chamber during the measurement (or outside for winter fluxes), and with a constant atmospheric pressure value of 0.96 atm using equation (2):

$$Flux = slope \frac{P.v}{R.T.A} \quad (2)$$

where slope is the rate of change ($second^{-1}$) of gas concentration in the chamber over the measurement period; P is atmospheric pressure (1 atm); V is chamber volume (L); R is the universal gas constant (L atm K^{-1} mol^{-1}); T is the average temperature inside the chamber during the measurement period (K); and A is the base area of the chamber (0.12 m^2). Each greenhouse gas flux was measured for 5 minutes. The first 2 minutes of each measurement were discarded for the flux calculation to ensure fluxes with $R^2 > 0.75$ following inspection of the change in concentration over time. We report CO_2 fluxes (NEE and ER) in g C-CO_2 m^{-2} day^{-1} and CH_4 fluxes in g C-CH_4 m^{-2} day^{-1}, with positive fluxes indicating fluxes to the atmosphere and negative fluxes as uptake from the atmosphere.

Sampling began in May 2016 and was conducted over three full growing seasons (May 10th – October 26th) and two-nongrowing seasons, ending in November 2018. The 2016 growing season had 15 measurement days from May 10th – October 9th. Non-growing season flux measurements occurred three times in 2017 on February 2nd, March 22nd, and April 24th. The 2017 growing season had 13 growing season measurement days between May 20th – October

26th. Flux measurements in 2018 began with three non-growing season flux measurement days on February 10th, March 20th, March 31st, and April 24th. Growing season flux measurements in 2018 began May 16th and ended September 24th with a total of five flux measurement days. One final non-growing season flux measurement day occurred on November 11th, 2018. A total of 662 NEE, 731 ER, 613 GPP, and 664 CH_4 flux measurements were accepted after data quality checks. This included 311 and 351 NEE, 354 and 377 ER, 287 and 326 GPP, and 322 and 342 CH_4 fluxes measured from the YB and MB bog stages respectively. The greatest number of fluxes were measured in 2017 (293 NEE, 300 ER, 271 GPP, and 296 CH_4) and lowest in 2018 (141 NEE, 181 ER, 105 GPP, and 174 CH_4).

3.2.4 Data modelling and statistical analysis

In order to assess the control of abiotic variables on ER, GPP, and CH_4 fluxes we used both linear and non-linear mixed effects models. All mixed effects models were built in R Studio (Team 2016) using the nlme package (Pinheiro, Bates, and DebRoy 2017). Models were built individually for each flux (ER, GPP, and CH_4) in each bog stage (young and mature bog). We used forward stepwise selection in identifying significant abiotic variables to retain for model building and those retained included water table position (WT), soil temperatures (°C) at 5 and 40 cm, and PAR (µE). Non-linear mixed effects models included abiotic variables as fixed effects and collar ID as a random effect to account for the grouping of bog stages from two separate transects and the lack of independence of repeated measures. All abiotic variables were tested for collinearity prior to model parameter selection and variables with a variance inflation factor greater than 5 were removed. The adequacy of each model was determined via the Akaike Information Criterion (AIC) value, root square mean error (RMSE), and inspection of residuals. Data from both transects were pooled for analysis to ensure significant model parameters. Model parameters and abiotic variables presented below include error that represent 95% confidence intervals unless otherwise stated.

Statistical analysis was carried out in R studio (Team, 2016) using the nlme (Pinheiro, Bates, and DebRoy, 2017) and multcomp (Hothorn, Bretz, and Westfall, 2008) packages. We performed ANOVAs and Bonferroni post-hoc tests on linear mixed effects models to test for significant annual trends and evaluate differences in measured fluxes and abiotic variables between years for both the YB and MB. We used t-tests to test for differences between model parameter outputs

and average NECF between the YB and MB. For all t-tests, the homogeneity of variances was checked using an F test. We define the statistical significance level at 5% and error presented represents ± 95% Confidence Interval bounds unless otherwise stated.

3.3 Results

3.3.1 Climate and environmental variables

Climate measurements indicate that 2016 was a warm year with relatively high precipitation given the warmest average annual air temperatures (-0.28 ± 1.02 °C; Fig. 3.2a) and second highest precipitation (248 mm; Fig. 3.2b) occurred in 2016. The year with the greatest precipitation, with also the highest solar irradiation, was 2017 when 262.8 mm of precipitation fell and a average growing season PAR of 390 ± 20 µE (Fig. 3.2c) was recorded, along with the second warmest average annual air temperatures (-0.64 ± 1.10 °C). As such 2017 was a warm year with high precipitation and solar irradiance. Solar irradiation was similar for both 2016 (386 ± 21 µE) and 2018 (368 ± 20 µE). The climate in 2018 was cool with low precipitation, with the lowest average annual air temperature (-1.85 ± 1.07 °C) and precipitation (138.4 mm).

Precipitation was not the main driver of interannual wetness and water table position (Fig. 3.2d), which seemed to be more closely linked with the non-growing season snowpack that we unfortunately do not have measurements of. There was a general trend of water table lowering throughout all growing seasons, interrupted by precipitation inputs. Thus, we use water table position as a measure of wetness, not precipitation.

The wettest year was 2016, with an average water table depth of 0.98 ± 0.60 cm in the young bog and -20.04 ± 0.72 cm in the mature bog. The second highest average water tables were measured in 2018 (young bog = -1.33 ± 0.53 cm. mature bog = -22.21 ± 0.41 cm). The lowest average water tables in the young bog (-4.04 ± 0.37 cm) and mature bog (-28.32 ± 0.41 cm) were recorded during 2017. The water table position demonstrated significant interannual variability in both the young bog ($F_{(2, 273)} = 40.59$, $P < 0.001$) and mature bog ($F_{(2, 260)} = 42.78$, $P < 0.001$), with 2016 and 2018 being classified as wet years and 2017 a dry year, particularly in the young bog where the water table was above the peat surface for a large proportion of the growing season.

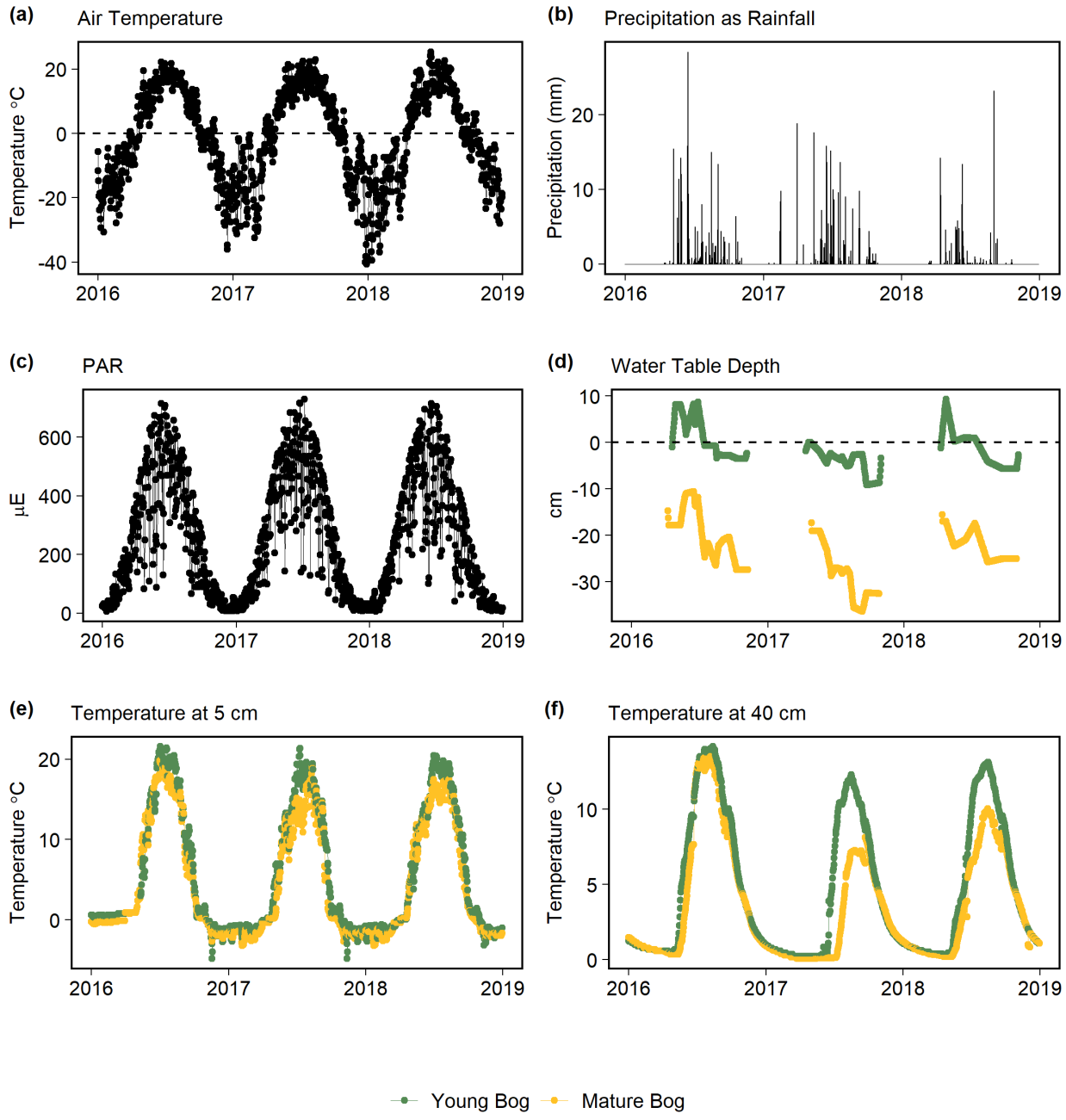

Figure 3.2. Daily average data from January 1st 2016 to December 31st 2018 including (a) air temperature (°C), (b) precipitation (mm) as rainfall, (c) photosynthetically active radiation (PAR; µE), (d) water table position (cm) from peat surface with negative values representing water table beneath the peat surface, (e) soil temperature (°C) at 5cm, and (f) soil temperature (°C) at 40cm. Green represents data measured from the young bog and yellow represents data measured from the mature bog.

In both the young bog and mature bog average annual soil temperatures at 5 cm (Fig. 3.2e) and 40 cm (Fig. 3.2f) were highest in 2016. Warm soil temperatures in 2016 were likely due to both high air temperatures and water table position allowing heat to transfer down the peat column. The second warmest average annual soil temperatures were recorded in 2018 when air temperature was cooler, but the water table remained high. While 2017 had the second highest average annual air temperatures, the lower soil temperatures are likely due to the lower water tables measured during 2017 and restriction of heat transfer to depth as a result.

Differences in soil temperatures between years, and between the young bog and mature bog, were more pronounced during the growing season. Patterns of interannual variability observed in average annual soil temperatures prevailed for average growing season soil temperatures. Warm and wet conditions in 2016 led to the highest average growing season temperatures at 5 cm and at 40 cm. The lowest water table position in 2017 and reduced transfer of heat to depth, resulted in the lowest average growing season soil temperatures at 5 cm and 40 cm in the young bog and mature bog, thus 2017 was a cool and dry year. Whereas the higher water table positions and cooler air temperatures in 2018 lead to the second warmest temperatures at 5 cm and 40 cm in both the young bog and mature bog, resulting in 2018 being classified as a mild, wet year.

3.3.2 Ecosystem respiration measurements

Ecosystem respiration (ER) measurements (Fig. 3.3a) demonstrated interannual variability in both the young bog ($F_{(2, 273)} = 6.25$, $P < 0.01$) and mature bog ($F_{(2, 260)} = 7.32$, $P < 0.01$), with higher average fluxes measured in both over the warm, wet 2016 measurement period. Both the mature bog and young bog had clear seasonal ER patterns with peak rates measured in July – August each year (Fig. 3.3a), and the lowest emissions measured between November – April each year. ER measurements were significantly higher in the mature bog compared to the young bog throughout the three-year measurement period ($F_{(2, 21)} = 98.48$, $P < 0.001$) likely due to lower water tables and an upper oxic zone in the mature bog resulting in more efficient aerobic respiration. Average measured growing season ER over the three years in the mature bog was 2.03 ± 0.11 g $C\text{-}CO_2$ m^{-2} day^{-1} and 0.84 ± 0.08 g $C\text{-}CO_2$ m^{-2} day^{-1} in the young bog. Similarly, average non-growing measurements were higher in the mature bog (0.44 ± 0.10 g $C\text{-}CO_2$ m^{-2} day^{-1}) than the young bog (0.25 ± 0.06 g $C\text{-}CO_2$ m^{-2} day^{-1}).

3.3.3 Measured gross primary production

Significant interannual variability in gross primary production (GPP) measurements were observed in both the young bog ($F_{(2, 208)} = 34.78$, $P < 0.001$) and mature bog ($F_{(2, 240)} = 11.14$, $P < 0.001$) with higher rates measured over the cool and dry 2017 measurement period when PAR was highest, and the water table was lowest in both. Measured GPP in both the mature bog and young bog exhibited seasonal patterns with peak rates measured in July – August each year (Fig. 3.3b) when PAR and temperatures were at their highest, and plant phenology is at its apex (Peichl et al., 2018). Average GPP measurements in the drier mature bog (-3.23 ± 0.19 g $C\text{-}CO_2$ m^{-2} day^{-1}) were significantly higher ($F_{(1, 21)} = 20.88$, $P < 0.01$) than those measured in the young bog (-1.95 ± 0.21 g $C\text{-}CO_2$ m^{-2} day^{-1}) over the three growing seasons (Fig. 3.3b).

3.3.4 Methane (CH_4) fluxes

No significant interannual variability was observed in methane (CH_4) fluxes (Fig. 3.3c) in either the young bog ($F_{(2, 213)} = 0.83$, $P = 0.44$) or mature bog ($F_{(2, 210)} = 1.67$, $P = 0.19$). CH_4 fluxes in the young bog and mature bog exhibited seasonal patterns, with peak emissions measured between June – August when soil temperatures at 40 cm were highest. Methane (CH_4) fluxes (Fig. 3.3c) were significantly higher in the young bog than in the mature bog ($F_{(1, 21)} = 43.28$, $P < 0.001$) and average growing season CH_4 fluxes measured in the young bog were 0.075 ± 0.006 and 0.028 ± 0.004 g $C\text{-}CH_4$ m^{-2} day^{-1} in the mature bog respectively. Interestingly, average non-growing season CH_4 emissions in the young bog (0.032 ± 0.009 g $C\text{-}CH_4$ m^{-2} day^{-1}) were considerably higher than those measured in the mature bog (0.005 ± 0.001 g $C\text{-}CH_4$ m^{-2} day^{-1}).

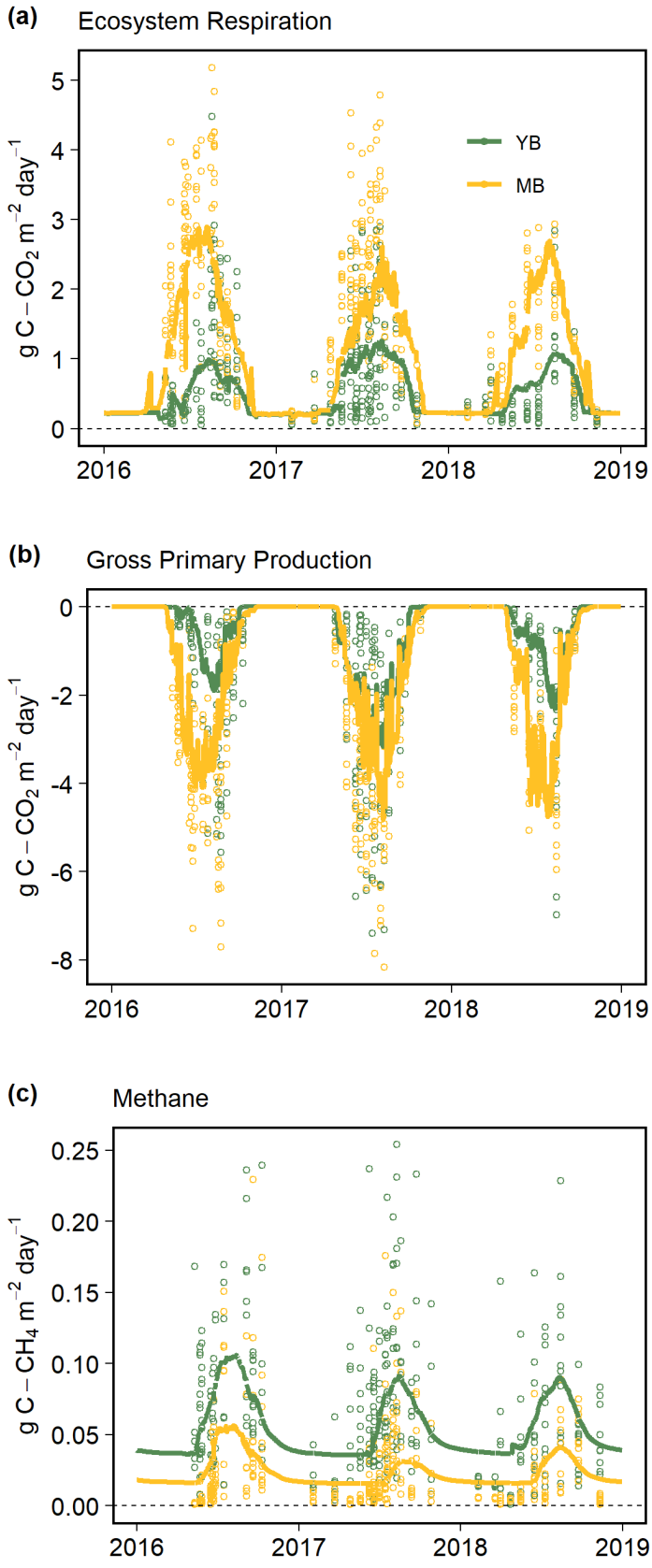
(a)
Ecosystem Respiration
g C – CO2 m–2 day–1
5
4
3
2
1
0
YB
MB
2016
2017
2018
2019
(b)
Gross Primary Production
g C – CO2 m–2 day–1
0
-2
-4
-6
-8
2016
2017
2018
2019
(c)
Methane
g C – CH4 m–2 day–1
0.25
0.20
0.15
0.10
0.05
0.00
2016
2017
2018
2019

Figure 3.3. Individual measured fluxes (circles) and modelled daily fluxes (lines) for (a) ecosystem respiration, (b) gross primary production, and (c) methane from January 1st, 2016 to December 31st, 2018. Green represents fluxes from the young bog (YB) and yellow represents fluxes from the mature bog (MB). Dashed line represents zero. Positive values represent a flux to the atmosphere, negative values represent a flux from the atmosphere (uptake). Fluxes in each stage were measured from 12 individual collars but the figure does not indicate individual collars, only which stage they were collected from.

3.3.5 Ecosystem respiration models

Following stepwise selection soil temperature at 5 cm and water table position were found to be significant environmental variables ($P < 0.05$ for both) influencing growing season ER in both the young bog and mature bog. In the young bog, the most parsimonious ER model, based on AIC values, (Table A2.1) used water table position and temperature in a quadratic parabola and exponential function (Table 3.1. Eqn. 3) (Alm et al., 2007). Models that used only water table or temperature had higher AIC values and not all model parameters were found to be significant (Table A2.1. Eqn. 3.1 – 3.4). A similar model that used a sigmoidal response to water table position had a similar AIC value to our selected model, however not all model parameters were found to be significant (Table A2.1. Eqn. 3.5). Model fit was reasonably good (Table 3.1. RMSE = 0.6) and all model parameters were found to be significant (Table A2.1), yielding confidence in the use of interpolated water table depths and continuous soil temperature at 5 cm data for estimating growing season ER in the young bog.

The most parsimonious ER model in the mature bog (Table A2.1. Eqn. 4 – 4.4) also used temperature in an exponential function, but water table position was used in a linear function (Table 3.1. Eqn. 4). Models that used only water table or temperature, and a combination of temperature and water table similar to Eqn. 3 used in the young bog, had higher AIC values and not all model parameters were found to be significant (Table A2.1. Eqn. 4.1 – 4.4). Model fit was good (Table 3.1. RMSE = 0.7) and all model parameters were found to be significant (Table A2.1), yielding confidence in the use of interpolated water table depths and continuous soil temperature at 5 cm data for estimating growing season ER in the mature bog.

For non-growing season (NGS) ER models in the young bog and mature bog the most parsimonious model (Table A2.1. Eqn. 5 – 5.11) used temperature in a similar exponential function as for growing season models, but thaw depth was used in a linear function (Table 3.1. Eqn. 5). Average non-growing season thaw depth in the young bog is -6.3 ± 2.7 cm (median is 0 cm) and -6.8 ± 1.5 cm (median is 0 cm) in the mature bog. Models that used only temperature had higher AIC values, reduced overall model fit (Table A2.1. Eqn. 5.1 – 5.11) or yielded ecologically unrealistic results.

Our non-linear mixed effects models indicated that the water table and soil temperature at 5 cm had a significant influence on measured ER fluxes in both the young bog and mature bog (Fig. 3.4; Table 3.1). However, ER responded to both of these abiotic variables differently between the young bog and mature bog (Fig. 3.4). In the mature bog, ER increased linearly with lowering water tables and exponentially with increases in soil temperature at 5 cm (Eqn. 5), and soil temperature was the most important predictor of ER (Fig. 3.4b, c). Whereas in the young bog (Eqn. 3), while the exponential response of ER to soil temperature at 5 cm was significant, the quadratic parabolic response of ER to water table was the most important predictor (Fig. 3.4a, c).

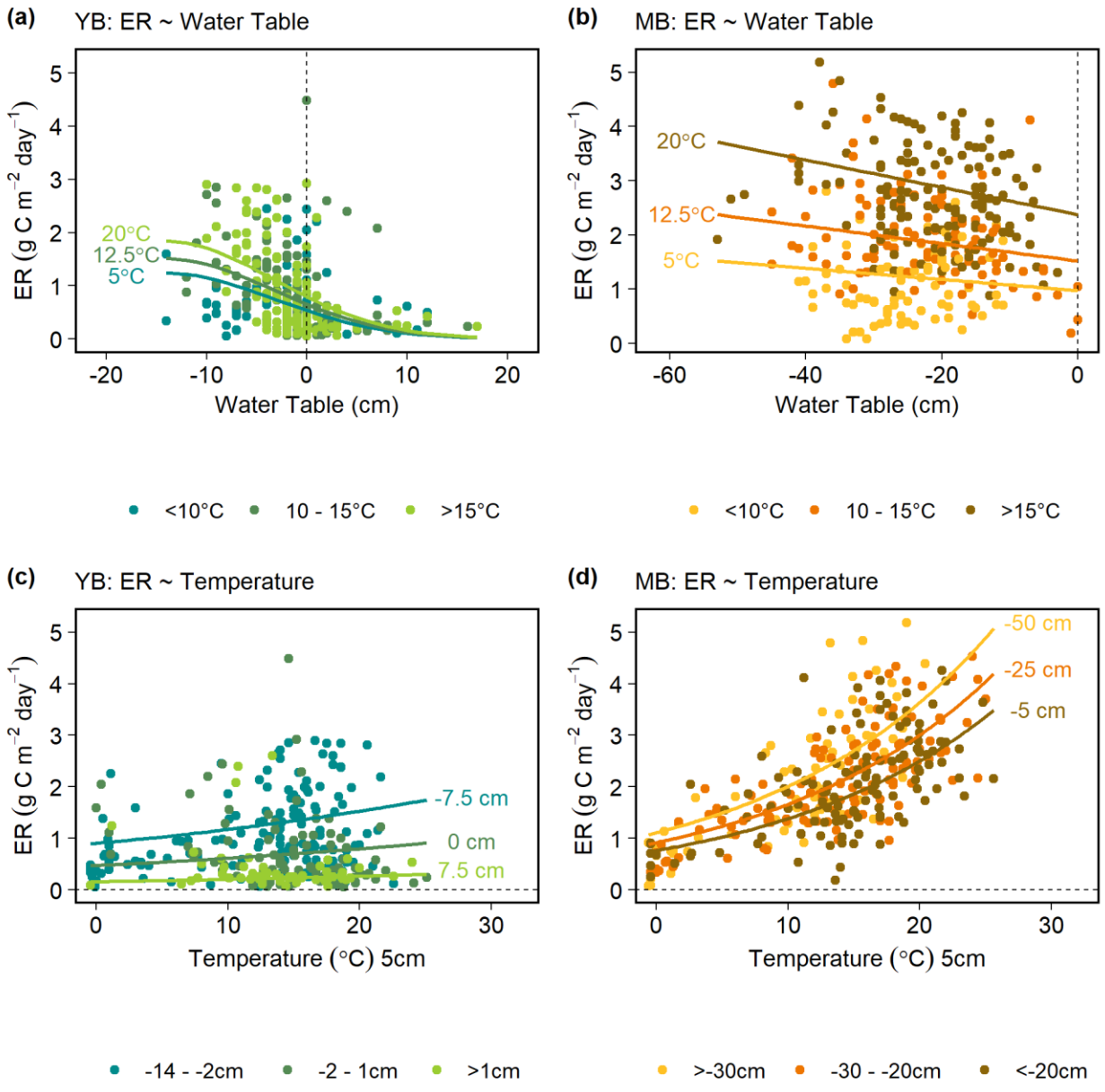

Figure 3.4. Ecosystem respiration (ER) functional response to abiotic variables used in models for young bog (young bog; green circles) and mature bog (mature bog; golden circles). (a) Functional response of ER to water table depth in the young bog at three different temperatures (°C) at 5 cm depth (20 °C, 12.5 °C, and 5 °C). (b) Functional response of ER to water table depth in the mature bog at three different temperatures (°C) at 5 cm depth (20 °C, 12.5 °C, and 5 °C). (c) Functional response of ER to temperature (°C) in the young bog at three different water table depths (-7.5 cm, 0 cm, and 7.5 cm). (d) Functional response of ER to temperature (°C) in the mature bog at three different water table depths (-50 cm, -25 cm, and -5 cm).

Negative water table (cm) values = water table beneath the peat surface. Positive water table (cm) values = water table above the peat surface.

3.3.6 Gross primary production models

Water table position, soil temperature at 5 cm, and PAR were found to be significant environmental variables ($P < 0.05$ for both) influencing growing season GPP in the young bog following stepwise selection. Whereas following stepwise selection in the mature bog, soil temperature at 5 cm and PAR were found to be significant environmental variables ($P < 0.05$ for both) influencing growing season GPP, with no influence of water table on the model. To address the identification of soil temperature at 5 cm as a significant explanatory variable we impose a seasonality factor of $\frac{mT_5}{mT_{season}}$ on GPP, where mT_5 is the 7-day running average peat temperature at 5 cm and mT_{season} is the average seasonal temperature at 5 cm, by multiplying the rectangular hyperbolic in our models by this seasonality factor (Bubier et al., 1999). By imposing this seasonal phenological factor with peat temperature, both k and $GPP_{(max)}$ can respond to seasonal progresses.

The most parsimonious GPP model in the young bog (Table A2.1 Eqn. 6 – 6.2) was the non-linear dependence of GPP to PAR and water table using a modified rectangular hyperbola and quadratic parabola (Table 3.1. Eqn. 6) (Olefeldt et al., 2017; Alm et al., 2007). Modelling attempts using water table and PAR separately yielded higher AIC values, although model parameters were significant across all models. Model fit was good (Table 3.1. RMSE = 1.2) and all model parameters were found to be significant (Table A2.1), yielding confidence in the use of interpolated water table depths and continuous PAR data for estimating GPP in the young bog.

In the mature bog the most parsimonious GPP model (Table A2.1. Eqn. 7 – 7.2) was the non-linear dependence of GPP to PAR using a modified rectangular hyperbola (Table 3.1. Eqn. 7) (Olefeldt et al., 2017; Alm et al., 2007). Attempts using water table alone (Table A2.1. Eqn. 7.1) yielded higher AIC values and not all parameters were significant. Using a combination of water table and PAR as in Eqn. 6 to model GPP in the mature bog resulted in a similar AIC value (Table A2.1. Eqn. 7.2), however not all models' parameters were significant. Overall, we have

confidence in the use of continuous PAR data to model GPP in the mature bog due to the significance of our model parameters and good model fit (Table 3.1. RMSE = 1.3).

In both the young bog and mature bog non-linear rectangular hyperbolic response curve models and the light response curve parameter, GPP_{max} (Eqn. 6 and 7 respectively), demonstrated a significant influence of PAR on measured GPP (Fig. 3.5; Table A2.1). Modelled GPP in the young bog and mature bog increased along a light response curve with increasing PAR (Fig. 3.5a, b). However, the most important predictor of GPP in the young bog was its quadratic parabolic response to water table position (Fig. 3.5c; Table A2.1). The non-linear model showed that young bog GPP had its greatest magnitude, i.e. highest productivity, when the water table was -5.9 ± 1.4 cm beneath the peat surface (Fig. 3.5c; Table A2.1). The seasonal phenology factor, using peat temperature at 5 cm, imposed on GPP had a similar seasonal pattern to measured GPP fluxes in both the young bog and mature bog over the three years (Fig. A2.1). The young bog seasonality factor was lower than that in the mature bog over the three years, likely due to the larger effect of water table position, rather than phenology and temperature, on GPP in the young bog.

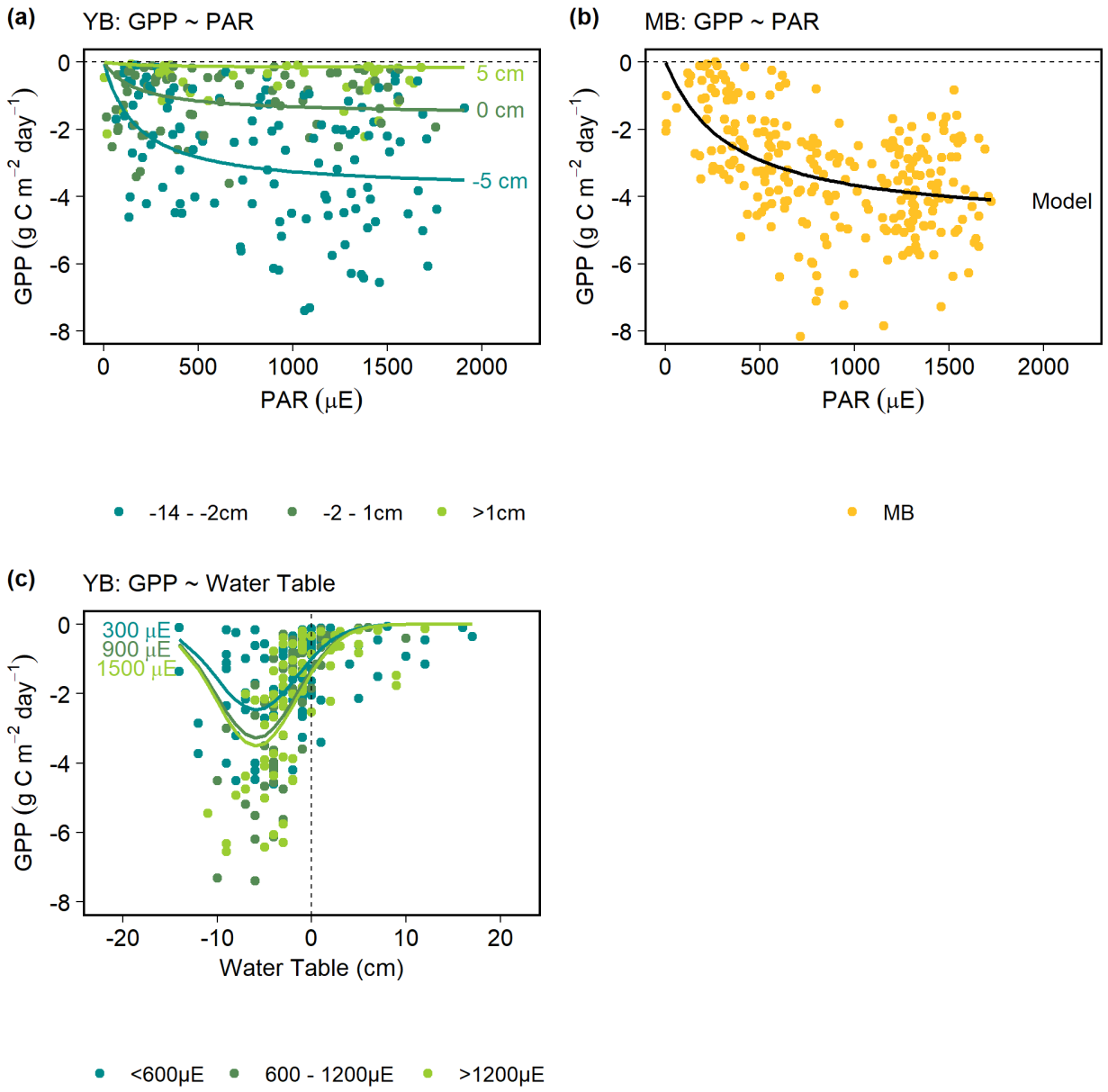

Figure 3.5. Gross primary production (GPP) functional response to abiotic variables used in models for young bog (young bog; green circles) and mature bog (mature bog; golden circles). (a) Functional response of GPP to photosynthetically active radiation (PAR; µE) in the young bog at three different water table (cm) depths (-5 cm, 0 cm, and 5 cm). (b) Functional response (model; black line) of GPP to PAR (µE) in the mature bog. (c) Functional response of GPP to water table (cm) depth in the young bog at three different levels of PAR (µE) (300 µE, 900 µE, and 1500 µE). Negative water table (cm) values = water table beneath the peat surface. Positive water table (cm) values = water table above the peat surface.

Table 3.1 Equations and estimate parameters for models examining the nonlinear effects of abiotic variables for both growing and non-growing season measured CO_2 and CH_4 fluxes. Parameters include 95% confidence intervals. RMSE = root square mean error. All model parameters were significant ($P < 0.05$) except in non-growing season ecosystem respiration models.

Bog Stage	Model	Model Parameters	RMSE
Young Bog	Equation 3. Ecosystem Respiration $\left[ER_{(max)} \times \exp\left(-0.5 \times \left(\frac{(\mathrm{WT} - uER)^2}{tER^2}\right)\right)\right] \times exp^{(x,\mathrm{T5cm})}$	$ER_{(max)}$ = 1.1 ± 0.5 g C-CO_2 m^{-2} day^{-1}. *uER* = -14.4 ± 11.3 cm. *tER* = -11.1 ± 6.1 cm. *x* = 0.03 ± 0.02	0.6
Mature Bog	Equation 4. Ecosystem Respiration $\left(a + \left(b \times \mathrm{WT}\right)\right) \times exp^{(x,\mathrm{T5cm})}$	*a* = 0.7 ± 0.1. *b* = -0.007 ± 0.004. *x* = 0.06 ± 0.01	0.7
Young and Mature Bog	Equation 5. Non-growing Season Ecosystem Respiration $\left(a + \left(b \times \mathrm{TD}\right)\right) \times exp^{(x,\mathrm{T5cm})}$	YB: *a* = 0.25. *b* = 0.006. *x* = 0.14 MB: *a* = 0.22. *b* = -0.03. *x* = 0.06	YB: 0.2 MB: 0.3
Young Bog	Equation 6. Gross Primary Production $GPP_{(max)} \times \left(\frac{\mathrm{PAR}}{k + \mathrm{PAR}}\right) \times \exp\left(-0.5 \times \left(\frac{(\mathrm{WT} - uGPP)^2}{tGPP^2}\right)\right)$	$GPP_{(max)}$ = -3.8 ± 1.2 g C-CO_2 m^{-2} day^{-1}. *k* = 176.5 ± 88.5 µE. *uGPP* = -5.9 ± 1.4 cm. *tGPP* = 4.4 ± 0.7 cm	1.2
Mature Bog	Equation 7. Gross Primary Production $GPP_{(max)} \times \left(\frac{\mathrm{PAR}}{k + \mathrm{PAR}}\right)$	$GPP_{(max)}$ = -4.7 ± 0.8 g C-CO_2 m^{-2} day^{-1} *k* = 344.2 ± 157.8 µE	1.3
Young and Mature Bog	Equation 8. Methane $z \times Q_{10}^{(\frac{T_{40}}{10})}$	YB: *z* = 0.04 ± 0.01 g C-CH_4 m^{-2} day^{-1}. *Q10* = 2.03 ± 0.44 MB: *z* = 0.02 ± 0.01 g C-CH_4 m^{-2} day^{-1}. Q_{10} = 2.36 ± 0.91	YB: 60.8 MB: 44.3

$ER_{(max)}$ = maximum rate of ER (g C-CO_2 m^{-2} day^{-1}) under optimal conditions. *uER* = optimum water table position (cm) for ER. *tER* = the range of water table position (cm) in which *uER* can occur. *x* = the rate and direction of change in ER along the range of soil temperature at 5 cm. $GPP_{(max)}$ = maximum rate of GPP (g C-CO_2 m^{-2} day^{-1}) under optimal conditions. PAR = photosynthetically active radiation (µE). *k* = range around *uGPP* over which GPP_{max} is found (µE). *uGPP* = optimum water table position (cm) for GPP. *tGPP* = the range of water table position (cm) in which *uGPP* can occur. *z* = CH_4 flux at 0 °C (g C-CH_4 m^{-2} day^{-1}). Q_{10} = temperature dependency of CH_4 flux. T_{40} = temperature (°C) at 40 cm. *a* and *b* are model estimate.

3.3.7 Methane (CH_4) flux models

Following stepwise selection soil temperature at 40 cm was found to be the significant environmental variable ($P < 0.05$) influencing CH_4 fluxes in both the young bog and mature bog. In both, the most parsimonious CH_4 model, based on AIC values, (Table A2.1) used temperature in a Q_{10} function (Table 3.1. Eqn. 8) (A. Baird et al., 2019). Models using temperature in an exponential function, similar to Eqn. 3, 4, and 5, had higher AIC values (Table A2.1. Eqn. 8.1 – 8.2). Model fit was reasonably good (Table 3.1. RMSE = 60.8 in the young bog and 44.3 in the mature bog) and all model parameters were found to be significant (Table A2.1), yielding confidence in the use of continuous soil temperature at 40 cm data for estimating CH_4 fluxes in the young bog and mature bog.

The non-linear model (Eqn. 8) indicated that temperature (°C) at 40 cm had a significant influence on measured CH_4 fluxes in both the young bog and mature bog (Fig. 3.6; Table A2.1). Modelled CH_4 fluxes increased exponentially with increasing soil temperature at 40 cm in both the young bog and mature bog. The estimated Q_{10} value for the young bog (2.03 ± 0.44) is lower than in the mature bog. While not found to be a significant explanatory variable in our models, water table depth is likely to play an important role in the higher CH_4 fluxes measured (Fig. 3.3c) in the young bog than in the mature bog. Water table coupled with differences in soil temperature at 40 cm (Fig. 3.2f) and higher modelled CH_4 at lower temperatures (a and Q_{10}) in the young bog (Table 3.1. Fig. 3.6).

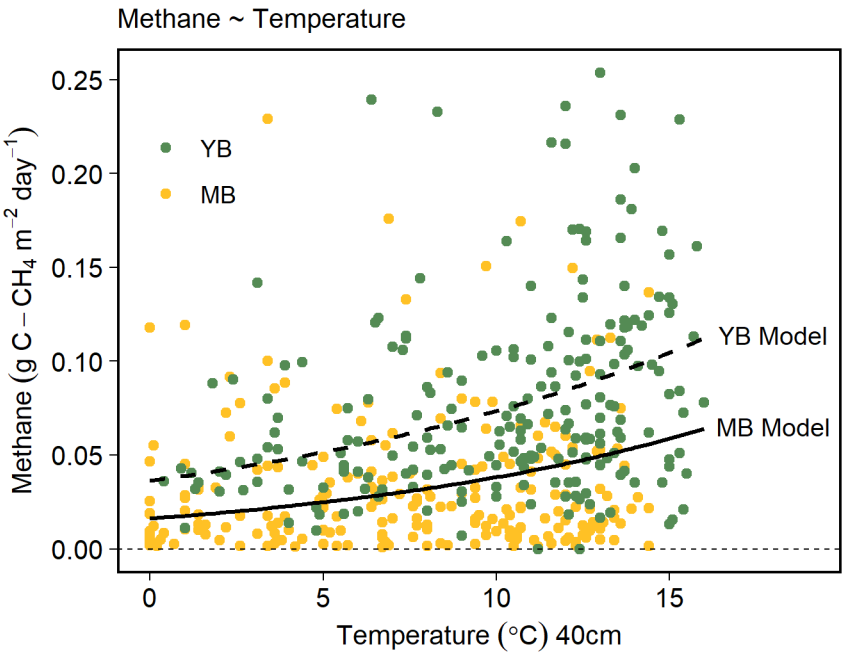

Figure 3.6. Sensitivity of methane fluxes to soil temperature at 40 cm depth (Q_{10}) in the young bog (young bog; green circles) and mature bog (mature bog; golden circles). Dashed line is the young bog Q_{10} model (Q_{10} = 2.03 ± 0.44), solid line is the mature bog Q_{10} model (Q_{10} = 2.36 ± 0.91).

3.3.8 Annual modelled greenhouse gas fluxes

In the YB modelled ER was highest during the cool, dry 2017 growing season (Fig. 3.3a) and cumulative annual ER was greatest during this year (Fig. 3.7a). Modelled ER is reduced in the YB in years when the water table is high (2016 and 2018) and wet, saturated conditions lead to the dominance of anaerobic respiration and reduced GPP and autotrophic respiration. The highest modelled ER in the MB was during the wet, warm 2016 growing season (Fig. 3.3a) and 2016 had the highest cumulative ER (Fig. 3.7a). Modelled ER is reduced in years (2017 and 2018) when soil temperature at 5 cm are lower. While both water table position and soil temperature at 5 cm are important factors in determining annual ER in the young and mature bog, water table plays a more important role in the young bog whereas soil temperature plays a more important role in the mature bog (Fig. 3.5). Non-growing season modelled ER (Fig. 3.3a) was similar across for all years in the YB, however higher modelled ER was found in the mature

bog during 2016 when soil temperature at 5 cm was higher (Fig. 3.2). Modelled ER was found to be higher in the mature bog (Fig. 3.3a) and annual cumulative ER (Fig. 3.7a) was significantly greater in the mature bog ($F_{(1, 2188)} = 294.69$, $P < 0.001$) than in the young bog for all years. Higher ER in the mature bog is due to the drier conditions that support more efficient aerobic respiration and higher GPP which leads to a greater contribution from autotrophic respiration.

The cool, dry, and high PAR conditions during the 2017 measurement period resulted in the highest modelled GPP in the young and mature bog (Fig. 3.3b) and cumulative annual GPP was greatest for both the young and mature bog during this year (Fig. 3.7b). Modelled GPP is reduced in the YB in wet years when the water table is high (2016 and 2018) particularly during the first half off the growing as saturated conditions lead to reduced GPP. Our models found no influence of water table on GPP in the mature bog and the highest modelled GPP in the mature bog was due to the higher PAR in 2017, and modelled GPP was reduced in the mature bog in years with lower PAR (2016 and 2018). While lowered water tables can lead to moisture stress for vegetation and reduced GPP (Breeuwer et al., 2009), the lower water tables in 2017 did not have a negative impact on modelled GPP, likely due to the higher precipitation measured that year (Fig. 3.2b). While PAR and seasonality is an important factor in determining modelled GPP in both the young and mature bog (Fig. 3.5. Fig. A2.1), the water table position plays a more important role in GPP in the young bog only. Annual GPP was higher ($F_{(1, 2188)} = 250.05$, $P < 0.001$) in the mature bog for all years (Fig. 3.7b) due to the drier conditions and no reduction in GPP due to saturation, and a higher vascular green area for photosynthesis due to the presence of ericaceous shrubs (Wilson et al., 2007).

Modelled CH_4 fluxes (Fig. 3.3c) and annual cumulative CH_4 fluxes (Fig. 3.7c) were highest in the young and mature bog during the warm and wet 2016 measurement period. In both the young and mature bog modelled CH_4 is reduced in years when the soil temperature at 40 cm is lower (2017 and 2018) and soil temperature was found to be the main factor influencing modelled CH_4 in both (Fig. 3.6). However, while not identified as a significant factor in our models the difference in water tables likely plays a role in both interannual variations in modelled CH_4 and differences between in modelled CH_4 between the young and mature bog. The wetter conditions in 2016 would have led to increased anaerobic respiration and methanogenesis compared to drier conditions and lower modelled CH_4 in 2017 and 2018. Annual cumulative CH_4 fluxes were

greater in the young bog ($F_{(1, 2188)} = 627.87$, $P < 0.001$) than in the mature bog (Fig. 3.7c) for all years. This is due to the warmer soil temperatures at 40 cm and greater sensitivity of modelled CH_4 to temperature in the young bog, particularly during the non-growing season where modelled CH_4 was greater in the young bog across all years. While, our models likely overestimate non-growing season CH_4 fluxes (Fig. 3.3c), the discrepancy between growing and non-growing season CH_4 model estimates is similar to differences in CH_4 production at <10 °C and 10 – 20 °C (Treat et al., 2015).

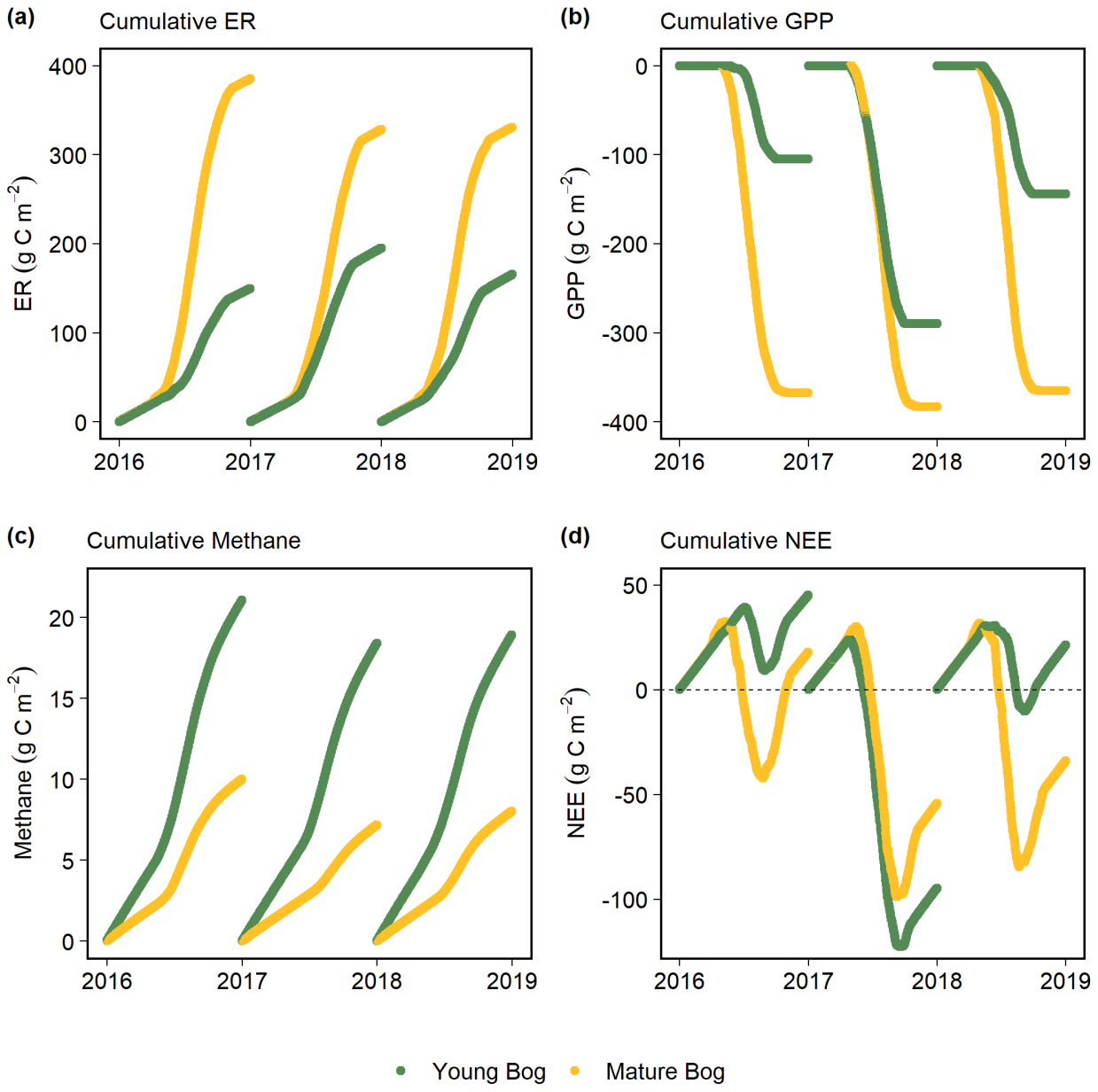

Figure 3.7. Annual cumulative modelled carbon fluxes for 2016, 2017, and 2018 for the young bog (green) and mature bog (golden) estimated from models Eqn. 3 – 8 (Table 3.1). Positive values represent a flux to the atmosphere (loss), negative values represent a flux from the atmosphere (uptake). ER = ecosystem respiration. GPP = gross primary production. NEE = net ecosystem exchange.

3.3.9 Net annual carbon balance

The cumulative net ecosystem exchange (NEE) over the three years (Fig. 3.7d) exhibited interannual variability in both the young bog and mature bog. Both the young and the mature bog exhibited at least one year where they acted as a net source (positive NEE) and net sink (negative NEE) of atmospheric CO_2. In the young bog, the magnitude of net losses (i.e. positive NEE) followed the same trend as the water table position. The largest net loss in the young bog was observed following the warm and wet conditions in 2016, whereas the largest net gain was seen in the cool and dry 2017. In the mature bog, the magnitude of net losses followed the same trend as soil temperature at 5 cm and net losses were observed following the warm and wet conditions in 2016. A net gain was found for both 2017 and 2018 in the mature bog when soil temperatures at 5 cm were lower. Net losses are found in the young bog during wet years, largely due to the suppression of GPP, whereas soil temperature and its impact on ER is the main determinant of annual net losses in the mature bog.

The net ecosystem C flux (NECF), the balance of C lost to the atmosphere as both CO_2 and CH_4 and C, as CO_2, sequestered from the atmosphere was calculated using:

$$NECF = GPP + ER + CH_4 \quad (9)$$

The magnitude of NECF losses followed the same trend as NEE whereby the largest net NECF losses in the young and mature bog were in 2016 due to warm and wet conditions. The average annual cumulative NECF over the three years in the young bog was a net loss of +10 (-46 – +66: 95 % CI) g C m^{-2} whereas there was a net gain of -15 (-74 – +44 % CI) g C m^{-2} in the mature bog. However, despite the asynchronous response of greenhouse gas fluxes to environmental variables between the young and mature bog there was no significant difference between their average cumulative NECF ($P = 0.47$; two-sample t-test. Fig. A2.2). While their NECF does not statistically differ overall, the individual fluxes that comprise the NECF in the young and mature bog do differ. Most importantly the contribution of CH_4 to overall C emissions differs, with 10.8 ± 1.7 % of C emissions as CH_4 in the young bog compared to 2.1 ± 0.1 % of C emissions as CH_4 in the mature bog.

3.4 Discussion

In this study we monitored greenhouse gas exchange (CO_2 and CH_4) over three years along a thermokarst bog thaw transect, contrasting the net greenhouse gas balance of recently thawed young bogs with mature bogs. We found that both CO_2 and CH_4 fluxes were sensitive to environmental conditions, such as water table position and soil temperatures, but the functional relationship and dominant controls of fluxes varied between the young and mature bog stage. This led to largely asynchronous cumulative net annual fluxes, where the young bog was sensitive to wetness and the water table position whereas the mature bog was sensitive to variability in soil temperature. Given the interannual variability in environmental conditions, and the sensitivity of the net ecosystem carbon flux (NECF) to these drivers, three years was not sufficient to determine whether long-term NECFs differed between the young and mature bog stage, or even whether the sites act as a long-term sink or source of atmospheric C. Our findings did however show that recently thawed thermokarst bogs, in our study region of western Canada, are unlikely to act as large sources of greenhouse gas emissions to the atmosphere (Wickland et al., 2006; Johnston et al., 2014) due to rapid mineralization of previously frozen C as has been suggested for thermokarst peatlands in other regions (O'Donnell et al., 2012; Jones et al., 2017). Below we expand on our findings of differences in the functional relationship and dominant controls on greenhouse gas fluxes between the young and mature bog, and the potential implications of these findings for the future net C balance of rapidly thawing peatlands in the sporadic-discontinuous permafrost zone.

3.4.1 Unique environmental conditions and vegetation composition in the young bog

The young and mature areas of the studied thermokarst bogs had distinct differences with regards to vegetation composition, but also environmental variables such as water table position and soil temperatures. The vegetation community in the young bog was dominated by hydrophilic species such as *Sphagnum riparium* and sedges in response to the saturated conditions, that included surface inundation in the wettest years, and an average water table position of -1.5 ± 0.3 cm. The mature bog surface was never inundated, even in the wettest years, and the average water table depth of -23.3 ± 0.5 cm led to the colonization of more drought tolerant *Sphagnum fuscum* and ericaceous shrubs. High water tables in the young bog led to consistently higher soil temperatures at 5 and 40 cm depth, with deep soil temperatures in the mature bog particularly

influenced by seasonal water table variations. In both the young and mature bog wetter years resulted in warmer soil temperatures, whereas cooler temperatures at depth occurred during dry years. While average air temperatures and precipitation over the three years is similar to long-term averages for the area (Alberta Government, 2016), we unfortunately do not know how representative these three years are of long-term water table depth and soil temperatures.

Currently, recently thawed young bogs cover 5.3 – 8.6% of peatland complexes within the sporadic-discontinuous permafrost region of western Canada (Gibson et al., 2018) and their areal extent is expected to increase to its maximum potential within the 21st century (Chasmer and Hopkinson, 2017). However, these young bogs, sometimes called moats, collapse scar bogs or internal lawns, are found anywhere we have peatlands across the circumpolar sporadic-discontinuous region. These characteristic thermokarst bogs with wetter edges and hydrophilic *Sphagnum* spp, and sedge dominated vegetation, giving them a distinct green colour easily visible from publicly available satellite imagery, are found across Alaska (Jorgenson et al., 2001), western Canada (Vitt, Halsey, and Zoltai, 2000), the Hudson Bay Lowlands (Camill et al., 2001), Scandinavia (Johansson et al., 2006), and eastern (De Klerk et al., 2011) and western Siberia (Kremenetski et al., 2003). Further permafrost thaw and the development of thermokarst bogs is expected to occur in peatland complexes across all these C rich regions due to climatic warming (Lawrence, Slater, and Swenson, 2012).

3.4.2 Direct and indirect effects of water table position on CO2 fluxes

We found that the water table position acted as a threshold for both ecosystem respiration (ER) and gross primary production (GPP) in the young bog, whereby both ER and GPP were dramatically reduced when the water table position was above the peat surface and *Sphagnum* capitulum. Such a threshold was not observed under experimentally high water tables in an Alaskan boreal peatland due to the presence of emergent vegetation that continued to photosynthesize even under high water table position (Olefeldt et al., 2017). While variations in the water table position had a much smaller effect in the mature bog, the drier conditions overall led to higher ER and GPP than in the young bog due to a greater contribution from aerobic respiration and no moisture stress on the vegetation.

We found that the annual net ecosystem exchange (NEE) in the young bog (Fig. 3.7d) was highly sensitive to interannual variability in the water table position and wetness, particularly the response of GPP to water table position (Fig. 3.5a, c), resulting in net losses of CO_2 to the atmosphere during wet years and net uptake in the dry year. The lower GPP in the young bog was somewhat unexpected given previous estimates of high rates of net primary productivity in recently thawed thermokarst bogs (Camill et al., 2001) and high measured rates of hydrophilic *Sphagnum* spp. GPP in saturated microforms (Alm et al., 1999). However, in very wet years, such as 2016 and 2018, the amount of available light reaching the vegetation for photosynthesis may be significantly reduced due to surface reflection (Sand-Jensen, 1989) and a higher proportion of aromatic dissolved organic C runoff from the adjacent plateau following snowmelt (Olefeldt and Roulet, 2012; Burd et al., 2018) absorbing UV-light (Vähätalo et al., 2003). ER in the young bog is dependant on water table directly through aerobic/anaerobic conditions for heterotrophic respiration (Walz et al., 2017), but also indirectly though the influence on GPP and the contribution from autotrophic respiration (Frolking et al., 2002). Thus, lower ER in wet years when GPP is reduced suggests that autotrophic is a large component of ER (Crow and Wieder, 2005) and that there is limited contribution of deep, heterotrophic respiration of previously frozen peat to surface CO_2 emissions (Estop-Aragonés, Czimczik, et al., 2018; Voigt et al., 2019).

In contrast, the annual NEE in the mature bog was much less sensitive to interannual variations in the water table position and there was no evidence of a similar water table threshold effect on ER and GPP as found in the young bog. The water table influence on GPP in the mature bog is indirect as it promotes colonization of *Sphagnum fuscum*, a species proficient at wicking water up to the capitula (Rydin, 1985). There was no evidence of reduced GPP due to drying induced vegetation damage (Mezbahuddin, Grant, and Flanagan, 2016) even in dry years. Unlike in the young bog, the peat surface was never inundated and the average water table depth in the mature bog over the three years is within range of optimal water table depths for northern peatland GPP and the success of mesic *Sphagnum* spp. found there (Silvola and Aaltonen, 1984; Tuittila, Vasander, and Laine, 2004; Munir et al., 2015). Higher ER in the mature bog than in the young bog is due to the upper oxic zone supporting more efficient aerobic respiration (Blodau and Moore, 2003). While ER did increase with a deepening of the water table (Fig. 3.4b), suggesting that heterotrophic respiration in the mature bog is sensitive to the water table position, this did

not yield higher ER in dry years as drier conditions also led to lower temperatures which acted to reduce ER.

3.4.3 Impact of soil temperatures on CO_2 fluxes

We found that ER was driven by near-surface soil temperatures at 5 cm depth, rather than at 40 cm depth. ER in the mature bog was particularly sensitive to temperature variability at 5 cm depth (Fig. 3.4b, d), but less so to water table fluctuations as changes in water table position well below the surface are unlikely to have a significant impact of ER (Juszczak et al., 2013). Whereas any temperature response of ER in the YB was largely masked by the overriding effect of the water table (Fig. 3.4a, c) and whether it was just above or below the peat surface.

The mature bog had the highest soil temperatures at 5 cm in 2016 (Fig. 3.2a), but more importantly water table position and wetness (Fig. 3.2d) were highest. Wetter years, as in 2016 and 2018, led to higher soil temperatures, and as a result higher annual ER (Fig. 3.7a). As GPP did not vary between years, we found that annual NEE in the mature bog was highly sensitive to the response of ER to interannual variability of soil temperatures at 5 cm, which has been shown to be the major driver of peatland ER under oxic conditions (Basiliko et al., 2005; Updegraff et al., 2001; Dorrepaal et al., 2009)

Non-growing season ER was similar between the young and mature bog. ER from the non-growing season contributed 25.8 ± 3.8% and 15.7 ± 0.5% to the annual cumulative ER in the young and mature bog respectively, and these estimates are similar to non-growing season ER estimates from other thermokarst bogs (Euskirchen et al., 2014). In both the young and mature bog roughly two-thirds of these non-growing season CO_2 emissions were observed in early winter, i.e. October – December. Increased availability of labile substrates following a full growing season and warm soil temperatures near 0 °C can lead to enhanced non-growing season CO_2 losses (Larsen et al., 2007; Mauritz et al., 2017). Rising winter temperatures and increased snow accumulation could lead to enhanced winter microbial respiration and large losses of CO_2 (Natali et al., 2019), however this is unlikely at our study site as ER is controlled by temperatures at 5 cm depth with no evidence of a contribution from depth.

3.4.4 Increased CH_4 emissions in the recently thawed thermokarst bog

We found that the young bog had substantially higher CH_4 emissions than the mature bog (Fig. 3.3c), with average annual emissions of 19.5 ± 1.6 g C-CH_4 m^{-2} and 8.4 ± 1.7 g C-CH_4 m^{-2} respectively (Fig. 3.7c). Annual CH_4 emissions were found to be highly sensitive to temperature at 40 cm (Fig. 3.6), resulting in increased CH_4 during warmer years (Turetsky et al., 2014). Interestingly, temperature at 40 cm and water table depth were found to not be independent. Wetter years were found to have substantially warmer deep temperatures in both the young and mature bogs, and the higher water depth in the young bog resulted in consistently higher temperatures at 40 cm than in the mature bog. The higher water table and resulting higher soil temperatures at 40 cm (Fig. 3.2f) in the young bog is likely an important factor is explaining the greater CH_4 emissions found in the young bog compared to the mature bog, and the higher emissions found in wet, warm, years (Fig. 3.7c).

Together with temperature, the oxic/anoxic boundary defined by the water table depth, and the vegetation community control the magnitude of CH_4 emissions (Olefeldt et al., 2013). The saturated, anoxic conditions in the young bog, along with a vegetation community consisting of *Sphagnum* and vascular plant spp. associated with quick decomposition and labile litter inputs, provided prime conditions for CH_4 production and increase the sensitivity of methanogenesis to increasing temperatures (Bridgham et al., 2013; Turetsky et al., 2008; Öquist and Svensson, 2002). Predicted increases in thermokarst development in carbon-rich, boreal permafrost peatlands (Olefeldt et al., 2016), along with the temperature sensitivity of sedge dominated, saturated areas such as recently thawed thermokarst bogs (Hartley et al., 2015), may lead to increased CH_4 emissions and a net radiative greenhouse gas forcing effect at the landscape level (Helbig, Chasmer, Kljun, et al., 2017).

3.4.5 Effect of thaw on annual C balances

Our three-year average NECF in the young and mature bog exhibits high interannual variability (Fig. A2.2) and it has been suggested that to accurately estimate whether the long-term NECF is significantly different from 0 g C m^{-2} i.e. whether the peatland is a long-term sink or source, several decades of measurements may be required (Roulet et al., 2007). However, over our three-year measurement period we found no evidence of a large net source or sink of atmospheric C

following permafrost thaw. Similar to previous studies (Euskirchen et al., 2014), the annual C balance of thermokarst bogs is highly dependant on interannual variability in climate and environmental variables. However, we show here that while changes in the hydrological regime following thaw directly and indirectly govern C fluxes, the C sink or source potential of recently thawed and mature sites are controlled by differing functional responses. Previous studies have indicated little impact to the C sink potential at the landscape level with thawing in boreal permafrost peatlands (Helbig, Chasmer, Desai, et al., 2017; Myers-Smith et al., 2007), an increase in C sequestration (Myers-Smith et al., 2008; Camill et al., 2001), while others have suggested thawing will result in increased C losses (Wickland et al., 2006; Johnston et al., 2014) Under an exceedingly warmer climate this delicate balance between C uptake and losses may shift leading to increased net losses of atmospheric C and a reduction in boreal peatlands C sequestration ability.

3.5 Conclusions

In this study we showed that interannual variability in the NECF was asynchronous for a young and mature thermokarst bog where the young bog was most sensitive to the water table position and its control on GPP, while the mature bog was most sensitive to the response of ER to soil temperatures. Our results highlight that for modelling attempts of the permafrost C feedback to improve, future work should include the incorporation of the functional response of greenhouse gas fluxes from differing stages of thermokarst peatland succession into process-based models predicting the impact of thaw on boreal permafrost peatlands. Due to interannual variability of environmental controls we are unable to determine whether the long-term NECF differs between young and mature bog stages or whether they act as long-term net sinks or sources. However similar to previous findings (Johnston et al., 2014) the initial decades post-thaw represent a large source of CH_4 that may have important implications for net radiative forcing at the landscape level (Helbig, Chasmer, Kljun, et al., 2017). We do not find evidence of a significant contribution of deep, previously frozen peat to surface emissions which supports previous findings from the study site of little to no losses or decomposition of previously frozen peat following thaw (Estop-Aragonés, Czimczik, et al., 2018; Heffernan et al., 2020). Despite not being able to determine the long-term NECF of the young and mature bog, we show that it is

unlikely that recently thawed peatlands in western Canada act as significant C sources during the young thermokarst stage.

4. Stability of soil carbon following permafrost thaw: no evidence of increased soil enzyme activity in recently thawed peat and elevated activity in near-surface peat is driven by vegetation succession

Abstract

Boreal peatlands are important carbon sinks characterized by slow rates of microbial decomposition due to cool, waterlogged conditions and recalcitrant plant material. However, recent studies in permafrost peatlands have indicated that warming temperatures, shifts in vegetation, and increased microbial activity on previously frozen peat in the initial decades following permafrost thaw and thermokarst collapse can lead to rapid carbon loss and increased greenhouse gas emissions. We investigated the factors controlling soil enzyme activity, and the stability of previously frozen, deep peat, following thaw in a boreal permafrost peatland in western Canada. We collected shallow (near-surface) and deep (previously frozen) peat samples in a thermokarst bog that thawed ~30 years (young bog) and ~200 years (mature bog) ago, along with six peat mesocosms from the young and mature bogs surface that were maintained under either oxic or anoxic conditions. The young bog surface was saturated and dominated by *Sphagnum riparium* and sedges. The drier mature bog had an average water table 24 cm below the surface and was dominated by *Sphagnum fuscum* and ericaceous shrubs. Analysis of soil enzyme activities exhibited no evidence of elevated peat decomposition at depth in the initial decades following permafrost thaw. Both field and mesocosms approaches demonstrate that availability of labile litter inputs and reduced peat quality, assessed by FTIR ratios, are the main factors constraining enzyme activity at depth. Our study highlights that deep, previously frozen peat may be resilient to increased microbial decomposition following permafrost thaw in boreal peatlands when substrate availability is limited.

4.1 Introduction

Northern peatlands are a globally important store of soil organic carbon (C) and 345 ± 50 Pg C of their 500 ± 100 Pg C stores are found within the permafrost region (Yu, 2012; Hugelius et al., 2014). Long-term accumulation of peat C stores is due to slow rates of microbial decomposition (Clymo, 1984) facilitated by cold, waterlogged conditions and the production of recalcitrant litter by *Sphagnum* mosses (Moore and Basiliko, 2006; Verhoeven and Toth, 1995). Increased rates of permafrost thaw in ice-rich peatlands driven by warming temperatures leads to thermokarst development (Kokelj and Jorgenson, 2013) and currently ~20% of the permafrost region's areal extent are thermokarst landscapes (Olefeldt et al., 2016). Thermokarst development exposes previously frozen C stores (Schuur et al., 2008), and can lead to enhanced microbial decomposition and mineralization of previously frozen C into greenhouse gases (Dorrepaal et al., 2009). However, if recalcitrant upon thawing there may be little to no contribution of previously frozen C to greenhouse gas emissions in thermokarst peatlands (Estop-Aragonés, Cooper, et al., 2018). Previous studies using a chronosequence approach to estimate the change in C stores following thaw have indicated large losses of C (Jones et al., 2017) and have ruled out large losses of C (Heffernan et al., 2020), but are limited by the large uncertainties and poor precision of the chronosequence approach. Direct approaches measuring the impacts of thawing on the net C balance using eddy-covariance (Helbig, Chasmer, Desai, et al., 2017) or chamber based (Wickland et al., 2006) flux measurements are also limited due to spatial and temporal heterogeneity in the response of fluxes to environmental drivers (Myers-Smith et al., 2007). It is currently unknown to what degree permafrost thaw will impact microbial decomposition, however focusing on microbial activity may provide an indication of the long-term stability of previously frozen C stores and compliment chronosequence and flux measurement studies.

Thermokarst collapse along peat plateau margins leads to a successional trajectory over several centuries that have distinct stages in terms of environmental conditions and vegetation composition (Camill, 1999; Jorgenson et al., 2010). In subsequent autogenic peatland development, there is a shift from raised, well drained permafrost peat plateaus characterized by a dry, aerobic active layer and *Picea mariana* and *Cladonia* spp. to thermokarst bogs that have a near-surface water table position (Quinton *et al.,* 2009). This causes a ~30% increase in species diversity characterized by *Sphagnum* spp., *Carex* spp., and other common bog vascular plant

species (Beilman, 2001; Camill, 2005). The early stages of thaw are characterised by an inundated surface and fast-growing vegetation, such as flood tolerant *Sphagnum riparium*, that has relatively labile plant litter (Camill, 1999; Turetsky, 2003). Following a century or more, peatland succession and accumulation results in drier surface conditions and more drought tolerant *Sphagnum* species with less labile litter, such as *S. fuscum* and *S. magellanicum*, are dominant along with ericaceous shrubs (Johnson and Damman, 1991). Historically, when these dry conditions persist for centuries to millennia thermokarst peatlands have re-aggraded permafrost in a natural cycle of permafrost degradation and aggradation (Zoltai, 1993). However, this is unlikely to happen within the sporadic-discontinuous permafrost region, where the abundance of thermokarst peatlands is predicted to increase (Quinton et al., 2011; Carpino et al., 2018).

Peat decomposition is governed directly by the impact of water table position on temperature and oxygen availability, and indirectly by impacts on the vegetation community and its litter inputs (Laiho, 2006). The water table position determines oxygen availability for respiration, with 1 – 3 cm beneath the water table being anoxic (Blodau et al., 2004) and influences the structure of the vegetation community (Robroek et al., 2007) which in turn impacts the quality of litter inputs (Laiho et al., 2003) and root exudates (Robroek et al., 2016). Litter and plant-root exudate inputs regulate the composition and activity of the microbial community as they provide the substrate and nutrients used as an energy source (Borga et al., 1994). The activity of extracellular enzymes produced by the microbial community control the rate limiting step of decomposition and at which solubilized substrates become available for microbial metabolism (Bell et al., 2013; Luo et al., 2017). The microbial communities activity is determined by the sensitivity of these extracellular enzymes to the water table position and its influence on peat substrate and nutrient availability (Briones et al., 2014; Sinsabaugh et al., 2008), however the main drivers among these still remains poorly known.

Litter type and chemistry, in particular that derived from *Sphagnum* spp., are important controls on microbial decomposition and C mineralization in to CO_2 and CH_4 (Limpens et al., 2017; Sjögersten et al., 2016; Strakova et al., 2011). *Sphagnum* mosses produce decay resistant litter with poor organic matter quality (Hájek et al., 2011) and phenolic compounds that inhibit the activity of extracellular hydrolytic enzymes and microbial decomposition (Jassey et al., 2011).

Oxidative enzymes are involved in the degradation of phenolic compounds (Sinsabaugh, 2010), but their activity has been shown to be limited in conditions with low oxygen, temperature, and pH (Freeman et al., 2001; Freeman et al., 2002; Pind et al., 1994). Studies have shown that seasonal variations and increases in temperature (Jassey et al., 2013; Pinsonneault et al., 2016), changes to water table position (Toberman et al., 2008), and short periods of oxygenation (Brouns et al., 2014) can increase oxidative enzyme activity and release the phenolic inhibition on hydrolytic enzymes leading to enhanced C decomposition (D'Andrilli et al., 2010).

Recent research has highlighted that variations in plant litter inputs are of greater importance to decomposition than water table position and oxygen availability (Kaštovská et al., 2018; Straková et al., 2012). Shifts in vascular plant communities due to changing water tables, temperature, and nutrient status (Bragazza, 2006; Dieleman et al., 2015) can have important implications for microbial communities and activity, leading to increased C decomposition (Bragazza et al., 2015; Robroek et al., 2016; Walker et al., 2016). Following permafrost thaw the shifts in the abiotic and biotic controls on microbial decomposition may have cascading effects on the microbial community structure and activity, potentially driving deep, old C losses and impacting the long-term stability of permafrost peatland C (Keuper et al., 2012; Finger et al., 2016).

In this study the main objective was to assess the vulnerability of deep, previously frozen C to enhanced microbial decomposition and determine the main drivers of enzymatic activity following permafrost thaw in a boreal peatland complex. We measured enzymatic activity along a space-for-time chronosequence in areas that thawed ~30 and ~200 years ago. In both areas we measure activity on shallow near-surface peat that accumulated post-permafrost thaw and deep peat that accumulated pre-permafrost thaw. This allowed us to determine whether previously frozen peat demonstrated evidence of elevated enzyme activity that would be an indicator of rapid peat decomposition in the initial decades following thaw. We also used a laboratory-based peat mesocosms experiment on surface peat to evaluate whether water table position or vegetation type was the main control on enzyme activity. We hypothesize that; (1) deep, pre-thaw peat has increased rates of hydrolytic enzymatic activity in the initial decades following thaw that declines following centuries of thaw and (2) the greatest enzymatic activity will occur on shallow, post-thaw peat. We further hypothesize that (3) higher rates on enzymatic activity will be driven by vegetation type and not oxic/anoxic state. This study highlights the importance

of litter inputs and peat lability when considering the impact of permafrost thaw on boreal peatland C stores.

4.2 Methods

4.2.1 Study site

This research was carried out at a permafrost peatland complex in the sporadic-discontinuous permafrost zone of the Mackenzie River Basin in western Canada (59.5°N, 117.2°W) (Brown et al., 1997; Heginbottom, Dubreuil, and Harker, 1995) (Fig. 4.1a). The site has a continental climate with an average annual rainfall at Meander River (50 km south of the site) of 391 mm and an average annual temperature of -1.8°C (Climate-Data.org, 2019). Permafrost peatland complexes cover ~25% of the region and the study area is a heterogenous landscape of peatlands and upland forests (Hugelius et al., 2014; Vitt et al., 2000). These peatland complexes are a mix of peat plateaus interspersed with thermokarst bogs, channel fens, and ponds (Quinton et al., 2011). Permafrost is primarily found in black spruce dominated peatland ecosystems in the area, although it has also been found in areas with shallow organic layers overlaying coarse grained substrates (Holloway and Lewkowicz, 2019). Permafrost here is warm (near 0 °C), fragmented, and susceptible to thaw (Smith et al., 2005, 2009) and complete permafrost loss is predicted to occur over the next ~50 years (Chasmer and Hopkinson, 2017).

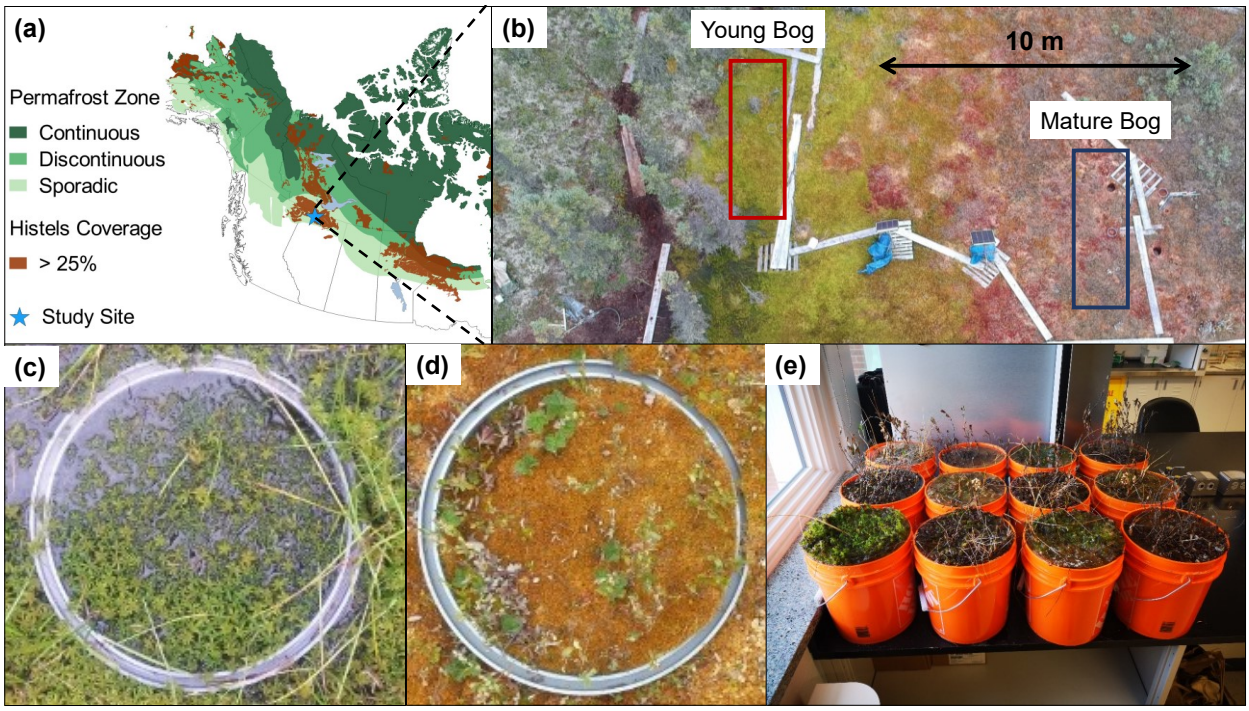

Figure 4.1. Study area for assessing impact of permafrost thaw on enzymatic controls on peat decomposition. (a) Map of Western Canada depicting permafrost zonation (Brown et al., 1997) in green, areas with > 25% coverage of permafrost peatland soils (Hugelius et al., 2014) in brown, and a blue star indicating the study site in Alberta, Canada (59.5°N, 117.2°W). (b) Aerial image from 2018 growing season of transect. Red box indicates areas where Young Bog samples were taken from, blue box indicates area where Mature Bog samples were taken. (c) Close up image of surface vegetation and water table position in the Young Bog. (d) Close up image of surface vegetation in the Mature Bog. (e) Image of peat mesocosms used in lab experiment. (Aerial photo credit: Olefeldt, David).

Organic matter began accumulating in the study area ~8,800 years ago (Heffernan et al., 2020). The study site transitioned through multiple developmental peat stages; initiating as marsh and then, transitioned to a fen and later a bog stage (Heffernan et al., 2020). The site transitioned from a bog to a peat plateau once permafrost aggradation occurred at the site ~1,800 years ago. This timing is consistent with other peatlands within the current sporadic-discontinuous permafrost zone of western Canada (Loisel et al., 2014; Pelletier et al., 2017). Permafrost thaw at the study site began ~200 years ago and continues to occur today. Hereafter, peat that

accumulated prior to permafrost thaw in referred to as old deep peat, and peat that accumulated after permafrost thaw and thermokarst bog development is referred to as new, shallow peat.

The study site is a transect along a thermokarst bog that is adjacent to a raised (1 – 2 m) intact permafrost peat plateau. The thermokarst bog is differentiated in to a young and mature bog stage based on proximity to the thawing edge of the peat plateau, the vegetation community, and water table position (Fig. 4.1b). The young bog thawed most recently, ~30 years ago, and is directly adjacent to the peat plateau. The mature bog thawed ~200 years ago and is >10m from the peat plateau. The depth of new, shallow peat from the surface (i.e. the depth in the peat profile from the surface to the transition from peat plateau to thermokarst bog indicating thaw) in the young bog is 29 cm and 71 cm in the mature bog. The young bog (YB) is saturated with an average growing season water table depth of -1.1 ± 3.5 cm and its vegetation community is dominated by the hydrophilic species *Sphagnum riparium,* rannoch rush (*Scheuchzeria palustris)*, bog-sedge (*Carex limosa)*, and cotton-grass (*Eriophorum vaginatum)* (Fig. 4.1c). The drier mature bog (MB) has an average growing season water table depth of -23.5 ± 3.9 and its vegetation community consists of *Sphagnum fuscum, Sphagnum magellanicum,* leather leaf (*Chamaedaphne calyculata),* bog rosemary *(Andromeda polifolia),* cloudberry *(Rubus chamaemorus), Eriophorum vaginatum* tussocks, and some black spruce (*Picea mariana)* regrowth (Fig. 4.1d).

4.2.2 Field sampling

We extracted peat cores from two locations along a space-for-time thaw chronosequence to assess the vulnerability of peat to increased extracellular enzyme activity following permafrost thaw. Cores were extracted once a month from May – September 2018 along a 20 m transect from each location, totalling 5 cores from both the YB and MB to a depth of 160 cm. Surface cores for the top 0 – 30 cm were extracted manually using a cutting tool. Below 30 cm we used a Russian peat corer (4.5 cm inner-diameter, Eijkelkamp, Giesbeek, Netherlands). Using the Russian corer, cores were taken at each location from two boreholes located ~30 cm apart, alternating between both in 50 cm long sections with a 10 cm overlap. Each core section was then placed in a halved PVC tube and divided into 15 segments based on the following depths; 0 – 5 cm, 5 – 10 cm, 10 – 20 cm, 20 – 30 cm, 30 – 40 cm, 40 – 50 cm, 50 – 60 cm, 60 – 70 cm, 70 – 80 cm, 80 – 90 cm, 90 – 100 cm, 100 – 110 cm, 110 – 120 cm, 130 – 140 cm, and 150 – 160

cm. A total of 132 peat samples were extracted over the study period. Each peat sample segment was then placed in zipper plastic storage bags and transported back to the laboratory in a cooled container. Peat samples were stored at 4°C in the laboratory before homogenization and analysis.

In order to assess whether deep, pre-thaw peat that accumulated before permafrost thaw was vulnerable to increased enzyme activity following thaw, we categorized the 15 peat measurement depths into deep peat that accumulated pre-thaw and shallow peat that accumulated post-thaw. This resulted in four categories of peat layer based on whether the core was taken from either the YB or MB, and whether the peat from each was from a shallow or deep peat depth. These four categories of peat layer are hereafter referred to as (a) YB Shallow (YB; depth 0 – 31 cm), YB Deep (YB; depth 32 – 160 cm), MB Shallow (MB; depth 0 – 71 cm), MB Deep (MB; depth 72 – 160 cm). All measured extracellular enzyme activities, peat pore water chemistry, and environmental variables are presented in each of these four peat layer categories.

Peat pore water samples were taken at all 15 peat sampling depths mentioned above from pre-installed pore water peepers. Three 60 ml pore water samples were taken at the same time as peat extraction and each water sample was filtered immediately through 0.7 μm pore size glass fiber filters (GF/F Whatman) into amber glass bottles. One of every 60 ml sample depth was acidified with 0.6 mL 2N HCl to prevent further microbial activity during transport back to the laboratory (Burd et al., 2018). Pore water samples were transported in a cooled container and stored at 4 °C prior to analysis.

We used Fourier transform infrared (FTIR) spectroscopy from peat elemental analysis to determine peat humification on peat samples collected from cores in 2015 (Heffernan et al., 2020). We analyzed 8 and 10 samples from the YB and MB respectively for FTIR using an Agilent 660 FT-IR spectrometer (Agilent Technologies Inc., Santa Clara, CA, USA) and each sample was organised into its relevant peat layer based on sample depth. Peak height ratios were calculated for absorption at ~1630 cm^{-1} and 1090 cm^{-1} to determine the abundance of aromatic and carboxylate moieties relative to polysaccharides (Artz et al., 2008; Broder et al., 2012), and higher values represent higher humification, i.e. degree of peat decomposition.

4.2.3 Pore water analyses

Chemistry of peat pore water samples was monitored for dissolved organic carbon, dissolved nitrogen, phenolics, pH, and anion analysis, as well as the absorbance over the full UV-visible (UV-vis) spectra. Differences in number of porewater samples analyzed between the YB and MB are due to the differences in water table depths and availability of sufficient porewater samples. The lower water table depth in the MB resulted in less field samples collected. Continuous bihourly measurements of soil temperature (°C) at 5, 10, 40, 100, and 150 cm were taken using installed Hobo 8k Pendant (Onset Computer, Bourne, MA, USA) loggers in all bog stages throughout the measurement period. Pore water pH was measured on 98 (YB: 57, MB: 41) filtered samples within 12 hours of sampling using a ProfiLine pH 3310 meter (Xylem Analytics, Germany). We determined the concentrations of 68 (YB: 38, MB: 30) phosphate (PO_4^{3-}; $\mu g\ L^{-1}$) filtered but not acidified peat pore water samples using colorimetric methods on a SmartChem® 200 discrete wet chemistry analyzer (Westco Scientific, Milford, MA, USA). Lower number of analyzed PO_4^{3-} samples included in data analysis is due to certain samples being removed as they were under limit of quantification.

Dissolved organic carbon (DOC) and total dissolved nitrogen (TN) concentrations were determined from 101 (YB: 58, MB: 42) acidified pore water samples collected over the growing season using the combustion catalyst method on a TOC-L combustion analyser with a TNM-L module (Shimadzu, Kyoto, Japan). The concentration of phenolic compounds was determined for 101 (YB: 56, MB: 45) peat pore water samples throughout the growing season and lower sample numbers that DOC and TN due to sampling error. We quantified the phenolic contents in a 3.5 mL aliquot of filtered sample using a Folin-Ciocalteau assay and standard curves based on gallic acid equivalent (GAE) (Jassey et al., 2011). Absorbance of each sample was measured at 760 nm (A_{760}) wavelength on a Synergy™ HT spectrophotometer (Biotek, Winooski, VT, USA) and results were expressed as GAE per litre of peat pore water (GAE mg L^{-1}).

We measured the spectra of UV-vis absorbance, between 230 and 600 nm, for 101 (YB: 58, MB: 42) pore water samples collected over the growing season to assess relative aromatic content and average molecular weight using the specific UV absorbance at 254 nm (SUVA, L mg C^{-1} m^{-1}) and spectral slope between 250 – 465 nm ($S_{250-465}$, nm^{-1}) respectively. A 4 mL aliquot of filtered sample was transferred to a 1 cm path-length quartz cuvette and analysed using a Flame-DA-

CUV-UV-VIS light source and Flame-S spectrophotometer (Ocean Optics, Dunedin, FL, USA). The decadal absorbance at 254 nm (cm^{-1}) was divided with DOC concentration (mg C L^{-1}) and multiplied the value by 100 to calculate SUVA (Weishaar et al., 2003). Spectral slopes ($S_{250-465}$) were estimated using a linear fit of the log-transformed absorption spectra between 250 – 465 nm. High SUVA values indicate a high aromatic content while high $S_{250-465}$ values indicate a low average molecular weight or decreasing aromaticity (Hansen et al., 2016).

4.2.4 Enzyme activity assays

We performed hydrolytic enzyme assays for four enzymes; phosphatase (PHOS), β-N-glucosaminidase (NAG), β-glucosidase (BG), and β-cellobiosidase (CB) using fluorogenic 4-methylumbelliferone (MUF) labelled substrates (Dunn et al., 2014). These enzymes are involved in the degradation of carbohydrates and polysaccharides (carbon acquisition; BG and CB), the mineralization of nitrogen from chitin and proteins (NAG), and phosphorus mineralization (PHOS) (Machmuller et al., 2016). We assayed oxidative enzyme activity by measuring laccase (LAC) activity using syringaldazine (Criquet et al., 2000; Jassey et al., 2012).

We extracted enzymes by adding 5 g of homogenised wet peat to 50 mL 0.1 M $CaCl_2$, 0.5 mL Tween 80 and 20 g polyvinylpolypyrrolidone and shaking at room temperature for 90 minutes (Criquet et al., 1999). This mixture was then centrifuged, and the supernatant was filtered through 0.2 µm pore size glass fiber filters (GF/C Whatman). This filtrate was then placed inside cellulose dialysis tubing (10 kDa molecular mass cut-off) and covered with polyethylene glycol to concentrate the filtrate. Concentrated extracts were brought back to 40% of their initial volume by adding 20 ml of phosphate buffer (pH 5.6) and separated into two equal fractions. One of these fractions was then stored at 4 °C overnight and contained the active enzymatic extract, whereas the other fraction was boiled for 3 hours at 90 °C and was used as the control assay. Hydrolytic enzyme activities were measured spectrophotometrically at 365 nm excitation and 450 nm emission in black 96 well microplates. Plates had 250 µL of enzymatic extract or control and 38 µL of enzymatic substrate (PHOS, NAG, BG, CB) added to each well and were then incubated for 3 hours at 25°C. Phenol oxidases were measured in clear 96 well plates. Each well contained 150 µL of enzyme extract with 2 µL of LAC (5 mM; $\varepsilon^M = 65{,}000\ M^{-1}\ cm^{-1}$) and was monitored at 525 nm (Jassey et al., 2012; Criquet et al., 2000). To determine dry weight, peat material was dried at 100 °C for 24 hours. Data for hydrolytic enzyme activities were

expressed as nanomole per gram of dry soil per hour (nmol g^{-1} $hour^{-1}$) and as micromole per gram of dry soil per hour (μ mol g^{-1} $hour^{-1}$) for oxidative enzyme activity.

4.2.5 Peat mesocosms

In September 2018 we extracted 6 near-surface, shallow peat mesocosms from both the YB and MB for a total of 12 mesocosms (Fig. 4.1e). Mesocosms were extracted as a single section to a depth of 23 ± 1 cm using cutting tools and placed inside 25 × 20 cm plastic buckets. Careful consideration was taken when extracting each mesocosm from the peatland to not disturb or damage the vegetation. Collected peat mesocosms were then transported back to the laboratory and stored out of direct sunlight and at room temperature (19 – 23 °C). Once in the laboratory each mesocosm was completely saturated with distilled water and waterlogged conditions were maintained by adding distilled water every 1 -2 days for 4 months to develop and maintain anoxic conditions. We tested the dissolved oxygen (DO) concentration (%), temperature, and pH of pore water at 5, 10, 15, and 20 cm depth in each mesocosm. We consider pore water that has a DO concentration lower than 10% to be anoxic. After 4 months, 3 YB and 3 MB peat mesocosms were chosen to be drained. To drain each of these 6 mesocosms, multiple holes were drilled on the bottom and sides of each plastic bucket and it was left to drain for 72 hours. We then measured the DO, temperature, and pH of each mesocosm using the YSI Professional Plus multiparameter water quality instrument to ensure that a) the undrained mesocosms remained anoxic and b) the DO concentration of the drained mesocosms was >10% at all depths indicating that it was under oxic conditions. This resulted in 4 groups of peat mesocosm conditions; (1) YB vegetation under anoxic condition; YB Anoxic, (2) YB vegetation under oxic conditions; YB Oxic, (3) MB vegetation under anoxic condition; MB Anoxic, (4) MB vegetation under oxic conditions; MB Oxic.

We extracted peat samples at 0 – 5 cm, 5 – 10 cm, and 10 – 20 cm in each mesocosm using cutting tools 96 hours after draining. A total of 36 peat samples were collected, 8 samples from each peat mesocosm group, and stored at 4 °C before homogenization and analysis. Assays for enzyme activity were carried out on all 36 mesocosm peat samples (18 each from the YB and MB) as described for field samples above. Peat pore water samples were collected at 5, 10, and 15 cm in every peat mesocosm. These pore water samples were treated the same as pore water

samples collected from the field (as described above) and used to determine phenolic concentrations, pH, DOC concentrations, SUVA, and $S_{250-465}$.

4.2.6 Statistical analyses

We evaluated whether enzymatic activity from field measurements was different in both shallow and deep peat layers between the YB and MB using the principal response curve (PRC) method (Van Den Brink and Ter Braak, 1999). PRCs were used to assess the differences in enzyme activity over the growing season between the YB and MB in both shallow and deep peat layers and was applied on standardized enzyme activity data to normalize measured rates. In diagrams, the curves represent the seasonal trajectory for enzyme activity in the MB as a horizontal line maintained at 0 and deviation of enzyme activity in the YB from activity in the MB is represented by a dashed line with points. Species (enzyme activity) scores plotted on the right Y-axis are used to infer about the response of the activity of individual enzymes between the YB and MB where a positive score indicates higher activity in the MB and a negative score indicates higher activity in the YB.

We performed ANOVAs and Bonferroni post-hoc tests on linear mixed effects models to test for significant seasonal trends and evaluate differences between the four different peat layers (YB Shallow, YB Deep, MB Shallow, MB Deep) in; a) site hydrology and pore water chemistry and b) enzymatic activity. In all model's sampling month and peat layer were included as fixed effects and sample depth was included as a random effect.

To evaluate the drivers of enzyme activity in field samples redundancy analysis (RDA) was applied to log-transformed and standardized enzymatic data using biotic and abiotic environmental data as explanatory variables. The selection of explanatory variables used were determined using automatic stepwise model selection permutation tests, that included 1,000 permutations, and Akaike Information Criterion (AIC). The significance of our RDA model and each explanatory variable was tested using 1,000 permutations (Jassey et al., 2011). Additionally, we performed variance partitioning using RDA and adjusted R^2 to compare the individual effect of each explanatory variable on enzyme activity (Peres-Neto et al., 2006).

The influence of peat quality on field enzyme activity measurements was tested using a linear regression of the response of enzyme activity to peat humification (FTIR). We summarized the

activity of multiple enzymes, including both hydrolytic and oxidative, using a multifunctionality index based on *z*-scores (Allan et al., 2015). This enzyme activity proxy summarizes the activity of multiple enzymes so that high enzyme multifunctionality values indicate high activity of many, but not necessarily all, measured enzymes. The enzyme multifunctionality values for each peat layer (YB Shallow, YB Deep, MB Shallow, MB Deep) over the measurement period were averaged (± one standard deviation) and the response of enzyme multifunctionality to the average FTIR ratio (± one standard deviation) for each corresponding peat layer was tested using linear regression.

Our peat mesocosm experiment was used to assess whether water table position or vegetation type was the main control on enzyme activity and the activity of the four hydrolytic enzymes measured were summarized to calculate a hydrolytic enzyme multifunctionality ($Hydro_{enz}$) estimate similar to our enzyme multifunctionality estimate of field based enzyme measurements. To test for differences in $Hydro_{enz}$ between the YB Oxic, YB Anoxic, MB Oxic, and MB Anoxic mesocosms we used two-way ANOVAs and Tukey post-hoc tests. Furthermore, we built a structural equation model (SEM) to investigate the influence of vegetation, pore-water quality, and oxidative enzyme activity on hydrolytic enzyme activity ($Hydro_{enz}$) in our mesocosms. The determination of explanatory variables that were the main drivers of $Hydro_{enz}$ in our SEM was based on step-wise selection of variables guided by AIC scores (Jassey et al., 2018). The adequacy of our model was tested using AIC values and goodness of fit index (CFI), including Fischer's C statistic and p-values based on chi-square tests (Grace et al., 2010; Jonsson and Wardle, 2010). All pathways of our SEM model included mesocosm as a random effect.

All statistical analysis was carried out in R (Version 3.4.4) (R Core Team, 2015) using the nlme, vegan, piecewiseSEM, and ggpubr packages (Pinheiro, Bates, and DebRoy 2017; Oksanen et al., 2013; Lefcheck, 2016; Kassambara, 2018). For ANOVAs distribution of the data was inspected visually and with the Shapiro-Wilk test. We tested homogeneity of variances using the car package and the Levene (Fox and Weisberg, 2011). We define the statistical significance level at 5%.

4.3 Results

4.3.1 Site hydrology and chemistry

Over the growing season the average water table depth (Table 4.1) in the MB (-23.5 ± 3.9 cm) was lower than that measured in the YB (-1.1 ± 3.5 cm). The seasonally average peat temperatures were non-significantly highest in the shallow YB and MB peat layers at 11.0 ± 4.4 and 8.4 ± 5.0 °C respectively, with peak temperatures occurring in July and August. Seasonal average temperatures in the YB deep peat layers were non-significantly higher in the YB (7.0 ± 3.7 °C) than those measured in the MB deep peat layer (3.9 ± 2.8 °C). The seasonally average pore-water pH varied between peat layers, with the highest pH found in the shallow and deep layers in the YB, 4.2 ± 0.3 and 4.1 ± 0.2 respectively, which was higher than both the shallow (3.9 ± 0.2) and deep (4.0 ± 0.2) MB pH (see Table 4.1 for statistics).

Across the growing season average pore-water DOC concentrations varied among the four peat layers, with the highest concentrations found in the shallow and deep peat layers in the MB (68.6 ± 23.1 and 70.0 ± 10.9 mg C L^{-1} respectively). DOC concentrations in the YB deep layer were on average 54.1 ± 5.8 mg C L^{-1} and were higher than the average 52.5 ± 3.3 mg C L^{-1} in the YB shallow layer, with DOC concentrations in both increasing over the growing season (Table 4.1). The highest seasonal average SUVA value (3.6 ± 0.1 L mg C^{-1} m^{-1}) was found in the YB shallow peat layer and second highest (3.1 ± 0.4 L mg C^{-1} m^{-1}) was found in the YB deep peat layer. SUVA values did not differ between shallow and deep MB peat layers, at 2.7 ± 0.4 and 2.4 ± 0.4 L mg C^{-1} m^{-1} respectively. The seasonally average concentration of phenolics and spectral slope ($S_{250-465}$) did not vary among the four peat layers (Table 4.1).

The average TN concentrations differed amongst the peat layers and measured TN in the MB shallow and deep peat layers, at 1.52 ± 1.8 and 1.5 ± 0.5 mg L^{-1} respectively, were higher than those measured in the YB shallow (0.92 ± 0.1 mg L^{-1}) and deep (0.9 ± 0.1 mg L^{-1}). Seasonally averaged PO_4 concentrations did not significantly differ across the four peat layers (Table 4.1).

Table 4.1. Average (average ± SD) growing season (May – September 2018) characteristics of porewater chemistry from four different peat types. YB Shallow = near-surface young bog peat (0 – 29 cm) that accumulated post-thaw; YB Deep = deep young bog peat (32 – 160 cm) that accumulated pre-thaw; MB Shallow = near-surface mature bog peat (0 – 71 cm) that accumulated post-thaw; MB Deep = deep mature bog peat (72 – 160 cm) that accumulated pre-thaw. DOC = dissolved organic carbon. PO_4^{3-} = phosphate. SUVA = specific ultraviolet absorbance at 254 nm.$S_{250-465}$ = spectral slope between 250 – 465 nm (nm^{-1}).

	YB Shallow	YB Deep	MB Shallow	MB Deep
Water Table (cm)	-1.1 ± 3.5 ^{a}		-23.5 ± 3.9 ^{b}	
pH	4.2 ± 0.3 ^{a}	4.1 ± 0.2 ^{a*}	3.9 ± 0.2 ^{b*}	4.0 ± 0.2 ^{b}
Temperature (°C)	11.0 ± 4.4 ^{a*}	7.0 ± 3.7 ^{a}	8.4 ± 5.0 ^{a*}	3.9 ± 2.8 ^{a}
PO_4^{3-} (µg L^{-1})	10.1 ± 14.4 ^{a}	8.6 ± 14.5 ^{a}	5.8 ± 2.3 ^{a*}	8.0 ± 3.4 ^{a}
TN (mg L^{-1})	0.92 ± 0.1 ^{a}	0.9 ± 0.12 ^{a*}	1.52± 1.8 ^{b}	1.5 ± 0.5 ^{b}
DOC (mg C L^{-1})	52.5 ± 3.3 ^{a*}	54.1 ± 5.8 ^{b*}	68.6 ± 23.1 ^{c}	70.0 ± 10.9 ^{c}
$S_{250-465}$ (nm^{-1})	-0.016 ± 0.001 ^{a*}	-0.016 ± 0.002 ^{a*}	-0.017 ± 0.003 ^{a}	-0.018 ± 0.003 ^{a*}
SUVA (L mg C^{-1} m^{-1})	3.6 ± 0.1 ^{a*}	3.1 ± 0.4 ^{b*}	2.7 ± 0.4 ^{c}	2.4 ± 0.4 ^{c}
Phenolics (mg L^{-1})	0.60 ± 0.19 ^{a}	0.64 ± 0.19 ^{a*}	0.58 ± 0.21 ^{a}	0.56 ± 0.15 ^{a}

Letters indicate significant variations between four peat types ($P < 0.05$). * indicates significant monthly variation within each peat type ($P < 0.05$).

4.3.2 Enzyme activities

The measured enzyme activity over the entire growing in YB shallow peat layer clearly deviated from that in the MB shallow peat layer ($F_{(1, 44)} = 20.7$, $P < 0.05$) as shown by the PRC (Fig. 4.2a), whereas the PRC in the deep peat layers (Fig. 3.2b) shows no significant deviation of enzyme activity ($F_{(1, 58)} = 3.2$, $P = 0.46$) between the YB and MB. Examination of the PRCs in shallow peat over the growing season demonstrates a strong impact of thaw stage on enzyme activity, particularly the hydrolytic enzymes, with greater enzyme activity found in the YB. Such a clear influence of peatland stage (YB or MB) is not evident in the deeper peat layers.

In all four peat layers, no significant seasonal trend was observed (Fig. 4.3a – e; Table A3.1). Across the growing season, the activity of all enzymes was higher in the shallow peat layers than the deep peat layers of both the YB and MB, the only exception is LAC activity in the YB

towards the end of the growing season (Fig. 4.3e). As no seasonal trends were found, we combined all monthly measurements for further analyses on the differences in enzyme activity between the four peat layers.

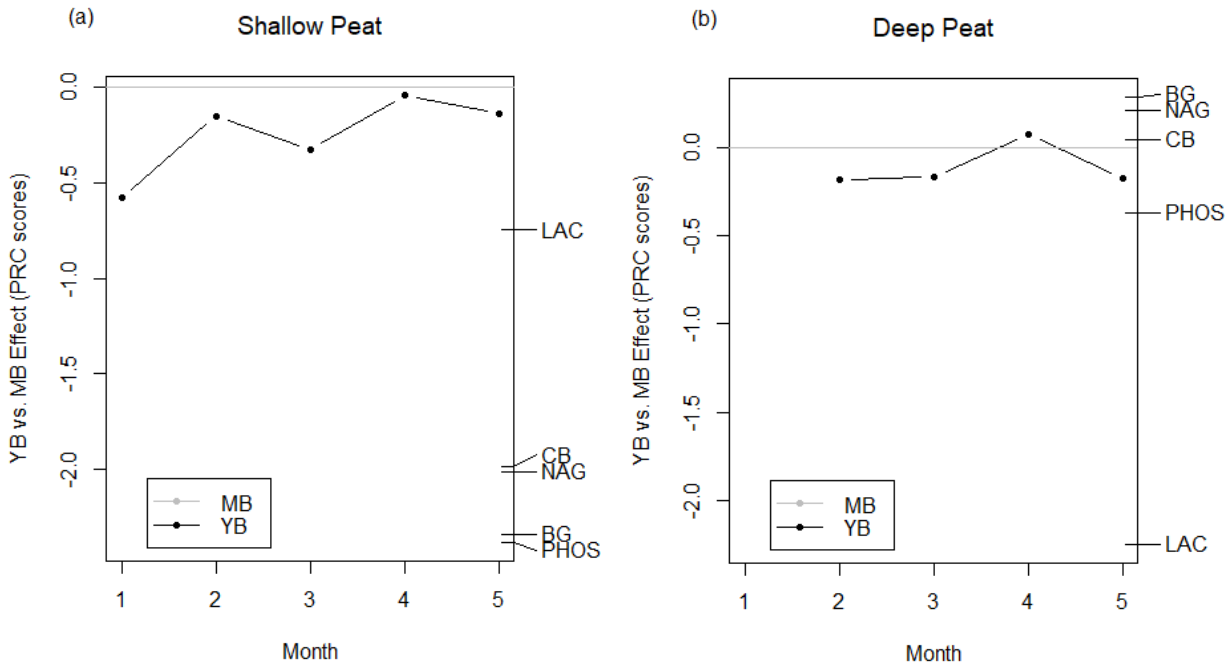

Figure 4.2. Peat enzyme potential activity in the recently thawed young bog (YB) compared to the relatively stable mature bog (MB). Principal response curve (PRC) diagrams with scores for enzyme activity on (a) shallow peat that accumulated post-thaw ($P < 0.05$) and (b) deep peat that accumulated pre-thaw ($P = 0.46$). PHOS = phosphatase activity. NAG = glucosaminidase activity. BG = glucosidase activity. CB = cellobiosidase activity. LAC = laccase activity. Month; 1 = May, 2 = June, 3 = July, 4 = August, 5 = September.

Overall, we found higher potential enzyme activity in shallow peat than deep peat layers, and the greatest activity overall in the YB shallow peat layer (Fig. 4.3f – o; Table A3.2). The majority of hydrolytic enzyme activity was observed in the shallow peat layers, with significantly greater activity measured in the shallow peat layer than deep peat for both the YB and MB (Table A3.2). Similar to the PRCs (Fig. 4.2) the activity of all four hydrolytic enzymes measured was greater in YB shallow peat than the MB shallow (Fig. 4.3f – i), whereas there was no difference in hydrolytic enzyme activity between the deep YB and MB peat layers (Fig. 4.3k – n). Laccase

activity of deep peat layers was similar to the activity of the four measured hydrolytic enzymes, and there was no difference in measured activity between the YB and MB (Fig. 4.3o). However, higher laccase activity rates observed in the shallow layers compared to the deep layers of both YB and MB, and between the shallow YB and MB peat layers were not significantly higher (Fig. 4.3j; Table A3.2)

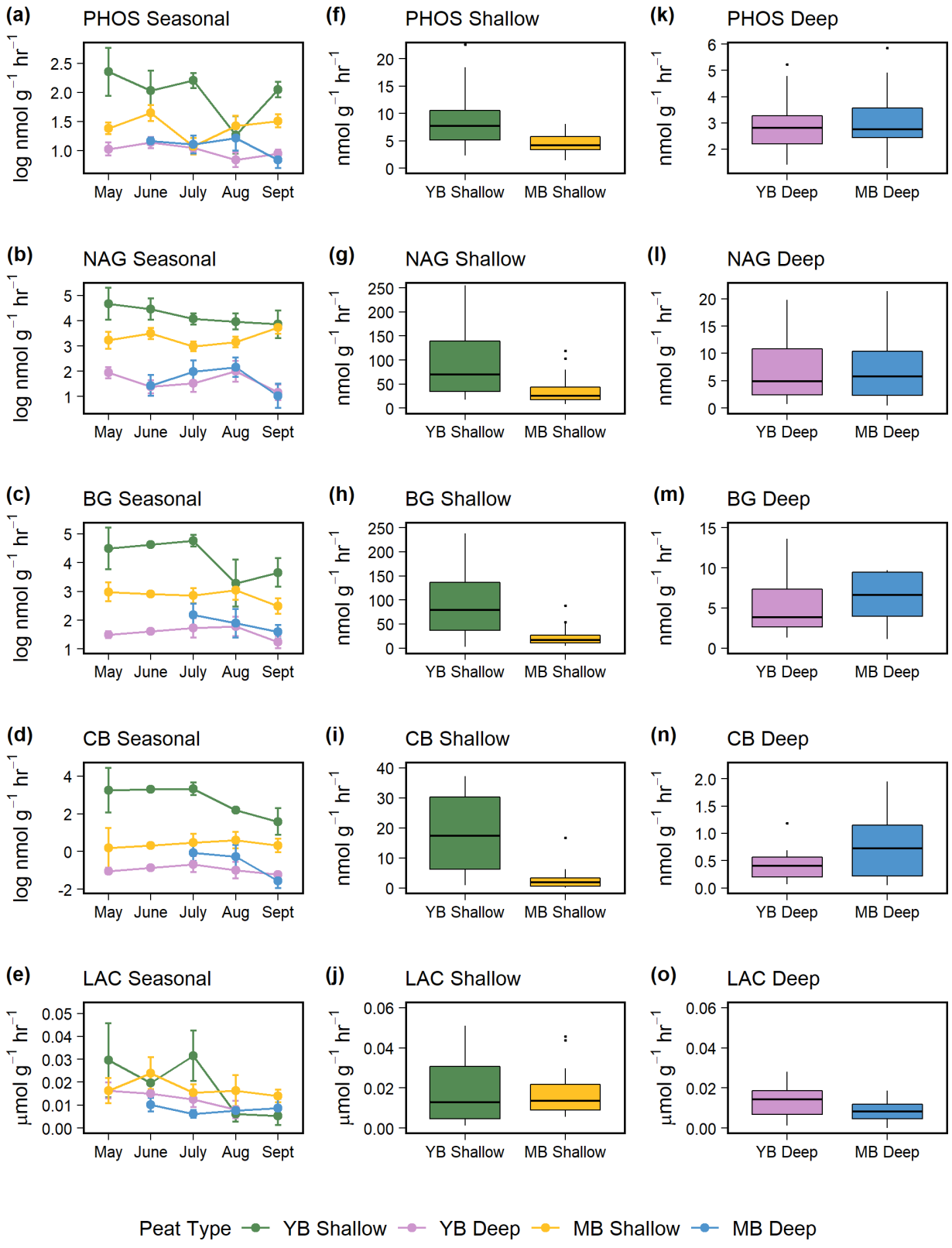
(a)
PHOS Seasonal
log nmol g−1 hr−1
May June July Aug Sept
(f)
PHOS Shallow
nmol g−1 hr−1
YB Shallow MB Shallow
(k)
PHOS Deep
nmol g−1 hr−1
YB Deep MB Deep
(b)
NAG Seasonal
(g)
NAG Shallow
(l)
NAG Deep
(c)
BG Seasonal
(h)
BG Shallow
(m)
BG Deep
(d)
CB Seasonal
(i)
CB Shallow
(n)
CB Deep
(e)
LAC Seasonal
µmol g−1 hr−1
(j)
LAC Shallow
(o)
LAC Deep
Peat Type YB Shallow YB Deep MB Shallow MB Deep

Figure 4.3. Potential enzyme activities from different peat types. YB Shallow = near-surface young bog peat (0 – 29 cm) that accumulated post-thaw; YB Deep = deep young bog peat (32 – 160 cm) that accumulated pre-thaw; MB Shallow = near-surface mature bog peat (0 – 71 cm) that accumulated post-thaw; MB Deep = deep mature bog peat (72 – 160 cm) that accumulated pre-thaw.. PHOS = phosphatase activity (nmol g^{-1} hr^{-1}). NAG = glucosaminidase activity (nmol g^{-1} hr^{-1}). BG = glucosidase activity (nmol g^{-1} hr^{-1}). CB = cellobiosidase activity (nmol g^{-1} hr^{-1}). LAC = laccase activity (μmol g^{-1} hr^{-1}). (a) – (d) activities in log scale. (a) – (e) seasonal trends in enzyme activity and no significant seasonal trends ($P > 0.05$) observed (Table A3.1). (f) – (j) enzyme activity on shallow peat that accumulated post-thaw, with significantly higher ($P < 0.05$) activity of all enzymes observed in YB shallow peat than MB shallow (Table A3.2). (k) – (o) enzyme activity on peat that accumulated pre-thaw, with no significant difference ($P > 0.05$) in activity of all enzymes between YB and MB deep (Table A3.2).

4.3.3 Response of enzyme activity to site factors

Following stepwise selection, the YB shallow and MB shallow peat layers, porewater pH and DOC concentration were found to be significant environmental variables ($P < 0.01$ for all) influencing enzyme activity and no collinearity was found between any of these explanatory variables. Our model, and both RDA biplot axes 1 and 2, were significant ($P < 0.05$). Overall, 32.5% of enzyme activity was explained by environmental variables and peat layer. Variation partitioning and adjusted R^2 showed that the YB shallow peat layer alone explained 20.4% of the variation of enzyme activity, further supporting the finding of greatest enzyme activity in the YB shallow peat layer. Shallow peat in the MB explains only 3.3% of the variation in enzyme activity. Whereas pH and DOC explained 2.0% and 1.7% respectively of the variation in enzyme activity (Fig. 4.4). Linear regression found that the activity of each of the four hydrolytic enzyme activities was positively correlated ($P < 0.05$) with oxidative (LAC) enzyme activity (Fig. A3.1).

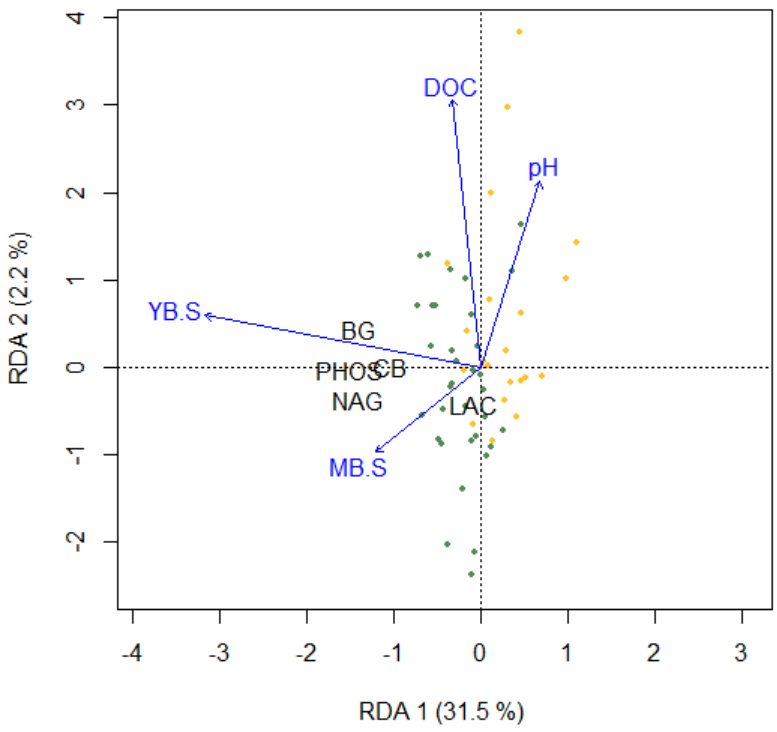

Figure 4.4. Redundancy analysis (RDA) biplot of log transformed and standardized environmental variables and enzyme activity data. Enzymes are represented by an abbreviation around each one's centroid. PHOS = phosphatase activity. NAG = glucosaminidase activity. BG = glucosidase activity. CB = cellobiosidase activity. LAC = laccase activity. Environmental variables are represented by blue vectors and only those that were shown to have a significant impact ($P < 0.05$) on hydrolytic and laccase enzyme activity are used. Environmental variables include: DOC = dissolved organic carbon; YB.S = young bog shallow peat; MB.S = mature bog shallow peat. Species of both sites are represented by points. Green points = YB.S species. Yellow points = MB.S species. Both RDA axes 1 and 2 are significant ($P < 0.05$) and the overall RDA model was significant ($F_{(4, 124)} = 16.4$; $P < 0.001$). YB.S explains 20.4%, MB.S explains 3.3%, and pH and DOC combined explain 3.6% of the variation in enzyme activity.

Furthermore, we found that that enzyme multifunctionality strongly decreased as peat humification increased ($R^2 = 0.86$, $P = 0.07$; Fig. 4.5). This negative correlation demonstrates that as the degree of decomposition of peat increases, i.e. as peat quality decreases, the rate of

hydrolytic enzyme activity also decreases. Enzyme multifunctionality, as with individual enzyme measurements, varied significantly amongst the four peat layers. Overall, it was greater in the shallow peat layers than the deep peat, and the greatest enzyme multifunctionality was found in the YB shallow peat layer. The opposite trend was observed for FTIR (1630 cm^{-1}/1090 cm^{-1}) ratios, where the highest FTIR ratios were observed in the deep peat layers and the lowest FTIR ratio in the YB shallow layer. Thus, peat in the shallow layers was less humified than that observed in the deeper peat layers. Peat in the shallow YB layer was the least humified and had the highest enzyme multifunctionality estimate, with enzyme multifunctionality decreasing with increasing FTIR ratios and peat humification, suggesting that peat quality is an important controlling factor on enzyme activity.

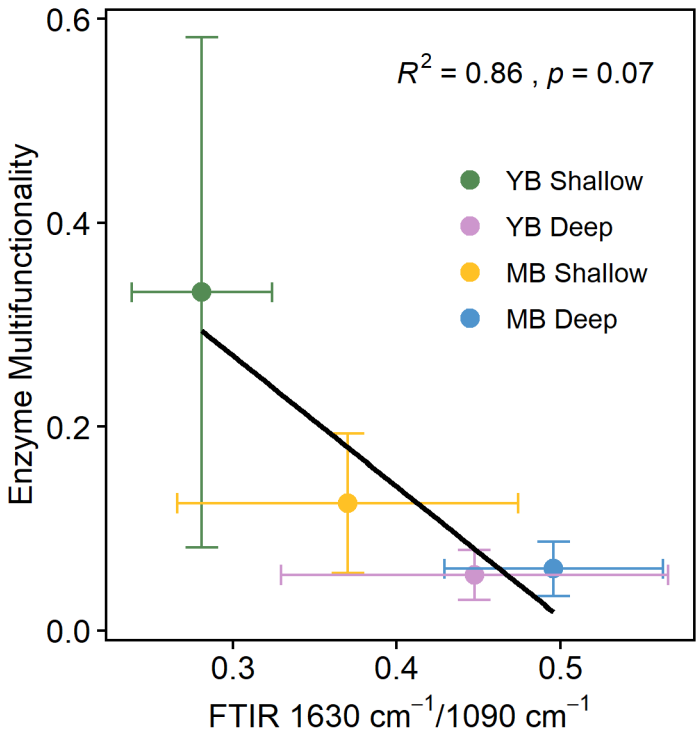

Figure 4.5. Negative relationship between enzyme multifunctionality and FTIR 1630 cm^{-1}/1090 cm^{-1} ratios for each peat type. Vertical error bars represent ± 1 standard deviation of enzyme multifunctionality for each peat type over the growing season. Horizontal error bars represent ± 1 standard deviation of FTIR 1630 cm^{-1}/1090 cm^{-1} ratios for each peat type. Regression line in black is non-significant (R^2 = 0.86, P = 0.07). YB Shallow = near-surface young bog peat (0 – 29 cm) that accumulated post-thaw; YB Deep = deep young bog peat (32 – 160 cm) that

accumulated pre-thaw; MB Shallow = near-surface mature bog peat (0 – 71 cm) that accumulated post-thaw; MB Deep = deep mature bog peat (72 – 160 cm) that accumulated pre-thaw.

4.3.4 Mesocosm porewater chemistry

The average DO concentration (%) in the YB Anoxic and MB Anoxic peat mesocosms was 1 ± 0.4% and 5 ± 4% respectively, both of which are less than 10% which we consider to be anoxic. The average DO concentration (%) in the YB Oxic and MB Oxic peat mesocosms was 76 ± 26% and 56 ± 32% respectively, both of which are greater than 10% which we consider to be oxic. Overall, there was no significant variations observed between the YB Oxic, YB Anoxic, MB Oxic, and MB Anoxic in DOC concentrations, phenolic concentration, $S_{250-465}$, and pH. The only significant variation observed was a lower pH in the MB Anoxic mesocosm than the YB Anoxic mesocosm.

4.3.5 Peat mesocosm enzyme activities

Vegetation type, but not oxic state, was shown to be a key driver of enzyme activity in our peat mesocosms (Fig. 4.5). Hydrolytic enzyme activity in peat mesocosms was summarized to an enzyme multifunctionality estimate ($Hydro_{enz}$) as was performed for enzyme activity from field samples, however unlike the field measurements, oxidative enzyme activity (LAC) was kept separate. There was no difference in enzyme multifunctionality between the YB oxic and anoxic mesocosms, and similarly there was no difference between MB oxic and anoxic mesocosms. Higher enzyme multifunctionality was observed in the both YB oxic and anoxic mesocosms than in the MB oxic and anoxic mesocosms (Fig. 4.5a). The activity of the majority of all four individual hydrolytic enzymes measured from peat mesocosms demonstrated similar patterns (Table A3.3).

When oxic and anoxic mesocosm data was combined, laccase activity was higher in YB vegetation peat mesocosms that that measured in MB mesocosms (Fig. A3.2). When separated while laccase activity was higher in the YB mesocosms, only laccase activity in the YB and MB anoxic peat mesocosms were significantly different ($P < 0.05$).

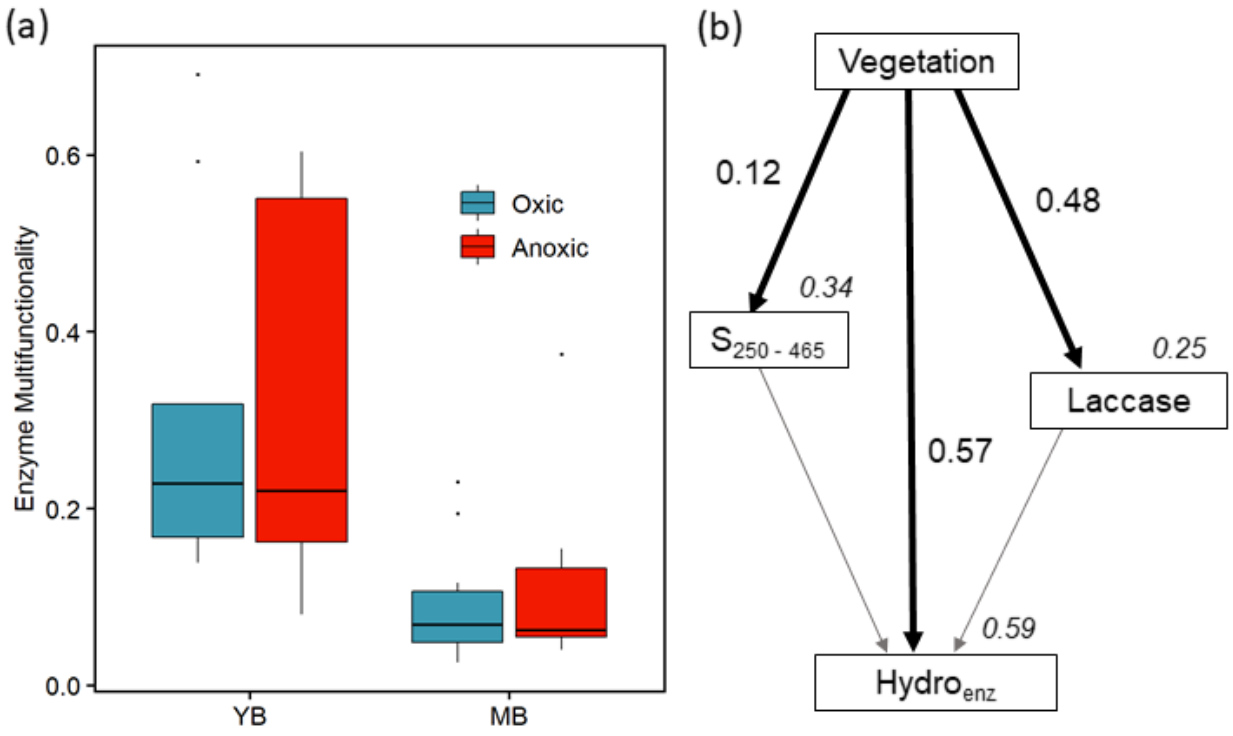

Figure 4.6. (a) Boxplots of enzyme multifunctionality in young bog (YB) and mature bog (MB) peat mesocosms under both oxic (blue) and anoxic (red) conditions. No difference in enzyme multifunctionality between oxic and anoxic in the YB (P = 0.99) and MB (P = 0.94) mesocosms. Enzyme multifunctionality significantly higher in the YB oxic mesocosms than in the MB oxic (P < 0.01) and MB anoxic (P < 0.05) mesocosms, and higher in the YB anoxic mesocosms than in both MB oxic (P < 0.01) and anoxic (P < 0.05) mesocosms. (b) Structural equation model (SEM) representing connections between the YB and MB vegetation type (Vegetation), spectral slope ($S_{250-465}$), laccase activity (Laccase; μmol g^{-1} $hour^{-1}$), and enzyme multifunctionality ($Hydro_{enz}$) from peat mesocosm experiment. Grey lines represent non-significant paths, black lines represent significant paths. Only standardized path coefficients with P < 0.05 are shown. The amount of variance explained (R^2, in italics) for each response variable are given above their respective box. SEM incorporates the random effect of mesocosm sampled. Model fits are on average good, CFI = 0.28, and P = 0.87.

Our structural equation model (SEM) explained 59% of the variance in $Hydro_{enz}$ in the peat mesocosms (Fig. 4.6b). Vegetation type was found to be the major control on $Hydro_{enz}$ in the model (path = 0.57, P < 0.05), which is supported by our previous observations of both field and

mesocosm hydrolytic enzyme patterns (Fig. 4.3, Fig. 4.6a). Similarly, both $S_{250-465}$ and laccase activity were significantly influenced by vegetation type. Laccase activity was shown to have a positive, but not significant, effect on $Hydro_{enz}$ (path = 0.25, $P = 0.12$). Similarly, $S_{250-465}$ was shown to have a positive, but not significant, effect on $Hydro_{enz}$ (path = 0.17, $P = 0.21$). Overall, vegetation type was the major control on enzymatic activity, but there is evidence of a priming effect on hydrolytic enzyme activity by oxidative enzymes and a negative influence of increasing pore water aromaticity and peat humification on hydrolytic enzyme activity.

4.4 Discussion

Permafrost peatlands within the sporadic-discontinuous permafrost zone are currently undergoing rapid permafrost thaw and thermokarst formation (Chasmer and Hopkinson, 2017), exposing vast stores of soil organic C to microbial activity and potential release as greenhouse gases into the atmosphere (Schuur et al., 2008). Previous studies have indicated that soil C is rapidly mineralized in the initial decades following thaw resulting in large net losses of previously frozen C stores (Jones et al., 2017) and enhanced emissions of greenhouse gases (Helbig, Chasmer, Kljun, et al., 2017; Helbig, Chasmer, Desai, et al., 2017). However, no direct evidence of rapid decomposition of previously frozen peat following thaw has so far been found. Here, we find no evidence of elevated enzyme activity at depth in a recently thawed (~30 years) thermokarst bog when compared to deep peat of the same age in a mature bog stage along the same thaw transect, but has been thawed for ~200 years. Unsurprisingly, enzyme activity at depth was much lower that rates observed in near-surface peat. We found consistently higher potential enzyme activities in the near-surface, shallow peat of the recently thawed young bog (YB) than in the mature bog (MB) stage, due to peat and pore water quality and a potential priming effect of oxidative enzymes on hydrolytic enzyme activity. Contrary to previous findings (Fenner and Freeman, 2011; Freeman et al., 2002), our peat mesocosm experiment established that this difference was due to differences in the dominant vegetation species, rather than due to differences in inundation conditions and oxygen availability. Interestingly, we conclude that greater enzyme activity near the surface in the YB compared to the MB does not extend into the older, deeper peat and thus is unlikely to be responsible for any priming effect and mineralization of deeper peat

4.4.1 Links between soil enzyme activity and decomposition

Microbes produces enzymes to degrade insoluble complex organic compounds into soluble molecules that can be assimilated, and *in situ* rates of this enzymatic degradation activity are controlled by temperature, substrate availability, and enzyme concentrations (Wallenstein and Weintraub, 2008). While soil enzyme activity measurements are not a direct measure of *in situ* rates of enzymatically catalyzation reactions, they are informative of overall enzyme concentrations (Nannipieri et al., 2018) and can be interpreted as an indicator of substrate availability and microbial activity. Thus, while not a direct measure of peat decomposition, potential soil enzyme activity measurements coupled with peat temperature and substrate availability, as in this study, provides a suitable surrogate when assessing the potential long-term decomposition of peat following permafrost thaw. Direct comparison of measured enzyme activity rates between studies can be difficult due to differences in methodology. However our measured activities from post-thaw peat were comparable in magnitude to those measured from 0 – 15cm in tundra organic soils (Wallenstein et al., 2009) and from 0 – 25cm in a northern ombrotrophic bog (Steinweg et al., 2018). Furthermore, many studies have used enzyme activity measurements to assess microbial activity (Preston et al., 2012), the vulnerability of peat to increased decomposition (Strakova et al., 2011), and variability in ecosystem respiration (Jassey et al., 2018), supporting the use of enzyme activities as a measure of peat decomposition following thaw.

4.4.2 Seasonality, temperature, and enzyme activity

Our lack of a seasonal pattern in potential enzyme activities is unsurprising as previous studies have had mixed results when assessing the seasonality of enzyme concentrations and activity. Enzyme activity has been shown to rise throughout the growing season peaking in the fall (Fenner et al., 2005), peak mid-growing season (Pinsonneault et al., 2016), and have no observable peak over the growing season (Steinweg et al., 2018). Previous studies reporting a lack of seasonal effect on enzyme activity have suggested it may be due to limited substrate supply (Wallenstein et al., 2009; Weintraub and Schimel 2005), which may be a factor in the deeper peat layers and in the hydrologically isolated MB (Quinton et al., 2009). Runoff from peat plateaus, particularly following spring snowmelt (Olefeldt and Roulet, 2012) leads to increasing runoff of DOC and nutrients from the plateau into the adjacent recently thawed YB (Burd et al.,

2018; Keuper et al., 2012; Finger et al., 2016). It is unlikely, therefore, that substrate limitation is controlling the lack of a seasonal effect observed in the YB shallow peat layer (Fig. 4.3a – e). Given this lack of seasonal effect and higher enzyme activities measured in the YB shallow layer, it is possible that enzymatic turnover is so great that even if the microbial community produce higher quantities of enzymes, the overall concentration remains the same. Or, conversely, the turnover of enzymes is slow so that the concentration remains the same.

Temperature is an important control for *in situ* enzyme activities (Koch et al., 2007) and has been shown to be a strong driver of enzyme activity (Trasar-Cepeda et al., 2007; Steinweg et al., 2012), as well as destabilizing microbial food-webs and stimulating microbial activity (Jassey et al., 2013). Seasonal temperature fluctuations can play an important role in driving seasonal variations in enzyme activity (Machmuller et al., 2016), however we find no evidence of seasonal variations in enzyme concentrations being driven by the observed seasonal fluctuations in soil temperatures amongst the four peat layers. Soil enzyme activities were greater in the near-surface, shallow peat layers where temperatures were higher, and the size of the enzyme pool may be sensitive to the differences in temperature between the different peat layers. This sensitivity of enzyme activity to temperature varied with peat depth across the peat layers, but not with season (Steinweg et al., 2018), suggests that while temperature is likely an important control on enzyme concentrations and activity it is not as important as substrate availability.

4.4.3 Peatland succession and implications for enzyme activity

Substrate availability, governed by the quality of litter inputs from vegetation, along with oxygen availability have been identified as two of the main factors influencing microbial activity and decomposition in peatlands (Belyea, 1996; Laiho, 2006). Soil enzymes are sensitive to substrate and oxygen availability, and respond rapidly to changes in environmental conditions (Henry, 2013; García-Ruiz et al., 2009). Previous studies have shown that lower water tables and increased oxygen availability can result in favourable conditions for enzyme activity leading to enhanced peat decomposition (Fenner and Freeman, 2011; Saraswati et al., 2019; Freeman et al., 2012). However, our results do not indicate any influence from water table position and oxygen availability on microbial activity. The greatest rates of enzyme activity were observed in the shallow YB peat layer (Fig. 4.2, Fig. 4.3) despite the high-water table position and surface inundation (Table 4.1). This same pattern was observed in the peat mesocosm experiment where

regardless of whether the mesocosm was under oxic or anoxic conditions, there was higher enzyme activity in YB mesocosms than MB mesocosms (Fig. 4.6). Increased rates of hydrolytic enzyme activity under such saturated, anoxic conditions have previously been observed (Romanowicz et al., 2015; Sun et al., 2010; Saraswati et al., 2016) and these enzymes are well-suited to low oxygen environments as oxygen itself is not a direct regulator of hydrolytic enzyme activity (Nybroe et al., 1992; Lee et al., 1999; Freeman et al., 2004). Also, while contrary to previous findings (Toberman et al., 2008; Bonnett et al., 2017), our observation of a non-negative impact of saturated conditions on oxidative enzyme activity (Fig. A3.2) has been observed before (Sun et al., 2010; Toberman et al., 2010; Williams et al., 2000).

Our results suggest an intrinsic control on enzyme activity by the vegetation community and that enzyme activity is a property of peatland successional stage (Fig. 4.6). This finding is supported by previous studies reporting that vegetation community composition and litter type are the main influence on decomposition and microbial activity (Hobbie, 1996; Thormann et al., 2001; Cornwell et al., 2008; Strakova et al., 2011). *Sphagnum* is the dominant vegetation in both the YB and MB and while in general *Sphagnum* mosses decompose slowly due to specific chemical qualities, such a polyphenol, that have an inhibitory effect on microbial activity (Bragazza et al., 2007), within the *Sphagnum* mosses there are significant chemical variations with certain species and groups decomposing at different rates (Bengtsson, Granath, and Rydin, 2016; Chiapusio et al., 2018). The hummock *Sphagnum* spp. found in the MB, such *S. fuscum* and *S. magellanicum*, typically have higher cellulose contents, polyphenols, and structural:metabolic carbohydrates ratios than hollow species such as *S. riparium* (Straková et al., 2010; Turetsky et al., 2008). Hemicellulose contents are generally higher in hollow *Sphagnum* spp. (Straková et al., 2010) and degradation of hemicellulose begins before cellulose degradation (Berg and McClaugherty 2014). The dominant species in the YB, *S. riparium,* is associated with nitrogen fixation (Basilier et al., 1978) and high nitrogen availability can reduce the polyphenol content in litter (Bragazza and Freeman, 2007). As a result, the wet hummock species found in the YB decompose quicker and easier than the hummock species of the MB (Johnson and Damman, 1991; Limpens and Berendse, 2003; Turetsky et al., 2008). The decrease in enzyme activity with depth may be not be due to the distance from water table position but rather the distance from vegetation inputs, substrate availability, and associated higher microbial biomass (Straková et al., 2012; Tfaily et al., 2014; Lin et al., 2014).

4.4.4 Constraints on enzyme activity

Similar to previous studies (Fisk et al., 2003; Preston et al., 2012), we found that enzymatic activity decreased with depth (Fig. 4.3) and that shallow, near-surface peat in the YB explained the majority of the variation observed in measured enzyme activity (Fig. 4.4). Decreasing enzyme activity at depth may be due to the temperature sensitivity of soil enzymes (Wallenstein et al., 2010), increased humic substances (Allison, 2006) and sub-optimal conditions for enzyme activity such as low pH and oxygen availability (Freeman et al., 2002). Previous studies have shown that the impact of nutrient and water table levels on substrate lability is minor when compared to the effect of vegetation type (Straková et al., 2010) and that even under aerobic conditions microbial respiration and potential for microbial respiration decreases with depth in thawing permafrost peatlands (Monteux et al., 2018). These studies, coupled with our findings of porewater chemistry, including pH and DOC explaining only 3.6% of the variation in enzyme activity and no influence of oxygen availability on enzyme activity, suggest that there are other constraints limiting enzyme activity at depth.

Peat and dissolved organic matter (DOM) lability can have large implications for enzyme activity, for example peatland DOC with high aromaticity is generally seen to have low bioavailability as a decomposition substrate for microbial communities (Peuravuori and Pihlaja, 1997; Kalbitz et al., 2003). In the initial decades following permafrost thaw, there is a shift in thermokarst DOM towards more biodegradable, lower molecular weight compounds with lower aromaticity (Burd 2017) which can have a significant impact on potential peat mineralization and CO_2 and CH_4 production, leading to increased peat humification (Hodgkins et al., 2014). We find that as peat humification increases with depth, and time-since-thaw, enzyme activity decreases (Fig. 4.5), and decreasing peat quality with depth is a major constraint on enzyme activity at depth. This finding further supports the idea that peat and DOM quality is a major control on enzyme activity and highlights the importance of peat quality in governing decomposition following permafrost thaw.

Interestingly, our results suggest an additional driver of hydrolytic enzyme activity may be a possible priming effect due to oxidative enzyme activity. Previously, oxidative enzyme activity has been shown to release hydrolytic enzyme activity from constraints by reducing phenolic concentrations in peat (Freeman et al., 2002; Freeman et al., 2004; Saraswati et al., 2016).

Similar to previous studies (Romanowicz et al., 2015; Strickland et al., 2009), we find no evidence of constraints on oxidative and hydrolytic enzyme activity due to low oxygen availability or phenolic concentrations. We do however find consistent evidence of a positive influence of oxidative enzyme activity on hydrolytic enzyme activity (Fig. 4.5, Fig. A3.1) in the near-surface YB peat from both field and mesocosm measurements. The higher rates of both hydrolytic and oxidative enzyme activities in the YB may be a result of inputs from vegetation with higher concentrations of hemicellulose and suitable as a substrate for microbially decomposers (Straková et al., 2010). However, previous work has shown that in peat lawns, with a similar water table position and vegetation community to the YB, the microbial community is less dependant on plant derived labile C and hydrolytic enzyme activity increases as the availability of easily degradable C decreases (Robroek et al., 2016). This suggests that as the microbial community preferentially expends the plant-derived labile C source there is increased decomposition of recalcitrant DOM, which in other ecosystem types, has been shown to be primed by oxidative enzyme activity (Phillips et al., 2011; Bird et al., 2011).

4.4.5 Stability of deep peat following thaw

Results from this study would suggest that deep, previously frozen peat is relatively stable following permafrost thaw, and is unlikely to experience rapid increases in rates of enzyme activity and mineralization. The transportation of labile substrates up to depths of 3 m can occur in peatlands and prime microbial decomposition at depth (Chanton et al., 2008). However, despite increased enzyme activity and more labile DOM at the surface, along with higher soil temperatures at depth (Table 4.1) we found no evidence of deep peat priming. The lack of evidence of any change in enzyme concentrations at depth in the YB may be a result of greater turnover of enzymes, such that the overall concentration remains the same, this is unlikely due to the distance from fresh litter inputs, increased peat humification, and decreased oxidative enzyme activity. Our findings of limited enzyme activity and decomposition in previously frozen, deep peat are complimented by previous work from the research site. Soil C stock measurements were unable to detect a significant decline in previously frozen, deep peat C stores following 200 years of thaw (Heffernan et al., 2020) and $^{14}CO_2$ measurements were unable to detect a contribution of aged soil C to late-season soil respiration in the YB and MB thermokarst

bog locations, however it is possible that losses of C from deep peat may be too small to be identified using this method (Estop-Aragonés, Czimczik, et al., 2018).

Extracellular enzyme activity is a regulator of anaerobic decomposition (Limpens et al., 2008) and enzyme activity at depth may stimulate CH_4 production leading to loss of old, deep C. However when considering the estimated ~30 g C-CH_4 m^{-2} $year^{-1}$ emitted from thermokarst landscapes within the last 100 years (Olefeldt et al., 2013), losses via this pathway are unlikely to compensate for such large losses of C as previously indicated from other thawing boreal permafrost peatlands (O'Donnell et al., 2012; Jones et al., 2017). Furthermore, studies from thermokarst peatlands have suggested that there is a limited contribution of aged soil C to CH_4 emissions from the surface (Klapstein et al., 2014; Cooper et al., 2017).

4.5 Conclusion

In this study we show that despite warmer temperatures, potentially more labile DOM from the peat surface, and no constraint on enzymes due to oxygen availability, there is no evidence of increased enzyme activity in deeper peat layers in the initial decades following permafrost thaw, and that deep, previously frozen peat is relatively stable upon thawing. Our findings of stable previously frozen peat following permafrost thaw are reinforced by previous studies demonstrating no significant loss of C stores or contribution of deep soil organic C to CO_2 respired at the surface (Estop-Aragonés, Czimczik, et al., 2018; Heffernan et al., 2020). Despite seasonal variations in soil temperature, there is no seasonal impact on soil enzyme activities and while higher surface temperatures may play a role in the increased rates of activity consistently observed in the shallow peat layers, substrate availability is the main driver of enzyme activity. Contrary to previous studies (Bonnett et al., 2017), but supportive of others (Straková et al., 2012), we show that vegetation type and not water table position is the main driver of enzyme activity. Distance from labile litter inputs, and increasing peat humification, were key constraints on enzyme activity at depth and these findings suggest that peat quality following permafrost thaw is a major factor in controlling the potential rapid loss of C as has been described elsewhere (Jones et al., 2017; O'Donnell et al., 2012). We show that oxidative enzyme activity may be an important driver of hydrolytic enzyme activity, a priming effect that has only previously been observed in grassland and forest soils and is potentially an important driver of organic matter

decomposition previously unexplored in peatlands. Future work should include complimentary approaches such as microbial community composition and activity analysis and assessment of the pathways and rates of deep peat mineralization and methanogenesis following thaw to further elucidate direct impacts of permafrost thaw on peatland C stores. In conclusion, our study shows that deep, previously frozen C stores in thawing boreal peatlands may be more stable than previously thought and proposes that substrate availability and peat quality are important factors in controlling peat decomposition following permafrost thaw.

5. Summary, Conclusions, and Directions for Future Research

5.1 Summary of Findings

This research investigated the effects of permafrost thaw and thermokarst formation on soil carbon (C) cycling in a boreal peatland complex in the sporadic-discontinuous permafrost region of western Canada. Permafrost thaw in boreal peatlands alters the hydrological regime resulting in inundation of the peat profile, leads to drastic shifts in the vegetation community, and exposes vast stores of previously frozen C to enhanced microbially decomposition. The stability of boreal peatlands' globally significant function as a long-term sink of atmospheric C is at risk under accelerated rates of permafrost thaw. In this thesis I have shown that thawing does not 1) result in any significant change to long-term net C storage, 2) lead to any significant increase in a C sink or source effect, and 3) lead to increase the microbial degradation of previously frozen peat. This work highlights that site developmental history, peat properties and quality, and spatial variations in the controls of greenhouse gas emissions are vital when considering the future C sink capacity of boreal permafrost peatlands and that thawing boreal peatlands can show resilience against the impacts of permafrost thaw.

Previous studies from boreal permafrost peatland thaw chronosequences in Alaska have indicated the up 30% of the original, previously frozen, C store is lost following thaw and that the majority of this loss occurs in the initial decades post-thaw resulting in a net source effect that reverts to a net sink centuries after thaw (O'Donnell et al., 2012; Jones et al., 2017). Permafrost thaw exposes previously frozen peat to increased temperatures and enhanced microbial decomposition that can result in peat mineralization and C loss via increased surface emissions of carbon dioxide (CO_2) and methane (CH_4) (Helbig, Chasmer, Desai, et al., 2017; Johnston et al., 2014). Alternatively, others studies found rapid C gains and accumulation at the surface post thaw following a shift from a slow growing, black spruce dominated forest to a fast-growing *Sphagnum* moss dominated thermokarst bog (Camill et al., 2001; Robinson and Moore, 2000). This switch in vegetation community leads to increased net primary productivity (Turetsky et al., 2007) and the inundation of the peat profile results in anaerobic conditions and a reduction in aerobically respired CO_2 emissions (Schädel et al., 2016) but increased CH_4 emissions (Turetsky et al., 2002). In this dissertation, Chapter 2 and 3 highlight the long-term

and short-term stability of permafrost peatland C to thawing and thermokarst formation, and significantly contributes to the growing body of literature on the stability and accumulation of soil organic C pools across northern permafrost regions. Chapter 4 addresses the vulnerability of previously frozen peat to enhanced microbial decomposition, reinforces the observed effects of thawing on C stores and surface C fluxes from Chapter 2 and 3, and is one of the first studies to use soil enzyme activity to assess the impact of thaw on peat decomposition in boreal thermokarst peatlands. This dissertation addresses the contrasting findings in the literature of the impacts of permafrost thaw on boreal peatland C and provides new insights into the mechanisms controlling decomposition post-thaw.

In Chapter 2, I address the assumptions of the space-for-time chronosequence approach used to assess the impact of permafrost thaw on peatland C and report the long-term net effect of permafrost thaw on C stocks and peat humification indices. Using plant macrofossils and ^{14}C dated peat samples I reconstructed the developmental history of the study site and found that the assumptions of the chronosequence approach, i.e. all sites have undergone the same developmental history up until the most recent thaw event, were satisfied and that permafrost aggraded epigenetically at the site. This study supports the use of a chronosequence approach to assess the impact of thawing on peatland C stores provided this assumption is met. Using this approach, I ruled out any change greater than a loss of 16.8% or gain of 4.3% of the net C store over the first 200 years following thaw, and that the estimated 6.8% loss of previously frozen C post-thaw were compensated by the accumulation of new C at the surface. Using peat humification indices, there was no evidence of a detectable increase in peat decomposition following thaw. These findings are contrary to the large losses previously indicated in Alaskan boreal peatlands where permafrost aggraded syngenetically (O'Donnell et al., 2012; Jones et al., 2017), and this discrepancy may be due to differences in site history and the influence of epigenetic vs. syngenetic aggradation on the properties and quality of peat available for decomposition upon thawing in boreal peatlands.

In Chapter 3, I build upon the findings of Chapter 2 by exploring the impact of permafrost thaw on the short-term, or annual, net C balance of the recently thawed and mature thermokarst bog sites and ruling out a large net C source or sink effect over 200 years following permafrost thaw at the site. There was no evidence of a significant contribution of deep, previously frozen peat to

surface emissions and C fluxes were controlled by conditions at or near the peat surface. The water table via direct and indirect constraints, was the major control on C gas fluxes following thaw, however individual gas fluxes had differing functional responses to water table, temperature, and vegetation community between the young and mature thermokarst areas. Net losses in the recently thawed YB were not due to enhanced respiration and loss of C, but rather due to a suppression of CO_2 uptake under saturated conditions. Increased CH_4 emissions in the recently thawed YB were nearly three times as high as those from the MB and these high emissions can result in a positive net radiative forcing effect at the landscape level with over 200 g C-CO_2 m^{-2} $year^{-1}$ net uptake required to offset this effect (Helbig, Chasmer, Kljun, et al., 2017). While in terms of positive radiative forcing these increased CH_4 emissions are significant, they do not represent a great enough loss of C to supplement CO_2 emissions and constitute the net C source required to result in the large losses indicated by previous studies (Jones et al., 2017; O'Donnell et al., 2012). Overall, this study demonstrated that annual cumulative fluxes were asynchronistic, where the young bog was sensitive to wetness and the water table position whereas the mature bog was sensitive to variability in soil temperature. The predicted widespread thawing of boreal permafrost peatlands in western Canada (Chasmer and Hopkinson, 2017), an area sensitive to thaw induced thermokarst bog development (Helbig, Pappas, and Sonnentag, 2016) that also induces regional cooling and wetting (Helbig et al., 2016), may result in the emergence of saturated, recently thawed thermokarst bogs characterized by low net CO_2 uptake and high CH_4 emissions across the southern portion of the Mackenzie River Basin. Predicted increases in temperature, water table drawdown, extended growing season length, and shifts in peatland vegetation will play an important role in the interannual variability of thawing boreal peatlands annual C balance and the stability of their function as net sinks of atmospheric C.

The results of Chapter 4 supported the findings of Chapters 2 and 3 where I showed that post-thaw there was no evidence of enhanced losses or decomposition of previously frozen peat and there was no observed large net source of atmospheric C. Despite increased temperatures at depth, the availability of a recently thawed peat substrate for microbial decomposition, and more labile dissolved organic matter at the surface, there was no evidence of increased enzymatic activity on previously frozen peat in the recently thawed thermokarst bog. The availability of labile litter inputs and reduced peat quality are the main factors controlling enzyme activity and

peat decomposition at depth following thaw. There were however differences in enzymatic activity at the surface and despite the saturated, waterlogged conditions, enzyme activity was greatest in the recently thawed thermokarst bog. This study showed results contrary to a previously proposed latch mechanism that constrains decomposition in peatlands (Freeman et al., 2002), but supports previous studies that report that litter inputs and the vegetation community are the main control on microbial and enzyme activity (Straková et al., 2010; Strakova et al., 2011). The results of Chapter 4 support previous findings of limited to no contribution of deep, old soil organic C to CO_2 and CH_4 emissions from thermokarst bogs in western Canada (Estop-Aragonés, Czimczik, et al., 2018; Estop-Aragonés, Cooper, et al., 2018; Cooper et al., 2017), suggesting that the vast C stores found here are relatively stable following permafrost thaw.

Chapters 2 and 3 clearly demonstrate that permafrost thaw in boreal peatlands at the southernly extent of the permafrost regions in western Canada does not result in large losses of old, previously frozen C or a large net C source or sink effect, and that the C stores found in this region are resilient to permafrost thaw. Chapter 4 corroborates these findings by demonstrating that despite increased temperatures and the availability of a previously frozen peat substrate, there is no evidence of increased enzymatic activity or priming effect on deep peat decomposition following thaw. Together, these findings suggest that while permafrost thaw has been shown to lead to enhanced net losses of C from boreal permafrost peatlands (Jones et al., 2017; Johnston et al., 2014), these losses are not as substantial as previously thought and that deep, previously frozen peat remains stable and largely unaffected following permafrost thaw. This dissertation proposes that differences in site developmental history, peat properties, regional water table position and climatic variables, and peatland autogenic succession are the important factors controlling the magnitude of the impact of permafrost thaw on C cycling in boreal permafrost peatlands.

5.2 Directions for Future Research

Based on the findings from my dissertation, I recommend that the most pressing direction for future research to advance our understanding of the response of boreal peatland soil C to permafrost thaw is to improve our understanding of the role site developmental history has in

governing the response to thaw. Previous studies have demonstrated how heterogeneous the landscape, permafrost history, and peat properties are across the circumpolar north, and that permafrost aggradation plays a large role in the peat type and quality that is accumulated (Jorgenson et al., 2001; Treat et al., 2016; Turetsky et al., 2007). The results from Chapter 2 in this dissertation showing no evidence of old C loss post-thaw can be directly compared to previous studies in Alaskan peatlands where permafrost aggraded syngenetically and large losses of previously frozen C were indicated following thaw (Jones et al., 2017; O'Donnell et al., 2012). While the study design between Chapter 2 and these studies are slightly different, the contrasting results are likely driven by differences in site developmental history and the aggradation of permafrost epigenetically vs. syngenetically.

To address the role site history plays in the response of C stores to thawing I propose three lines of future investigation. First, future research should quantify the sensitivity and rates of decomposition of intact frozen peat plateau peat that has aggraded epigenetically, syngenetically, and epigenetically that after time transitioned to syngenetic aggradation in a laboratory based thermokarst simulating, anoxic incubation experiment. The results from this should be compared to chronosequence studies from sites with different developmental histories, with all these findings synthesized to comment of the influence of thawing on boreal peatland C stores at sites where permafrost has aggraded differently over the Holocene. Second, permafrost aggradation and thawing should be incorporated into conceptual process-based peatland development models, such as the Digibog model (Baird, Morris, and Belyea, 2012; Morris, Baird, and Belyea, 2012), to investigate how the drastic shifts in hydrological regime associated with permafrost aggradation and degradation impacts peat properties and accumulation. And finally, using findings from previous studies on global peatland development and circumpolar permafrost aggradation trends (Treat and Jones, 2018; Treat et al., 2019), coupled with more regional estimates of both (e.g. Pelletier et al., 2017 for western Canada, Jones et al., 2013 for Alaska, Kuhry, 2008 for the Hudson Bay lowlands in Canada, and Oksanen et al., 2003 for western Russia) develop a circumpolar map of permafrost aggradation in boreal peatlands. Findings from these three proposed lines of future research will provide valuable insights in to how site developmental history will impact the C stores found in boreal permafrost peatlands, how vulnerable these C stores are to loss following thaw, and the proportion of circumpolar boreal

peatlands that are likely to experience large losses of previously frozen C post-thaw and lead to an enhanced permafrost C climate feedback.

Finally, Chapter 4 of this dissertation is one of the first studies to measure soil enzyme activity in boreal permafrost peatlands and showed that there was no evidence of increased enzymatic degradation of previously frozen peat following thaw that would be required to drive losses of this C. Previous studies have shown that labile surface dissolved organic matter can be transported to depths of up to 3 m and drive deep peat heterotrophic respiration (Chanton et al., 1995; Corbett et al., 2013), however despite warmer temperatures we found no evidence of a priming a peat decomposition at depth. Future work should include further measurements of soil enzyme activities and the vulnerability of previously frozen peat to enhanced microbial degradation following thaw in sites where permafrost aggraded syngenetically and may have a more labile substrate available for microbial activity. Study sites should also include sites (both with epigenetic and syngenetic permafrost histories) with thinner peat layer than the 6 m deep deposit found at the research site in this dissertation where the entire peat profile may be more susceptible to changes in biotic and abiotic conditions at the surface. Furthermore, peat degrading enzymes are released by the microbial community and studies on the vulnerability of peat to increased enzyme activity should be supplemented with composition analysis of the microbial community present. Decomposition is driven by the activity of the microbial community, thus a better understanding of the composition of microbial community present post-thaw and the activity of this community will greatly improve our efforts in monitoring, modelling, and upscaling the stability of previously frozen peat following permafrost thaw in boreal peatlands.

Bibliography

Abbott, Benjamin W., Jeremy B. Jones, Edward A.G. Schuur, F. Stuart Chapin, William B. Bowden, M. Syndonia Bret-Harte, Howard E. Epstein, et al. 2016. "Biomass Offsets Little or None of Permafrost Carbon Release from Soils, Streams, and Wildfire: An Expert Assessment." *Environmental Research Letters* 11 (3): 34014. https://doi.org/10.1088/1748-9326/11/3/034014.

Ahlström, Anders, Jianyang Xia, Almut Arneth, Yiqi Luo, and Benjamin Smith. 2015. "Importance of Vegetation Dynamics for Future Terrestrial Carbon Cycling." *Environmental Research Letters*. https://doi.org/10.1088/1748-9326/10/5/054019.

Alberta Government. 2016. "Current and Historical Alberta Weather Station Data Viewer." AgroClimatic Information Service (ACIS). 2016.

Alexandrov, Georgii A., Victor A. Brovkin, Thomas Kleinen, and Zicheng Yu. 2020. "The Capacity of Northern Peatlands for Long-Term Carbon Sequestration." *Biogeosciences* 17 (1): 47–54. https://doi.org/10.5194/bg-17-47-2020.

Allan, Eric, Pete Manning, Fabian Alt, Julia Binkenstein, Stefan Blaser, Nico Blüthgen, Stefan Böhm, et al. 2015. "Land Use Intensification Alters Ecosystem Multifunctionality via Loss of Biodiversity and Changes to Functional Composition." *Ecology Letters*. https://doi.org/10.1111/ele.12469.

Allison, Steven D. 2006. "Soil Minerals and Humic Acids Alter Enzyme Stability: Implications for Ecosystem Processes." *Biogeochemistry*. https://doi.org/10.1007/s10533-006-9046-2.

Alm, Jukka, Leif Schulman, Jari Walden, Hannu Nykänen, Pertti J. Martikainen, and Jouko Silvola. 1999. "Carbon Balance of a Boreal Bog during a Year with an Exceptionally Dry Summer." *Ecology*. https://doi.org/10.1890/0012-9658(1999)080[0161:CBOABB]2.0.CO;2.

Alm, Jukka, Narasinha J. Shurpali, Eeva Stiina Tuittila, Tuomas Laurila, Marja Maljanen, Sanna Saarnio, and Kari Minkkinen. 2007. "Methods for Determining Emission Factors for the Use of Peat and Peatlands - Flux Measurements and Modelling." *Boreal Environment Research* 12 (2): 85–100.

Artz, Rebekka R.E., Stephen J. Chapman, A. H. Jean Robertson, Jacqueline M. Potts, Fatima Laggoun-Défarge, Sébastien Gogo, Laure Comont, Jean Robert Disnar, and Andre Jean Francez. 2008. "FTIR Spectroscopy Can Be Used as a Screening Tool for Organic Matter Quality in Regenerating Cutover Peatlands." *Soil Biology and Biochemistry* 40 (2): 515–27. https://doi.org/10.1016/j.soilbio.2007.09.019.

Baird, A., S. Green, E. Brown, and G. Dooling. 2019. "Modelling Time-Integrated Fluxes of CO2 and CH4 in Peatlands: A Review." *Mires and Peat*. https://doi.org/10.19189/MaP.2019.DW.395.

Baird, Andy J., Paul J. Morris, and Lisa R. Belyea. 2012. "The DigiBog Peatland Development Model 1: Rationale, Conceptual Model, and Hydrological Basis." *Ecohydrology*. https://doi.org/10.1002/eco.230.

Baltzer, Jennifer L., Tyler Veness, Laura E. Chasmer, Anastasia E. Sniderhan, and William L. Quinton. 2014. "Forests on Thawing Permafrost: Fragmentation, Edge Effects, and Net Forest Loss." *Global Change Biology* 20 (3): 824–34. https://doi.org/10.1111/gcb.12349.

Basilier, Karl, Ulf Granhall, Thor-Axel Stenström, and Thor-Axel Stenstrom. 1978. "Nitrogen Fixation in Wet Minerotrophic Moss Communities of a Subarctic Mire." *Oikos*. https://doi.org/10.2307/3543568.

Basiliko, Nathan, Tim R. Moore, Peter M. Lafleur, and Nigel T. Roulet. 2005. "Seasonal and Inter-Annual Decomposition, Microbial Biomass, and Nitrogen Dynamics in a Canadian Bog." *Soil Science*. https://doi.org/10.1097/01.ss.0000196765.59412.14.

Bauer, Ilka E, L Dennis Gignac, and Dale H Vitt. 2003. "Development of a Peatland Complex in Boreal Western Canada: Lateral Site Expansion and Local Variability in Vegetation Succession and Long-Term Peat Accumulation." *Canadian Journal of Botany* 81 (8): 833–47. https://doi.org/10.1139/b03-076.

Beer, Julia, and Christian Blodau. 2007. "Transport and Thermodynamics Constrain Belowground Carbon Turnover in a Northern Peatland>." *Geochimica et Cosmochimica Acta*. https://doi.org/10.1016/j.gca.2007.03.010.

Beer, Julia, Kern Lee, Michael Whiticar, and Christian Blodau. 2008. "Geochemical Controls on Anaerobic Organic Matter Decomposition in a Northern Peatland." *Limnology and Oceanography* 53 (4): 1393–1407. https://doi.org/10.4319/lo.2008.53.4.1393.

Beilman, David W. 2001. "Plant Community and Diversity Change Due to Localized Permafrost Dynamics in Bogs of Western Canada." *Canadian Journal of Botany* 79 (8): 983–93. https://doi.org/10.1139/cjb-79-8-983.

Beilman, David W., Dale H. Vitt, Jagtar S. Bhatti, and Silvie Forest. 2008. "Peat Carbon Stocks in the Southern Mackenzie River Basin: Uncertainties Revealed in a High-Resolution Case Study." *Global Change Biology* 14 (6): 1221–32. https://doi.org/10.1111/j.1365-2486.2008.01565.x.

Bell, Colin W., Barbara E. Fricks, Jennifer D. Rocca, Jessica M. Steinweg, Shawna K. McMahon, and Matthew D. Wallenstein. 2013. "High-Throughput Fluorometric Measurement of Potential Soil Extracellular Enzyme Activities." *Journal of Visualized Experiments*. https://doi.org/10.3791/50961.

Belyea, Lisa R. 1996. "Separating the Effects of Litter Quality and Microenvironment on Decomposition Rates in a Patterned Peatland." *Oikos* 77 (3): 529. https://doi.org/10.2307/3545942.

Bengtson, Per, and Göran Bengtsson. 2007. "Rapid Turnover of DOC in Temperate Forests Accounts for Increased CO 2 Production at Elevated Temperatures." *Ecology Letters*. https://doi.org/10.1111/j.1461-0248.2007.01072.x.

Bengtsson, Fia, Gustaf Granath, and Håkan Rydin. 2016. "Photosynthesis, Growth, and Decay Traits in Sphagnum - a Multispecies Comparison." *Ecology and Evolution*. https://doi.org/10.1002/ece3.2119.

Berg, Björn, and Charles McClaugherty. 2014. *Plant Litter: Decomposition, Humus Formation,*

Carbon Sequestration. *Plant Litter: Decomposition, Humus Formation, Carbon Sequestration*. https://doi.org/10.1007/978-3-642-38821-7_9.

Biester, H., K. H. Knorr, J. Schellekens, A. Basler, and Y. M. Hermanns. 2014. "Comparison of Different Methods to Determine the Degree of Peat Decomposition in Peat Bogs." *Biogeosciences*. https://doi.org/10.5194/bg-11-2691-2014.

Bird, Jeffrey A., Donald J. Herman, and Mary K. Firestone. 2011. "Rhizosphere Priming of Soil Organic Matter by Bacterial Groups in a Grassland Soil." *Soil Biology and Biochemistry*. https://doi.org/10.1016/j.soilbio.2010.08.010.

Blaauw, Maarten, and J. Andrés Christen. 2011. "Flexible Paleoclimate Age-Depth Models Using an Autoregressive Gamma Process." *Bayesian Analysis* 6 (3): 457–74. https://doi.org/10.1214/11-BA618.

Blodau, C. 2002. "Carbon Cycling in Peatlands — A Review of Processes and Controls." *Environmental Reviews* 10 (2): 111–34. https://doi.org/10.1139/a02-004.

Blodau, Christian. 2002. "Carbon Cycling in Peatlands - A Review of Processes and Controls." *Environmental Reviews*. https://doi.org/10.1139/a02-004.

Blodau, Christian, Nathan Basiliko, and Tim R. Moore. 2004. "Carbon Turnover in Peatland Mesocosms Exposed to Different Water Table Levels." *Biogeochemistry*. https://doi.org/10.1023/B:BIOG.0000015788.30164.e2.

Blodau, Christian, and Tim R. Moore. 2003. "Experimental Response of Peatland Carbon Dynamics to a Water Table Fluctuation." *Aquatic Sciences* 65 (1): 47–62. https://doi.org/10.1007/s000270300004.

Bonnett, Samuel Alexander Festing, Edward Maltby, and Chris Freeman. 2017. "Hydrological Legacy Determines the Type of Enzyme Inhibition in a Peatlands Chronosequence." *Scientific Reports*. https://doi.org/10.1038/s41598-017-10430-x.

Borga, Peter, Mats Nilsson, and Anders Tunlid. 1994. "Bacterial Communities in Peat in Relation to Botanical Composition as Revealed by Phospholipid Fatty Acid Analysis." *Soil Biology and Biochemistry*. https://doi.org/10.1016/0038-0717(94)90300-X.

Borgmark, Anders, and Kristian Schoning. 2006. "A Comparative Study of Peat Proxies from Two Eastern Central Swedish Bogs and Their Relation to Meteorological Data." *Journal of Quaternary Science*. https://doi.org/10.1002/jqs.959.

Bragazza, L., C. Siffi, P. Iacumin, and R. Gerdol. 2007. "Mass Loss and Nutrient Release during Litter Decay in Peatland: The Role of Microbial Adaptability to Litter Chemistry." *Soil Biology and Biochemistry*. https://doi.org/10.1016/j.soilbio.2006.07.014.

Bragazza, Luca. 2006. "A Decade of Plant Species Changes on a Mire in the Italian Alps: Vegetation-Controlled or Climate-Driven Mechanisms?" *Climatic Change*. https://doi.org/10.1007/s10584-005-9034-x.

Bragazza, Luca, Richard D. Bardgett, Edward A.D. Mitchell, and Alexandre Buttler. 2015. "Linking Soil Microbial Communities to Vascular Plant Abundance along a Climate Gradient." *New Phytologist* 205 (3): 1175–82. https://doi.org/10.1111/nph.13116.

Bragazza, Luca, and Chris Freeman. 2007. “High Nitrogen Availability Reduces Polyphenol Content in Sphagnum Peat.” *Science of the Total Environment*. https://doi.org/10.1016/j.scitotenv.2007.02.016.

Bragazza, Luca, Julien Parisod, Alexandre Buttler, and Richard D. Bardgett. 2013. “Biogeochemical Plant-Soil Microbe Feedback in Response to Climate Warming in Peatlands.” *Nature Climate Change* 3 (3): 273–77. https://doi.org/10.1038/nclimate1781.

Breeuwer, Angela, Bjorn J.M. Robroek, Juul Limpens, Monique M.P.D. Heijmans, Matthijs G.C. Schouten, and Frank Berendse. 2009. “Decreased Summer Water Table Depth Affects Peatland Vegetation.” *Basic and Applied Ecology*. https://doi.org/10.1016/j.baae.2008.05.005.

Bridgham, Scott D., Hinsby Cadillo-Quiroz, Jason K. Keller, and Qianlai Zhuang. 2013. “Methane Emissions from Wetlands: Biogeochemical, Microbial, and Modeling Perspectives from Local to Global Scales.” *Global Change Biology*. https://doi.org/10.1111/gcb.12131.

Bridgham, Scott D., Carol A. Johnston, John Pastor, and Karen Updegraff. 1995. “Potential Feedbacks of Northern Wetlands on Climate Change.” *BioScience*. https://doi.org/10.2307/1312419.

Brink, Paul J. Van Den, and Cajo J.F. Ter Braak. 1999. “Principal Response Curves: Analysis of Time-Dependent Multivariate Responses of Biological Community to Stress.” *Environmental Toxicology and Chemistry*. https://doi.org/10.1897/1551-5028(1999)018<0138:PRCAOT>2.3.CO;2.

Briones, María Jesús I, Niall P. Mcnamara, Jan Poskitt, Susan E. Crow, and Nicholas J. Ostle. 2014. “Interactive Biotic and Abiotic Regulators of Soil Carbon Cycling: Evidence from Controlled Climate Experiments on Peatland and Boreal Soils.” *Global Change Biology* 20 (9): 2971–82. https://doi.org/10.1111/gcb.12585.

Broder, T., C. Blodau, H. Biester, and K. H. Knorr. 2012. “Peat Decomposition Records in Three Pristine Ombrotrophic Bogs in Southern Patagonia.” *Biogeosciences* 9 (4): 1479–91. https://doi.org/10.5194/bg-9-1479-2012.

Brouns, Karlijn, Jos T.A. Verhoeven, and Mariet M. Hefting. 2014. “Short Period of Oxygenation Releases Latch on Peat Decomposition.” *Science of the Total Environment*. https://doi.org/10.1016/j.scitotenv.2014.02.030.

Brown, Jerry, O.J. Ferrians Jr., J. Alan Heginbottom, and E.S. Melnikov. 1997. “Circum-Arctic Map of Permafrost and Ground Ice Conditions.” *USGS Numbered Series*, 1. https://doi.org/10.1016/j.jallcom.2010.03.054.

Bubier, J. L., S. Frolking, P. M. Crill, and E. Linder. 1999. “Net Ecosystem Productivity and Its Uncertainty in a Diverse Boreal Peatland.” *Journal of Geophysical Research Atmospheres*. https://doi.org/10.1029/1999JD900219.

Bubier, Jill, Patrick Crill, Andrew Mosedale, Steve Frolking, and Ernst Linder. 2003. “ Peatland Responses to Varying Interannual Moisture Conditions as Measured by Automatic CO 2 Chambers .” *Global Biogeochemical Cycles*. https://doi.org/10.1029/2002gb001946.

Bubier, Jill L. 1995. “The Relationship of Vegetation to Methane Emission and Hydrochemical Gradients in Northern Peatlands.” *The Journal of Ecology*. https://doi.org/10.2307/2261594.

Burd, Katheryn. 2017. “Influence of Wildfire and Permafrost Thaw on DOC in Northern Peatlands.” University of Alberta. https://doi.org/https://doi.org/10.7939/R3FB4X10G.

Burd, Katheryn, Suzanne E. Tank, Nicole Dion, William L. Quinton, Christopher Spence, Andrew J. Tanentzap, and David Olefeldt. 2018. “Seasonal Shifts in Export of DOC and Nutrients from Burned and Unburned Peatland-Rich Catchments, Northwest Territories, Canada.” *Hydrology and Earth System Sciences*, 4455–72. https://doi.org/10.5194/hess-22-4455-2018.

Burger, Magdalena, Sina Berger, Ines Spangenberg, and Christian Blodau. 2016. “Summer Fluxes of Methane and Carbon Dioxide from a Pond and Floating Mat in a Continental Canadian Peatland.” *Biogeosciences*. https://doi.org/10.5194/bg-13-3777-2016.

Cai, Tiebo, Lawrence B. Flanagan, and Kamran H. Syed. 2010. “Warmer and Drier Conditions Stimulate Respiration More than Photosynthesis in a Boreal Peatland Ecosystem: Analysis of Automatic Chambers and Eddy Covariance Measurements.” *Plant, Cell and Environment*. https://doi.org/10.1111/j.1365-3040.2009.02089.x.

Camill, Philip. 1999. “Peat Accumulation and Succession Following Permafrost Thaw in the Boreal Peatlands of Manitoba, Canada.” *Ecoscience* 6 (4): 592–602. https://doi.org/10.1080/11956860.1999.11682561.

Camill, Philip. 2005. “Permafrost Thaw Accelerates in Boreal Peatlands during Late-20th Century Climate Warming.” *Climatic Change* 68 (1–2): 135–52. https://doi.org/10.1007/s10584-005-4785-y.

Camill, Philip, Ann Barry, Evie Williams, Christian Andreassi, Jacob Limmer, and Donald Solick. 2009. “Climate-Vegetation-Fire Interactions and Their Impact on Long-Term Carbon Dynamics in a Boreal Peatland Landscape in Northern Manitoba, Canada.” *Journal of Geophysical Research: Biogeosciences* 114 (4): 1–10. https://doi.org/10.1029/2009JG001071.

Camill, Philip, Jason A. Lynch, James S. Clark, J. Brad Adams, and B. Jordan. 2001. “Changes in Biomass, Aboveground Net Primary Production, and Peat Accumulation Following Permafrost Thaw in the Boreal Peatlands of Manitoba, Canada.” *Ecosystems* 4 (5): 461–78. https://doi.org/10.1007/s10021-001-0022-3.

Carpino, Olivia A., Aaron A. Berg, William L. Quinton, and Justin R. Adams. 2018. “Climate Change and Permafrost Thaw-Induced Boreal Forest Loss in Northwestern Canada.” *Environmental Research Letters*. https://doi.org/10.1088/1748-9326/aad74e.

Carroll, Paul, and Patrick Crill. 1997. “Carbon Balance of a Temperate Poor Fen.” *Global Biogeochemical Cycles*. https://doi.org/10.1029/97GB01365.

Chambers, F.M., D.W. Beilman, and Z. Yu. 2011. “- Methods for Determining Peat Humification and for Quantifying Peat Bulk Density.” *Mires and Peat* 7 (7): 1–10. http://www.mires-and-peat.net/pages/volumes/map07/map0707.php.

Chanton, J. P., P. H. Glaser, L. S. Chasar, D. J. Burdige, M. E. Hines, D. I. Siegel, L. B.

Tremblay, and W. T. Cooper. 2008. “Radiocarbon Evidence for the Importance of Surface Vegetation on Fermentation and Methanogenesis in Contrasting Types of Boreal Peatlands.” *Global Biogeochemical Cycles* 22 (4): 1–11. https://doi.org/10.1029/2008GB003274.

Chanton, Jeffrey P., James E. Bauer, Paul A. Glaser, Donald I. Siegel, Cheryl A. Kelley, Stanley C. Tyler, Edwin H. Romanowicz, and Allen Lazrus. 1995. “Radiocarbon Evidence for the Substrates Supporting Methane Formation within Northern Minnesota Peatlands.” *Geochimica et Cosmochimica Acta* 59 (17): 3663–68. https://doi.org/10.1016/0016-7037(95)00240-Z.

Chasmer, Laura E., and C. Hopkinson. 2017. “Threshold Loss of Discontinuous Permafrost and Landscape Evolution,” 2672–86. https://doi.org/10.1111/gcb.13537.

Chaudhary, Nitin, Paul A. Miller, and Benjamin Smith. 2018. “Biotic and Abiotic Drivers of Peatland Growth and Microtopography: A Model Demonstration.” *Ecosystems* 21 (6): 1196–1214. https://doi.org/10.1007/s10021-017-0213-1.

Chiapusio, Geneviève, Vincent E.J. Jassey, Floriant Bellvert, Gilles Comte, Leslie A. Weston, Frederic Delarue, Alexandre Buttler, Marie Laure Toussaint, and Philippe Binet. 2018. “Sphagnum Species Modulate Their Phenolic Profiles and Mycorrhizal Colonization of Surrounding Andromeda Polifolia along Peatland Microhabitats.” *Journal of Chemical Ecology*. https://doi.org/10.1007/s10886-018-1023-4.

Chimner, Rodney A., Thomas G. Pypker, John A. Hribljan, Paul A. Moore, and James M. Waddington. 2017. “Multi-Decadal Changes in Water Table Levels Alter Peatland Carbon Cycling.” *Ecosystems*. https://doi.org/10.1007/s10021-016-0092-x.

Chivers, M. R., M. R. Turetsky, J. M. Waddington, J. W. Harden, and A. D. McGuire. 2009. “Effects of Experimental Water Table and Temperature Manipulations on Ecosystem CO2 Fluxes in an Alaskan Rich Fen.” *Ecosystems*. https://doi.org/10.1007/s10021-009-9292-y.

Churchill, Amber C., Merritt R. Turetsky, A. David McGuire, and Teresa N. Hollingsworth. 2014. “Response of Plant Community Structure and Primary Productivity to Experimental Drought and Flooding in an Alaskan Fen1.” *Canadian Journal of Forest Research*. https://doi.org/10.1139/cjfr-2014-0100.

Climate-Data.org. 2019. “2019. 2019.” ة. https://en.climate-data.org/north-america/canada/alberta/meander-river-11380/.

Clymo, R. S. 1984. “The Limits to Peat Bog Growth.” *Philosophical Transactions of the Royal Society B: Biological Sciences* 303 (1117): 605–54. https://doi.org/10.1098/rstb.1984.0002.

Clymo, R. S., J. Turunen, and K. Tolonen. 1998. “Carbon Accumulation in Peatland.” *Oikos* 81 (2): 368. https://doi.org/10.1016/j.compositesb.2018.11.026.

Commane, Róisín, Jakob Lindaas, Joshua Benmergui, Kristina A. Luus, Rachel Y.W. Chang, Bruce C. Daube, Eugénie S. Euskirchen, et al. 2017. “Carbon Dioxide Sources from Alaska Driven by Increasing Early Winter Respiration from Arctic Tundra.” *Proceedings of the National Academy of Sciences of the United States of America*. https://doi.org/10.1073/pnas.1618567114.

Cooper, Mark D.A., Cristian Estop-Aragonés, James P. Fisher, Aaron Thierry, Mark H. Garnett, Dan J. Charman, Julian B. Murton, et al. 2017. "Limited Contribution of Permafrost Carbon to Methane Release from Thawing Peatlands." *Nature Climate Change* 7 (7): 507–11. https://doi.org/10.1038/nclimate3328.

Corbett, Elizabeth J., David J. Burdige, Malak M. Tfaily, Angela R. Dial, William T. Cooper, Paul H. Glaser, and Jeffrey P. Chanton. 2013. "Surface Production Fuels Deep Heterotrophic Respiration in Northern Peatlands." *Global Biogeochemical Cycles* 27 (4): 1163–74. https://doi.org/10.1002/2013GB004677.

Cornwell, William K., Johannes H.C. Cornelissen, Kathryn Amatangelo, Ellen Dorrepaal, Valerie T. Eviner, Oscar Godoy, Sarah E. Hobbie, et al. 2008. "Plant Species Traits Are the Predominant Control on Litter Decomposition Rates within Biomes Worldwide." *Ecology Letters*. https://doi.org/10.1111/j.1461-0248.2008.01219.x.

Criquet, S., A. M. Farnet, S. Tagger, and J. Le Petit. 2000. "Annual Variations of Phenoloxidase Activities in an Evergreen Oak Litter: Influence of Certain Biotic and Abiotic Factors." *Soil Biology and Biochemistry*. https://doi.org/10.1016/S0038-0717(00)00027-4.

Criquet, S., S. Tagger, G. Vogt, G. Iacazio, and J. Le Petit. 1999. "Laccase Activity of Forest Litter." *Soil Biology and Biochemistry*. https://doi.org/10.1016/S0038-0717(99)00038-3.

Crow, Susan E., and R. Kelman Wieder. 2005. "Sources of CO2emission from a Northern Peatland: Root Respiration, Exudation, and Decomposition." *Ecology*. https://doi.org/10.1890/04-1575.

D'Andrilli, Juliana, Jeffrey P. Chanton, Paul H. Glaser, and William T. Cooper. 2010. "Characterization of Dissolved Organic Matter in Northern Peatland Soil Porewaters by Ultra High Resolution Mass Spectrometry." *Organic Geochemistry* 41 (8): 791–99. https://doi.org/10.1016/j.orggeochem.2010.05.009.

Davidson, Eric A., and Ivan A. Janssens. 2006. "Temperature Sensitivity of Soil Carbon Decomposition and Feedbacks to Climate Change." *Nature*. https://doi.org/10.1038/nature04514.

Deng, J., C. Li, S. Frolking, Y. Zhang, K. Bäckstrand, and P. Crill. 2014. "Assessing Effects of Permafrost Thaw on C Fluxes Based on Multiyear Modeling across a Permafrost Thaw Gradient at Stordalen, Sweden." *Biogeosciences* 11 (17): 4753–70. https://doi.org/10.5194/bg-11-4753-2014.

Dieleman, Catherine M., Brian A. Branfireun, James W. Mclaughlin, and Zoe Lindo. 2015. "Climate Change Drives a Shift in Peatland Ecosystem Plant Community: Implications for Ecosystem Function and Stability." *Global Change Biology* 21 (1): 388–95. https://doi.org/10.1111/gcb.12643.

Dorrepaal, Ellen, Sylvia Toet, Richard S.P. Van Logtestijn, Elferra Swart, Martine J. Van De Weg, Terry V. Callaghan, and Rien Aerts. 2009. "Carbon Respiration from Subsurface Peat Accelerated by Climate Warming in the Subarctic." *Nature* 460 (7255): 616–19. https://doi.org/10.1038/nature08216.

Dunn, Christian, Timothy G. Jones, Astrid Girard, and Chris Freeman. 2014. "Methodologies for

Extracellular Enzyme Assays from Wetland Soils." *Wetlands* 34 (1): 9–17. https://doi.org/10.1007/s13157-013-0475-0.

Durán, Nelson, Maria A. Rosa, Alessandro D'Annibale, and Liliana Gianfreda. 2002. "Applications of Laccases and Tyrosinases (Phenoloxidases) Immobilized on Different Supports: A Review." *Enzyme and Microbial Technology*. https://doi.org/10.1016/S0141-0229(02)00214-4.

Estop-Aragonés, Cristian, Mark D.A. Cooper, James P. Fisher, Aaron Thierry, Mark H. Garnett, Dan J. Charman, Julian B. Murton, et al. 2018. "Limited Release of Previously-Frozen C and Increased New Peat Formation after Thaw in Permafrost Peatlands." *Soil Biology and Biochemistry* 118 (December 2017): 115–29. https://doi.org/10.1016/j.soilbio.2017.12.010.

Estop-Aragonés, Cristian, Claudia I. Czimczik, Liam Heffernan, Carolyn Gibson, Jennifer C. Walker, Xiaomei Xu, and David Olefeldt. 2018. "Respiration of Aged Soil Carbon during Fall in Permafrost Peatlands Enhanced by Active Layer Deepening Following Wildfire but Limited Following Thermokarst." *Environmental Research Letters* 13 (8). https://doi.org/10.1088/1748-9326/aad5f0.

Euskirchen, E. S., C. W. Edgar, M. R. Turetsky, M. P. Waldrop, and J. W. Harden. 2014. "Differential Response of Carbon Fluxes to Climate in Three Peatland Ecosystems That Vary in the Presence and Stability of Permafrost." *Journal of Geophysical Research G: Biogeosciences* 119 (8): 1576–95. https://doi.org/10.1002/2014JG002683.

Everett, K. R. 1989. "Glossary of Permafrost and Related Ground-Ice Terms." *Arctic and Alpine Research*. https://doi.org/10.2307/1551636.

Fenner, N., C. Freeman, and B. Reynolds. 2005. "Observations of a Seasonally Shifting Thermal Optimum in Peatland Carbon-Cycling Processes; Implications for the Global Carbon Cycle and Soil Enzyme Methodologies." *Soil Biology and Biochemistry* 37 (10): 1814–21. https://doi.org/10.1016/j.soilbio.2005.02.032.

Fenner, Nathalie, and Chris Freeman. 2011. "Drought-Induced Carbon Loss in Peatlands." *Nature Geoscience* 4 (12): 895–900. https://doi.org/10.1038/ngeo1323.

Fenner, Nathalie, Christopher Freeman, and Brian Reynolds. 2005. "Hydrological Effects on the Diversity of Phenolic Degrading Bacteria in a Peatland: Implications for Carbon Cycling." *Soil Biology and Biochemistry* 37 (7): 1277–87. https://doi.org/10.1016/j.soilbio.2004.11.024.

Fierer, Noah, Joseph M. Craine, Kendra Mclauchlan, and Joshua P. Schimel. 2005. "Litter Quality and the Temperature Sensitivity of Decomposition." *Ecology*. https://doi.org/10.1890/04-1254.

Finger, Rebecca A., Merritt R. Turetsky, Knut Kielland, Roger W. Ruess, Michelle C. Mack, and Eugénie S. Euskirchen. 2016. "Effects of Permafrost Thaw on Nitrogen Availability and Plant–Soil Interactions in a Boreal Alaskan Lowland." *Journal of Ecology* 104 (6): 1542–54. https://doi.org/10.1111/1365-2745.12639.

Fisk, Melany C., Kristin F. Ruether, and Joseph B. Yavitt. 2003. "Microbial Activity and Functional Composition among Northern Peatland Ecosystems." *Soil Biology and*

Biochemistry. https://doi.org/10.1016/S0038-0717(03)00053-1.

Fox, John, and Sanford Weisberg. 2011. "An R Companion to Applied Regression, Sec- Ond Ed." Sage, Thousand Oaks CA. 2011. https://doi.org/10.1016/j.stomax.2010.07.001.

Fraser, C. J.D., N. T. Roulet, and T. R. Moore. 2001. "Hydrology and Dissolved Organic Carbon Biogeochemistry in an Ombrotrophic Bog." *Hydrological Processes*. https://doi.org/10.1002/hyp.322.

Freeman, C., C. D. Evans, D. T. Monteith, B. Reynolds, and N. Fenner. 2001. "Export of Organic Carbon from Peat Soils." *Nature*. https://doi.org/10.1038/35090628.

Freeman, C., N. J. Ostle, N. Fenner, and H. Kang. 2004. "A Regulatory Role for Phenol Oxidase during Decomposition in Peatlands." In *Soil Biology and Biochemistry*. https://doi.org/10.1016/j.soilbio.2004.07.012.

Freeman, Chris, Nick Ostle, and Hojeong Kang. 2002. "An Enzymic 'latch' on a Global Carbon Store." *Nature*. https://doi.org/10.1038/35051650.

Freeman, Christopher, Nathalie Fenner, and Anil H. Shirsat. 2012. "Peatland Geoengineering: An Alternative Approach to Terrestrial Carbon Sequestration." *Philosophical Transactions of the Royal Society A: Mathematical, Physical and Engineering Sciences*. https://doi.org/10.1098/rsta.2012.0105.

Frolking, Steve, Nigel Roulet, and Jan Fuglestvedt. 2006. "How Northern Peatlands Influence the Earth's Radiative Budget: Sustained Methane Emission versus Sustained Carbon Sequestration." *Journal of Geophysical Research: Biogeosciences* 111 (1): 1–10. https://doi.org/10.1029/2005JG000091.

Frolking, Steve, and Nigel T. Roulet. 2007. "Holocene Radiative Forcing Impact of Northern Peatland Carbon Accumulation and Methane Emissions." *Global Change Biology* 13 (5): 1079–88. https://doi.org/10.1111/j.1365-2486.2007.01339.x.

Frolking, Steve, Nigel T. Roulet, Tim R. Moore, Peter M. Lafleur, Jill L. Bubier, and Patrick M. Crill. 2002. "Modeling Seasonal to Annual Carbon Balance of Mer Bleue Bog, Ontario, Canada." *Global Biogeochemical Cycles*. https://doi.org/10.1029/2001gb001457.

Frolking, Steve, Nigel T. Roulet, Tim R. Moore, Pierre J.H. Richard, Martin Lavoie, and Serge D. Muller. 2001. "Modeling Northern Peatland Decomposition and Peat Accumulation." *Ecosystems*. https://doi.org/10.1007/s10021-001-0105-1.

Frolking, Steve, Julie Talbot, Miriam C. Jones, Claire C. Treat, J. Boone Kauffman, Eeva Stiina Tuittila, and Nigel Roulet. 2011. "Peatlands in the Earth's 21st Century Climate System." *Environmental Reviews*. https://doi.org/10.1139/a11-014.

Gallego-Sala, Angela V., Dan J. Charman, Simon Brewer, Susan E. Page, I. Colin Prentice, Pierre Friedlingstein, Steve Moreton, et al. 2018. "Latitudinal Limits to the Predicted Increase of the Peatland Carbon Sink with Warming." *Nature Climate Change*. https://doi.org/10.1038/s41558-018-0271-1.

García-Ruiz, Roberto, V. Ochoa, B. Viñegla, M. B. Hinojosa, R. Peña-Santiago, G. Liébanas, J. C. Linares, and J. A. Carreira. 2009. "Soil Enzymes, Nematode Community and Selected

Physico-Chemical Properties as Soil Quality Indicators in Organic and Conventional Olive Oil Farming: Influence of Seasonality and Site Features." *Applied Soil Ecology*. https://doi.org/10.1016/j.apsoil.2008.12.004.

Gibson, Carolyn M., Laura E. Chasmer, Dan K. Thompson, William L. Quinton, Mike D. Flannigan, and David Olefeldt. 2018. "Wildfire as a Major Driver of Recent Permafrost Thaw in Boreal Peatlands." *Nature Communications* 9 (1). https://doi.org/10.1038/s41467-018-05457-1.

Gill, Allison L., Marc André Giasson, Rieka Yu, and Adrien C. Finzi. 2017. "Deep Peat Warming Increases Surface Methane and Carbon Dioxide Emissions in a Black Spruce-Dominated Ombrotrophic Bog." *Global Change Biology* 23 (12): 5398–5411. https://doi.org/10.1111/gcb.13806.

Gorham, E. 1991. "Northern Peatlands: Role in the Carbon Cycle and Probable Responses to Climatic Warming." *Ecological Applications*. https://doi.org/10.2307/1941811.

Gorham, Eville, Clarence Lehman, Arthur Dyke, Joannes Janssens, and Lawrence Dyke. 2007. "Temporal and Spatial Aspects of Peatland Initiation Following Deglaciation in North America." *Quaternary Science Reviews*. https://doi.org/10.1016/j.quascirev.2006.08.008.

Grace, James B., T. Michael Anderson, Olff Han, and Samuel M. Scheiner. 2010. "On the Specification of Structural Equation Models for Ecological Systems." *Ecological Monographs*. https://doi.org/10.1890/09-0464.1.

Grosse, Guido, Scott Goetz, A. Dave McGuire, Vladimir E. Romanovsky, and Edward A.G. Schuur. 2016. "Changing Permafrost in a Warming World and Feedbacks to the Earth System." *Environmental Research Letters*. https://doi.org/10.1088/1748-9326/11/4/040201.

Grosse, Guido, Jennifer Harden, Merritt Turetsky, A. David McGuire, Philip Camill, Charles Tarnocai, Steve Frolking, et al. 2011. "Vulnerability of High-Latitude Soil Organic Carbon in North America to Disturbance." *Journal of Geophysical Research: Biogeosciences* 116 (3): 1–23. https://doi.org/10.1029/2010JG001507.

Hájek, T., Simon Ballance, Juul Limpens, Mink Zijlstra, and Jos T.A. Verhoeven. 2011. "Cell-Wall Polysaccharides Play an Important Role in Decay Resistance of Sphagnum and Actively Depressed Decomposition in Vitro." *Biogeochemistry*. https://doi.org/10.1007/s10533-010-9444-3.

Halsey, Linda A., Dale H. Vitt, and Ilka E. Bauer. 1998. "Peatland Initiation during the Holocene in Continental Western Canada." *Climatic Change*. https://doi.org/10.1023/A:1005425124749.

Hansen, Angela M., Tamara E.C. Kraus, Brian A. Pellerin, Jacob A. Fleck, Bryan D. Downing, and Brian A. Bergamaschi. 2016. "Optical Properties of Dissolved Organic Matter (DOM): Effects of Biological and Photolytic Degradation." *Limnology and Oceanography*. https://doi.org/10.1002/lno.10270.

Hartley, Iain P., Timothy C. Hill, Thomas J. Wade, Robert J. Clement, John B. Moncrieff, Ana Prieto-Blanco, Mathias I. Disney, et al. 2015. "Quantifying Landscape-Level Methane Fluxes in Subarctic Finland Using a Multiscale Approach." *Global Change Biology*.

https://doi.org/10.1111/gcb.12975.

Heffernan, Liam, Cristian Estop-Aragonés, Klaus-Holger Knorr, Julie Talbot, and David Olefeldt. 2020. “Long-Term Impacts of Permafrost Thaw on Carbon Storage in Peatlands: Deep Losses Offset by Surficial Accumulation.” *Journal of Geophysical Research: Biogeosciences* 2011 (2865): e2019JG005501. https://doi.org/10.1029/2019JG005501.

Heginbottom, J.A., M.H. Dubreuil, and P.T. Harker. 1995. “Canada, Permafrost.” *National Atlas of Canada*.

Helbig, M., C. Pappas, and O. Sonnentag. 2016. “Permafrost Thaw and Wildfire: Equally Important Drivers of Boreal Tree Cover Changes in the Taiga Plains, Canada.” *Geophysical Research Letters*. https://doi.org/10.1002/2015GL067193.

Helbig, Manuel, Laura E. Chasmer, Ankur R. Desai, Natascha Kljun, William L. Quinton, and Oliver Sonnentag. 2017. “Direct and Indirect Climate Change Effects on Carbon Dioxide Fluxes in a Thawing Boreal Forest–Wetland Landscape.” *Global Change Biology* 23 (8): 3231–48. https://doi.org/10.1111/gcb.13638.

Helbig, Manuel, Laura E. Chasmer, Natas Cha Kljun, William L. Quinton, Claire C. Treat, and Oliver Sonnentag. 2017. “The Positive Net Radiative Greenhouse Gas Forcing of Increasing Methane Emissions from a Thawing Boreal Forest-Wetland Landscape.” *Global Change Biology*. https://doi.org/10.1111/gcb.13520.

Helbig, Manuel, Karoline Wischnewski, Natascha Kljun, Laura E. Chasmer, William L. Quinton, Matteo Detto, and Oliver Sonnentag. 2016. “Regional Atmospheric Cooling and Wetting Effect of Permafrost Thaw-Induced Boreal Forest Loss.” *Global Change Biology*. https://doi.org/10.1111/gcb.13348.

Henry, Hugh A.L. 2013. “Reprint of ‘Soil Extracellular Enzyme Dynamics in a Changing Climate.’” *Soil Biology and Biochemistry*. https://doi.org/10.1016/j.soilbio.2012.10.022.

Heslop, J.K., M. Winkel, K.M. Walter Anthony, R.G.M. Spencer, D.C. Podgorski, P. Zito, A. Kholodov, M. Zhang, and S. Liebner. 2019. “Increasing Organic Carbon Biolability with Depth in Yedoma Permafrost: Ramifications for Future Climate Change.” *Journal of Geophysical Research: Biogeosciences*. https://doi.org/10.1029/2018jg004712.

Hobbie, Sarah E. 1996. “Temperature and Plant Species Control over Litter Decomposition in Alaskan Tundra.” *Ecological Monographs*. https://doi.org/10.2307/2963492.

Hodgkins, S. B., M. M. Tfaily, C. K. McCalley, T. A. Logan, P. M. Crill, S. R. Saleska, V. I. Rich, and J. P. Chanton. 2014. “Changes in Peat Chemistry Associated with Permafrost Thaw Increase Greenhouse Gas Production.” *Proceedings of the National Academy of Sciences* 111 (16): 5819–24. https://doi.org/10.1073/pnas.1314641111.

Holland, M. M., and C. M. Bitz. 2003. “Polar Amplification of Climate Change in Coupled Models.” *Climate Dynamics*. https://doi.org/10.1007/s00382-003-0332-6.

Holloway, Jean E., and Antoni G. Lewkowicz. 2019. “Half a Century of Discontinuous Permafrost Persistence and Degradation in Western Canada.” *Permafrost and Periglacial Processes*. https://doi.org/10.1002/ppp.2017.

Hothorn, Torsten, Frank Bretz, and Peter Westfall. 2008. “Simultaneous Inference in General Parametric Models.” *Biometrical Journal*. https://doi.org/10.1002/bimj.200810425.

Hugelius, G., J. Strauss, S. Zubrzycki, J. W. Harden, E. A.G. Schuur, C. L. Ping, L. Schirrmeister, et al. 2014. “Estimated Stocks of Circumpolar Permafrost Carbon with Quantified Uncertainty Ranges and Identified Data Gaps.” *Biogeosciences* 11 (23): 6573–93. https://doi.org/10.5194/bg-11-6573-2014.

IPCC. 2019. “The Ocean and Cryosphere in a Changing Climate.” *In Press*. https://doi.org/https://www.ipcc.ch/report/srocc/.

Jassey, Vincent E.J., Geneviève Chiapusio, Edward A.D. Mitchell, Philippe Binet, Marie Laure Toussaint, and Daniel Gilbert. 2011. “Fine-Scale Horizontal and Vertical Micro-Distribution Patterns of Testate Amoebae Along a Narrow Fen/Bog Gradient.” *Microbial Ecology*. https://doi.org/10.1007/s00248-010-9756-9.

Jassey, Vincent E.J., Monika K. Reczuga, Małgorzata Zielińska, Sandra Słowińska, Bjorn J.M. Robroek, Pierre Mariotte, Christophe V. W Seppey, et al. 2018. “Tipping Point in Plant–Fungal Interactions under Severe Drought Causes Abrupt Rise in Peatland Ecosystem Respiration.” *Global Change Biology*. https://doi.org/10.1111/gcb.13928.

Jassey, Vincent E J, Geneviève Chiapusio, Daniel Gilbert, Marie Laure Toussaint, and Philippe Binet. 2012. “Phenoloxidase and Peroxidase Activities in Sphagnum-Dominated Peatland in a Warming Climate.” *Soil Biology and Biochemistry* 46: 49–52. https://doi.org/10.1016/j.soilbio.2011.11.011.

Jassey, Vincent Ej, Geneviève Chiapusio, Philippe Binet, Alexandre Buttler, Fatima Laggoun-Défarge, Frédéric Delarue, Nadine Bernard, et al. 2013. “Above- and Belowground Linkages in Sphagnum Peatland: Climate Warming Affects Plant-Microbial Interactions.” *Global Change Biology* 19 (3): 811–23. https://doi.org/10.1111/gcb.12075.

Jensen, Anna M., Jeffrey M. Warren, Anthony W. King, Daniel M. Ricciuto, Paul J. Hanson, and Stan D. Wullschleger. 2019. “Simulated Projections of Boreal Forest Peatland Ecosystem Productivity Are Sensitive to Observed Seasonality in Leaf Physiology.” *Tree Physiology*. https://doi.org/10.1093/treephys/tpy140.

Johansson, Torbjörn, Nils Malmer, Patrick M. Crill, Thomas Friborg, Jonas H. Åkerman, Mikhail Mastepanov, and Torben R. Christensen. 2006. “Decadal Vegetation Changes in a Northern Peatland, Greenhouse Gas Fluxes and Net Radiative Forcing.” *Global Change Biology*. https://doi.org/10.1111/j.1365-2486.2006.01267.x.

Johnson, Loretta C., and Antoni W. H. Damman. 1991. “Species-Controlled Sphagnum Decay on a South Swedish Raised Bog.” *Oikos* 61 (2): 234. https://doi.org/10.2307/3545341.

Johnston, Carmel E., Stephanie A. Ewing, Jennifer W. Harden, Ruth K. Varner, Kimberly P. Wickland, Joshua C. Koch, Christopher C. Fuller, Kristen Manies, and M. Torre Jorgenson. 2014. “Effect of Permafrost Thaw on CO<inf>2</Inf> and CH<inf>4</Inf> Exchange in a Western Alaska Peatland Chronosequence.” *Environmental Research Letters* 9 (8): 085004. https://doi.org/10.1088/1748-9326/9/8/085004.

Jones, Miriam C., Robert K. Booth, Zicheng Yu, and Paul Ferry. 2013. “A 2200-Year Record of

Permafrost Dynamics and Carbon Cycling in a Collapse-Scar Bog, Interior Alaska." *Ecosystems* 16 (1): 1–19. https://doi.org/10.1007/s10021-012-9592-5.

Jones, Miriam C., Jennifer Harden, Jonathan O'Donnell, Kristen Manies, Torre Jorgenson, Claire Treat, and Stephanie Ewing. 2017. "Rapid Carbon Loss and Slow Recovery Following Permafrost Thaw in Boreal Peatlands." *Global Change Biology* 23 (3): 1109–27. https://doi.org/10.1111/gcb.13403.

Jones, Miriam C., and Zicheng Yu. 2010. "Rapid Deglacial and Early Holocene Expansion of Peatlands in Alaska." *Proceedings of the National Academy of Sciences of the United States of America*. https://doi.org/10.1073/pnas.0911387107.

Jonsson, Micael, and David A. Wardle. 2010. "Structural Equation Modelling Reveals Plant-Community Drivers of Carbon Storage in Boreal Forest Ecosystems." *Biology Letters*. https://doi.org/10.1098/rsbl.2009.0613.

Jorgenson, M. Torre, Charles H. Racine, James C. Walters, and Thomas E. Osterkamp. 2001. "Permafrost Degradation and Ecological Changes Associated with a Warming Climate in Central Alaska." *Climatic Change* 48 (4): 551–79. https://doi.org/10.1023/A:1005667424292.

Jorgenson, Torre, Vladimir Romanovsky, Jennifer Harden, Yuri Shur, Jonathan O'Donnell, E. A. G. Schuur, Mikhail Kanevskiy, and Sergei Marchenko. 2010. "Resilience and Vulnerability of Permafrost to Climate Change." *Canadian Journal of Forest Research*. https://doi.org/10.1139/X10-098.

Juggins, S. 2003. "C2 User Guide: Software for Ecological and Palaeoecological Data Analysis and Visualization." *User Guide*. Newcastle upon Tyne, UK: Newcastle University. http://scholar.google.com/scholar?hl=en&btnG=Search&q=intitle:C2+Software+for+ecological+and+palaeoecological+data+analysis+and+visualisation#0.

Juszczak, Radosław, Elyn Humphreys, Manuel Acosta, Maria Michalak-Galczewska, Dariusz Kayzer, and Janusz Olejnik. 2013. "Ecosystem Respiration in a Heterogeneous Temperate Peatland and Its Sensitivity to Peat Temperature and Water Table Depth." *Plant and Soil*. https://doi.org/10.1007/s11104-012-1441-y.

Kalbitz, K., J. Schmerwitz, D. Schwesig, and E. Matzner. 2003. "Biodegradation of Soil-Derived Dissolved Organic Matter as Related to Its Properties." In *Geoderma*. https://doi.org/10.1016/S0016-7061(02)00365-8.

Kanevskiy, Mikhail, Torre Jorgenson, Yuri Shur, Jonathan A. O'Donnell, Jennifer W. Harden, Qianlai Zhuang, and Daniel Fortier. 2014. "Cryostratigraphy and Permafrost Evolution in the Lacustrine Lowlands of West-Central Alaska." *Permafrost and Periglacial Processes* 25 (1): 14–34. https://doi.org/10.1002/ppp.1800.

Kassambara, Alboukadel. 2018. "Ggpubr: 'ggplot2' Based Publication Ready Plots. R Package Version 0.2. Https://CRAN.R-Project.Org/Package=ggpubr." *Https://CRAN.R-Project.Org/Package=ggpubr*. https://doi.org/R package version 0.1.8.

Kaštovská, Eva, Petra Straková, Keith Edwards, Zuzana Urbanová, Jiří Bárta, Jiří Mastný, Hana Šantrůčková, and Tomáš Picek. 2018. "Cotton-Grass and Blueberry Have Opposite Effect

on Peat Characteristics and Nutrient Transformation in Peatland." *Ecosystems* 21 (3): 443–58. https://doi.org/10.1007/s10021-017-0159-3.

Keller, Jason K., and Scott D. Bridgham. 2007. "Pathways of Anaerobic Carbon Cycling across an Ombrotrophic-Minerotrophic Peatland Gradient." *Limnology and Oceanography*. https://doi.org/10.4319/lo.2007.52.1.0096.

Kettridge, N., and A. Baird. 2008. "Modelling Soil Temperatures in Northern Peatlands." *European Journal of Soil Science*. https://doi.org/10.1111/j.1365-2389.2007.01000.x.

Keuper, Frida, Peter M. van Bodegom, Ellen Dorrepaal, James T. Weedon, Jurgen van Hal, Richard S.P. van Logtestijn, and Rien Aerts. 2012. "A Frozen Feast: Thawing Permafrost Increases Plant-Available Nitrogen in Subarctic Peatlands." *Global Change Biology* 18 (6): 1998–2007. https://doi.org/10.1111/j.1365-2486.2012.02663.x.

Klapstein, Sara J., Merritt R. Turetsky, A. David McGuire, Jennifer W. Harden, Claudia I. Czimczik, Xiaomei Xu, Jeffrey P. Chanton, and James M. Waddington. 2014. "Controls on Methane Released through Ebullition in Peatlands Affected by Permafrost Degradation." *Journal of Geophysical Research: Biogeosciences*. https://doi.org/10.1002/2013JG002441.

Klerk, Pim De, Norman Donner, Nikolay S. Karpov, Merten Minke, and Hans Joosten. 2011. "Short-Term Dynamics of a Low-Centred Ice-Wedge Polygon near Chokurdakh (NE Yakutia, NE Siberia) and Climate Change during the Last ca 1250 Years." *Quaternary Science Reviews*. https://doi.org/10.1016/j.quascirev.2011.06.016.

Knoblauch, Christian, Christian Beer, Alexander Sosnin, Dirk Wagner, and Eva Maria Pfeiffer. 2013. "Predicting Long-Term Carbon Mineralization and Trace Gas Production from Thawing Permafrost of Northeast Siberia." *Global Change Biology*. https://doi.org/10.1111/gcb.12116.

Koch, Oliver, Dagmar Tscherko, and Ellen Kandeler. 2007. "Temperature Sensitivity of Microbial Respiration, Nitrogen Mineralization, and Potential Soil Enzyme Activities in Organic Alpine Soils." *Global Biogeochemical Cycles*. https://doi.org/10.1029/2007GB002983.

Kokelj, S. V., and M. T. Jorgenson. 2013. "Advances in Thermokarst Research." *Permafrost and Periglacial Processes* 24 (2): 108–19. https://doi.org/10.1002/ppp.1779.

Korhola, Atte, Meri Ruppel, Heikki Seppä, Minna Väliranta, Tarmo Virtanen, and Jan Weckström. 2010. "The Importance of Northern Peatland Expansion to the Late-Holocene Rise of Atmospheric Methane." *Quaternary Science Reviews*. https://doi.org/10.1016/j.quascirev.2009.12.010.

Koven, C. D., E. A.G. Schuur, C. Schädel, T. J. Bohn, E. J. Burke, G. Chen, X. Chen, et al. 2015. "A Simplified, Data-Constrained Approach to Estimate the Permafrost Carbon-Climate Feedback." *Philosophical Transactions of the Royal Society A: Mathematical, Physical and Engineering Sciences* 373 (2054). https://doi.org/10.1098/rsta.2014.0423.

Koven, Charles D., William J. Riley, and Alex Stern. 2013. "Analysis of Permafrost Thermal Dynamics and Response to Climate Change in the CMIP5 Earth System Models." *Journal of Climate* 26 (6): 1877–1900. https://doi.org/10.1175/JCLI-D-12-00228.1.

Kremenetski, K. V., A. A. Velichko, O. K. Borisova, G. M. MacDonald, L. C. Smith, K. E. Frey, and L. A. Orlova. 2003. “Peatlands of the Western Siberian Lowlands: Current Knowledge on Zonation, Carbon Content and Late Quaternary History.” *Quaternary Science Reviews*. https://doi.org/10.1016/S0277-3791(02)00196-8.

Kuhry, P., Vitt, D. 1996. “Fossil Carbon / Nitrogen Ratios as a Measure of Peat Decomposition.” *Ecology* 77 (1): 271–75.

Kuhry, Peter. 2008. “Palsa and Peat Plateau Development in the Hudson Bay Lowlands, Canada: Timing, Pathways and Causes.” *Boreas*. https://doi.org/10.1111/j.1502-3885.2007.00022.x.

Lafleur, P. M., T. R. Moore, N. T. Roulet, and S. Frolking. 2005. “Ecosystem Respiration in a Cool Temperate Bog Depends on Peat Temperature but Not Water Table.” *Ecosystems*. https://doi.org/10.1007/s10021-003-0131-2.

Laiho, Raija. 2006. “Decomposition in Peatlands: Reconciling Seemingly Contrasting Results on the Impacts of Lowered Water Levels.” *Soil Biology and Biochemistry* 38 (8): 2011–24. https://doi.org/10.1016/j.soilbio.2006.02.017.

Laiho, Raija, Harri Vasander, Timo Penttilä, and Jukka Laine. 2003. “Dynamics of Plant-Mediated Organic Matter and Nutrient Cycling Following Water-Level Drawdown in Boreal Peatlands.” *Global Biogeochemical Cycles*. https://doi.org/10.1029/2002gb002015.

Laine, Anna M., Päivi Mäkiranta, Raija Laiho, Lauri Mehtätalo, Timo Penttilä, Aino Korrensalo, Kari Minkkinen, Hannu Fritze, and Eeva Stiina Tuittila. 2019. “Warming Impacts on Boreal Fen CO 2 Exchange under Wet and Dry Conditions.” *Global Change Biology*. https://doi.org/10.1111/gcb.14617.

Lara, Mark J., Hélène Genet, Anthony D. Mcguire, Eugénie S. Euskirchen, Yujin Zhang, Dana R.N. Brown, Mark T. Jorgenson, Vladimir Romanovsky, Amy Breen, and William R. Bolton. 2016. “Thermokarst Rates Intensify Due to Climate Change and Forest Fragmentation in an Alaskan Boreal Forest Lowland.” *Global Change Biology*. https://doi.org/10.1111/gcb.13124.

Larsen, Klaus S., Paul Grogan, Sven Jonasson, and Anders Michelsen. 2007. “Respiration and Microbial Dynamics in Two Subarctic Ecosystems during Winter and Spring Thaw: Effects of Increased Snow Depth.” *Arctic, Antarctic, and Alpine Research*. https://doi.org/10.1657/1523-0430(2007)39[268:RAMDIT]2.0.CO;2.

Lawrence, David M., Andrew G. Slater, and Sean C. Swenson. 2012. “Simulation of Present-Day and Future Permafrost and Seasonally Frozen Ground Conditions in CCSM4.” *Journal of Climate* 25 (7): 2207–25. https://doi.org/10.1175/JCLI-D-11-00334.1.

Lee, S. S., K. J. Shin, W. Y. Kim, J. K. Ha, and In K. Han. 1999. “The Rumen Ecosystem : As a Fountain Source of Nobel Enzymes - Review.” *Asian-Australasian Journal of Animal Sciences*. https://doi.org/10.5713/ajas.1999.988.

Lefcheck, Jonathan S. 2016. “PiecewiseSEM: Piecewise Structural Equation Modelling in r for Ecology, Evolution, and Systematics.” *Methods in Ecology and Evolution* 7 (5): 573–79. https://doi.org/10.1111/2041-210X.12512.

Limpens, J., F. Berendse, C. Blodau, J. G. Canadell, C. Freeman, J. Holden, N. Roulet, H. Rydin,

and G. Schaepman-Strub. 2008. “Peatlands and the Carbon Cycle: From Local Processes to Global Implications - A Synthesis.” *Biogeosciences* 5 (5): 1475–91. https://doi.org/10.5194/bg-5-1475-2008.

Limpens, Juul, and Frank Berendse. 2003. “How Litter Quality Affects Mass Loss and N Loss from Decomposing Sphagnum.” *Oikos*. https://doi.org/10.1034/j.1600-0706.2003.12707.x.

Limpens, Juul, Elisabet Bohlin, and Mats B. Nilsson. 2017. “Phylogenetic or Environmental Control on the Elemental and Organo-Chemical Composition of Sphagnum Mosses?” *Plant and Soil* 417 (1–2): 69–85. https://doi.org/10.1007/s11104-017-3239-4.

Lin, Xueju, Malak M. Tfaily, J. Megan Steinweg, Patrick Chanton, Kaitlin Esson, Zamin K. Yang, Jeffrey P. Chanton, William Cooper, Christopher W. Schadt, and Joel E. Kostka. 2014. “Microbial Community Stratification Linked to Utilization of Carbohydrates and Phosphorus Limitation in a Boreal Peatland at Marcell Experimental Forest, Minnesota, USA.” *Applied and Environmental Microbiology*. https://doi.org/10.1128/AEM.00205-14.

Liu, Futing, Dan Kou, Benjamin W. Abbott, Chao Mao, Yongliang Chen, Leiyi Chen, and Yuanhe Yang. 2019. “Disentangling the Effects of Climate, Vegetation, Soil and Related Substrate Properties on the Biodegradability of Permafrost-Derived Dissolved Organic Carbon.” *Journal of Geophysical Research: Biogeosciences*, 3377–89. https://doi.org/10.1029/2018JG004944.

Loisel, Julie, Zicheng Yu, David W. Beilman, Philip Camill, Jukka Alm, Matthew J. Amesbury, David Anderson, et al. 2014. “A Database and Synthesis of Northern Peatland Soil Properties and Holocene Carbon and Nitrogen Accumulation.” *Holocene* 24 (9): 1028–42. https://doi.org/10.1177/0959683614538073.

Luo, Ling, Han Meng, and Ji Dong Gu. 2017. “Microbial Extracellular Enzymes in Biogeochemical Cycling of Ecosystems.” *Journal of Environmental Management*. https://doi.org/10.1016/j.jenvman.2017.04.023.

MacDonald, Glen M., David W. Beilman, Konstantine V. Kremenetski, Yongwei Sheng, Laurence C. Smith, and Andrei A. Velichko. 2006. “Rapid Early Development of Circumarctic Peatlands and Atmospheric CH 4 and CO2 Variations.” *Science*. https://doi.org/10.1126/science.1131722.

Machmuller, Megan B., Jacqueline E. Mohan, Jeffrey M. Minucci, Carly A. Phillips, and Nina Wurzburger. 2016. “Season, but Not Experimental Warming, Affects the Activity and Temperature Sensitivity of Extracellular Enzymes.” *Biogeochemistry* 131 (3): 255–65. https://doi.org/10.1007/s10533-016-0277-6.

Mäkiranta, Päivi, Raija Laiho, Hannu Fritze, Jyrki Hytönen, Jukka Laine, and Kari Minkkinen. 2009. “Indirect Regulation of Heterotrophic Peat Soil Respiration by Water Level via Microbial Community Structure and Temperature Sensitivity.” *Soil Biology and Biochemistry*. https://doi.org/10.1016/j.soilbio.2009.01.004.

Mäkiranta, Päivi, Raija Laiho, Lauri Mehtätalo, Petra Straková, Janne Sormunen, Kari Minkkinen, Timo Penttilä, Hannu Fritze, and Eeva Stiina Tuittila. 2018. “Responses of Phenology and Biomass Production of Boreal Fens to Climate Warming under Different Water-Table Level Regimes.” *Global Change Biology*. https://doi.org/10.1111/gcb.13934.

Malmer, Nils, and Bo Wallén. 1999. “The Dynamics of Peat Accumulation on Bogs: Mass Balance of Hummocks and Hollows and Its Variation throughout a Millennium.” *Ecography*. https://doi.org/10.1111/j.1600-0587.1999.tb00523.x.

Manabe, S., and R. T. Wetherald. 1986. “Reduction in Summer Soil Wetness Induced by an Increase in Atmospheric Carbon Dioxide.” *Science*. https://doi.org/10.1126/science.232.4750.626.

Marx, M. C., M. Wood, and S. C. Jarvis. 2001. “A Microplate Fluorimetric Assay for the Study of Enzyme Diversity in Soils.” *Soil Biology and Biochemistry*. https://doi.org/10.1016/S0038-0717(01)00079-7.

Mauquoy, Dmitri., Pdm. Hughes, and B. van Geel. 2010. “A Protocol for Plant Macrofossil Analysis of Peat Deposits.” *Mires and Peat* 7 (06): 1–5. https://doi.org/http://www.mires-and-peat.net/map07/map_07_06.htm.

Mauritz, Marguerite, Rosvel Bracho, Gerardo Celis, Jack Hutchings, Susan M. Natali, Elaine Pegoraro, Verity G. Salmon, Christina Schädel, Elizabeth E. Webb, and Edward A.G. Schuur. 2017. “Nonlinear CO2 Flux Response to 7 Years of Experimentally Induced Permafrost Thaw.” *Global Change Biology*. https://doi.org/10.1111/gcb.13661.

Mezbahuddin, M., R. F. Grant, and L. B. Flanagan. 2016. “Modeling Hydrological Controls on Variations in Peat Water Content, Water Table Depth, and Surface Energy Exchange of a Boreal Western Canadian Fen Peatland.” *Journal of Geophysical Research: Biogeosciences*. https://doi.org/10.1002/2016JG003501.

Michaelis, L, Maud L Menten, Roger S Goody, and Kenneth A Johnson. 1913. “Die Kinetik Der Invertinwirkung/ The Kinetics of Invertase Action.” *Biochemistry*. https://doi.org/10.1021/bi201284u.

Monteux, Sylvain, James T. Weedon, Gesche Blume-Werry, Konstantin Gavazov, Vincent E.J. Jassey, Margareta Johansson, Frida Keuper, Carolina Olid, and Ellen Dorrepaal. 2018. “Long-Term in Situ Permafrost Thaw Effects on Bacterial Communities and Potential Aerobic Respiration.” *ISME Journal*. https://doi.org/10.1038/s41396-018-0176-z.

Moore, T. R., and M. Dalva. 1993. “The Influence of Temperature and Water Table Position on Carbon Dioxide and Methane Emissions from Laboratory Columns of Peatland Soils.” *Journal of Soil Science* 44 (4): 651–64. https://doi.org/10.1111/j.1365-2389.1993.tb02330.x.

Moore, T. R., N. T. Roulet, and J. M. Waddington. 1998. “Uncertainty in Predicting the Effect of Climatic Change on the Carbon Cycling of Canadian Peatlands.” *Climatic Change*. https://doi.org/10.1023/A:1005408719297.

Moore, Tim, and Nate Basiliko. 2006. “Decomposition in Boreal Peatlands.” In *Boreal Peatland Ecosystems*. https://doi.org/10.1007/978-3-540-31913-9_7.

Moore, Tim R., Jill L. Bubier, and Leszek Bledzki. 2007. “Litter Decomposition in Temperate Peatland Ecosystems: The Effect of Substrate and Site.” *Ecosystems* 10 (6): 949–63. https://doi.org/10.1007/s10021-007-9064-5.

Morris, Paul J., Andy J. Baird, and Lisa R. Belyea. 2012. “The DigiBog Peatland Development

Model 2: Ecohydrological Simulations in 2D." *Ecohydrology*. https://doi.org/10.1002/eco.229.

Morris, Paul J., Graeme T. Swindles, Paul J. Valdes, Ruza F. Ivanovic, Lauren J. Gregoire, Mark W. Smith, Lev Tarasov, Alan M. Haywood, and Karen L. Bacon. 2018. "Global Peatland Initiation Driven by Regionally Asynchronous Warming." *Proceedings of the National Academy of Sciences of the United States of America*. https://doi.org/10.1073/pnas.1717838115.

Munir, T. M., M. Perkins, E. Kaing, and M. Strack. 2015. "Carbon Dioxide Flux and Net Primary Production of a Boreal Treed Bog: Responses to Warming and Water-Table-Lowering Simulations of Climate Change." *Biogeosciences*. https://doi.org/10.5194/bg-12-1091-2015.

Myers-Smith, I. H., J. W. Harden, M. Wilmking, C. C. Fuller, A. D. McGuire, and F. S. Chapin. 2008. "Wetland Succession in a Permafrost Collapse: Interactions between Fire and Thermokarst." *Biogeosciences* 5 (5): 1273–86. https://doi.org/10.5194/bg-5-1273-2008.

Myers-Smith, Isla H., A. David McGuire, Jennifer W. Harden, and F. Stuart Chapin. 2007. "Influence of Disturbance on Carbon Exchange in a Permafrost Collapse and Adjacent Burned Forest." *Journal of Geophysical Research: Biogeosciences*. https://doi.org/10.1029/2007jg000423.

Nannipieri, Paolo, Carmen Trasar-Cepeda, and Richard P. Dick. 2018. "Soil Enzyme Activity: A Brief History and Biochemistry as a Basis for Appropriate Interpretations and Meta-Analysis." *Biology and Fertility of Soils*. https://doi.org/10.1007/s00374-017-1245-6.

Natali, Susan M., Jennifer D. Watts, Brendan M. Rogers, Stefano Potter, Sarah M. Ludwig, Anne Katrin Selbmann, Patrick F. Sullivan, et al. 2019. "Large Loss of CO2 in Winter Observed across the Northern Permafrost Region." *Nature Climate Change*. https://doi.org/10.1038/s41558-019-0592-8.

Nybroe, Ole, Per Elberg Jørgensen, and Mogens Henze. 1992. "Enzyme Activities in Waste Water and Activated Sludge." *Water Research*. https://doi.org/10.1016/0043-1354(92)90230-2.

O'Donnell, Jonathan A., M. Torre Jorgenson, Jennifer W. Harden, A. David McGuire, Mikhail Z. Kanevskiy, and Kimberly P. Wickland. 2012. "The Effects of Permafrost Thaw on Soil Hydrologic, Thermal, and Carbon Dynamics in an Alaskan Peatland." *Ecosystems* 15 (2): 213–29. https://doi.org/10.1007/s10021-011-9504-0.

Oksanen, Jari, F. Guillaume Blanchet, Roeland Kindt, Maintainer Jari Oksanen, and MASS Suggests. 2013. "Package 'Vegan.'" *Community Ecology Package Version*.

Oksanen, Pirita O. 2006. "Holocene Development of the Vaisjeäggi Palsa Mire, Finnish Lapland." *Boreas* 35 (1): 81–95. https://doi.org/10.1111/j.1502-3885.2006.tb01114.x.

Oksanen, Pirita O., Peter Kuhry, and Rimma N. Alekseeva. 2003. "Holocene Development and Permafrost History of the Usinsk Mire, Northeast European Russia." *Geographie Physique et Quaternaire*. https://doi.org/10.7202/011312ar.

Olefeldt, D., S. Goswami, G. Grosse, D. Hayes, G. Hugelius, P. Kuhry, A. D. Mcguire, et al.

2016. “Circumpolar Distribution and Carbon Storage of Thermokarst Landscapes.” *Nature Communications* 7: 13043. https://doi.org/10.1038/ncomms13043.

Olefeldt, David, Eugénie S. Euskirchen, Jennifer Harden, Evan Kane, A. David McGuire, Mark P. Waldrop, and Merritt R. Turetsky. 2017. “A Decade of Boreal Rich Fen Greenhouse Gas Fluxes in Response to Natural and Experimental Water Table Variability.” *Global Change Biology* 23 (6): 2428–40. https://doi.org/10.1111/gcb.13612.

Olefeldt, David, Nigel Roulet, Reiner Giesler, and Andreas Persson. 2013. “Total Waterborne Carbon Export and DOC Composition from Ten Nested Subarctic Peatland Catchments-Importance of Peatland Cover, Groundwater Influence, and Inter-Annual Variability of Precipitation Patterns.” *Hydrological Processes*. https://doi.org/10.1002/hyp.9358.

Olefeldt, David, and Nigel T. Roulet. 2012. “Effects of Permafrost and Hydrology on the Composition and Transport of Dissolved Organic Carbon in a Subarctic Peatland Complex.” *Journal of Geophysical Research: Biogeosciences*. https://doi.org/10.1029/2011JG001819.

Olefeldt, David, Nigel T. Roulet, Onil Bergeron, Patrick Crill, Kristina Bäckstrand, and Torben R. Christensen. 2012. “Net Carbon Accumulation of a High-Latitude Permafrost Palsa Mire Similar to Permafrost-Free Peatlands.” *Geophysical Research Letters*. https://doi.org/10.1029/2011GL050355.

Olefeldt, David, Merritt R. Turetsky, Patrick M. Crill, and A. David Mcguire. 2013. “Environmental and Physical Controls on Northern Terrestrial Methane Emissions across Permafrost Zones.” *Global Change Biology* 19 (2): 589–603. https://doi.org/10.1111/gcb.12071.

Öquist, M. G., and B. H. Svensson. 2002. “Vascular Plants as Regulators of Methane Emissions from a Subarctic Mire Ecosystem.” *Journal of Geophysical Research Atmospheres*. https://doi.org/10.1029/2001JD001030.

Park, Hotaek, Youngwook Kim, and John S. Kimball. 2016. “Widespread Permafrost Vulnerability and Soil Active Layer Increases over the High Northern Latitudes Inferred from Satellite Remote Sensing and Process Model Assessments.” *Remote Sensing of Environment*. https://doi.org/10.1016/j.rse.2015.12.046.

Payette, Serge, Ann Delwaide, Marco Caccianiga, and Michel Beauchemin. 2004. “Accelerated Thawing of Subarctic Peatland Permafrost over the Last 50 Years.” *Geophysical Research Letters* 31 (18): 1–4. https://doi.org/10.1029/2004GL020358.

Peichl, Matthias, Michal Gažovič, Ilse Vermeij, Eefje De Goede, Oliver Sonnentag, Juul Limpens, and Mats B. Nilsson. 2018. “Peatland Vegetation Composition and Phenology Drive the Seasonal Trajectory of Maximum Gross Primary Production.” *Scientific Reports*. https://doi.org/10.1038/s41598-018-26147-4.

Pelletier, Nicolas, Julie Talbot, David Olefeldt, Merritt Turetsky, Christian Blodau, Oliver Sonnentag, and William L. Quinton. 2017. “Influence of Holocene Permafrost Aggradation and Thaw on the Paleoecology and Carbon Storage of a Peatland Complex in Northwestern Canada.” *Holocene* 27 (9): 1391–1405. https://doi.org/10.1177/0959683617693899.

Peres-Neto, Pedro R., Pierre Legendre, Stéphane Dray, and Daniel Borcard. 2006. "Variation Partitioning of Species Data Matrices: Estimation and Comparison of Fractions." *Ecology*. https://doi.org/10.1890/0012-9658(2006)87[2614:VPOSDM]2.0.CO;2.

Peuravuori, Juhani, and Kalevi Pihlaja. 1997. "Molecular Size Distribution and Spectroscopic Properties of Aquatic Humic Substances." *Analytica Chimica Acta*. https://doi.org/10.1016/S0003-2670(96)00412-6.

Phillips, Richard P., Adrien C. Finzi, and Emily S. Bernhardt. 2011. "Enhanced Root Exudation Induces Microbial Feedbacks to N Cycling in a Pine Forest under Long-Term CO2 Fumigation." *Ecology Letters*. https://doi.org/10.1111/j.1461-0248.2010.01570.x.

Pind, A., C. Freeman, and M. A. Lock. 1994. "Enzymic Degradation of Phenolic Materials in Peatlands - Measurement of Phenol Oxidase Activity." *Plant and Soil*. https://doi.org/10.1007/BF00009285.

Pinheiro J, Bates D, DebRoy S, Sarkar D and R Core Team. 2017. "Nlme: Linear and Nonlinear Mixed Effects Models. R Package Version 3.1-131, Https://CRAN.R-Project.Org/Package=nlme." *R Package Version 3.1-131, Https://CRAN.R-Project.Org/Package=nlme.* https://doi.org/10.1016/j.tibs.2011.05.003.

Pinsonneault, Andrew J., Tim R. Moore, and Nigel T. Roulet. 2016. "Temperature the Dominant Control on the Enzyme-Latch across a Range of Temperate Peatland Types." *Soil Biology and Biochemistry* 97: 121–30. https://doi.org/10.1016/j.soilbio.2016.03.006.

Porter, Trevor J., Spruce W. Schoenemann, Lauren J. Davies, Eric J. Steig, Sasiri Bandara, and Duane G. Froese. 2019. "Recent Summer Warming in Northwestern Canada Exceeds the Holocene Thermal Maximum." *Nature Communications*. https://doi.org/10.1038/s41467-019-09622-y.

Prater, James L., Jeffrey P. Chanton, and Gary J. Whiting. 2007. "Variation in Methane Production Pathways Associated with Permafrost Decomposition in Collapse Scar Bogs of Alberta, Canada." *Global Biogeochemical Cycles*. https://doi.org/10.1029/2006GB002866.

Preston, Michael D., Kurt A. Smemo, James W. McLaughlin, and Nathan Basiliko. 2012. "Peatland Microbial Communities and Decomposition Processes in the James Bay Lowlands, Canada." *Frontiers in Microbiology*. https://doi.org/10.3389/fmicb.2012.00070.

Quinton, W. L., and J. L. Baltzer. 2013. "The Active-Layer Hydrology of a Peat Plateau with Thawing Permafrost (Scotty Creek, Canada)." *Hydrogeology Journal*. https://doi.org/10.1007/s10040-012-0935-2.

Quinton, W. L., M. Hayashi, and L. E. Chasmer. 2011. "Permafrost-Thaw-Induced Land-Cover Change in the Canadian Subarctic: Implications for Water Resources." *Hydrological Processes* 25 (1): 152–58. https://doi.org/10.1002/hyp.7894.

Quinton, W. L., M. Hayashi, and A. Pietroniro. 2003. "Connectivity and Storage Functions of Channel Fens and Flat Bogs in Northern Basins." *Hydrological Processes*. https://doi.org/10.1002/hyp.1369.

Quinton, W.L., M. Hayashi, and L.E. Chasmer. 2009. "Peatland Hydrology of Discontinuous Permafrost in the Northwest Territories: Overview and Synthesis." *Canadian Water*

Resources Journal 34 (4): 311–28. https://doi.org/10.4296/cwrj3404311.

R Core Team. 2015. "R: A Language and Environment for Statistical Computing. Vienna, Austria; 2014." *URL Http://Www. R-Project. Org*. Vienna, Austria: R Foundation for Statistical Computing. https://doi.org/10.1007/978-3-540-74686-7.

Rasmussen, Susanne, Christian Wolff, and Hansjörg Rudolph. 1995. "Compartmentalization of Phenolic Constituents in Sphagnum." *Phytochemistry* 38 (1): 35–39. https://doi.org/10.1016/0031-9422(94)00650-I.

Reimer, Paula J, Edouard Bard, Alex Bayliss, J Warren Beck, Paul G Blackwell, Christopher Bronk Ramsey, Caitlin E Buck, et al. 2013. "IntCal13 and Marine13 Radiocarbon Age Calibration Curves 0–50,000 Years Cal BP." *Radiocarbon* 55 (04): 1869–87. https://doi.org/10.2458/azu_js_rc.55.16947.

Riutta, Terhi, Jukka Laine, and Eeva Stiina Tuittila. 2007. "Sensitivity of CO2 Exchange of Fen Ecosystem Components to Water Level Variation." *Ecosystems*. https://doi.org/10.1007/s10021-007-9046-7.

Robinson, D, Tim R Moore, and Fort Simpson. 1999. "Carbon and Peat Accumulation over the Past 1200 Years in a Landscape with Discontinuous Permafrost , Permafrost Peat Fen and Bog Accumulation Rates Survey 2 . Study Area and Sites." *Carbon* 13 (2): 591–601.

Robinson, S. D., and T. R. Moore. 2000. "The Influence of Permafrost and Fire upon Carbon Accumulation in High Boreal Peatlands, Northwest Territories, Canada." *Arctic, Antarctic, and Alpine Research* 32 (2): 155–66. https://doi.org/10.2307/1552447.

Robroek, Bjorn J.M., Remy J.H. Albrecht, Samuel Hamard, Adrian Pulgarin, Luca Bragazza, Alexandre Buttler, and Vincent Ej Jassey. 2016. "Peatland Vascular Plant Functional Types Affect Dissolved Organic Matter Chemistry." *Plant and Soil*. https://doi.org/10.1007/s11104-015-2710-3.

Robroek, Bjorn J.M., Juul Limpens, Angela Breeuwer, and Matthijs G.C. Schouten. 2007. "Effects of Water Level and Temperature on Performance of Four Sphagnum Mosses." *Plant Ecology*. https://doi.org/10.1007/s11258-006-9193-5.

Romanowicz, Karl J., Evan S. Kane, Lynette R. Potvin, Aleta L. Daniels, Randall K. Kolka, and Erik A. Lilleskov. 2015. "Understanding Drivers of Peatland Extracellular Enzyme Activity in the PEATcosm Experiment: Mixed Evidence for Enzymic Latch Hypothesis." *Plant and Soil* 397 (1–2): 371–86. https://doi.org/10.1007/s11104-015-2746-4.

Roulet, Nigel, Tim Moore, Jill Bubier, and Peter Lafleur. 1992. "Northern Fens: Methane Flux and Climatic Change." *Tellus B* 44 (2): 100–105. https://doi.org/10.1034/j.1600-0889.1992.t01-1-00002.x.

Roulet, Nigel T., Peter M. Lafleur, Pierre J.H. Richard, Tim R. Moore, Elyn R. Humphreys, and Jill Bubier. 2007. "Contemporary Carbon Balance and Late Holocene Carbon Accumulation in a Northern Peatland." *Global Change Biology* 13 (2): 397–411. https://doi.org/10.1111/j.1365-2486.2006.01292.x.

Rydin, Håkan. 1985. "Effect of Water Level on Desiccation of Sphagnum in Relation to Surrounding Sphagna." *Oikos*. https://doi.org/10.2307/3565573.

Sadoh, T., M. Kurosawa, K. Toko, and M. Miyao. 2014. “Coherent Lateral-Growth of Ge over Insulating Film by Rapid-Melting- Crystallization.” *Thin Solid Films* 557: 135–38. https://doi.org/10.1016/j.soilbio.2017.11.020.

Sand-Jensen, Kaj. 1989. “Environmental Variables and Their Effect on Photosynthesis of Aquatic Plant Communities.” *Aquatic Botany*. https://doi.org/10.1016/0304-3770(89)90048-X.

Sannel, A. Britta K., and Peter Kuhry. 2008. “Long-Term Stability of Permafrost in Subarctic Peat Plateaus, West-Central Canada.” *Holocene* 18 (4): 589–601. https://doi.org/10.1177/0959683608089658.

Saraswati, Saraswati, Christian Dunn, William J. Mitsch, and Chris Freeman. 2016. “Is Peat Accumulation in Mangrove Swamps Influenced by the ‘Enzymic Latch’ Mechanism?” *Wetlands Ecology and Management* 24 (6): 641–50. https://doi.org/10.1007/s11273-016-9493-z.

Saraswati, Saraswati, Christopher T. Parsons, and Maria Strack. 2019. “Access Roads Impact Enzyme Activities in Boreal Forested Peatlands.” *Science of the Total Environment*. https://doi.org/10.1016/j.scitotenv.2018.09.280.

Schädel, Christina, Martin K.F. Bader, Edward A.G. Schuur, Christina Biasi, Rosvel Bracho, Petr Capek, Sarah De Baets, et al. 2016. “Potential Carbon Emissions Dominated by Carbon Dioxide from Thawed Permafrost Soils.” *Nature Climate Change* 6 (10): 950–53. https://doi.org/10.1038/nclimate3054.

Schuur, E. A.G., A. D. McGuire, C. Schädel, G. Grosse, J. W. Harden, D. J. Hayes, G. Hugelius, et al. 2015. “Climate Change and the Permafrost Carbon Feedback.” *Nature* 520 (7546): 171–79. https://doi.org/10.1038/nature14338.

Schuur, Edward A. G., James Bockheim, Josep G. Canadell, Eugenie Euskirchen, Christopher B. Field, Sergey V. Goryachkin, Stefan Hagemann, et al. 2008. “Vulnerability of Permafrost Carbon to Climate Change: Implications for the Global Carbon Cycle.” *BioScience*. https://doi.org/10.1641/B580807.

Shur, Y. L., and M. T. Jorgenson. 2007. “Patterns of Permafrost Formation and Degradation in Relation to Climate and Ecosystems.” *Permafrost and Periglacial Processes*. https://doi.org/10.1002/ppp.582.

Silvola, J., and H. Aaltonen. 1984. “Water Content and Photosynthesis in the Peat Mosses Sphagnum Fuscum and S. Angustifolium.” *Annales Botanici Fennici*.

Silvola, Jouko, Jukka Alm, Urpo Ahlholm, Hannu Nykanen, and Pertti J. Martikainen. 1996. “CO 2 Fluxes from Peat in Boreal Mires under Varying Temperature and Moisture Conditions.” *The Journal of Ecology*. https://doi.org/10.2307/2261357.

Sinsabaugh, Robert L. 2010. “Phenol Oxidase, Peroxidase and Organic Matter Dynamics of Soil.” *Soil Biology and Biochemistry* 42 (3): 391–404. https://doi.org/10.1016/j.soilbio.2009.10.014.

Sinsabaugh, Robert L., Marcy E. Gallo, Christian Lauber, Mark P. Waldrop, and Donald R. Zak. 2005. “Extracellular Enzyme Activities and Soil Organic Matter Dynamics for Northern

Hardwood Forests Receiving Simulated Nitrogen Deposition." *Biogeochemistry*. https://doi.org/10.1007/s10533-004-7112-1.

Sinsabaugh, Robert L., Christian L. Lauber, Michael N. Weintraub, Bony Ahmed, Steven D. Allison, Chelsea Crenshaw, Alexandra R. Contosta, et al. 2008. "Stoichiometry of Soil Enzyme Activity at Global Scale." *Ecology Letters*. https://doi.org/10.1111/j.1461-0248.2008.01245.x.

Sjögersten, S., S. Caul, T. J. Daniell, A. P.S. Jurd, O. S. O'Sullivan, C. S. Stapleton, and J. J. Titman. 2016. "Organic Matter Chemistry Controls Greenhouse Gas Emissions from Permafrost Peatlands." *Soil Biology and Biochemistry* 98: 42–53. https://doi.org/10.1016/j.soilbio.2016.03.016.

Smith, Sharon L., Margo M. Burgess, Dan Riseborough, and F. Mark Nixon. 2005. "Recent Trends from Canadian Permafrost Thermal Monitoring Network Sites." *Permafrost and Periglacial Processes* 16 (1): 19–30. https://doi.org/10.1002/ppp.511.

Smith, Sharon L., Stephen A. Wolfe, Daniel W. Riseborough, and F. Mark Nixon. 2009. "Active-Layer Characteristics and Summer Climatic Indices, Mackenzie Valley, Northwest Territories, Canada." *Permafrost and Periglacial Processes* 20 (2): 201–20. https://doi.org/10.1002/ppp.651.

Soong, Jennifer L., Claire L. Phillips, Catherine Ledna, Charles D. Koven, and Margaret S. Torn. 2020. "CMIP5 Models Predict Rapid and Deep Soil Warming over the 21 St Century." *Journal of Geophysical Research: Biogeosciences*, no. 100 cm (January). https://doi.org/10.1029/2019JG005266.

Sottocornola, Matteo, Anna Laine, Gerard Kiely, Kenneth A. Byrne, and Eeva Stiina Tuittila. 2009. "Vegetation and Environmental Variation in an Atlantic Blanket Bog in South-Western Ireland." *Plant Ecology*. https://doi.org/10.1007/s11258-008-9510-2.

Steinweg, J. Megan, Jeffrey S. Dukes, and Matthew D. Wallenstein. 2012. "Modeling the Effects of Temperature and Moisture on Soil Enzyme Activity: Linking Laboratory Assays to Continuous Field Data." *Soil Biology and Biochemistry*. https://doi.org/10.1016/j.soilbio.2012.06.015.

Steinweg, J. Megan, Joel E. Kostka, Paul J. Hanson, and Christopher W. Schadt. 2018. "Temperature Sensitivity of Extracellular Enzymes Differs with Peat Depth but Not with Season in an Ombrotrophic Bog." *Soil Biology and Biochemistry*. https://doi.org/10.1016/j.soilbio.2018.07.001.

Strack, M., and J. M. Waddington. 2007. "Response of Peatland Carbon Dioxide and Methane Fluxes to a Water Table Drawdown Experiment." *Global Biogeochemical Cycles*. https://doi.org/10.1029/2006GB002715.

Strack, M., J. M. Waddington, L. Rochefort, and E. S. Tuittila. 2006. "Response of Vegetation and Net Ecosystem Carbon Dioxide Exchange at Different Peatland Microforms Following Water Table Drawdown." *Journal of Geophysical Research: Biogeosciences*. https://doi.org/10.1029/2005JG000145.

Strakova, P., R. M. Niemi, C. Freeman, K. Peltoniemi, H. Toberman, I. Heiskanen, H. Fritze,

and R. Laiho. 2011. “Litter Type Affects the Activity of Aerobic Decomposers in a Boreal Peatland More than Site Nutrient and Water Table Regimes.” *Biogeosciences*. https://doi.org/10.5194/bg-8-2741-2011.

Straková, Petra, Jani Anttila, Peter Spetz, Veikko Kitunen, Tarja Tapanila, and Raija Laiho. 2010. “Litter Quality and Its Response to Water Level Drawdown in Boreal Peatlands at Plant Species and Community Level.” *Plant and Soil*. https://doi.org/10.1007/s11104-010-0447-6.

Straková, Petra, Timo Penttilä, Jukka Laine, and Raija Laiho. 2012. “Disentangling Direct and Indirect Effects of Water Table Drawdown on Above- and Belowground Plant Litter Decomposition: Consequences for Accumulation of Organic Matter in Boreal Peatlands.” *Global Change Biology*. https://doi.org/10.1111/j.1365-2486.2011.02503.x.

Strauss, J., L. Schirrmeister, K. Mangelsdorf, L. Eichhorn, S. Wetterich, and U. Herzschuh. 2015. “Organic-Matter Quality of Deep Permafrost Carbon - A Study from Arctic Siberia.” *Biogeosciences*. https://doi.org/10.5194/bg-12-2227-2015.

Strickland, Michael S., Ernest Osburn, Christian Lauber, Noah Fierer, and Mark A. Bradford. 2009. “Litter Quality Is in the Eye of the Beholder: Initial Decomposition Rates as a Function of Inoculum Characteristics.” *Functional Ecology*. https://doi.org/10.1111/j.1365-2435.2008.01515.x.

Stuiver, M., P.J. Reimer, and R.W. Reimer. 2019. “CALIB 7.1 [WWW Program].” Http://Calib.Org. 2019. http://calib.org/CALIBomb/.

Sulman, B. N., A. R. Desai, B. D. Cook, N. Saliendra, and D. S. MacKay. 2009. “Contrasting Carbon Dioxide Fluxes between a Drying Shrub Wetland in Northern Wisconsin, USA, and Nearby Forests.” *Biogeosciences*. https://doi.org/10.5194/bg-6-1115-2009.

Sun, Xingting, Wu Xiang, Ling He, and Yulong Zhao. 2010. “Impacts of Hydrological Conditions on Enzyme Activities and Phenolic Concentrations in Peatland Soil: An Experimental Simulation.” *Frontiers of Earth Science in China*. https://doi.org/10.1007/s11707-010-0140-3.

Swindles, Graeme T., Paul J. Morris, Donal Mullan, Elizabeth J. Watson, T. Edward Turner, Thomas P. Roland, Matthew J. Amesbury, et al. 2015. “The Long-Term Fate of Permafrost Peatlands under Rapid Climate Warming.” *Scientific Reports*. https://doi.org/10.1038/srep17951.

Szumigalski, Anthony R., and Suzanne E. Bayley. 1996. “Decomposition along a Bog to Rich Fen Gradient in Central Alberta, Canada.” *Canadian Journal of Botany* 74 (4): 573–81. https://doi.org/10.1139/b96-073.

Tarnocai, C., J. G. Canadell, E. A.G. Schuur, P. Kuhry, G. Mazhitova, and S. Zimov. 2009. “Soil Organic Carbon Pools in the Northern Circumpolar Permafrost Region.” *Global Biogeochemical Cycles* 23 (2). https://doi.org/10.1029/2008GB003327.

Team, R Core. 2016. “R: A Language and Environment for Statistical Computing.” *R Foundation for Statistical Computing*.

Tfaily, Malak M., William T. Cooper, Joel E. Kostka, Patrick R. Chanton, Christopher W.

Schadt, Paul J. Hanson, Colleen M. Iversen, and Jeffrey P. Chanton. 2014. “Organic Matter Transformation in the Peat Column at Marcell Experimental Forest: Humification and Vertical Stratification.” *Journal of Geophysical Research: Biogeosciences*. https://doi.org/10.1002/2013JG002492.

Tfaily, Malak M., Rasha Hamdan, Jane E. Corbett, Jeffrey P. Chanton, Paul H. Glaser, and William T. Cooper. 2013. “Investigating Dissolved Organic Matter Decomposition in Northern Peatlands Using Complimentary Analytical Techniques.” *Geochimica et Cosmochimica Acta* 112: 116–29. https://doi.org/10.1016/j.gca.2013.03.002.

Thormann, M. N., S. E. Bayley, and R. S. Currah. 2001. “Comparison of Decomposition of Belowground and Aboveground Plant Litters in Peatlands of Boreal Alberta, Canada.” *Canadian Journal of Botany*. https://doi.org/10.1139/cjb-79-1-9.

Toberman, H., C. Freeman, R. R.E. Artz, C. D. Evans, and N. Fenner. 2008. “Impeded Drainage Stimulates Extracellular Phenol Oxidase Activity in Riparian Peat Cores.” *Soil Use and Management*. https://doi.org/10.1111/j.1475-2743.2008.00174.x.

Toberman, H., R. Laiho, C. D. Evans, R. R.E. Artz, N. Fenner, P. Straková, and C. Freeman. 2010. “Long-Term Drainage for Forestry Inhibits Extracellular Phenol Oxidase Activity in Finnish Boreal Mire Peat.” *European Journal of Soil Science*. https://doi.org/10.1111/j.1365-2389.2010.01292.x.

Toberman, Hannah, Chris D. Evans, Christopher Freeman, Nathalie Fenner, Marie White, Bridget A. Emmett, and Rebekka R.E. Artz. 2008. “Summer Drought Effects upon Soil and Litter Extracellular Phenol Oxidase Activity and Soluble Carbon Release in an Upland Calluna Heathland.” *Soil Biology and Biochemistry* 40 (6): 1519–32. https://doi.org/10.1016/j.soilbio.2008.01.004.

Trasar-Cepeda, C., F. Gil-Sotres, and M. C. Leirós. 2007. “Thermodynamic Parameters of Enzymes in Grassland Soils from Galicia, NW Spain.” *Soil Biology and Biochemistry*. https://doi.org/10.1016/j.soilbio.2006.08.002.

Treat, C. C., M. C. Jones, P. Camill, A. Gallego-Sala, M. Garneau, J. W. Harden, G. Hugelius, et al. 2016. “Effects of Permafrost Aggradation on Peat Properties as Determined from a Pan-Arctic Synthesis of Plant Macrofossils.” *Journal of Geophysical Research: Biogeosciences* 121 (1): 78–94. https://doi.org/10.1002/2015JG003061.

Treat, C. C., W. M. Wollheim, R. K. Varner, A. S. Grandy, J. Talbot, and S. Frolking. 2014. “Temperature and Peat Type Control CO2and CH4production in Alaskan Permafrost Peats.” *Global Change Biology* 20 (8): 2674–86. https://doi.org/10.1111/gcb.12572.

Treat, Claire C., Jill L. Bubier, Ruth K. Varner, and Partick M. Crill. 2007. “Timescale Dependence of Environmental and Plant-Mediated Controls of CH4 Flux in a Temperate Fen.” *Journal of Geophysical Research: Biogeosciences*. https://doi.org/10.1029/2006JG000210.

Treat, Claire C., and Miriam C. Jones. 2018. “Near-Surface Permafrost Aggradation in Northern Hemisphere Peatlands Shows Regional and Global Trends during the Past 6000 Years.” *Holocene*. https://doi.org/10.1177/0959683617752858.

Treat, Claire C., Thomas Kleinen, Nils Broothaerts, April S. Dalton, René Dommaine, Thomas A. Douglas, Judith Z. Drexler, et al. 2019. "Widespread Global Peatland Establishment and Persistence over the Last 130,000 Y." *Proceedings of the National Academy of Sciences of the United States of America*. https://doi.org/10.1073/pnas.1813305116.

Treat, Claire C., Susan M. Natali, Jessica Ernakovich, Colleen M. Iversen, Massimo Lupascu, Anthony David Mcguire, Richard J. Norby, et al. 2015. "A Pan-Arctic Synthesis of CH4 and CO2 Production from Anoxic Soil Incubations." *Global Change Biology* 21 (7): 2787–2803. https://doi.org/10.1111/gcb.12875.

Trumbore, S. E., and J. W. Harden. 1997. "Accumulation and Turnover of Carbon in Organic and Mineral Soils of the BOREAS Northern Study Area." *Journal of Geophysical Research: Atmospheres* 102 (D24): 28817–30. https://doi.org/10.1029/97JD02231.

Tuittila, Eeva Stiina, Harri Vasander, and Jukka Laine. 2004. "Sensitivity of C Sequestration in Reintroduced Sphagnum to Water-Level Variation in a Cutaway Peatland." *Restoration Ecology*. https://doi.org/10.1111/j.1061-2971.2004.00280.x.

Turetsky, M. R., R. K. Wieder, L. Halsey, and D. H. Vitt. 2002. "Current Disturbance and the Diminishing Peatland Carbon Sink." *Geophysical Research Letters*. https://doi.org/10.1029/2001GL014000.

Turetsky, M. R., R. K. Wieder, D. H. Vitt, R. J. Evans, and K. D. Scott. 2007. "The Disappearance of Relict Permafrost in Boreal North America: Effects on Peatland Carbon Storage and Fluxes." *Global Change Biology* 13 (9): 1922–34. https://doi.org/10.1111/j.1365-2486.2007.01381.x.

Turetsky, Merritt R. 2003. "The Role of Bryophytes in Carbon and Nitrogen Cycling." *The Bryologist* 106 (3): 395–409. https://doi.org/10.1639/05.

Turetsky, Merritt R., Susan E. Crow, Robert J. Evans, Dale H. Vitt, and R. Kelman Wieder. 2008. "Trade-Offs in Resource Allocation among Moss Species Control Decomposition in Boreal Peatlands." *Journal of Ecology* 96 (6): 1297–1305. https://doi.org/10.1111/j.1365-2745.2008.01438.x.

Turetsky, Merritt R., Agnieszka Kotowska, Jill Bubier, Nancy B. Dise, Patrick Crill, Ed R.C. Hornibrook, Kari Minkkinen, et al. 2014. "A Synthesis of Methane Emissions from 71 Northern, Temperate, and Subtropical Wetlands." *Global Change Biology*. https://doi.org/10.1111/gcb.12580.

Turetsky, Merritt R., R. Kelman Wieder, Christopher J. Williams, and Dale H. Vitt. 2000. "Organic Matter Accumulation, Peat Chemistry, and Permafrost Melting in Peatlands of Boreal Alberta." *Écoscience* 7 (3): 115–22. https://doi.org/10.1080/11956860.2000.11682608.

Turunen, J, E Tomppo, K Tolonen, and A Reinikainen. 2002. "Estimating Carbon Accumulating Rates of Undrained Mires in Finland - Application to Boreal and Subarctic Regions." *The Holocene* 12 (2002): 69–80.

Updegraff, K., J. Pastor, S. D. Bridgham, and C. A. Johnston. 1995. "Environmental and Substrate Controls over Carbon and Nitrogen Mineralization in Northern Wetlands."

Ecological Applications. https://doi.org/10.2307/1942060.

Updegraff, Karen, Scott D. Bridgham, John Pastor, Peter Weishampel, and Calvin Harth. 2001. "Response of CO2 and CH4 Emissions from Peatlands to Warming and Water Table Manipulation." *Ecological Applications*. https://doi.org/10.2307/3060891.

Vähätalo, Anssi V., Kalevi Salonen, Uwe Münster, Marko Järvinen, and Robert G. Wetzel. 2003. "Photochemical Transformation of Allochthonous Organic Matter Provides Bioavailable Nutrients in a Humic Lake." *Archiv Fur Hydrobiologie*. https://doi.org/10.1127/0003-9136/2003/0156-0287.

Verhoeven, J. T.A., and E. Toth. 1995. "Decomposition of Carex and Sphagnum Litter in Fens: Effect of Litter Quality and Inhibition by Living Tissue Homogenates." *Soil Biology and Biochemistry*. https://doi.org/10.1016/0038-0717(94)00183-2.

Vitt, Dale H., Linda A. Halsey, Ilka E. Bauer, and Celina Campbell. 2000. "Spatial and Temporal Trends in Carbon Storage of Peatlands of Continental Western Canada through the Holocene." *Canadian Journal of Earth Sciences* 37 (5): 683–93. https://doi.org/10.1139/e99-097.

Vitt, Dale H., Linda A. Halsey, and Stephen C. Zoltai. 1994. "The Bog Landforms of Continental Western Canada in Relation to Climate and Permafrost Patterns." *Arctic and Alpine Research* 26 (1): 1. https://doi.org/10.2307/1551870.

———. 2000. "The Changing Landscape of Canada's Western Boreal Forest: The Current Dynamics of Permafrost." *Canadian Journal of Forest Research* 30 (2): 283–87. https://doi.org/10.1139/x99-214.

Voigt, Carolina, Richard E. Lamprecht, Maija E. Marushchak, Saara E. Lind, Alexander Novakovskiy, Mika Aurela, Pertti J. Martikainen, and Christina Biasi. 2017. "Warming of Subarctic Tundra Increases Emissions of All Three Important Greenhouse Gases – Carbon Dioxide, Methane, and Nitrous Oxide." *Global Change Biology*. https://doi.org/10.1111/gcb.13563.

Voigt, Carolina, Maija E. Marushchak, Mikhail Mastepanov, Richard E. Lamprecht, Torben R. Christensen, Maxim Dorodnikov, Marcin Jackowicz-Korczyński, et al. 2019. "Ecosystem Carbon Response of an Arctic Peatland to Simulated Permafrost Thaw." *Global Change Biology*. https://doi.org/10.1111/gcb.14574.

Waddington, J. M., P. J. Morris, N. Kettridge, G. Granath, D. K. Thompson, and P. A. Moore. 2014. "Hydrological Feedbacks in Northern Peatlands." *Ecohydrology* 8 (1): 113–27. https://doi.org/10.1002/eco.1493.

Waddington, J. M., and N. T. Roulet. 2000. "Carbon Balance of a Boreal Patterned Peatland." *Global Change Biology* 6 (1): 87–97. https://doi.org/10.1046/j.1365-2486.2000.00283.x.

Walker, Anthony P., Kelsey R. Carter, Lianhong Gu, Paul J. Hanson, Avni Malhotra, Richard J. Norby, Stephen D. Sebestyen, Stan D. Wullschleger, and David J. Weston. 2017. "Biophysical Drivers of Seasonal Variability in Sphagnum Gross Primary Production in a Northern Temperate Bog." *Journal of Geophysical Research: Biogeosciences*. https://doi.org/10.1002/2016JG003711.

Walker, Tom N., Mark H. Garnett, Susan E. Ward, Simon Oakley, Richard D. Bardgett, and Nicholas J. Ostle. 2016. "Vascular Plants Promote Ancient Peatland Carbon Loss with Climate Warming." *Global Change Biology*. https://doi.org/10.1111/gcb.13213.

Wallenstein, Matthew, Steven D. Allison, Jessica Ernakovich, J. Megan Steinweg, and Robert Sinsabaugh. 2010. "Controls on the Temperature Sensitivity of Soil Enzymes: A Key Driver of In Situ Enzyme Activity Rates." In . https://doi.org/10.1007/978-3-642-14225-3_13.

Wallenstein, Matthew D., Shawna K. Mcmahon, and Joshua P. Schimel. 2009. "Seasonal Variation in Enzyme Activities and Temperature Sensitivities in Arctic Tundra Soils." *Global Change Biology*. https://doi.org/10.1111/j.1365-2486.2008.01819.x.

Wallenstein, Matthew D., and Michael N. Weintraub. 2008. "Emerging Tools for Measuring and Modeling the in Situ Activity of Soil Extracellular Enzymes." *Soil Biology and Biochemistry*. https://doi.org/10.1016/j.soilbio.2008.01.024.

Walter Anthony, Katey, Thomas Schneider von Deimling, Ingmar Nitze, Steve Frolking, Abraham Emond, Ronald Daanen, Peter Anthony, Prajna Lindgren, Benjamin Jones, and Guido Grosse. 2018. "21st-Century Modeled Permafrost Carbon Emissions Accelerated by Abrupt Thaw beneath Lakes." *Nature Communications*. https://doi.org/10.1038/s41467-018-05738-9.

Walz, Josefine, Christian Knoblauch, Luisa Böhme, and Eva Maria Pfeiffer. 2017. "Regulation of Soil Organic Matter Decomposition in Permafrost-Affected Siberian Tundra Soils - Impact of Oxygen Availability, Freezing and Thawing, Temperature, and Labile Organic Matter." *Soil Biology and Biochemistry*. https://doi.org/10.1016/j.soilbio.2017.03.001.

Wang, Meng, Tim R Moore, Julie Talbot, and John L Riley. 2014. "Global Biogeochemical Cycles in Peat Formation." *Global Biogeochemical Cycles*, 113–21. https://doi.org/10.1002/2014GB005000.Received.

Ward, Susan E., Kate H. Orwin, Nicholas J. Ostle, Maria J.I. Briones, Bruce C. Thomson, Robert I. Griffiths, Simon Oakley, Helen Quirk, and Richard D. Bardgett. 2015. "Vegetation Exerts a Greater Control on Litter Decomposition than Climate Warming in Peatlands." *Ecology* 96 (1): 113–23. https://doi.org/10.1890/14-0292.1.

Weintraub, Michael N., and Joshua P. Schimel. 2005. "Seasonal Protein Dynamics in Alaskan Arctic Tundra Soils." *Soil Biology and Biochemistry*. https://doi.org/10.1016/j.soilbio.2005.01.005.

Weishaar, James L., George R. Aiken, Brian A. Bergamaschi, Miranda S. Fram, Roger Fujii, and Kenneth Mopper. 2003. "Evaluation of Specific Ultraviolet Absorbance as an Indicator of the Chemical Composition and Reactivity of Dissolved Organic Carbon." *Environmental Science and Technology*. https://doi.org/10.1021/es030360x.

Weltzin, Jake F., Scott D. Bridgham, John Pastor, Jiquan Chen, and Calvin Harth. 2003. "Potential Effects of Warming and Drying on Peatland Plant Community Composition." *Global Change Biology*. https://doi.org/10.1046/j.1365-2486.2003.00571.x.

Weltzin, Jake F., Calvin Harth, Scott D. Bridgham, John Pastor, and Mark Vonderharr. 2001. "Production and Microtopography of Bog Bryophytes: Response to Warming and Water-

Table Manipulations." *Oecologia* 128 (4): 557–65. https://doi.org/10.1007/s004420100691.

Wickland, Kimberly P., Robert G. Striegl, Jason C. Neff, and Torsten Sachs. 2006. "Effects of Permafrost Melting on CO2 and CH4 Exchange of a Poorly Drained Black Spruce Lowland." *Journal of Geophysical Research: Biogeosciences* 111 (2): 1–13. https://doi.org/10.1029/2005JG000099.

Williams, Christopher J., Erica A. Shingara, and Joseph B. Yavitt. 2000. "Phenol Oxidase Activity in Peatlands in New York State: Response to Summer Drought and Peat Type." *Wetlands*. https://doi.org/10.1672/0277-5212(2000)020[0416:POAIPI]2.0.CO;2.

Wilson, David, Jukka Alm, Terhi Riutta, Jukka Laine, Kenneth A. Byrne, Edward P. Farrell, and Eeva Stiina Tuittila. 2007. "A High Resolution Green Area Index for Modelling the Seasonal Dynamics of CO2 Exchange in Peatland Vascular Plant Communities." *Plant Ecology*. https://doi.org/10.1007/s11258-006-9189-1.

Wilson, R. M., A. M. Hopple, M. M. Tfaily, S. D. Sebestyen, C. W. Schadt, L. Pfeifer-Meister, C. Medvedeff, et al. 2016. "Stability of Peatland Carbon to Rising Temperatures." *Nature Communications* 7: 1–10. https://doi.org/10.1038/ncomms13723.

Wu, Jianghua, Nigel T. Roulet, Tim R. Moore, Peter Lafleur, and Elyn Humphreys. 2011. "Dealing with Microtopography of an Ombrotrophic Bog for Simulating Ecosystem-Level CO2 Exchanges." *Ecological Modelling*. https://doi.org/10.1016/j.ecolmodel.2010.07.015.

Wu, Yuanqiao, Ed Chan, Joe R. Melton, and Diana L. Verseghy. 2017. "A Map of Global Peatland Distribution Created Using Machine Learning for Use in Terrestrial Ecosystem and Earth System Models." *Geoscientific Model Development Discussions*. https://doi.org/10.5194/gmd-2017-152.

Xia, Jianyang, Jiquan Chen, Shilong Piao, Philippe Ciais, Yiqi Luo, and Shiqiang Wan. 2014. "Terrestrial Carbon Cycle Affected by Non-Uniform Climate Warming." *Nature Geoscience*. https://doi.org/10.1038/ngeo2093.

Xin-Gang, Dai, and Wang Ping. 2010. "Zonal Mean Mode of Global Warming over the Past 50 Years." *Atmospheric and Oceanic Science Letters* 3 (1): 45–50. https://doi.org/10.1080/16742834.2010.11446835.

Xu, Jiren, Paul J. Morris, Junguo Liu, and Joseph Holden. 2018. "PEATMAP: Refining Estimates of Global Peatland Distribution Based on a Meta-Analysis." *Catena*. https://doi.org/10.1016/j.catena.2017.09.010.

Yu, Z. C. 2012. "Northern Peatland Carbon Stocks and Dynamics: A Review." *Biogeosciences* 9 (10): 4071–85. https://doi.org/10.5194/bg-9-4071-2012.

Yu, Zicheng. 2011. "Holocene Carbon Flux Histories of the World's Peatlands: Global Carbon-Cycle Implications." *Holocene* 21 (5): 761–74. https://doi.org/10.1177/0959683610386982.

Yu, Zicheng, Julie Loisel, Daniel P. Brosseau, David W. Beilman, and Stephanie J. Hunt. 2010. "Global Peatland Dynamics since the Last Glacial Maximum." *Geophysical Research Letters* 37 (13): 1–5. https://doi.org/10.1029/2010GL043584.

Zhang, Yu, Wenjun Chen, and Daniel W. Riseborough. 2008. "Transient Projections of

Permafrost Distribution in Canada during the 21st Century under Scenarios of Climate Change." *Global and Planetary Change*. https://doi.org/10.1016/j.gloplacha.2007.05.003.

Zimov, S. A., E. A.G. Schuur, and F. S. Chapin. 2006. "Permafrost and the Global Carbon Budget." *Science* 312 (5780): 1612–13. https://doi.org/10.1126/science.1128908.

Zoltai, S. C. 1993. "Cyclic Development of Permafrost in the Peatlands of Northwestern Alberta, Canada." *Arctic and Alpine Research* 25 (3): 240. https://doi.org/10.2307/1551820.

Zoltai, S. C., and D. H. Vitt. 1995. "Canadian Wetlands: Environmental Gradients and Classification." *Vegetatio*. https://doi.org/10.1007/BF00045195.

Zoltai, Stephen C. 1995. "Permafrost Distribution in Peatlands of West-Central Canada During the Holocene Warm Period 6000 Years BP." *Géographie Physique et Quaternaire* 49 (1): 45. https://doi.org/10.7202/033029ar.

Zoltai, Stephen C., and Charles Tarnocai. 1975. "Perennially Frozen Peatlands in the Western Arctic and Subarctic of Canada." *Canadian Journal of Earth Sciences* 12 (Brown 1967): 28–43. https://doi.org/10.1139/e75-004.

Zona, Donatella, Beniamino Gioli, Róisín Commane, Jakob Lindaas, Steven C. Wofsy, Charles E. Miller, Steven J. Dinardo, et al. 2016. "Cold Season Emissions Dominate the Arctic Tundra Methane Budget." *Proceedings of the National Academy of Sciences* 113 (1): 40–45. https://doi.org/10.1073/pnas.1516017113.

Appendices

Appendix 1. Supporting information for Chapter 2

All Chapter 2 data is available in the UAL Dataverse repository

[https://doi.org/10.7939/DVN/MKM0ZE]

Table A1.1. Summary of ^{14}C-dated peat samples, basal ages, and peat stages transitions in collected cores. Includes estimated *Bacon* model age (cal yr BP) of MB-1 and P-1 core sample, material used for dating, and the significance (if any) of that date in each peat core.

Lab ID	Core	Depth (cm)	Uncalibrated age (cal yr BP)	fM	Calibrated 1-sigma age range (cal yr BP)	*Bacon* model age (cal yr BP)	Material dated	Stratigraphic significance
UOC-2058	MB-1	32	126 ± 18	0.9844 ± 0.0022	-5 – 266	14	*Sphagnum*	
UOC-2059	MB-1	73	150 ± 33	0.9815 ± 0.004	-5 – 280	243	*Picea mariana* needles *Sphagnum*	Thaw transition
UOC-2060	MB-1	89	362 ± 21	0.9559 ± 0.0025	331 – 482	452	*Sphagnum*	
UOC-2061	MB-1	118	899 ± 20	0.8941 ± 0.0022	7782 – 902	787	*Sphagnum*	
UOC-2062	MB-1	159	1303 ± 20	0.8502 ± 0.0021	1187 – 1283	1225	*Sphagnum* *Picea mariana* needles	
UOC-2063	MB-1	206	1678 ± 21	0.8115 ± 0.0021	1553 – 1604	1608	*Sphagnum* *Picea mariana* needles	Bog – Peat Plateau transition
UOC-2064	MB-1	256	2442 ± 24	0.7378 ± 0.0022	2380 – 2682	2577	*Sphagnum*	

UOC-2065	MB-1	331	4344 ± 26	0.5823 ± 0.0019	4856 – 4959	4856	*Sphagnum*	
UOC-2066	MB-1	426	5632 ± 28	0.4960 ± 0.0017	6352 – 6449	6403	*Sphagnum* *Ericaceous* leaves	Marsh – Fen transition
UOC-2080	MB-1	524	8274 ± 101	0.3570 ± 0.0045	9131 – 9406	9061	*Ericaceous* leaves	Basal peat to mineral transition
UOC-2071	P-1	20	314 ± 19	0.9616 ± 0.0023	310 – 429	417	*Sphagnum*	
UOC-2072	P-1	56	1599 ± 20	0.8195 ± 0.0020	1418 – 1535	1444	*Sphagnum* *Ericaceous* leaves	
UOC-2073	P-1	88	1892 ± 22	0.7901 ± 0.0022	1823 – 1869	1820	*Sphagnum*	Bog – Peat Plateau transition
UOC-2074	P-1	130	2216 ± 25	0.7589 ± 0.0023	2158 – 2308	2134	*Sphagnum*	
UOC-2075	P-1	175	2191 ± 21	0.7613 ± 0.0020	2151 – 2302	2293	*Sphagnum* *Ericaceous* leaves	
UOC-2076	P-1	335	3559 ± 22	0.6421 ± 0.0017	3835 – 3883	3887	*Ericaceous* leaves	
UOC-2077	P-1	464	6170 ± 54	0.4639 ± 0.0031	7006 – 7159	7017	*Ericaceous* leaves Sedge	Marsh – Fen transition
UOC-2078	P-1	576	8235 ± 31	0.3587 ± 0.0014	9134 – 9266	9046	*Ericaceous* leaves	
UOC-2079	P-1	593	8103 ± 37	0.3647 ± 0.0017	8998 – 9085	9174	*Ericaceous* leaves	Deepest section of P-1 collected
205500	P-2	595	8170 ± 25	0.3618 ± 0.0009	9032 – 9124		Ligneous material Brown moss	Deepest section of P-2 collected
205495	YB-1	24	Modern	1.1185 ± 0.0020	-46.07 – -44.09		*Sphagnum*	Thaw transition

UOC-2081	YB-1	494	8301 ± 38	0.3558 ± 0.0017	9272 – 9405		Ligneous material *Ericaceous* leaves	Basal peat to mineral transition
UOC-2068	IB-1	42	76 ± 20	0.9905 ± 0.0025	-5 – 250		*Sphagnum*	Thaw transition
205496	YB-2	20	Modern	1.0592 ± 0.0018	-59.63 – -55.42		*Sphagnum*	Thaw transition
205500	IB-2	44	Modern	1.3670 ± 0.0022	-26.58 – -12.34		*Sphagnum*	Thaw transition
205499	OB-2	43	Modern	1.5958 ± 0.0028	-18.72 – -13.3		*Sphagnum*	
205498	OB-2	531	8835 ± 30	0.3329 ± 0.0012	9781 – 10118		Ligneous material *Ericaceous* leaves	Basal peat to mineral transition

(a)

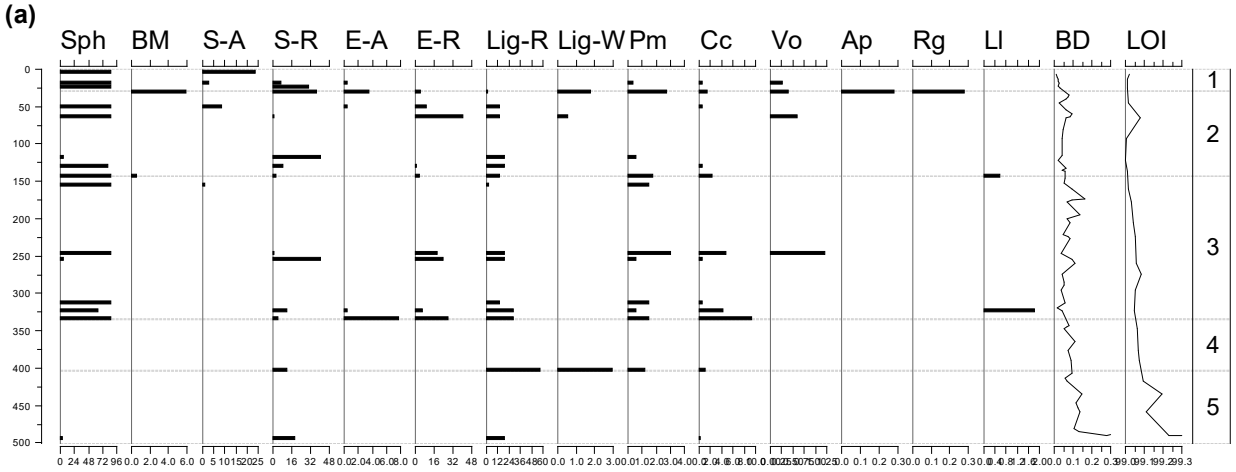
Sph
BM
S-A
S-R
E-A
E-R
Lig-R
Lig-W
Pm
Cc
Vo
Ap
Rg
Ll
BD
LOI
1
2
3
4
5

(b)

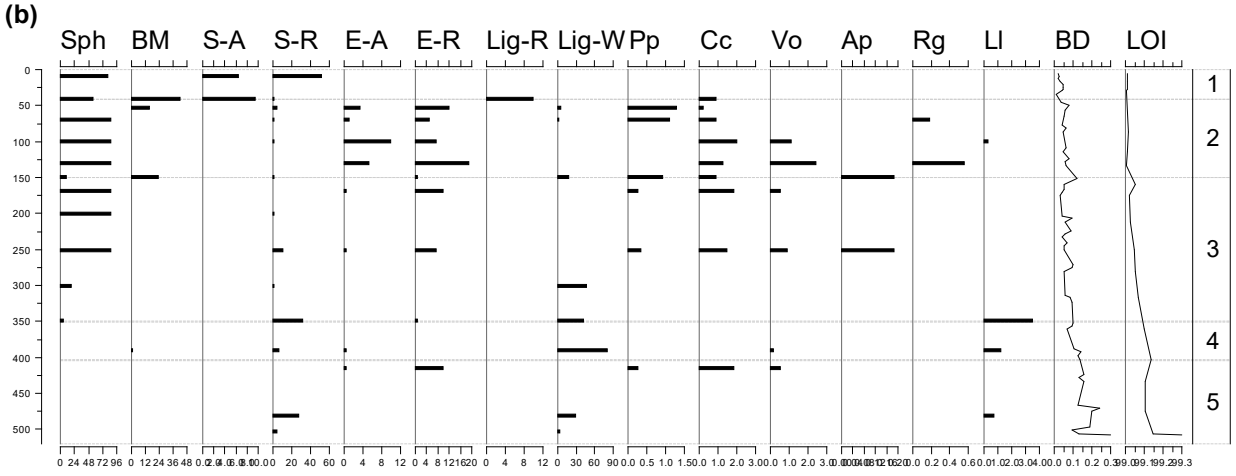
Sph
BM
S-A
S-R
E-A
E-R
Lig-R
Lig-W
Pp
Cc
Vo
Ap
Rg
Ll
BD
LOI
1
2
3
4
5

(c)

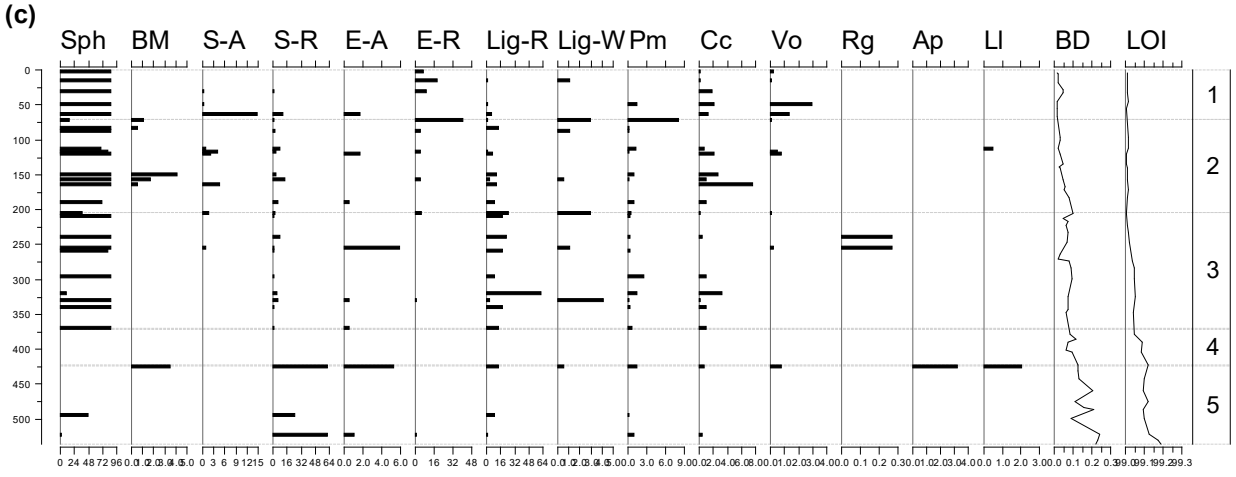
Sph
BM
S-A
S-R
E-A
E-R
Lig-R
Lig-W
Pm
Cc
Vo
Rg
Ap
Ll
BD
LOI
1
2
3
4
5

(d)

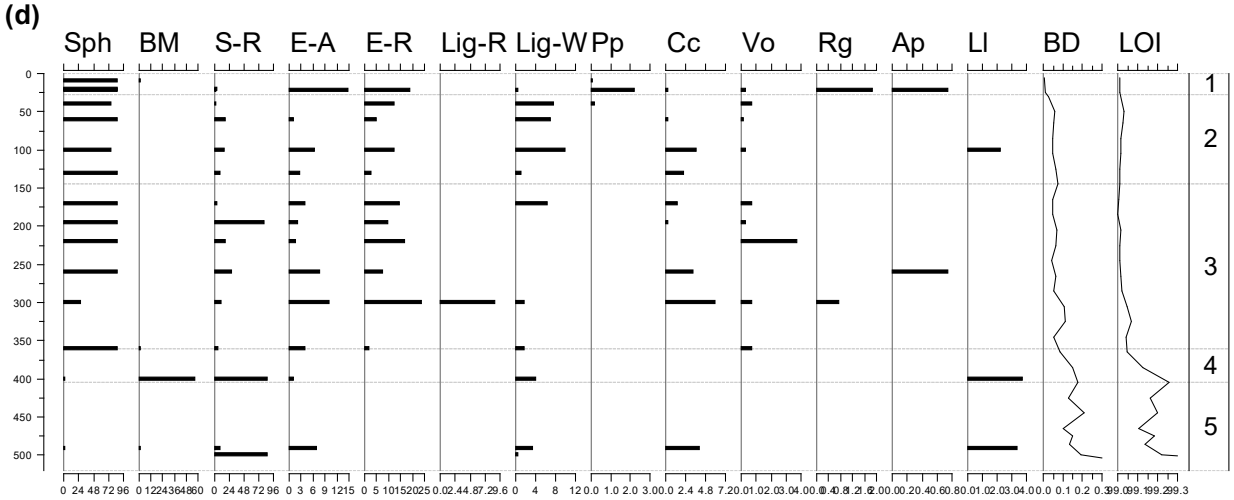
Sph
BM
S-R
E-A
E-R
Lig-R
Lig-W
Pp
Cc
Vo
Rg
Ap
Ll
BD
LOI
1
2
3
4
5

(e)

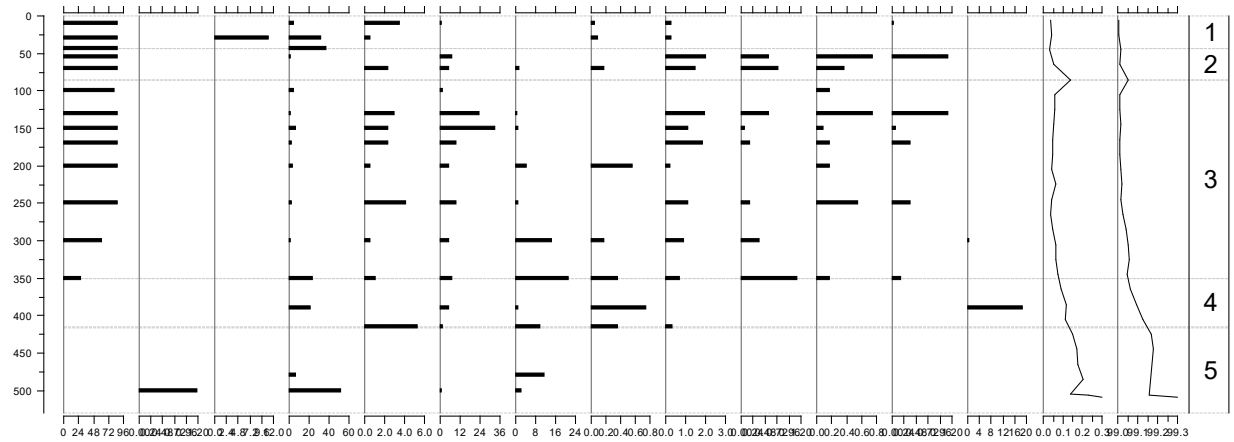
Sph
BM
S-A
S-R
E-A
E-R
Lig
Pm
Cc
Vo
Rg
Ap
Ll
BD
LOI
1
2
3
4
5

(f)

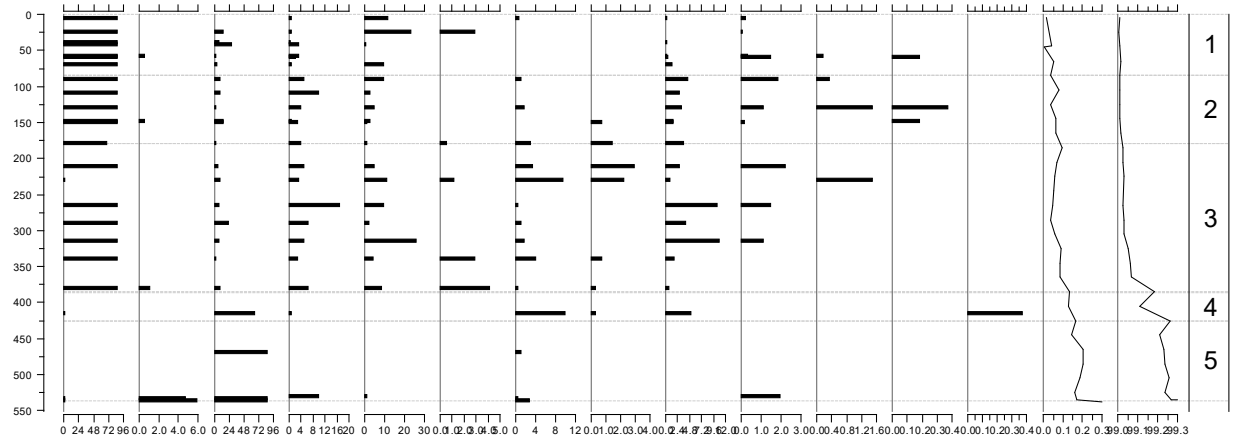
Sph
BM
S-R
E-A
E-R
Lig-R
Lig-W
Pm
Cc
Vo
Rg
Ap
Ll
BD
LOI
1
2
3
4
5

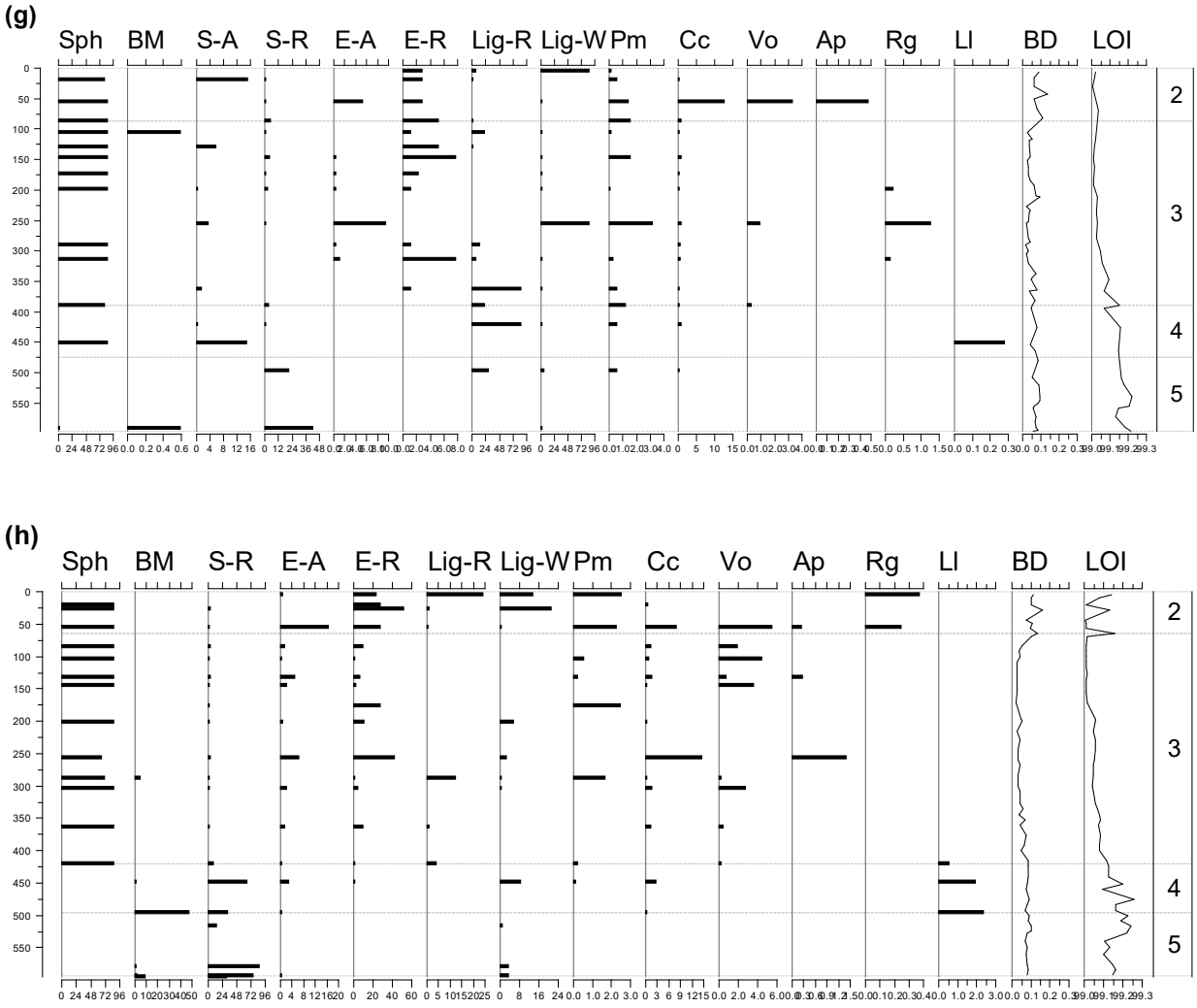

Figure A1.1. Summary of plant macrofossil data for all eight cores samples plotted using C2. Graphs (a) – (h) show main macrofossil groups, bulk density (BD), and loss-on-ignition (LOI) plotted with depth (y-axis = depth (cm)) used to determine different peat stages throughout all eight cores developmental history. (a) YB-1. (b) IB-1. (c) MB-1. (d) YB-2. (e) IB-2. (f) MB-2. (g) P-1. (h) P-2. Sph = *Sphagnum* spp;%. BM = brown moss spp;%. S-A = Sedge spp. – above-ground vegetation parts;%. S-R = Sedge spp. – roots:%. E-A = Ericaceous spp. – above-ground vegetation parts;%. E-R = Ericaceous spp. – roots:%. Lig-R = Unidentified wood – roots;%. Lig-W = Unidentified wood – above ground parts;%. Pm = *Picea mariana*; individuals per cm^3. Cc = *Chamaedaphne calyculata*; individuals per cm^3. Vo = *Vaccinium oxycoccos*; individuals per cm^3. Ap = *Andromeda polifolia*; individuals per cm^3. Rg = *Rhododendron groenlandicum*; individuals per cm^3. Ll = *Larix laricina*; individuals per cm^3. BD = bulk density; g cm^{-3}. LOI = Loss-on-

ignition;%. Zones 1 – 5 identified in column on right-hand side of each graph peatland developmental stage. 1 = Post-thaw; 2 = Peat plateau; 3 = Bog; 4 = Fen; 5 = Marsh.

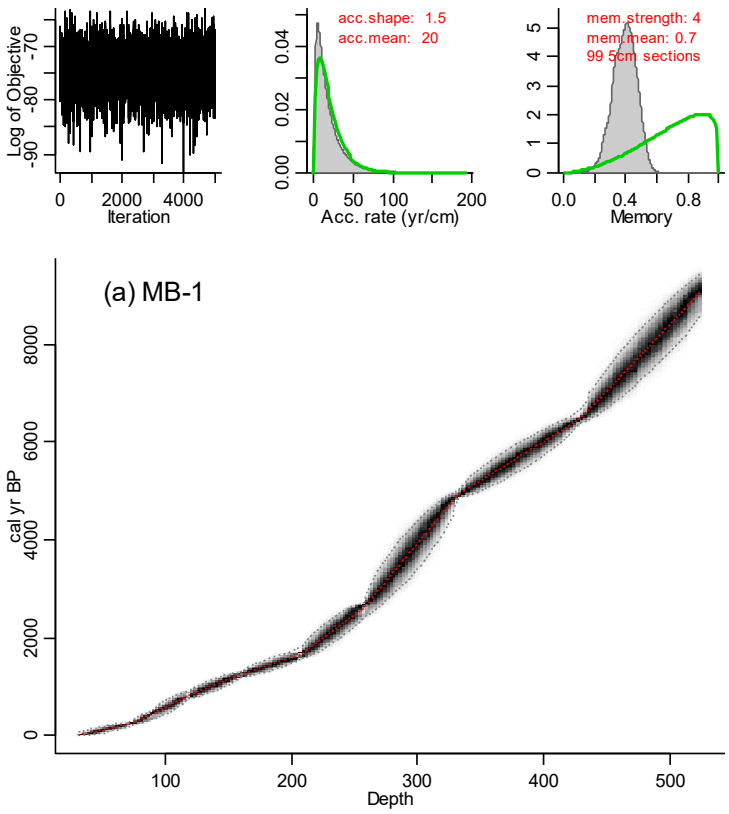
Log of Objective
-70
-80
-90
0
2000
4000
Iteration
acc.shape: 1.5
acc.mean: 20
0.00
0.02
0.04
0
50
100
200
Acc. rate (yr/cm)
mem.strength: 4
mem.mean: 0.7
99 5cm sections
0
1
2
3
4
5
0.0
0.4
0.8
Memory
(a) MB-1
cal yr BP
0
2000
4000
6000
8000
100
200
300
400
500
Depth

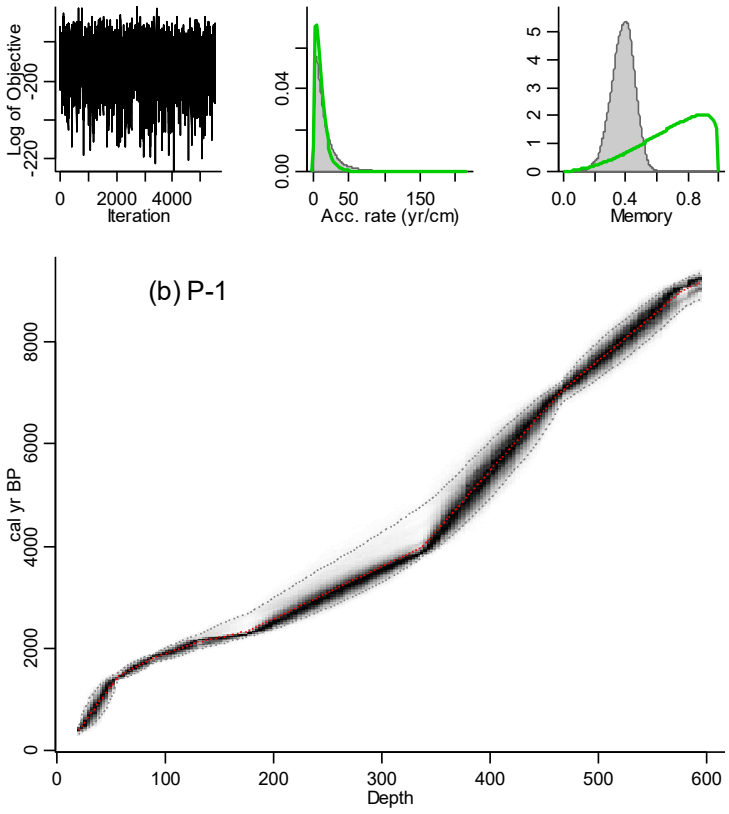
Log of Objective
-200
-220
0
2000
4000
Iteration
0.00
0.04
0
50
150
Acc. rate (yr/cm)
0
1
2
3
4
5
0.0
0.4
0.8
Memory
(b) P-1
cal yr BP
0
2000
4000
6000
8000
0
100
200
300
400
500
600
Depth

Figure A1.2. Bayesian age-depth models (*Bacon*) for (a) MB-1, and (b) P-1 cores. Blue shapes = ^{14}C calibrated ages. Red lines = average modelled ages. Gray lines = 1-σ distribution

Appendix 2. Supporting information for Chapter 3

Table A2.1 Equations, model fit, and indication of parameter significance for models examining the nonlinear effects of abiotic variables for both growing and non-growing season measured CO_2 and CH_4 fluxes. AIC = Akaike Information Criterion. RMSE = root square mean error. APS = all parameters significant. Eqn. = equation number. YB = young bog. MB = Mature bog. Models highlighted in bold are models used in main manuscript

	Model	AIC	RMSE	APS	Eqn.
YB	*Ecosystem Respiration*				
Water table (1)	$ER_{(max)} \times \exp\left(-0.5 \times \left(\frac{(\mathrm{WT} - uFlux)^2}{tFlux^2}\right)\right)$	608.2	0.7	No	3.1
Water table (2)	$ER_{(max)} \times \frac{a}{1 + \exp\left(\frac{WT - b_1}{-b_2}\right)}$	613.3	0.7	No	3.2
$Q_{10}^{(5cm)}$	$z \times Q_{10}^{\left(\frac{T_5}{10}\right)}$	645.5	0.7	Yes	3.3
$exp^{(T5)}$	$exp^{(x \times \mathrm{T5cm})}$	644.2	0.7	No	3.4
Water table (1) × $exp^{(T5)}$	$\boldsymbol{ER_{(max)} \times \exp\left(-0.5 \times \left(\frac{(\mathrm{WT} - uFlux)^2}{tFlux^2}\right)\right) \times exp^{(x \times \mathrm{T5cm})}}$	**593.7**	**0.6**	**Yes**	**3**
Water table (2) × $exp^{(T5)}$	$ER_{(max)} \times \frac{a}{1 + \exp\left(\frac{WT - b_1}{-b_2}\right)} \times exp^{(x \times \mathrm{T5cm})}$	593.7	0.6	No	3.5
MB	*Ecosystem Respiration*				
Water table (3)	$\left(a + (b \times \mathrm{WT})\right)$	910.5	0.9	No	4.1
$Q_{10}^{(5cm)}$	$z \times Q_{10}^{\left(\frac{T_5}{10}\right)}$	711.5	0.7	Yes	4.2

exp$^{(T5)}$	$exp^{(x \times \mathrm{T5cm})}$	714.9	0.7	Yes	4.3
Water table (1) × exp$^{(T5)}$	$ER_{(max)} \times \exp\left(-0.5 \times \left(\frac{(\mathrm{WT} - uFlux)^2}{tFlux^2}\right)\right) \times exp^{(x \times \mathrm{T5cm})}$	700.6	0.7	No	4.4
Water table (3) × exp$^{(T5)}$	$\boldsymbol{\left(a + (b \times \mathrm{WT})\right) \times exp^{(x \times \mathrm{T5cm})}}$	**699.6**	**0.7**	**Yes**	**4**
YB	*Non-growing Season Ecosystem Respiration*				
$Q_{10}^{(5cm)}$	$z \times Q_{10}^{(\frac{T_5}{10})}$	4.8	0.2	No	5.1
$Q_{10}^{(40cm)}$	$\mathrm{z} \times Q_{10}^{(\frac{T_{40}}{10})}$	4.4	0.2	No	5.2
exp$^{(T5)}$	$exp^{(x \times \mathrm{T5cm})}$	102.8	0.7	Yes	5.3
exp$^{(T40)}$	$exp^{(y \times \mathrm{T40cm})}$	72.0	0.5	Yes	5.4
exp$^{(T5)}$ × exp$^{(T40)}$	$exp^{(x \times \mathrm{T40cm})} \times exp^{(y \times \mathrm{T40cm})}$	70.4	0.5	No	5.5
Thaw depth × exp$^{(T5)}$	$\boldsymbol{\left(i + (j \times \mathrm{TD})\right) \times exp^{(x \times \mathrm{T5cm})}}$	**5.7**	**0.2**	**No**	**5**
Thaw depth × exp$^{(T40)}$	$\left(i + (j \times \mathrm{TD})\right) \times exp^{(y \times \mathrm{T40cm})}$	5.6	0.2	No	5.6
MB	*Non-growing Season Ecosystem Respiration*				
$Q_{10}^{(5cm)}$	$z \times Q_{10}^{(\frac{T_5}{10})}$	16.0	0.3	No	5.7
exp$^{(T5)}$	$exp^{(x \times \mathrm{T5cm})}$	28.6	0.3	Yes	5.8
exp$^{(T40)}$	$exp^{(y \times \mathrm{T40cm})}$	13.9	0.3	Yes	5.9

$exp^{(T5)} \times exp^{(T40)}$	$exp^{(x \times \mathrm{T40cm})} \times exp^{(y \times \mathrm{T40cm})}$	7.3	0.3	Yes	5.10
Thaw depth × $exp^{(T5)}$	$\boldsymbol{(i + (j \times \mathrm{TD})) \times exp^{(x \times \mathrm{T5cm})}}$	**14.5**	**0.3**	**No**	**5**
Thaw depth × $exp^{(T40)}$	$(i + (j \times \mathrm{TD})) \times exp^{(y \times \mathrm{T40cm})}$	16.0	0.3	No	5.11
YB	*Gross Primary Production*				
Water table (1)	$GPP_{(max)} \times \exp(-0.5 \times \left(\frac{(\mathrm{WT} - uFlux)^2}{tFlux^2}\right))$	717.6	1.3	Yes	6.1
PAR	$GPP_{(max)} \times \left(\frac{\mathrm{PAR}}{k + \mathrm{PAR}}\right)$	803.6	1.5	Yes	6.2
Water table (1) × PAR	$\boldsymbol{GPP_{(max)} \times \left(\frac{\mathrm{PAR}}{k + \mathrm{PAR}}\right) \times \exp(-0.5 \times \left(\frac{(\mathrm{WT} - uFlux)^2}{tFlux^2}\right))}$	**674.4**	**1.2**	**Yes**	**6**
MB	*Gross Primary Production*				
Water table (1)	$GPP_{(max)} \times \exp(-0.5 \times \left(\frac{(\mathrm{WT} - uFlux)^2}{tFlux^2}\right))$	946.4	1.5	No	7.1
PAR	$\boldsymbol{GPP_{(max)} \times \left(\frac{\mathrm{PAR}}{k + \mathrm{PAR}}\right)}$	**865.0**	**1.3**	**Yes**	**7**
Water table (1) × PAR	$GPP_{(max)} \times \left(\frac{\mathrm{PAR}}{k + \mathrm{PAR}}\right) \times \exp(-0.5 \times \left(\frac{(\mathrm{WT} - uFlux)^2}{tFlux^2}\right))$	864.8	1.3	No	7.2
YB	*Methane*				
$Q_{10}^{(40cm)}$	$\boldsymbol{g \times Q_{10}^{(\frac{T_{40}}{10})}}$	**2519.0**	**60.8**	**Yes**	**8**
$exp^{(T40)}$	$exp^{(y \times \mathrm{T40cm})}$	2669.0	83.9	Yes	8.1

MB	*Methane*				
$Q_{10}^{(40cm)}$	$\boldsymbol{g \times Q_{10}^{(\frac{T_{40}}{10})}}$	**2513.3**	**44.3**	**Yes**	**8**
$exp^{(T40)}$	$exp^{(x \times \mathrm{T40cm})}$	2577.0	50.9	Yes	8.2

$ER_{(max)}$ = maximum rate of ER (g C-CO_2 m^{-2} day^{-1}) under optimal conditions. $GPP_{(max)}$ = maximum rate of GPP (g C-CO_2 m^{-2} day^{-1}) under optimal conditions *uFlux* = optimum water table position (cm) for Flux (ER, GPP, or CH_4). *tFlux* = the range of water table position (cm) in which *uFlux* can occur. *x* = the rate and direction of change in ER along the range of soil temperature at 5 cm. *y* = the rate and direction of change in ER along the range of soil temperature at 40 cm. PAR = photosynthetically active radiation (µE). *k* = range around *uFlux* over which GPP_{max} is found (µE). *z* = Flux at 0 °C (g C-CO_2 m^{-2} day^{-1}). *g* = Flux at 0 °C (g C-CH_4 m^{-2} day^{-1}). Q_{10} = temperature dependency of Flux. T_5 = temperature (°C) at 5 cm. T_{40} = temperature (°C) at 40 cm.

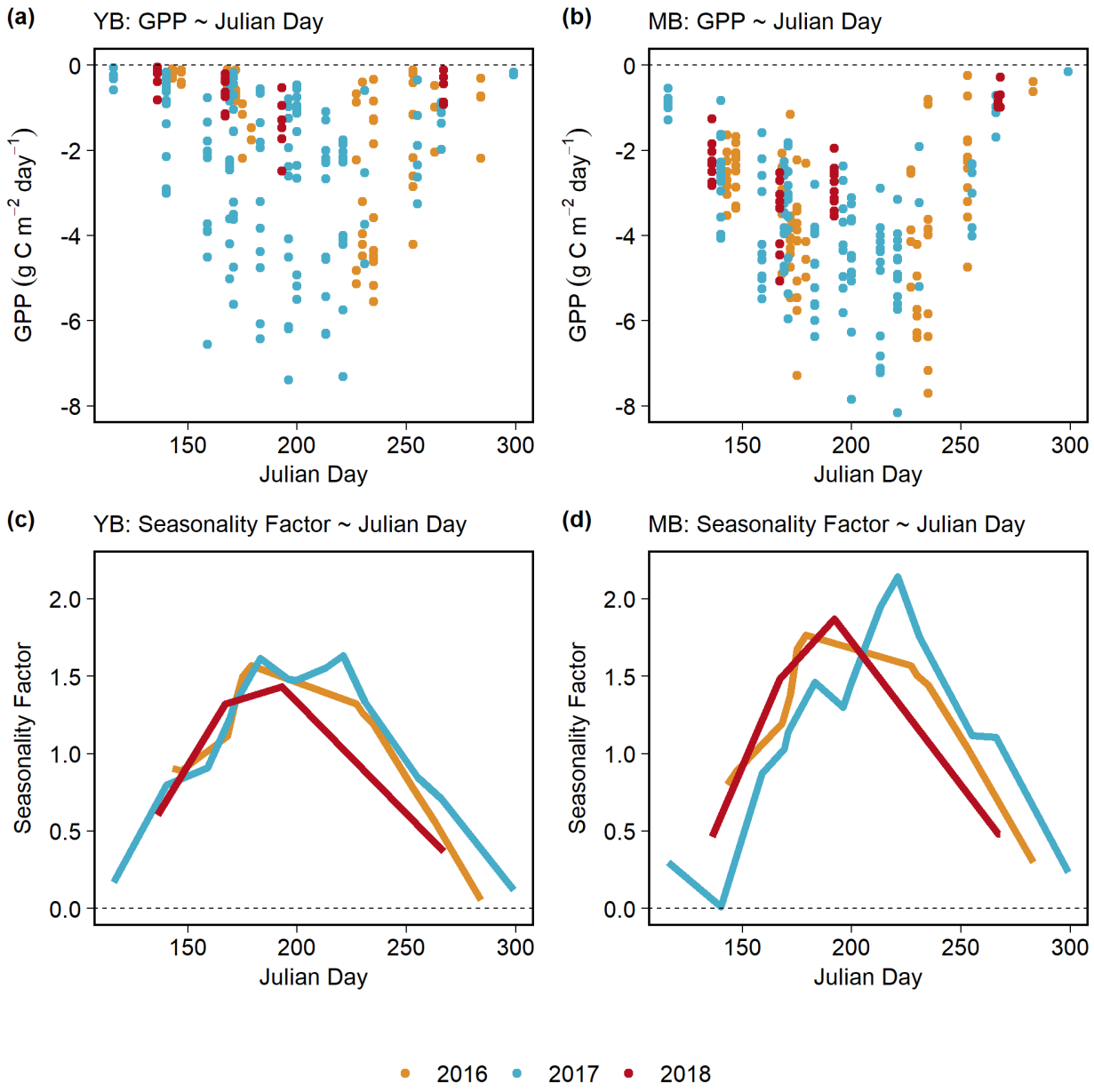

Figure A2.1. Measured gross primary production (GPP) fluxes and seasonality factor imposed on modelled GPP. Measured GPP fluxes over three years in (a) young bog (YB), and (b) mature bog (MB). GPP fluxes above *k* (PAR level where GPP is half its maximum) only shown in (a) and (b). Seasonality factor used in (c) YB and (d) MB when above 0. Seasonality factor represents 7-day average soil temperature (°C) at 5cm divided by seasonal average soil temperature (°C) at 5cm. Colours represent different years and data over all three years is used.

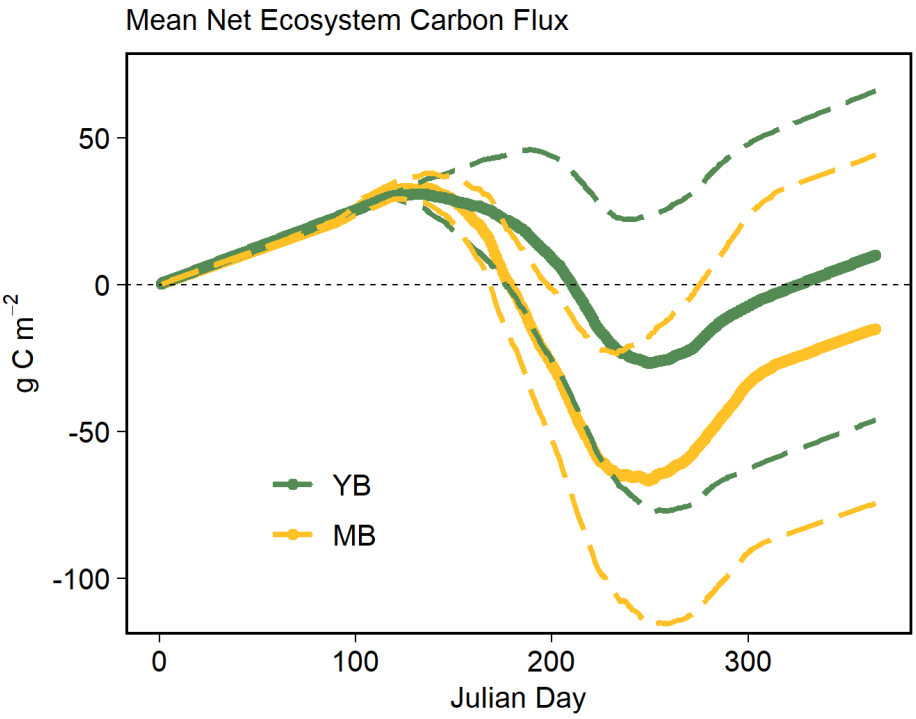

Figure A2.2. Average cumulative net annual ecosystem carbon flux from 2016 - 2018 for the young bog (YB; green) and mature bog (MB; golden). Solid lines represent average over three years. Dashed lines represent 95% confidence intervals.

Appendix 3. Supporting information for Chapter 4

Table A3.1. Statistical analysis of differences in monthly enzyme activity from four different peat layers (YB Shallow = near-surface young bog peat (0 – 29 cm) that accumulated post-thaw; YB Deep = deep young bog peat (32 – 160 cm) that accumulated pre-thaw; MB Shallow = near-surface mature bog peat (0 – 71 cm) that accumulated post-thaw; MB Deep = deep mature bog peat (72 – 160 cm) that accumulated pre-thaw.) measured throughout the 2018 growing season (May – September). PHOS = Phosphatase. NAG = Glucosaminidase. BG = Glucosidase. CB = Cellobiosidase. LAC = Laccase.

	PHOS		NAG		BG		CB		LAC	
Peat Layer	F ($_{Df}$)	P	F ($_{Df}$)	P	F ($_{Df}$)	P	F ($_{Df}$)	P	F ($_{Df}$)	P
YB Shallow	1.95 (3, 8)	0.201	1.71 (3, 8)	0.243	1.65 (3, 8)	0.254	1.77 (3, 8)	0.231	1.44 (4, 9)	0.30
YB Deep	0.95 (3, 19)	0.437	3.01 (3, 19)	0.056	2.07 (3, 19)	0.138	1.42 (3, 19)	0.269	1.28 (3, 15)	0.32
MB Shallow	1.42 (3, 14)	0.269	1.77 (3, 14)	0.199	0.38 (3, 14)	0.771	0.28 (3, 14)	0.840	0.66 (4, 11)	0.63
MB Deep	1.75 (2, 7)	0.242	1.93 (2, 7)	0.215	0.836 (2, 7)	0.472	3.29 (2, 7)	0.098	0.28 (3, 5)	0.84

Table A3.2. Statistical analysis of differences in hydrolytic enzyme activity (nmol g^{-1} $hour^{-1}$) from 4 different peat layers (YB Shallow = near-surface young bog peat (0 – 29 cm) that accumulated post-thaw; YB Deep = deep young bog peat (32 – 160 cm) that accumulated pre-thaw; MB Shallow = near-surface mature bog peat (0 – 71 cm) that accumulated post-thaw; MB Deep = deep mature bog peat (72 – 160 cm) that accumulated pre-thaw.) measured throughout the growing season. PHOS = Phosphatase. NAG = Glucosaminidase. BG = Glucosidase. CB = Cellobiosidase. LAC = Laccase. Bold emphasized P values indicate significance (P < 0.05). Df = degrees of freedom

	PHOS		NAG		BG		CB		LAC	
Peat Layer	F (Df)	P	F (Df)	P	F (Df)	P	F (Df)	P	F (Df)	P
Stage	26.2 (3, 100)	**< 0.001**	24.2 (3, 99)	**< 0.001**	29.2 (3, 75)	**< 0.001**	41.5 (3, 69)	**< 0.001**	2.7 (3, 61)	0.05
YB Shallow										
YB Deep		**< 0.001**		**< 0.001**		**< 0.001**		**< 0.001**		0.33
MB Shallow		**< 0.001**		**< 0.01**		**< 0.01**		**< 0.001**		1
MB Deep		**< 0.001**		**< 0.001**		**< 0.001**		**< 0.001**		0.12
MB Shallow										
MB Deep		**< 0.05**		**< 0.001**		0.101		**< 0.05**		0.20
YB Deep		**< 0.001**		**< 0.001**		**< 0.001**		**< 0.001**		0.15
YB Deep										
MB Deep		1		0.853		0.295		1		1

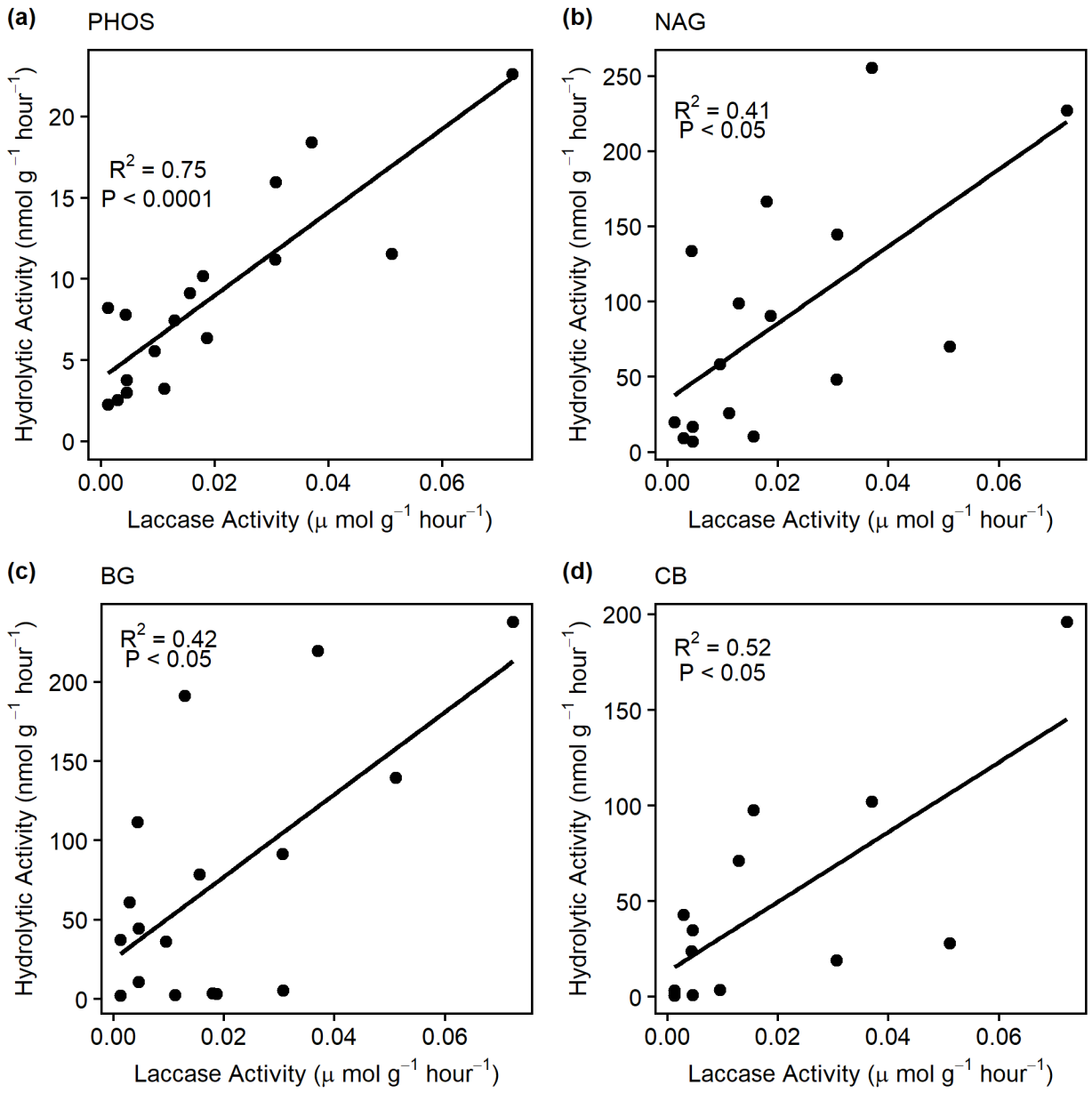

Figure A3.1. Positive relationship between measured hydrolytic enzyme activity (PHOS, NAG, BG, CB; nmol g^{-1} $hour^{-1}$) and oxidative (laccase) enzyme activity (μ mol g^{-1} $hour^{-1}$) in YB shallow peat. PHOS = Phosphatase. NAG = Glucosaminidase. BG = Glucosidase. CB = Cellobiosidase. All regression lines (in black) are significant ($P < 0.05$)

Table A3.3. Statistical analysis for differences in hydrolytic enzyme activity (nmol g^{-1} $hour^{-1}$) between different peat stages and oxic states (young bog oxic; young box anoxic; mature bog oxic; mature bog anoxic). PHOS = Phosphatase. NAG = Glucosaminidase. BG = Glucosidase. CB = Cellobiosidase. Bold emphasized P values indicate significance ($P < 0.05$). Df = degrees of freedom between peat types. Stage = Peat stage (YB; young bog or MB; mature bog). State = Oxic conditions (oxic or anoxic).

	PHOS		NAG		BG		CB		LAC	
	F (Df)	P	F (Df)	P	F (Df)	P	F (Df)	P	F (Df)	P
Stage	23.85 (1, 31)	**< 0.001**	11.16 (1, 26)	**< 0.01**	25.21 (1, 31)	**< 0.001**	26.07 (1, 31)	**< 0.001**	4.86 (1, 28)	**< 0.05**
State	0.07 (1, 31)	0.79	0.001 (1, 26)	0.98	0.19 (1, 31)	0.67	1.02 (1, 31)	0.32	0.07 (1, 28)	0.79
YB Oxic										
YB Anoxic		0.99		0.88		0.83		0.84		0.75
MB Oxic		**< 0.01**		**< 0.05**		**< 0.001**		**< 0.01**		0.94
MB Anoxic		**< 0.05**		0.14		**< 0.05**		0.07		0.31
YB Anoxic										
MB Anoxic		**< 0.05**		0.43		0.2		**< 0.05**		**< 0.05**
MB Oxic										
MB Anoxic		0.99		0.83		0.4		0.95		0.52

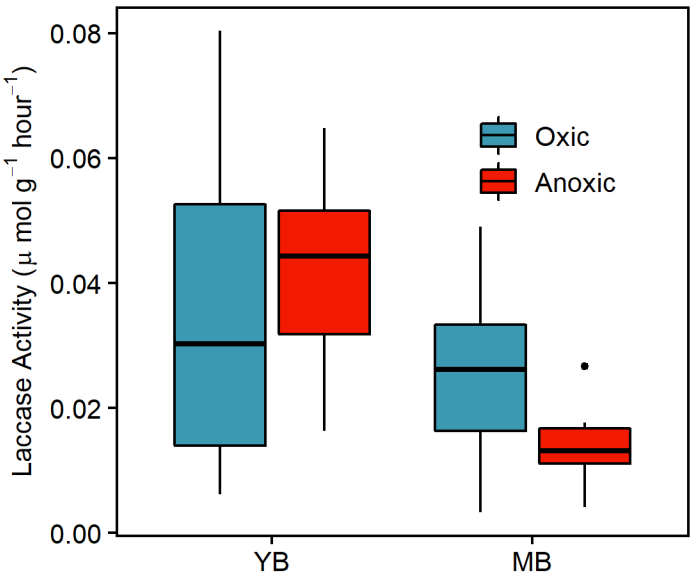

Figure A3.2. Laccase activity (μ mol g^{-1} $hour^{-1}$) from young bog (YB) and mature bog (MB) vegetation peat mesocosms under both oxic (blue) and anoxic (red) conditions. Overall, laccase activity in YB mesocosms (oxic and anoxic) is significantly higher ($F_{(1, 28)}$ = 6.8, P < 0.05) than laccase activity in MB mesocosms (oxic and anoxic). When separated, there is no significant difference (P > 0.05) in laccase activity between all four peat mesocosm types (YB Oxic, YB Anoxic, MB Oxic, MB Anoxic) except for YB Anoxic which had higher (P < 0.05) laccase activity than that observed in MB Anoxic.